

# A numerically efficient and holistic approach to design optimization of offshore wind turbine jacket substructures

Von der Fakultät für Bauingenieurwesen und Geodäsie der Gottfried Wilhelm Leibniz Universität Hannover zur Erlangung des Grades

Doktor-Ingenieur (Dr.-Ing.)

genehmigte Dissertation von

**Jan Häfele**

Erscheinungsjahr: 2019

Referent: Prof. Dr.-Ing. habil. Raimund Rolfes  
Gottfried Wilhelm Leibniz Universität Hannover

Korreferent: Prof. Dr. Michael Muskulus  
Norges teknisk-naturvitenskapelige universitet

Tag der Promotion: 27. Februar 2019

*“First, there is the power of the Wind, constantly exerted over the globe. [...] Nevertheless, here is an almost incalculable power at our disposal, yet how trifling the use we make of it! It only serves to turn a few mills, blow a few vessels across the ocean, and a few trivial ends besides. What a poor compliment do we pay to our indefatigable and energetic servant!”*

Henry David Thoreau, 1843<sup>1</sup>

---

<sup>1</sup>From “Paradise (to be) Regained” in *United States Magazine and Democratic Review*, XIII (XLV), pp. 451–463.

## Kurzfassung

Die Strukturoptimierung von Jacket-Tragstrukturen für Offshore-Windenergieanlagen birgt das Potenzial, signifikant zur Senkung der normierten Stromerzeugungskosten von Offshore-Windenergie beizutragen. In der Wissenschaft wurden in den letzten Jahren große Anstrengungen unternommen, um geeignete Ansätze hierfür zu entwickeln. Nichtsdestotrotz besteht weiterhin die Herausforderung, diese als unverzichtbare Optionen für die Dimensionierung von Jacket-Tragstrukturen nach dem Stand der Technik zu etablieren. In dieser Arbeit wird ein Optimierungsansatz vorgestellt, der das Problem ganzheitlich adressiert und sowohl hinsichtlich Genauigkeit als auch numerischer Effizienz Verbesserungen gegenüber dem Stand der Forschung darstellt. Dabei werden im Wesentlichen vier Aspekte thematisiert: Erstens, eine numerisch effiziente Implementierung der Boden-Bauwerk-Interaktion in Gesamtsimulationen von Offshore-Windenergieanlagen. Zweitens, eine umfangreiche Studie über reduzierte Lastsätze, die für die Berechnung der Ermüdungslebensdauern von Jacket-Tragstrukturen verwendet werden können. Der dritte Aspekt adressiert die Formulierung des Optimierungsproblems und beinhaltet die Entwicklung von Modellen für eine Zielfunktion, ein Kostenmodell auf Basis linear gewichteter Faktoren einzelner Kostenanteile, und nichtlineare Nebenbedingungen, für die Ersatzmodelle auf Basis der Gaußprozessregression zur numerisch effizienten Evaluation von Ermüdungs- und Extremlastnachweisen eingesetzt werden. Alle Entwicklungen werden im Rahmen des vierten Aspektes zu einem ganzheitlichen Optimierungsansatz zusammengeführt, der unter Verwendung gradientenbasierter Methoden am Beispiel der Optimierung von Jacket-Tragstrukturen für die NREL 5 MW-Referenzturbinen vielversprechende Ergebnisse liefert.

### **Schlagwörter:**

Jacket-Tragstrukturen, Offshore-Tragstrukturen, Offshore-Windenergie, Optimierung, Strukturoptimierung, Nichtlineare Programmierung

## Abstract

The structural optimization of jacket substructures for offshore wind turbines offers the potential to reduce the levelized costs of offshore wind energy significantly. In the recent past, science has made a major contribution to develop appropriate approaches in this field. Nevertheless, the challenge remains to improve these methods to represent an indispensable option for designing substructures in practical applications. This work presents an optimization approach that addresses the problem holistically and achieves improvements over the state of the art, both in terms of accuracy and numerical efficiency. Basically, four aspects are addressed: First, a numerically efficient implementation of the soil-structure interaction in simulations of offshore wind turbines. Second, a comprehensive study of reduced load sets, the input for the fatigue assessment of jacket substructures. The third aspect addresses the formulation of the optimization problem, incorporating the development of models for an objective function, a cost model based on linearly weighted factors of individual cost components, and nonlinear constraints, where surrogate models based on Gaussian process regression are used for the numerically efficient evaluation of structural code checks for fatigue and ultimate limit state. For the fourth aspect, all developments are combined in a holistic optimization approach for jacket substructures, which, using gradient-based methods, yields promising results, exemplarily shown for the NREL 5 MW reference turbine.

**Keywords:**

jacket substructures, offshore wind energy, optimization, structural optimization, nonlinear programming



## Vorwort

Diese Arbeit stellt den Abschluss meiner Tätigkeit als wissenschaftlicher Mitarbeiter am Institut für Statik und Dynamik im Zeitraum von 2013 bis 2018 dar. Die Optimierung von Jacket-Tragstrukturen für Offshore-Windenergieanlagen ist ein komplexes Thema, das verschiedenste Disziplinen der Ingenieurwissenschaften vereint. Im Laufe der Jahre sind daraus mehrere wissenschaftliche Publikationen entstanden, die in Form einer kumulativen Dissertation einen geschlossenen Themenkomplex behandeln. Ich möchte an dieser Stelle die Gelegenheit nutzen, um mich bei Menschen, die mich auf meinem Weg direkt oder indirekt unterstützt haben, zu bedanken.

Meinem Doktorvater, Herrn Professor Raimund Rolfes, gilt in mehrfacher Hinsicht mein besonderer Dank. Neben der kontinuierlichen Betreuung in Verbindung mit zahlreichen Fachdiskussionen bedanke ich mich insbesondere für die Freiheiten, die mir bei der Themenfindung eingeräumt wurden und die Unterstützung meiner persönlichen Weiterentwicklung. Auch möchte ich hervorheben, dass die Rahmenbedingungen am Institut für Statik und Dynamik zu einer kollegialen und produktiven Atmosphäre geführt haben, unter der ein Arbeiten auf hohem Niveau möglich ist. Ebenso möchte ich meinen herzlichen Dank an Herrn Professor Michael Muskulus richten, der sich – als ausgewiesener Experte im Bereich der Strukturoptimierung von Windenergieanlagen – bereit erklärt hat, das Korreferat zu übernehmen. Den Herren Professoren Udo Nackenhorst und Peter Schaumann gilt außerdem mein Dank für die Übernahme des Prüfungsbeisitzes und -vorsitzes. Ferner möchte ich mich bei Tanja Griebmann und Cristian Gebhardt für die sehr gute Betreuung meiner Arbeit auf Abteilungs- und Gruppenebene bedanken.

Von August bis Oktober 2017 verbrachte ich einen Forschungsaufenthalt am National Wind Technology Center des National Renewable Energy Laboratory (NREL) in Boulder, Colorado. Ich bedanke mich an dieser Stelle nochmals bei allen Forscherinnen und Forschern vom NREL, die meine Arbeit mit wertvollen Diskussionen, Anregungen und Informationen bereichert haben.

Ein guter Bürokollege ist die halbe Miete auf dem Weg zur Promotion. Daher bin ich sehr glücklich darüber, mein Büro anfangs mit Arne Schmoch und danach mit Tobias Bohne geteilt und viel Spaß gehabt haben zu dürfen. Auch meinen anderen Kollegen gilt mein herzlichster Dank für viele unvergessliche Momente, insbesondere Ricarda Berger, Martin Brod, Marlene Bruns, Aamir Dean, Andreas Ehrmann, Jasmin Hörmeyer, Benedikt Hofmeister, Clemens Hübler, Helge Jauken, Christian Karl und Susanne Martens. Eine unbesungene Heldin des Institutes ist Cornelia Kluge, bei der ich mich für alle Büromaterialien, Konferenzkekse und Ratschläge bedanken möchte, die ich von ihr bekommen habe. „Meinen Hiwis“, Qazi Asim Ijaz Ahmad, Manuela Böhm und Jennifer Dietrich danke ich für ihre stets zuverlässige und tolle Arbeit.

Nicht zuletzt bedanke ich mich bei meiner Familie und meinen Freunden, die immer für mich da waren, wenn ich sie gebraucht habe. Einen ganz besonderen Dank richte ich an meine großartige Partnerin Saskia, die viel Geduld aufgebracht hat, während ich diese Arbeit geschrieben habe.

Zum Schluss ist es mir ein großes Anliegen, meiner Mutter zu danken, die auch in den schwierigsten Zeiten immer so sehr für mich da war, sodass mein Weg immer ein leichter war. Ohne ihre Unterstützung würde es diese Arbeit nicht geben.

# Contents

<b>Kurzfassung</b>	<b>iv</b>
<b>Abstract</b>	<b>v</b>
<b>Vorwort</b>	<b>vi</b>
<b>1 Introduction</b>	<b>1</b>
1.1 Motivation . . . . .	1
1.2 State of the art . . . . .	3
1.2.1 Standards and guidelines for the design of offshore wind turbine support structures	3
1.2.2 Numerical simulation of offshore wind turbines . . . . .	4
1.2.3 Design and optimization approaches for wind turbine support structures . . . . .	9
1.3 Challenges and research gaps . . . . .	13
1.4 Objectives . . . . .	15
1.5 Outline . . . . .	15
<b>2 Improvement of offshore wind turbine time domain simulation codes</b>	<b>16</b>
<b>3 Load set reduction for the fatigue assessment of jacket substructure for offshore wind turbines</b>	<b>27</b>
<b>4 Accurate and numerically efficient formulation of the jacket optimization problem</b>	<b>42</b>
<b>5 Evaluation of optimal designs for offshore wind turbine jacket substructures</b>	<b>63</b>
<b>6 Conclusion</b>	<b>82</b>
6.1 Summary . . . . .	82
6.2 Innovations . . . . .	84
6.3 Concluding remarks . . . . .	85
6.4 Future work . . . . .	86
<b>Glossary</b>	<b>88</b>
<b>Bibliography</b>	<b>90</b>

# 1 Introduction

## 1.1 Motivation

Both the narrowness of fossil energy sources and the problematic nature of technical combustion have led to a substantial role of renewable energy sources. In 2017, the global renewable power capacity (not including hydropower) leaped the hurdle of 1 TW distinctly, attaining a value of 1.081 TW. This is an increase of 17% compared to 2016, where the installed global power added up to 0.922 TW. Approximately one half of the world-wide renewable power capacity is provided by wind power with a capacity of 0.539 TW, which is mainly produced by onshore wind farms to date (Renewable Energy Policy Network for the 21st Century 2018). Onshore wind turbines are technically more mature and less expensive than offshore wind turbines. However, offshore wind energy promises substantial advantages, mainly for the following two reasons:

1. **Environmental conditions.** The meteorological conditions off shore are beneficial in terms of a generally higher wind speed level. In addition, the inflow is not disturbed by the surrounding landscape or above-ground structures (when disregarding the influence of adjacent turbines in wind farms).
2. **Acceptance.** While onshore turbines are often considered as harmful impact on nature and humans, offshore wind energy benefits from a much higher acceptance.

To achieve an increased market share of offshore wind energy, the levelized costs of energy have to be diminished. The costs for offshore wind energy are indeed supposed to be decreasing. Germany's Federal Network Agency selected three out of four projects at zero-subsidy level in a recent wind farm tendering round in April 2017 (Kreiss et al. 2017). While a profitable production without subsidies is not possible right now, this can be seen as a bet on profitability of offshore wind energy in the near future by investors. To make this vision come true, cost reduction of wind turbine structures is highly desirable. One of the cost-driving parts of an offshore wind turbine is the substructure, which bridges the gap between sea bed and tower foot. According to BVGassociates (2013) or The Crown Estate (2012), the substructure causes about 20% of the entire capital expenditures. Among all substructures that have been installed yet, the monopile – a large steel tube acting both as foundation and substructure – is by far the most common type due to financial aspects and established manufacturing and logistic procedures. For instance, 97% of all European offshore wind turbines in 2015 were installed on monopiles (Ho et al. 2016). In 2016, this value decreased to 88% (Ho and Mbistrova 2017), which is still a very high portion. However, other substructures than the monopile are also considered as reasonable options considering turbines with high rated power. This becomes apparent in the decreasing share of installations. While 75% among the world-wide operating turbines in 2015 were installed on monopiles, this share was only 66% for turbines announced to be built between 2015 and 2020, as reported in 2015 (Smith et al. 2015). Among all substructures, the jacket – a welded truss-like tower with multiple legs and stiffened by diagonal and horizontal bracings, known from the oil and gas industry – has reached the second highest market share and is supposed to be an alternative to monopiles when facing turbines with high rated power or installations in deeper waters

(BVGassociates 2012). The exact limits of rated power or water depth, where this substructure type becomes competitive, depend on many hard and soft factors. Regarding recent installations, there is still a trend to monopile installations, even for turbines with 8 MW rating. However, several projects and studies show that jackets may be competitive, e.g.:

- Six of twelve turbines with a rated power of 5 MW in the first German offshore wind farm *alpha ventus* (Haake et al. 2009; Rolfes et al. 2013) with a water depth of about 30 m were installed on jackets (Seidel 2010), see Figure 1.1.
- Nordsee Ost, Thornton Bank (phase 2 and 3), and Ormonde are offshore wind farms in the North Sea with jacket substructures for turbines with ratings between 5 and 6.2 MW in water depths between 12 and 26 m (Oh et al. 2018).
- The wind farm Borkum Riffgrund 2 contains 36 monopile and 20 three-legged jacket substructures with suction bucket foundation for turbines with 8 MW rating (4C Offshore 2018).
- A comparison study for U.S. waters in the Gulf of Mexico revealed that jackets for turbines with 5 MW are more favorable than monopiles for waters deeper than 40 m (Damiani et al. 2016).
- The Block Island wind farm, the first one in the United States, consists of five 6 MW turbines installed on jackets (Walters 2016).

According to these examples, it can be stated that jacket substructure may be a reasonable option for the 5 MW and higher turbine classes to be installed in intermediate water depths.

Compared to the monopile, the jacket is lighter and transfers the loads to multiple foundation points, e.g. primarily axially-loaded piles. But although the jacket may be, under certain constraints, advantageous from a technical point of view, it is for multiple reasons still more expensive than the established monopile. This is why its market penetration is quite low at the time being. Nevertheless, innovative design methods may lead to a technological breakthrough (van Kuik et al. 2016). The jacket requires a complex design procedure (Seidel 2007). This enables many variants of topology and tube sizing, containing unexploited optimization potential that can lead to a reduction of levelized costs of energy.

Regarding state-of-the-art jackets, for instance from the research projects UpWind (Vemula et al. 2010) or INNWIND.EU (von Borstel 2013), thousands of time-domain simulations are performed to account for the effect of varying environmental conditions, mainly on fatigue limit state design load cases according to IEC 61400-3 (International Electrotechnical Commission 2009). The main obstacle in the jacket design process is the high numerical demand for (fatigue and ultimate limit state) structural code checks. For this reason, state-of-the-art design methods commonly get along with a few design iterations, eventually resulting in nonoptimal design solutions. In this sense, an optimization method for an efficient design of jackets for offshore wind turbines is highly desirable in order to obtain cheaper, cost-competitive structures. This thesis describes a novel approach to reach this goal.



**Figure 1.1:** Three REpower 5M offshore turbines with jacket substructures in the offshore wind farm alpha ventus, research platform FINO1 in the foreground (Rademacher 2012).

## 1.2 State of the art

### 1.2.1 Standards and guidelines for the design of offshore wind turbine support structures

General wind turbine requirements are imposed by the international standard IEC-61400, published in multiple parts by the International Electrotechnical Commission. In IEC 61400-1 (International Electrotechnical Commission 2010), general design requirements are formulated. The basis for the design of offshore wind turbines is IEC 61400-3 (International Electrotechnical Commission 2009). Requirements on steel constructions are stated by national standards, for example DIN EN 1993 (Deutsches Institut für Normung 2010) in Germany. Furthermore, multiple guidelines and recommended practices exist from various institutions, which have proven to be extremely useful for the design and dimensioning process of offshore structures. The American Petroleum Institute (2002) published a general guideline for the planning, design, and construction of offshore platforms, which is, in particular, helpful for the dimensioning of pile foundations. The American Bureau of Shipping (2010) provides guidance for fatigue design. Moreover, important notes to the design of offshore steel structures are moreover furnished by the Norwegian petroleum industry, assembled in the standards NORSOK N-001 (NORSOK 2004b) and N-004 (NORSOK 2004a). All these documents have in common that they apply generally to all offshore platforms or support structures, but are widely used for the design of offshore structures for wind turbines. In addition, some documents provided by DNV GL are of

considerable importance for the practical design of support structures for offshore wind turbines. The standard ST-0126 (DNV GL AS 2016b) contains general design notes, merging the offshore standard OS-J101 (Det Norske Veritas AS 2014) and the certification guideline by Germanischer Lloyd (2012). The recommended practices RP-C202 (Det Norske Veritas AS 2013) and RP-C203 (DNV GL AS 2016a) contain empirical approaches for the calculation of shells and the lifetime of welded connections, respectively. The above-mentioned rules and regulations primarily address the topics of fatigue and ultimate limit state, which are important for the design of offshore structures. In particular, the check for safety against fatigue failure requires a detailed numerical assessment, considering many environmental and operating states of the turbine (Kleineidam 2005; Sutherland 1999). The common procedure for fatigue assessment incorporates simulations of multiple design load cases in time domain to cover the effect of varying environmental conditions at the wind farm location, the application of stress concentration factors to account for the geometry and the scale of tubular joints (see Efthymiou 1988), a rainflow counting (Rychlik 1987) of stress signals, and the evaluation of S-N curves. The variability in the loads acting on the wind turbine both in fatigue and ultimate limit state leads, however, to uncertainty in simulation responses and therefore to significant errors (Zwick and Muskulus 2015). To reduce this uncertainty, many time-domain simulations have to be performed, which is related to high numerical expenses. In the design process of support structures for offshore wind turbines, this is a significant obstacle, as it limits the number of total design iterations, given that the numerical capacity for every structural design is predetermined.

### 1.2.2 Numerical simulation of offshore wind turbines

The numerical representation of a wind turbine involves various physical phenomena from different disciplines: structural, aero- and hydrodynamics (in the offshore case) as well as interactions of control and electrical systems with the structure are the essential impacts that need to be considered. There are indeed many approaches to modeling wind turbines, ranging from very simple to very complex ones. In this thesis, the focus is, however, on medium-fidelity engineering models. This means that the models to be used incorporate, if possible, physical-based assumptions and deploy, if necessary, simplifications to guarantee an adequate numerical efficiency. In other words, with the objective of simulation-based optimization, approaches with a high ratio of accuracy to numerical performance are desirable.

#### Multi-physical wind turbine simulation codes

Initially, strongly simplified models or frequency-domain analyses were often used to estimate the dynamic behavior of wind turbines (Quarton 1998). Examples originate, for example, from Kühn (1999), proposing analyses in the frequency domain for early development stages, or Meyer (2002), modeling the structural dynamics of the entire turbine with just a few generalized coordinates. Since the certification of plants requires the calculation of specified transient load cases, multiple time-domain simulation codes have been developed over the years (Passon and Kühn 2005) and reported in literature. Examples for established software packages are the proprietary codes Bladed from DNV GL, which can be called industrial standard, FLEX5, HAWC2, and FEDEM WindPower. These simulation codes are commonly based on a multi-body system formulation of the entire turbine with about 10 to 100 degrees of freedom, which can be considered as medium fidelity in the field of multi-physical wind turbine simulation codes. There are also open-source codes. The most popular one is FAST (National Wind Technology Center Information Portal 2016, 2018), which has been developed

by the National Renewable Energy Laboratory (NREL) and was extended to a modular framework (Jonkman 2013). The FAST model of the turbine including rotor blades, rotor-nacelle assembly, tower, and platform is based on a multi-body system formulation with about 20 degrees of freedom (depending on the turbine configuration and the desired level of accuracy) and on the so-called blade-element/momentum theory (Sørensen 2016) to determine the aerodynamic loading on the blades, which can be considered as a numerically efficient medium-fidelity method for this purpose. As the source code of FAST is accessible for no charge without any restrictions, many research studies are based on this framework. Examples are shown by Mohammadi et al. (2018), who analyzed tower shadow and yaw error impacts on the electrical system of the turbine, Pahn et al. (2017), using the code for inverse load calculation, or Tong et al. (2018), designing a tuned mass damper for floating wind turbines<sup>1</sup>. On the basis of good accessibility and code-to-code verifications within projects of the International Energy Agency, namely the Offshore Code Comparison Collaboration (OC3, Jonkman and Musial 2010; Passon et al. 2007) and the Offshore Code Comparison Collaboration, Continuation (OC4, Popko et al. 2014a) projects, it has matured into a serious alternative to proprietary codes. Recently, there is also an initiative to validate simulated to physical responses from measurements within the Offshore Code Comparison Collaboration, Continued, with Correlation (OC5) project. In a first phase, the focus was on hydrodynamic loads (Robertson et al. 2015, 2016). In a second phase, global loads on a semisubmersible wind turbine were validated using measurement data (Robertson et al. 2017). Further results are announced for the near future.

In the recent past, also a demand for codes being capable of simulating the response of geometrically nonlinear structures of wind turbines, mainly rotor blades, has emerged. This requirement arose from the trend towards turbines with very high rated power, where very slender rotor blades feature significant nonlinear behavior due to hardening or stiffening effects by large deformations and rotations, bending-twisting coupling, etc. At some point, it became apparent that linear codes were not suitable to predict responses of these structures accurately. For instance, FAST was enhanced with a module to consider the nonlinear structural behavior of rotor blades by nonlinear, geometrically exact beam elements (Wang et al. 2017). In HAWC2, this is modeled by a linear anisotropic beam element (Kim et al. 2013). The codes were compared in ad-hoc benchmarks and it turned out that both are suitable to model the complex response of large rotor blades (Pavese et al. 2015). There are also simulation codes focusing on the nonlinear dynamics of structures, not developed for certification purposes in the first instance, but gaining further insight into structural dynamics, like DeSiO (Gebhardt et al. 2018). It can be assumed that all these efforts will lead to a further improvement of wind turbine design in the mid-term.

## Numerical representation of offshore substructures

The simulation of substructures involves the representation of the structure itself, the foundation, and the loading.

There are mainly two approaches to simulate the response of substructures for offshore wind turbines. In the first one, it is assumed that interaction effects between substructure and surrounding structures are weak. It is called decoupled approach, when the substructure properties are not considered, and sequentially coupled approach, when the substructure properties are considered to some extent in the time-domain simulations, for instance, by lumped mass and stiffness matrices. The reaction force between tower and substructure is considered as external load on the substructure, which is commonly

---

<sup>1</sup>This is deliberately far off from a complete listing and only shown to illustrate the high variety of applications based on the simulation code FAST.

modeled in high detail. Decoupled or sequentially coupled approaches are state of the art for the design of substructures in industrial applications (Seidel et al. 2005) and allow for relatively accurate predictions of structural responses in many load cases (Chen Ong et al. 2017). The second one, called coupled approach, goes along with the assumption that the interaction between substructure and turbine is nonnegligible, requiring the structural model of the substructure to be integrated into the one of the entire turbine. This approach is more accurate, but is also connected to higher requirements on numerical capacities.

The actual simulation method is mainly governed by the type of the substructure. While monopile substructures are often modeled as extension of the tubular tower in simulation codes for offshore wind turbines, the modeling of multi-member substructures like, for instance, tripods or jackets, is generally more complicated. Commonly, finite-element models are deployed for this purpose. Depending on the requirements of fidelity, these models may be discretized by beam, shell, or solid elements, where the latter represents the highest potential concerning accuracy, but also the highest demand of numerical capacity, and vice versa. However, the most applications reported in literature utilize linear Bernoulli and Timoshenko beam element discretizations (see Kaufer et al. 2010), as this is considered as the best compromise between accuracy and numerical efficiency for most applications. There are also proposals to account for the stiffness of tubular joints by superelements (Dubois et al. 2013; Popko et al. 2016). As the stiffness properties strictly depend on the exact geometry of the joint, which is indeed unknown for most applications, these approaches are often disregarded.

The foundation model is often combined with the substructure model. One reason is that this is commonly easier than exchanging information at the transition between substructure and foundation. The simplest way of foundation modeling is to assume that the substructure is clamped to the ground at the lowermost leg elements. In this case, there is no soil-structure interaction. While this had been a common approach in simulation codes for many years, the demand for incorporating the soil-structure interaction emerged. Zaijjer (2006) described common approaches to the modeling of foundations for offshore wind turbines. A simple approach for this purpose is the apparent fixity length approach, where the substructure is extended to a fictive depth below ground to account for the foundation stiffness (Bartrop et al. 1991). More accurate but yet simple approaches assume discrete uncoupled or coupled springs at the transition between substructure and ground, where stiffness matrices represent the soil resistance. More complex approaches consider a model of the entire foundation. In case of a pile foundation and with sufficient numerical capacity, it is straightforward to use a finite-element beam model of the pile. The soil-structure interaction is commonly considered by  $p$ - $y$  and  $T$ - $z$  curves, an approach from the petroleum industry, where discrete stiffnesses – mimicking the soil resistance – in horizontal and vertical directions are distributed along the pile in fixed distances. For the design of monopile and jacket substructures, this procedure can be considered as state of the art. There are several proposals for the calculation of stiffness values presented in literature. The most common one was introduced by the API (American Petroleum Institute 2002), which was modified by Kallehave et al. (2012). However, for time-domain simulations of offshore wind turbines, the numerical representation of piles with many degrees of freedom may be related to a too high demand of numerical capacity, as the corresponding improvement in accuracy is considerable, but not vital. Therefore, also the coupled and uncoupled spring approaches are still prevalent.

The wave loading on substructures, which may have significant impact both on fatigue and extreme loads, is commonly calculated by the strip theory using Morison's equation (Morison et al. 1950). This equation comprises two components, accounting for drag and inertia forces on the flow-surrounded body, which can be adapted to measurements by empirical coefficients. While this theory is well established and appropriate for offshore structures comprising slender tubes, it may be inaccurate for



nonslender structures, because it is only valid for nondiffractive flows, where the flow acceleration is uniform at the location of the body, and does not allow for the consideration of radiation damping, which is the main energy-extracting effect in flows (Sarpkaya 2010). For nonslender structures, more accurate although numerically more expensive methods are required to obtain adequate results. Typically, the potential flow theory is deployed in this case. Wave kinematics are often derived by the linear airy theory, which is also applicable for irregular waves (Jonkman 2007).

Beam models of substructures with few nodes like monopiles usually do not incorporate many degrees of freedom and are hence computationally inexpensive. However, it may cause significant computational expenses when simulating the response of jackets and motivates using reduction methods. In the simplest case, a static reduction method according to Guyan (1965) can be applied for this purpose. However, this is often not accurate enough. State of the art is a component mode synthesis, based on a Ritz transformation with constraint and fixed-interface normal modes<sup>2</sup>, as proposed by Craig Jr. and Bampton (1968). Song et al. (2012) described the representation of jackets in FAST based on a discretization of the structure with linear beam elements and a subsequent reduction of system matrices. Thereby, it is possible to represent jacket substructures adequately with approximately ten generalized coordinates (Damiani et al. 2013). Moreover, it is possible to incorporate external loads into this reduction scheme. It has to be stated that a component mode synthesis goes along with limiting the structural response to a upper boundary in the frequency domain, which may lead to a nonconsideration of local modes. Local modes are modes, where single bracings oscillate in in-plane or out-of-plane bending motions<sup>3</sup>. Böker (2010), Schaumann et al. (2011), and Popko et al. (2014b) showed that these may impact the structural response significantly. Therefore, prior to each numerical study, it has to be evaluated, whether the omission of local modes is valid or not.

## Reference wind turbines and offshore substructures

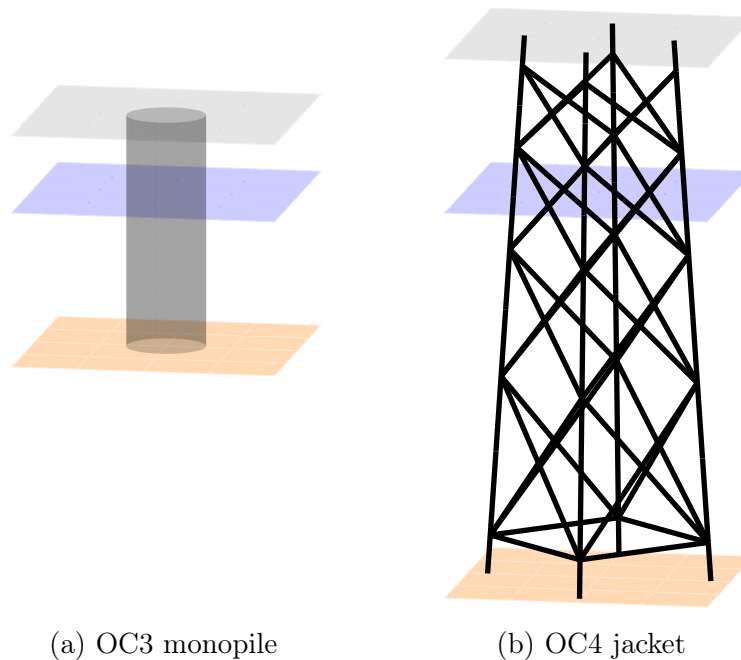
For a long time, it had been a big issue in the field of offshore wind research that turbine data and parameters were not freely accessible or that research results were not published due to nondisclosure agreements. To address these issues, reference turbines were designed to ease research on wind turbines. Jonkman et al. (2009) defined a test turbine with 5 MW rated power, based on the designs of the DOWEC 6 MW (Kooijman et al. 2003) and REpower 5M 5 MW (REpower Systems AG 2004) turbines. At the time being, the NREL 5 MW reference turbine is still the undisputed standard in this field due to excellent availability and documentation. Numerous studies presented in literature are based on this reference turbine. In addition, various reference substructures for the NREL 5 MW turbine emerged from the OC3 and OC4 projects for code-to-code verification purposes: In OC3, a monopile, shown in Figure 1.2(a), and a tripod structure were defined for 20 and 45 m water depths, respectively. In the OC4 project, a jacket substructure (OC4 jacket), shown in Figure 1.2(b), for a water depth of 50 m was derived from a reference jacket that was initially defined in the research project UpWind (Vemula et al. 2010). Reference load cases and sensor positions were elaborated, too (Vorpahl and Popko 2013). For the sake of numerical efficiency, the OC4 jacket lacks details of tubular joints and tube dimensions are constant from bay to bay (Vorpahl et al. 2011).


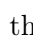

To address the arising issue that the rated power of installed turbines is increasing, reference turbines with higher rated power have been demanded and proposed in the recent past. In particular, the

---

<sup>2</sup>The Guyan reduction is a special case of the reduction method by Craig and Bampton, where only constraint modes are considered.

<sup>3</sup>The natural frequencies of other than in-plane or out-of-plane bending modes are of high frequency and therefore not considered as relevant for the structural response.



**Figure 1.2:** Topology of bottom-fixed reference substructures from the OC3 and the OC4 projects. Both structures are displayed in the same scale. The foundations are not shown. The ground layer is illustrated by , the mean sea level and transition piece layers by  and , respectively. The mean sea level layer is at constant height for both subfigures.

so-called DTU 10 MW turbine with 10 MW rating (Bak et al. 2012, 2013; Zahle et al. 2013) was proposed, which was supposed to supersede the 5 MW reference turbine from NREL, but has not been widely used yet. In the same research project, a reference jacket for the DTU 10 MW turbine and 50 m water depth was developed (von Borstel 2013). The initial design lacked sufficient fatigue damage resistance, featuring a computed lifetime of only four years. This issue was addressed in an improved design approach (Stolpe et al. 2016), which incorporated many innovations on component level. At the end of the research project INNWIND.EU, also the design of a conceptual 20 MW turbine was developed (Chaviaropoulos et al. 2017), which has already passed a preliminary aero-structural optimization of the rotor (Sartori et al. 2018). There is also a design solution for a support structure (Pontow et al. 2017), published at the same time.

## Design bases

To obtain loads for structural designs of wind turbines, environmental data is required, which is often related to a specific wind farm location. This data is often assembled in so-called design bases. In the research project UpWind, a design basis showing data for two offshore sites in the Dutch North Sea was developed (Fischer et al. 2010), which was used both for the structural designs of the UpWind and the INNWIND.EU reference jackets. The document provides data of wind and wave states and considers directionality of some parameters describing models of environmental conditions. As there had been no better alternative for a longer time, the UpWind design basis became a kind of standard for all kinds of studies on offshore wind energy that required knowledge about environmental

conditions to some extent. However, there are limitations to be mentioned. The data of both sites actually originates from two shallow locations with water depths from about 20 to 25 m. To obtain data for intermediate water depths, the normal sea states at the second site (“K13”) were assumed to be valid for 50 m water depth, too. Extreme sea states were obtained from an external database (ARGOSS) using oceanic modeling and satellite data. In addition, the UpWind design basis provides mainly scatter diagrams. More detailed climate data is available from the research platforms FINO1, FINO2, and FINO3 (Bachmann and Barton 2008). While FINO2 is located in the Baltic Sea, FINO1 (built in 2003) and FINO3 (built in 2009) are located in the North Sea and furnish – compared to the UpWind design basis – more comprehensive metocean data. There are several examples for research studies basing on data of these research platforms (see for instance Muñoz-Esparza et al. 2012; Schaumann and Böker 2007). The entire data basis of the FINO platforms was evaluated by Hübler et al. (2017), providing probability density functions of environmental state parameters, which may be the input for studies on offshore wind turbines.

### 1.2.3 Design and optimization approaches for wind turbine support structures

In the very most cases, wind turbines are subjects of investments. For this reason, the structural optimization of wind turbine support structures is almost as old as the technical use of wind energy itself. From an economical perspective, this optimization problem can be seen as a minimization of expenditures, respecting design constraints (Arora 2012). Often, it is stated in the following or a similar mathematical form, which is called the standard formulation according to Haftka and Gürdal (1992):

$$\begin{aligned} \min \quad & f(\vec{x}), \\ \text{such that} \quad & g_j(\vec{x}) = 0, \quad j = 1 \dots J, \\ \text{and} \quad & h_k(\vec{x}) \leq 0, \quad k = 1 \dots K, \end{aligned} \tag{1.1}$$

where  $\vec{x}$  is a vector of the design variables.  $f(\vec{x})$  is the objective function representing the costs of the structure or a related measure.  $g_j(\vec{x})$  and  $h_k(\vec{x})$  are the  $j$ th and  $k$ th equality and inequality constraints, respectively, that need to be satisfied by the optimal structural design. Although this formulation is quite abstract, it is a good starting point to characterize optimization approaches for wind turbine support structures. For instance, when imagining the structural optimization problem of a tubular wind turbine tower, the design variables may be geometrical properties on different heights and the mass has to be minimized under the constraint that the displacement under a certain design load must be limited. Even for this simple case, it becomes apparent that it has generally to be dealt with nonlinear inequality constraints. Therefore, the problem stated in equation 1.1 is in most approaches that will be presented in the following a nonlinear program. Another characterizing property of all approaches is, how the problem is solved, i.e., the solution process. There are mainly two families of optimization methods used for practical structural optimization of wind turbine support structures. The first one contains gradient-based methods. These methods usually guarantee local convergence with high numerical performance, in particular, when sensitivities of objectives and constraints are known. Excellent references in this field are the works of Gill et al. (1981), Fletcher (1987), and Nocedal and Wright (2006), where the latter incorporates all relevant gradient-based implementations being used in current optimization frameworks. The second ones are metaheuristic methods, a family of methods based on processes inspired by nature. In the field of metaheuristic optimization, the most widely used methods are genetic algorithms (Goldberg 1989) and particle swarm optimization (Kennedy and Eberhart 1995; Shi and Eberhart 1998). While these methods

need, compared to gradient-based ones, significantly more iterations to converge, they offer in many cases global convergence properties. This is the reason, why these methods are often deployed for nonconvex optimization problems, where a local minimum is not necessarily a global one.

Concerning wind turbine support structures, there is an extensive survey on the application of structural optimization approaches, elaborated by Muskulus and Schafhirt (2014), who divided the methods presented in literature into static, frequency-domain, and time-domain approaches. As this classification is meaningful from the author's point of view, it is adopted for the presentation of the state of the art given below.

## Static approaches

Static approaches to structural optimization in wind energy technology are based on static structural representations, often using detailed finite-element models, and have primarily been applied to tubular towers so far. Negm and Maalawi (2000) modeled tower structures with beam elements and discuss simple problem formulations for optimization problems of towers for wind turbines with 100 kW rating. Different problem formulations are compared, all incorporating a load case with constant extreme wind and constraints on maximum strength and deflection. The authors conclude that a weighted sum of natural frequencies is the most representative objective function with respect to major design goals. Another very early approach to wind turbine substructure optimization, yielding principle dimensions of support structures, originates from Zaaier (2001). This work contains basic features of modern optimization approaches like considering fatigue loads in a simple way and a relatively comprehensive cost model. Furthermore, the results are in good agreement with real structures that were installed. Bazeos et al. (2002) considered a prototype steel tower for a 450 kW wind turbine using a finite-element model discretized by shell elements, where static, stability, and seismic analyses were carried out. Lavassas et al. (2003) used a similar concept, but expanded the number of load cases and made detailed considerations of mechanical stress distribution in the foundation. In addition, a damage equivalent load procedure was applied to compute fatigue damages. A reliability-based optimization approach was reported by Sørensen and Tarp-Joansen (2005), using simplified models to compute failure modes. This work is not meant as a structural design optimization approach, but provides optimization models for inspection and maintenance planning of offshore wind turbines. The results of this work contain optimal reliability levels for the different failure modes. A method for the cost minimization of ring-stiffened cylindrical shells, proposed by Farkas and Jármai (1997), was used by Uys et al. (2007) to minimize the costs of a steel tower. An interesting aspect of this paper is that a cost function incorporating manufacturing costs (based on industrial data) was used. Gencturk et al. (2012) developed an approach to the optimization of latticed support structures for wind turbines with static loads, also considering geometrical nonlinearities in the finite-element analysis and eigenfrequency constraints, according to the model of Kang et al. (2001). Two main specialties are present in this study: First, the objective function includes the portions of manufacturing and foundation material costs. Second, a metaheuristic taboo search algorithm (Glover 1986) is used to obtain the optimal solution. A static approach to the design of latticed support structures was presented by Long et al. (2011), based on the NREL 5 MW reference turbine. While only static and buckling extreme load checks are performed in this work, the approach allows for topological design changes. Perelmuter and Yurchenko (2012) presented a parametric approach to tower optimization for onshore wind turbines, both based on very simple analytical inflow and structure calculations. Damiani and Song (2013) proposed a jacket sizing tool for systems engineering, which allows for the determination of basic topology and dimensions, also based on optimization. This tool is the first one presented in

literature enabling holistic design of the entire support structure (Damiani 2016). For instance, it was utilized for a realistic techno-economic study on jackets for U.S. waters (Damiani et al. 2017), which features application-oriented results in terms of a contrasting juxtaposition between jackets and monopiles.

### Frequency-domain approaches

In frequency-domain approaches, time series of loads are reduced to spectra to simplify numerical effort, which allows for considering fatigue damages by damage equivalent loads. This is particularly common when using decoupled simulation methods. Often, these approaches do not or just in a simplified way (if combined with other techniques) take the extreme load behavior into account, i.e., they are often coupled to static ones to compute extreme loads. Kühn (2001) discussed an optimization approach, where wind and wave loads are superposed in the frequency domain to compute fatigue damages and perform a design optimization of offshore wind turbines. A very detailed approach was proposed in the thesis of van der Tempel (2006). A focus of this work is on the applicability to practical problems. As a conclusion of this work, the main issue is that the entire fatigue estimation relies strongly on the damping of the turbine, both structurally and aerodynamically. Consequently, it turns out that appropriate results require a relatively exact predetermination of damping parameters. Thiry et al. (2011) presented a monopile optimization framework, relying on a simple structural model and making use of transfer functions to determine fatigue damages in the frequency domain. Also, modal and extreme load constraints are considered. The problem is solved by a metaheuristic genetic algorithm. Long and Moe (2012) applied a frequency-domain fatigue estimation method reported by Dirlik (1985) to determine fatigue loads for jacket substructures. As a novelty, three- and four-legged structures are considered in this work. The results show that three-legged jackets may be a promising, cheaper alternative to four-legged ones. Spectral approaches were also used to design floating structures. Although it is not particularly in the scope of this thesis, some ideas may be transferable to the design of bottom-fixed structures as well. Brommundt et al. (2012) proposed a spectral method to optimize the mooring system of a floating structure, where a spectral model was used to predict structural responses of a semi-submersible support structure. This work shows again that the estimation of damping parameters is crucial to obtain reliable results with frequency-domain methods. The authors proposed to utilize time-domain simulations for verification purposes. Michailides and Angelides (2012) considered a multi-objective problem formulation based on a genetic algorithm and a global criterion method. A similar work was presented by Hall et al. (2013), who proposed using a multi-objective formulation and a genetic algorithm to design floating structures, also in terms of topology.

### Time-domain approaches

Time-domain approaches offer the possibility to carry out a very detailed design assessment, which is close to the requirements of design standards and structural code checks. However, this is commonly related to high computing times. That is why the methods discussed in the following have mainly emerged in the current decade. One of the first approaches of this kind was reported by Yoshida (2006) for the dimensioning of a steel tower of an onshore turbine in the 2 MW class, based on a genetic algorithm and the simulation code *Bladed* to perform structural code checks. Maki et al. (2012) discussed the design of a wind turbine on system level. Although the focus is on the design of the rotor and the support structure is addressed only incidentally, it features some interesting ideas like

comprehensive cost functions and the utilization of meta-models. An alternative to empirical scaling laws is the simulation-based optimization methodology presented in the thesis of Ashuri (2012), providing forecasts for the design of very large offshore wind turbines, involving all components. The key idea of this study is to perform scaling not by empirical laws, but by optimization. The results are fairly comprehensive and answer questions concerning development of beyond-state-of-the-art turbines. However, the focus is not on the support structure or substructure. This was further elaborated by Haghi et al. (2012), designing a monopile for an offshore wind turbine with 3.6 MW. The mass of the entire support structure is decreased by about 12%, compared to the initial design. Interestingly, this involves a mass increase of the tower, while the monopile and the transition piece decrease in mass. An optimization framework based on FAST and being capable of performing design optimization of onshore wind turbines was presented by Gutierrez et al. (2013). Simulation-based optimization approaches focusing on jacket structures were introduced by Zwick et al. (2012) for the first time by taking up the full-height lattice tower concept (Muskulus 2012), where a gradient-based method was used to find a mass-optimal solution. The approach was further elaborated by Molde et al. (2014). Retrospectively, the work of Zwick et al. was the starting point of multiple studies, which all addressed simulation-based jacket optimization by a tube dimensioning problem, where the structural topology was given<sup>4</sup> and maintained. For instance, Chew et al. (2013, 2014) compared jacket substructures with three and four legs by an iterative approach. It turned out that three-legged structures may be beneficial from an economical point of view. To obtain a three-legged structure, the OC4 jacket was slightly modified in this study. Schafhirt et al. (2014) employed a metaheuristic genetic algorithm for jacket optimization to ensure global convergence. In order to address the problem of the significantly higher number of iterations compared to a gradient-based method, a reanalysis technique was implemented, where information from generations that had already been computed were reused. However, it becomes apparent by this study that, even when deploying efficient improvements, metaheuristics are too slow for a simulation-based optimization procedure, without simplifications of the problem statement. For this reason, most of the following approaches presented in literature were focusing on numerical efficiency, mainly in terms of efficient problem formulations. This was firstly addressed by Chew et al. (2015, 2016), who introduced the idea of analytically calculated gradients in the field of jacket optimization, which circumvents the need of finite differences in the computation of gradients and leads to faster convergence. The gradients were calculated using the equations of motion of the decoupled structure, where aero- and servodynamic impacts depicted external inputs. Furthermore, a sequential quadratic programming method was applied to find the optimal solution. Finally, the authors concluded that the presented framework was allowing for higher efficiency and accuracy compared to finite difference approaches. Schafhirt et al. (2016) employed a method for simplified fatigue load assessment by Zwick and Muskulus (2016) in a gradient-based approach, with the fundamental presumption that variations in single tube dimensions do not impact the structural response of the turbine, allowing for much less evaluations of structural code checks. Oest et al. (2016) presented a similar approach, applying analytically derived gradients and a sequential linear programming method to this type of problem, resulting in an entire mass reduction of around 40% of the OC4 jacket, which can be considered as a high value. Moreover, some interesting techniques guaranteeing a global solution when using gradient-based methods were deployed. A comparison of different time-domain simulation techniques – namely static, quasi-static, and dynamic simulations – within gradient-based optimization was shown by Oest et al. (2018), achieving even higher mass reductions of about 50% compared to the OC4 jacket. Sandal et al. (2018) integrated the foundation design into the optimization problem. An example with the DTU 10 MW reference turbine is discussed, where both piles and suction caissons are considered as possible

---

<sup>4</sup>In almost every case, the topology of the OC4 jacket was used.

foundation types. An approach to jacket optimization with discrete design variables, accounting for the practical problem of limited availability of tube size combinations, was presented by Stolpe and Sandal (2018). Recently, also metaheuristic optimization approaches based on genetic algorithms described by AlHamaydeh et al. (2015, 2017) and Kaveh and Sabeti (2017, 2018) were presented, however, incorporating limited load assumptions without appropriate structural code checks. A design optimization of a hybrid steel substructure by particle swarm optimization was reported by Chen et al. (2016), but it is unclear, why the number of ultimate limit state load cases is quite high, while there is only one fatigue load case considered in this work.

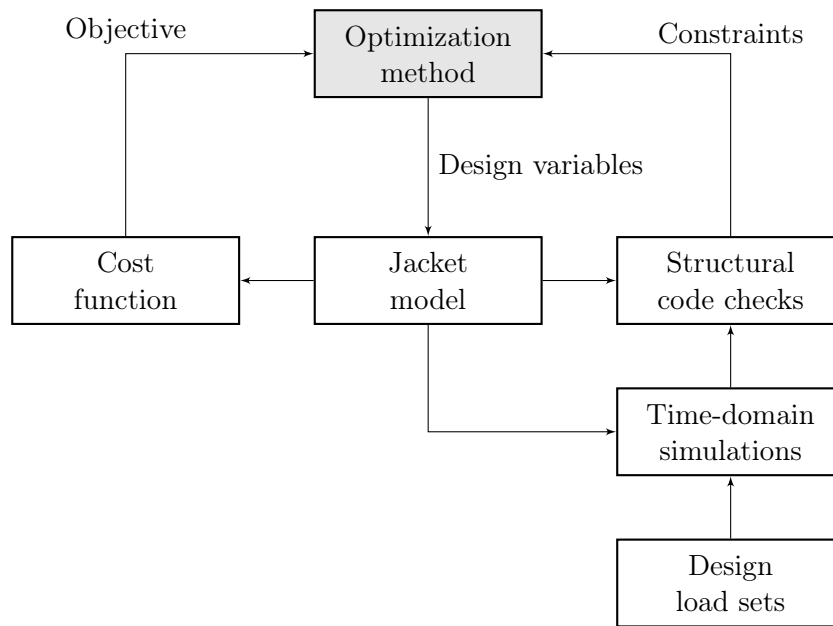
### 1.3 Challenges and research gaps

The previous section shows that a large number of jacket optimization approaches exists and this topic is both meaningful and relevant for industrial and scientific applications. From the industrial perspective, economical aspects are probably decisive, because jackets are still not cost-competitive to monopiles. From the scientific point of view, however, there is an additional motivation, as the topic is complex and involves certain research challenges. Muskulus and Schafhirt (2014) concluded that there are six specific challenges in the design of wind turbine structures in general, namely:

- **nonlinearities**, exhibited by wind turbines in many ways,
- **complex environment**, due to highly varying environmental conditions, which is particularly relevant for offshore wind turbines,
- **fatigue as design driver**, involving a large number of design load cases to be evaluated,
- **specialized analysis software**, accounting for the many different physical phenomena related to wind turbines,
- **tightly coupled and strongly interrelated systems**, implying that the system wind turbine cannot be considered as a sum of independent parts, physically and economically, and
- **many design variables and constraints**, which is particularly an issue in the design of jacket substructures.

In the author's opinion, this list precisely reflects the demands and challenges in this field and is likewise valid for the design of jacket substructures. It follows that a holistic approach needs to address all these challenges adequately to yield the best possible design. The state of the art shows that indeed many approaches to jacket optimization considering these challenges do exist. They have led to significant improvements of design methodologies, especially within the past five years. However, all aforementioned works – discussed in the presentation of the state of the art – involve massive simplifications, mainly for the sake of numerical efficiency. Figure 1.3 shows a general optimization scheme for single-objective jacket optimization with nonlinear constraints. Every approach can be transferred to this scheme. The existing research gaps can be directly related to the corresponding topics:

- **Optimization methods.** The state of the art reveals that gradient-based optimization is favorable, when global convergence can be guaranteed, especially, when analytically calculated gradients are available. Sequential quadratic programming or interior-point methods are considered as extremely accurate and efficient (Nocedal and Wright 2006) and have already been deployed numerous times. In addition, some studies revealed that metaheuristic optimization



**Figure 1.3:** Scheme of state-of-the-art approaches to time-domain jacket optimization with nonlinear structural code check constraints.

methods are too slow to be considered as an alternative for this kind of problem. Therefore, this factor does not offer much improvement potential.

- **Jacket model.** Many jacket optimization approaches consider the problem as a pure tube sizing task, where the design variables are tube sizes and wall thicknesses of single tubes. For this purpose, the structural topology is assumed to be fixed and usually adopted from reference structures. An approach incorporating the entire jacket design is highly desirable.
- **Cost function.** In the optimization scheme, a cost model serves as an objective function. The common cost modeling approach in approaches reported in literature is to consider the substructure mass as objective function. This is, to some extent, meaningful in terms of tube sizing, but disregards the real cost breakdown, which involves contributions like manufacturing, transport, or installation costs.
- **Structural code checks.** Recent approaches already consider structural code checks as nonlinear constraints. However, this point offers opportunities to speed up the entire optimization process, when the simulation-based evaluation of structural code checks is replaced by a faster method, for instance, surrogate models.
- **Time-domain simulations.** In time-domain approaches, the computation time of one design iteration is directly proportional to the simulation efficiency. This can be improved by more efficient simulation codes, e.g. using reduced order modeling, or computation hardware.
- **Design load sets.** The number of design load cases per load set is the second factor, that is related proportionally to the computation time per iteration. Therefore, the number of load cases to be considered per structural code check iteration needs to and can be reduced to accelerate jacket optimization.



## 1.4 Objectives

The global aim of this work is the development of an holistic approach to jacket substructure optimization with improvements in accuracy and efficiency compared to the state of the art. It intends to provide a method that considers the jacket optimization problem from a multi-disciplinary perspective with physical, technical, and economical constraints.

In this sense, four objectives are defined that – according to the research gaps in this field – present the prospect of offering significant improvement potential:

1. Improvement of offshore wind turbine time-domain simulation codes
2. Load set reduction for the fatigue assessment of jacket substructures for offshore wind turbines
3. Accurate and numerically efficient formulation of the jacket optimization problem
4. Evaluation of optimal designs for offshore wind turbine jacket substructures

It is supposed that these objectives – when addressed appropriately – are crucial to reach a technological leap of jacket substructures.

## 1.5 Outline

This thesis addresses the aforementioned objectives in the respective chapters. Each comprises a journal article, written by the author of this thesis as the main author.

Subsequent to this introduction chapter, chapter 2 describes an approach to incorporate the soil-structure interaction into numerical simulations of offshore wind turbines in an efficient way. Among many imaginable opportunities to improve time-domain wind turbine simulation codes, this is an exemplary contribution to the improvement of offshore wind turbine simulation methodologies enabling fast simulations while improving the accuracy of the predicted system response. Moreover, the approach is valid for all types of substructures. Chapter 3 presents a load set reduction study for fatigue limit state of jacket substructures, which is essential for the optimization of jackets, as the numerical costs of structural code checks for jackets depend highly on the number of design load cases to be considered during the design process. The approach considers different types of reduction. Chapter 4 proposes a jacket model, incorporating topology and tube dimensioning parameters, a cost model, and surrogate models for structural code checks, allowing for quick evaluations of jacket designs concerning fatigue and ultimate limit state. These models are the basis for an optimization approach described in chapter 5, which deploys state-of-the-art gradient-based, nonlinear optimization methods and compares optimal jacket designs with different topologies. The work is finalized with a comprehensive conclusion (chapter 6), including a summary of all chapters, a list of innovations, some concluding remarks, and ideas for work that may be performed in the future.

## 2 Improvement of offshore wind turbine time domain simulation codes

This research paper describes an approach for numerically efficient consideration of soil-structure interaction in offshore wind turbine simulations and is published in Applied Ocean Research, Vol. 55, 2016, pp. 141–150 (DOI: 10.1016/j.apor.2015.12.001).

### Author contributions

Jan Häfele is the corresponding author of the publication and the main author of section 1 (Introduction), section 2 (Fundamentals), section 4 (Benefits and limits of the approach), and section 5 (Conclusion and outlook).

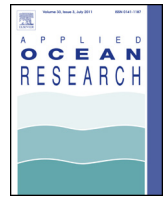
Clemens Hübler is the main author of section 3 (Test examples).

Cristian Guillermo Gebhardt performed a literature review and gave technical and editorial suggestions for improvement of the entire publication.

Raimund Rolfes gave technical and editorial suggestions for improvement of the entire publication and performed the final proofreading.

### Amendment

On page 145, last paragraph, it is stated that the NREL computed the mode shapes of the turbines with ADAMS. In fact, the NREL used BModes for this purpose.



# An improved two-step soil-structure interaction modeling method for dynamical analyses of offshore wind turbines



Jan Häfele\*, Clemens Hübler, Cristian Guillermo Gebhardt, Raimund Rolfes

*Institute of Structural Analysis, Leibniz Universität Hannover, Appelstr. 9a, D-30167 Hannover, Germany*

## ARTICLE INFO

### Article history:

Received 10 September 2015

Received in revised form 2 December 2015

Accepted 4 December 2015

### Keywords:

Soil-structure interaction  
Component-mode-synthesis  
Offshore substructure  
FAST

## ABSTRACT

The detailed modeling of soil-structure interaction is often neglected in simulation codes for offshore wind energy converters. This has several causes: On the one hand, soil models are in general sophisticated and have many degrees of freedom. On the other hand, for very stiff foundations the effect of soil-structure interaction could often be discounted. Therefore, very simple approaches are utilized or the whole structure is assumed to be clamped at the seabed. To improve the consideration of soil-structure interaction, a six-directional, coupled, linear approach is proposed, which contains an implementation of soil-structure interaction matrices in the system matrices of the whole substructure. The aero-hydro-servo-elastic simulation code FAST has been modified for this purpose. Subsequently, a 5 MW offshore wind energy converter with pile foundation is regarded in two examples.

© 2015 Elsevier Ltd. All rights reserved.

## 1. Introduction

According to standards and guidelines (e.g. [1]), the design and certification process of offshore wind energy converters is based on holistic time domain simulations. Therefore, the improvement of simulation techniques is a significant factor in research. With special regard to the foundation, several simulation codes with the ability to represent the dynamic behavior of support structures have been developed and verified in the last decade. Well-known verification efforts are the so called “Offshore Code Comparison Collaboration” (OC3) [2] and “Offshore Code Comparison Collaboration Continuation” (OC4) [3] projects. As there are diverging demands on results, different representations of soil-structure interaction models reaches from complex and non-linear finite element models to simplified  $p$ - $y$ -curves. However, all representations have in common that they add usually many degrees of freedom (DOFs) to the system assembly of an offshore wind energy converter model and time domain simulations are often performed with the structure assumed to be clamped at the seabed, which is in fact a massive simplification.

Zaaijer [4] presents a simplified dynamical model for the foundation of offshore wind turbines and considers the first two flexural frequencies of the structure as indicators of the dynamic response of the whole assembly. The author by means of a detailed analysis shows that the stiffness matrix at the mudline represents the best solution for monopiles. Pinto and Prato [5] developed a

symmetric formulation of the indirect boundary element method for buried frames and show how the formulation could be extended to account rotation of the piles due to combined loads acting on the buried structure. Bienen and Cassidy [6] introduced a software, which allows the analysis of fluid-structure-soil interactions in three dimensions. The authors analyze an offshore structure under combined loads and make the change of the response due to the loading direction and stresses evident. Bhattacharya and Adhikari [7] analyzed the dynamical behavior of wind turbines with monopile foundations, with focus on the soil-structure interaction. The authors validated a theoretical model against finite element calculations as well as against experimental results for some interesting cases and show that the frequencies of the complete system are strongly related to the stiffness of the foundation. AlHamayde and Hussain [8] performed the design optimization of multiple onshore wind towers under consideration of the soil-structure interaction. A detailed three-dimensional finite element model of the tower-foundation-pile system was created and soil springs were included in the model based on soil properties obtained from geotechnical investigations. Finally, the natural frequency from the model was verified against analytical and experimental values of the tower manufacturer. Harte et al. [9] investigated the along-wind forced vibration response of an onshore wind turbine. The study includes the dynamic interaction effects between the foundation and the underlying soil. The soil-structure interaction is shown to affect the response of the wind turbine. This was examined in terms of the turbine structural displacement, the base shear force, and the bending moment in the tower and the foundation. Bisoi and Haldar [10] conducted a comprehensive analysis of an offshore wind turbine structure with monopile foundation. The system was

\* Corresponding author. Tel.: +49 5117624208; fax: +49 5117622236.

modeled using a beam on nonlinear Winkler foundation model, and the soil resistance was modeled using  $p$ - $y$ - and  $T$ - $z$ -curves. The study proves that soil-monopile-tower interaction increases the response of tower and monopile, and the soil nonlinearities increase the system response at higher wind speeds. Damgaard et al. [11] evaluated the formulation and quality of an efficient numerical modeling for the surface foundation of offshore wind turbines, in which the geometrical dissipation related to the wave propagation was accounted. Finally, Damgaard et al. [12] developed a modeling approach to allow the integration of the soil-structure interaction into an aeroelastic software intended for offshore wind turbines by means of the employment of semi-analytical solutions in the frequency domain to include the impedance of the soil-pile system for a given discrete number of frequencies.

This article presents the development of an improved two-step soil-structure interaction modeling method for dynamical analyses of offshore wind turbines, which is fully implemented in FAST. After the definition of a desired operating point the method requires the calculation of the matrices for the soil-structure interaction at first. Secondly, the assembly of the system matrices and the reduction for the substructure representation are performed. The work is partitioned in four further sections: in Section 2 the fundamentals like Component-Mode-Synthesis in FAST, necessary modifications to account soil-structure interaction, derivation of the interaction matrices, and description of the method scheme are described. In Section 3, some results obtained with the current approach are presented and analyzed. Section 4 discusses the benefits and limits of the method. And lastly, in Section 5 some concluding remarks are drawn.

## 2. Fundamentals

As most simulation codes are proprietary, FAST – developed by the National Renewable Energy Laboratory and being open source – has become a well-accommodated code in research. Hence, it is an appropriate basis for the implementation of a new soil-structure interaction approach. Depending on the requests of the user, the structural model of a land-based wind energy converter in FAST comprises up to 23 DOFs, including 9 for the rotor blades (in case of a three-blade-rotor), 4 for rotor-teeter motion, drivetrain, generator and yaw rotation and 10 for tower bending and platform movement. While this limited number of DOFs allows adequate simulation times and qualifies FAST even for optimization applications, the implementation of offshore substructures in the model is challenging, because the dynamical behavior of bottom-fixed multi-member steel structures is commonly computed by FE-method using beam elements with hundreds of nodes and often thousands degrees of freedom. Therefore, a reduction method called Component-Mode-Synthesis has been implemented in FAST, which is based on the work of Craig and Bampton [13]. This reduction method allows an appropriate structural representation with about 5–15 degrees of freedom [14], but in the native implementation it is assumed that there are at least six DOFs as boundary conditions (so called reaction DOFs) to prevent the stiffness matrix from getting singular [15]. Therefore, integrating a soil-structure interaction in the fully assembled system requires an adjustment of the theory.

### 2.1. Component-Mode-Synthesis of multi-member substructures in FAST

The proposed procedure for the reduction of multi-member substructures in FAST [15] is described as under. For further information it is referred to [16].

It is presumed that the equations of motion have been derived within a linear frame finite-element beam model and are on hand in the general form:

$$\mathbf{M}\ddot{\bar{\mathbf{u}}} + \mathbf{C}\dot{\bar{\mathbf{u}}} + \mathbf{K}\bar{\mathbf{u}} = \bar{\mathbf{F}}. \quad (1)$$

In the above equation,  $\mathbf{M}$  is the mass matrix,  $\mathbf{C}$  the damping matrix,  $\mathbf{K}$  the stiffness matrix,  $\bar{\mathbf{u}}$  the displacement vector along all degrees of freedom and  $\bar{\mathbf{F}}$  comprises of the corresponding external forces. Dots represent derivatives with respect to time. In addition, the vector  $\bar{\mathbf{u}}$  is partitioned into the so called vectors of boundary displacements  $\bar{\mathbf{u}}_R$  and interior displacements  $\bar{\mathbf{u}}_L$  in the following way:

$$\bar{\mathbf{u}} = \begin{pmatrix} \bar{\mathbf{u}}_R \\ \bar{\mathbf{u}}_L \end{pmatrix}. \quad (2)$$

It is important to note that the rank of the stiffness matrix in Eq. (1) is lower than its dimension, as no constraints are applied.

Substituting Eq. (2) in (1) yields:

$$\begin{pmatrix} \mathbf{M}_{RR} & \mathbf{M}_{RL} \\ \mathbf{M}_{LR} & \mathbf{M}_{LL} \end{pmatrix} \begin{pmatrix} \ddot{\bar{\mathbf{u}}}_R \\ \ddot{\bar{\mathbf{u}}}_L \end{pmatrix} + \begin{pmatrix} \mathbf{C}_{RR} & \mathbf{C}_{RL} \\ \mathbf{C}_{LR} & \mathbf{C}_{LL} \end{pmatrix} \begin{pmatrix} \dot{\bar{\mathbf{u}}}_R \\ \dot{\bar{\mathbf{u}}}_L \end{pmatrix} + \begin{pmatrix} \mathbf{K}_{RR} & \mathbf{K}_{RL} \\ \mathbf{K}_{LR} & \mathbf{K}_{LL} \end{pmatrix} \begin{pmatrix} \bar{\mathbf{u}}_R \\ \bar{\mathbf{u}}_L \end{pmatrix} = \begin{pmatrix} \bar{\mathbf{F}}_R \\ \bar{\mathbf{F}}_L \end{pmatrix}. \quad (3)$$

$R$  and  $L$  as subscripts indicate the affiliation to the corresponding DOFs. While  $\bar{\mathbf{u}}_L$  is the vector of all remaining interior degrees of freedom, the vector  $\bar{\mathbf{u}}_R$  can be partitioned into the displacements at the interface  $\bar{\mathbf{u}}_{\text{int}}$  and the displacements at the bottom of the structure  $\bar{\mathbf{u}}_{\text{base}}$ :

$$\bar{\mathbf{u}}_R = \begin{pmatrix} \bar{\mathbf{u}}_{\text{int}} \\ \bar{\mathbf{u}}_{\text{base}} \end{pmatrix}. \quad (4)$$

To reduce the size of  $\bar{\mathbf{u}}_L$ , a Ritz transformation is applied and the vector of  $m$  generalized interior coordinates  $\bar{\mathbf{q}}_m$  is obtained:

$$\bar{\mathbf{u}}_L = \Phi \bar{\mathbf{q}}_m. \quad (5)$$

As the boundaries are unaffected, the new vector of displacements  $\bar{\mathbf{u}}$  is

$$\bar{\mathbf{u}} = \begin{pmatrix} \bar{\mathbf{u}}_R \\ \bar{\mathbf{q}}_m \end{pmatrix}. \quad (6)$$

Now, the essential supposition of the Component-Mode-Synthesis is that the matrix  $\Phi$  consists of constraint modes  $\Phi_R$  and fixed-interface normal modes  $\Phi_L$ :

$$\Phi = \begin{pmatrix} \mathbf{I} & \mathbf{0} \\ \Phi_R & \Phi_L \end{pmatrix}. \quad (7)$$

where  $\mathbf{I}$  is the identity matrix and  $\mathbf{0}$  the zero matrix.

Regarding the homogenous, static case (excitation and all derivatives zero) of the rigid body ( $\bar{\mathbf{q}}_m = \bar{\mathbf{0}}$ ) and setting all boundary DOFs to unit displacement, the matrix of constrained modes  $\Phi_R$  can be calculated according to

$$\begin{pmatrix} \mathbf{K}_{RR} & \mathbf{K}_{RL} \\ \mathbf{K}_{LR} & \mathbf{K}_{LL} \end{pmatrix} \begin{pmatrix} \mathbf{I} & \mathbf{0} \\ \Phi_R & \Phi_L \end{pmatrix} \begin{pmatrix} \bar{\mathbf{1}} \\ \bar{\mathbf{0}} \end{pmatrix} = \begin{pmatrix} \bar{\mathbf{0}} \\ \bar{\mathbf{0}} \end{pmatrix}. \quad (8)$$

It follows

$$\Phi_R = -\mathbf{K}_{LL}^{-1} \mathbf{K}_{LR}. \quad (9)$$

The matrix of fixed-interface normal modes  $\Phi_L$  comprises the first  $m$  eigenvectors of the eigenvalue problem:

$$\mathbf{K}_{LL} \Phi_L = \Omega_L^2 \mathbf{M}_{LL} \Phi_L. \quad (10)$$

The Ritz transformation is performed in Eq. (1):

$$\Phi^T \mathbf{M} \Phi \ddot{\mathbf{u}} + \Phi^T \mathbf{C} \Phi \dot{\mathbf{u}} + \Phi^T \mathbf{K} \Phi \mathbf{u} = \Phi^T \bar{\mathbf{F}}. \quad (11)$$

The following is obtained:

$$\begin{pmatrix} \mathbf{M}_{BB} & \mathbf{M}_{Bm} \\ \mathbf{M}_{mB} & \mathbf{I} \end{pmatrix} \begin{pmatrix} \ddot{\mathbf{u}}_R \\ \ddot{\mathbf{q}}_m \end{pmatrix} + \begin{pmatrix} \mathbf{0} & \mathbf{0} \\ \mathbf{0} & 2\xi \Omega_m \end{pmatrix} \begin{pmatrix} \dot{\mathbf{u}}_R \\ \dot{\mathbf{q}}_m \end{pmatrix} + \begin{pmatrix} \mathbf{K}_{BB} & \mathbf{0} \\ \mathbf{0} & \Omega_m^2 \end{pmatrix} \begin{pmatrix} \mathbf{u}_R \\ \mathbf{q}_m \end{pmatrix} = \begin{pmatrix} \bar{\mathbf{F}}_R + \Phi_R^T \bar{\mathbf{F}}_L \\ \Phi_m^T \bar{\mathbf{F}}_L \end{pmatrix} \quad (12)$$

with for example

$$\begin{pmatrix} \mathbf{I} & \Phi_R^T \\ \mathbf{0} & \Phi_m^T \end{pmatrix} \begin{pmatrix} \mathbf{M}_{RR} & \mathbf{M}_{RL} \\ \mathbf{M}_{LR} & \mathbf{M}_{LL} \end{pmatrix} \Phi = \begin{pmatrix} \mathbf{M}_{RR} + \Phi_R^T \mathbf{M}_{LR} & \mathbf{M}_{RL} + \Phi_R^T \mathbf{M}_{LL} \\ \Phi_m^T \mathbf{M}_{LR} & \Phi_m^T \mathbf{M}_{LL} \end{pmatrix} \times \begin{pmatrix} \mathbf{I} & \mathbf{0} \\ \Phi_R & \Phi_m \end{pmatrix} = \begin{pmatrix} \mathbf{M}_{BB} & \mathbf{M}_{Bm} \\ \mathbf{M}_{mB} & \mathbf{I} \end{pmatrix} \quad (13)$$

Therefore, the following applies:

$$\mathbf{M}_{BB} = \mathbf{M}_{RR} + \mathbf{M}_{RL} \Phi_R + \Phi_R^T \mathbf{M}_{LR} + \Phi_R^T \mathbf{M}_{LL} \Phi_R, \quad (14)$$

$$\mathbf{M}_{mB} = \Phi_m^T \mathbf{M}_{LR} + \Phi_m^T \mathbf{M}_{LL} \Phi_m, \quad (15)$$

$$\mathbf{M}_{Bm} = \mathbf{M}_{mB}^T, \quad (16)$$

$$\mathbf{K}_{BB} = \mathbf{K}_{RR} + \mathbf{K}_{RL} \Phi_R. \quad (17)$$

$\Phi_m$  is the truncated subset of  $\Phi_L$  and  $\Omega_m$  the diagonal matrix of the corresponding eigenvalues.  $\xi$  is the critical, viscous damping affecting the fixed-interface normal modes (if scalar, modes are damped proportionally to their corresponding eigen frequency).

The matrix  $\Phi^T \mathbf{K} \Phi$  is singular, because:

$$\det(\Phi^T \mathbf{K} \Phi) = \det \begin{pmatrix} \mathbf{K}_{BB} & \mathbf{0} \\ \mathbf{0} & \Omega_m^2 \end{pmatrix} = \underbrace{\det(\mathbf{K}_{BB})}_{=0} \det(\Omega_m^2) = 0. \quad (18)$$

One possibility to remove the singularity is to apply boundary conditions. The structure is fixed at the bottom. Thus, Eq. (4) is slightly adjusted:

$$\bar{\mathbf{u}}_R = \begin{pmatrix} \bar{\mathbf{u}}_{\text{int}} \\ \bar{\mathbf{0}} \end{pmatrix}. \quad (19)$$

This is applied to Eq. (12), which yields:

$$\begin{pmatrix} \bar{\mathbf{M}}_{BB} & \bar{\mathbf{M}}_{Bm} \\ \bar{\mathbf{M}}_{mB} & \mathbf{I} \end{pmatrix} \begin{pmatrix} \ddot{\bar{\mathbf{u}}}_{\text{int}} \\ \ddot{\bar{\mathbf{q}}}_m \end{pmatrix} + \begin{pmatrix} \mathbf{0} & \mathbf{0} \\ \mathbf{0} & 2\xi \Omega_m \end{pmatrix} \begin{pmatrix} \dot{\bar{\mathbf{u}}}_{\text{int}} \\ \dot{\bar{\mathbf{q}}}_m \end{pmatrix} + \begin{pmatrix} \bar{\mathbf{K}}_{BB} & \mathbf{0} \\ \mathbf{0} & \Omega_m^2 \end{pmatrix} \begin{pmatrix} \bar{\mathbf{u}}_{\text{int}} \\ \bar{\mathbf{q}}_m \end{pmatrix} = \begin{pmatrix} \bar{\mathbf{F}}_{\text{int}} + \Phi_R^T \bar{\mathbf{F}}_L \\ \Phi_m^T \bar{\mathbf{F}}_L \end{pmatrix}. \quad (20)$$

The bar denotes a matrix, where the rows and columns corresponding to the base degrees of freedom have been discarded. In this form the matrix  $\bar{\mathbf{K}}_{BB}$  is not singular any more.

## 2.2. Modifications to consider soil-structure interaction

Now it is supposed that the substructure is not clamped at the seabed, but connected to the soil by inertial and elastical coupling terms. The soil-structure interaction is represented by  $n$  mass and stiffness matrices  $\mathbf{M}_{\text{soil},i}$  and  $\mathbf{K}_{\text{soil},i}$ , respectively. The number of mass and stiffness matrices equals to the number of nodes, where the structure is connected to the ground (base reaction joints). For example, the soil-structure interaction of a monopile foundation is represented by one set of mass and stiffness matrices ( $n = 1$ ), a four-legged jacket needs four sets ( $n = 4$ ). Moreover, the matrices  $\mathbf{K}_{\text{soil},i}$  are assumed to be positive definite, and  $\mathbf{M}_{\text{soil},i}$  positive semidefinite. The dimension of these matrices is  $6 \times 6$ , because each node of the structure has six DOFs, three translational and three rotational. There are no other restrictions.

Origin of the following considerations is again Eq. (3). Changes are only made concerning the partition of the DOFs, in particular:

$$\bar{\mathbf{u}}_R^* = \bar{\mathbf{u}}_{\text{int}}, \quad (21)$$

$$\bar{\mathbf{u}}_L^* = \begin{pmatrix} \bar{\mathbf{u}}_I \\ \bar{\mathbf{u}}_{\text{base}} \end{pmatrix}, \quad (22)$$

with

$$\bar{\mathbf{u}}_{\text{base}} = \begin{pmatrix} u_{\text{base},1} \\ \vdots \\ u_{\text{base},6n} \end{pmatrix}. \quad (23)$$

A star denotes changes due to the implementation of soil-structure interaction. The vector  $\bar{\mathbf{u}}_I$  comprises all other (interior) DOFs except those at the base. The following is obtained from the new partition:

$$\mathbf{M}_{LL}^* = \begin{pmatrix} \mathbf{M}_I & \mathbf{M}_{I,\text{base}} \\ \mathbf{M}_{\text{base},I} & \mathbf{M}_{\text{base}} \end{pmatrix}, \quad (24)$$

$$\mathbf{K}_{LL}^* = \begin{pmatrix} \mathbf{K}_I & \mathbf{K}_{I,\text{base}} \\ \mathbf{K}_{\text{base},I} & \mathbf{K}_{\text{base}} \end{pmatrix}. \quad (25)$$

As the soil-structure interaction is of interest, the matrices  $\mathbf{M}_{\text{base}}$  and  $\mathbf{K}_{\text{base}}$  contain the terms from the structural system assembly  $\mathbf{M}_{\text{base},ij}$  and  $\mathbf{K}_{\text{base},ij}$  and the soil terms from the  $n$  mass and stiffness matrices  $\mathbf{M}_{\text{soil},i}$  and  $\mathbf{K}_{\text{soil},i}$  on the main diagonal:

$$\mathbf{M}_{\text{base}} = \begin{pmatrix} \mathbf{M}_{\text{base},11} + \mathbf{M}_{\text{soil},1} & \cdots & \mathbf{M}_{\text{base},1n} \\ \vdots & \ddots & \vdots \\ \mathbf{M}_{\text{base},n1} & \cdots & \mathbf{M}_{\text{base},nn} + \mathbf{M}_{\text{soil},n} \end{pmatrix}, \quad (26)$$

$$\mathbf{K}_{\text{base}} = \begin{pmatrix} \mathbf{K}_{\text{base},11} + \mathbf{K}_{\text{soil},1} & \cdots & \mathbf{K}_{\text{base},1n} \\ \vdots & \ddots & \vdots \\ \mathbf{K}_{\text{base},n1} & \cdots & \mathbf{K}_{\text{base},nn} + \mathbf{K}_{\text{soil},n} \end{pmatrix}, \quad (27)$$

and finally

$$\begin{pmatrix} \mathbf{M}_{RR}^* & \mathbf{M}_{RL}^* \\ \mathbf{M}_{LR}^* & \mathbf{M}_{LL}^* \end{pmatrix} \begin{pmatrix} \bar{\mathbf{u}}_R^* \\ \bar{\mathbf{u}}_L^* \end{pmatrix} + \begin{pmatrix} \mathbf{C}_{RR}^* & \mathbf{C}_{RL}^* \\ \mathbf{C}_{LR}^* & \mathbf{C}_{LL}^* \end{pmatrix} \begin{pmatrix} \dot{\bar{\mathbf{u}}}_R^* \\ \dot{\bar{\mathbf{u}}}_L^* \end{pmatrix} + \begin{pmatrix} \mathbf{K}_{RR}^* & \mathbf{K}_{RL}^* \\ \mathbf{K}_{LR}^* & \mathbf{K}_{LL}^* \end{pmatrix} \begin{pmatrix} \bar{\mathbf{u}}_R^* \\ \bar{\mathbf{u}}_L^* \end{pmatrix} = \begin{pmatrix} \bar{\mathbf{F}}_R^* \\ \bar{\mathbf{F}}_L^* \end{pmatrix}. \quad (28)$$

The further procedure can be adapted from equations (5) to (10) and results in:

$$\begin{pmatrix} \mathbf{M}_{BB}^* & \mathbf{M}_{Bm}^* \\ \mathbf{M}_{mB}^* & \mathbf{I} \end{pmatrix} \begin{pmatrix} \bar{\mathbf{u}}_{\text{int}} \\ \bar{\mathbf{q}}_m^* \end{pmatrix} + \begin{pmatrix} \mathbf{0} & \mathbf{0} \\ \mathbf{0} & 2\xi\boldsymbol{\Omega}_m^* \end{pmatrix} \begin{pmatrix} \bar{\mathbf{u}}_{\text{int}} \\ \bar{\mathbf{q}}_m^* \end{pmatrix} + \begin{pmatrix} \mathbf{K}_{BB}^* & \mathbf{0} \\ \mathbf{0} & \boldsymbol{\Omega}_m^{*2} \end{pmatrix} \begin{pmatrix} \bar{\mathbf{u}}_{\text{int}} \\ \bar{\mathbf{q}}_m^* \end{pmatrix} = \begin{pmatrix} \bar{\mathbf{F}}_{\text{int}} + \boldsymbol{\Phi}_R^{*T} \bar{\mathbf{F}}_L^* \\ \boldsymbol{\Phi}_m^{*T} \bar{\mathbf{F}}_L^* \end{pmatrix}. \quad (29)$$

The comparison to Eq. (20) shows that some terms can be carried over from the fixed interface structure:

$$\mathbf{M}_{BB}^* = \mathbf{M}_{RR}^* + \mathbf{M}_{RL}^* \boldsymbol{\Phi}_R^* + \boldsymbol{\Phi}_R^{*T} \mathbf{M}_{LR}^* + \boldsymbol{\Phi}_R^{*T} \mathbf{M}_{LL}^* \boldsymbol{\Phi}_R^*, \quad (30)$$

$$\mathbf{M}_{mB}^* = \boldsymbol{\Phi}_m^{*T} \mathbf{M}_{LR}^* + \boldsymbol{\Phi}_m^{*T} \mathbf{M}_{LL}^* \boldsymbol{\Phi}_m^*, \quad (31)$$

$$\mathbf{M}_{Bm}^* = \mathbf{M}_{mB}^{*T}, \quad (32)$$

$$\mathbf{K}_{BB}^* = \mathbf{K}_{RR}^* + \mathbf{K}_{RL}^* \boldsymbol{\Phi}_R^*. \quad (33)$$

### 2.3. Derivation of Soil-Structure Interaction System Matrices

The same properties (structural as well as soil) are presumed for all piles in case of foundations with more than one pile, for example jackets. However, the approach would allow the analysis of different piles, too.

To determine the system matrices of soil-structure interaction  $\mathbf{M}_{\text{soil}}$  and  $\mathbf{K}_{\text{soil}}$  (the index  $i$  has been dropped due to the above mentioned presumption), the corresponding pile is modeled with linear beam elements in ANSYS – of course another FE-solver would also be applicable. It is assembled with spring elements in all spatial coordinate directions along its length. The stiffnesses for the  $p$ - $y$ - and  $T$ - $z$ -curves are computed according to API [17]. As the system will be linearized in the next step, the operating point has to be chosen. No ultimate limit state is regarded in the examples load cases, hence a linearization in the neutral-deflection state is selected. Afterwards, the whole dynamic system behavior is condensed in the pile head or the uppermost point, respectively. The reduction method of Guyan [18] is utilized for this purpose. As the  $p$ - $y$ - and  $T$ - $z$ -curves do not specify a torsional stiffness  $k_\psi$ , a simple approach according to Georgiadis and Saflekou [19] is used to calculate the initial torsional stiffness. This yields the matrices for the soil-structure interaction in the following form:

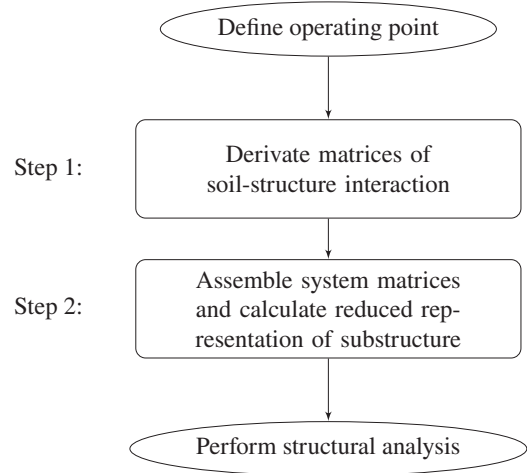
$$\mathbf{M}_{\text{soil}} = \begin{pmatrix} m_x & 0 & 0 & 0 & -m_{x\vartheta} & 0 \\ 0 & m_y & 0 & m_{y\varphi} & 0 & 0 \\ 0 & 0 & m_z & 0 & 0 & 0 \\ 0 & m_{y\varphi} & 0 & m_\varphi & 0 & 0 \\ -m_{x\vartheta} & 0 & 0 & 0 & m_\vartheta & 0 \\ 0 & 0 & 0 & 0 & 0 & m_\psi \end{pmatrix}, \quad (34)$$

$$\mathbf{K}_{\text{soil}} = \begin{pmatrix} k_x & 0 & 0 & 0 & -k_{x\vartheta} & 0 \\ 0 & k_y & 0 & k_{y\varphi} & 0 & 0 \\ 0 & 0 & k_z & 0 & 0 & 0 \\ 0 & k_{y\varphi} & 0 & k_\varphi & 0 & 0 \\ -k_{x\vartheta} & 0 & 0 & 0 & k_\vartheta & 0 \\ 0 & 0 & 0 & 0 & 0 & k_\psi \end{pmatrix}. \quad (35)$$

The coordinates  $x$ ,  $y$ , and  $z$  are defined according to the commonly used coordinate system defined by Germanischer Lloyd [20]. The corresponding rotational DOFs around  $x$ ,  $y$ , and  $z$  are  $\varphi$ ,  $\vartheta$ , and  $\psi$ . The values of the parameters for each corresponding test case are given in Table 1.

**Table 1**  
Soil parameters for the different foundation types regarded in the examples.

	$m_x$ [kg]	$m_y$ [kg]	$m_z$ [kg]	$m_\varphi$ [kg m <sup>2</sup> ]
OC3 monopile	$5.81 \times 10^4$	$5.81 \times 10^4$	$9.84 \times 10^4$	$7.34 \times 10^5$
OC4 jacket	$1.25 \times 10^4$	$1.25 \times 10^4$	$3.22 \times 10^4$	$5.59 \times 10^4$
	$m_\vartheta$ [kg m <sup>2</sup> ]	$m_\psi$ [kg m <sup>2</sup> ]	$m_{x\vartheta}$ [kg m]	$m_{y\varphi}$ [kg m]
OC3 monopile	$7.34 \times 10^5$	$2.79 \times 10^6$	$1.50 \times 10^5$	$1.50 \times 10^5$
OC4 jacket	$5.59 \times 10^4$	$1.38 \times 10^5$	$2.14 \times 10^4$	$2.14 \times 10^4$
	$k_x$ [N m <sup>-1</sup> ]	$k_y$ [N m <sup>-1</sup> ]	$k_z$ [N m <sup>-1</sup> ]	$k_\varphi$ [N m]
OC3 monopile	$1.30 \times 10^9$	$1.30 \times 10^9$	$8.33 \times 10^9$	$1.47 \times 10^{11}$
OC4 jacket	$3.56 \times 10^8$	$3.56 \times 10^8$	$2.91 \times 10^9$	$1.20 \times 10^{10}$
	$k_\vartheta$ [N m]	$k_\psi$ [N m]	$k_{x\vartheta}$ [N]	$k_{y\varphi}$ [N]
OC3 monopile	$1.47 \times 10^{11}$	$1.63 \times 10^{11}$	$1.05 \times 10^{10}$	$1.05 \times 10^{10}$
OC4 jacket	$1.20 \times 10^{10}$	$2.45 \times 10^{10}$	$1.62 \times 10^9$	$1.62 \times 10^9$



**Fig. 1.** Scheme of two-step-method for consideration of soil-structure interaction.

### 2.4. Method scheme

The proposed method requires a two-step pre-processing procedure according to Fig. 1: to assemble the system matrices, the mass and stiffness matrices of soil-structure interaction have to be evaluated at first. In other words, in contrast to most of the approaches for consideration of soil-structure interaction in literature the operating point has to be determined beforehand. This implies that the soil-structure interaction behavior has to be evaluated multiply, too. Subsequently, for every load case the appropriate soil matrices can be chosen.

### 3. Test examples

The new six-directional, linear approach for the implementation of soil-structure interaction that has been proposed is tested for two different configurations of the 5-MW NREL wind turbine [21]. At first, the OC3 monopile [2] with a flexible foundation is analyzed. Secondly, the new approach is tested for the OC4 jacket [22]. All calculations are conducted with the FASTv8-code [23] which has been recently verified [24] by the “National Renewable Energy Laboratory” (NREL). The FASTv8-code differs from older FAST versions by being totally modularized which makes it more flexible and robust. Hereinafter, FASTv8 is always meant if FAST is used.<sup>1</sup> The

<sup>1</sup> The FAST version v8.10.00a-bjj is the basis for all calculations.



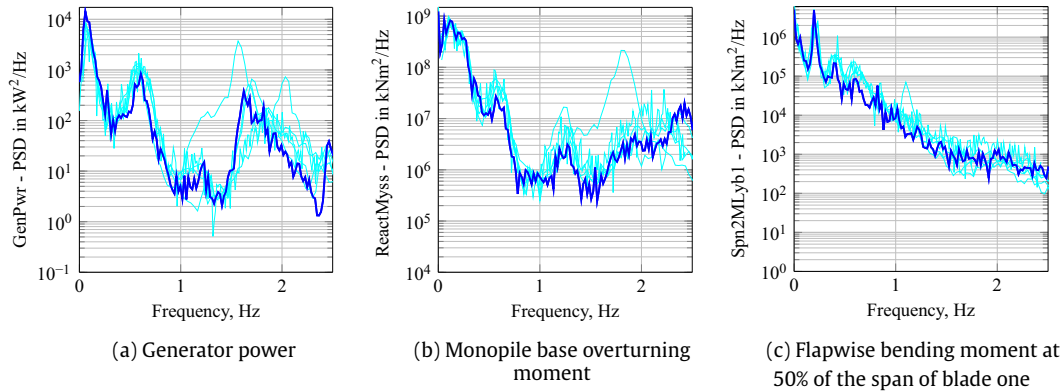


Fig. 2. Power spectral densities from load case 5.3 for OC3-monopile of FAST (—) and others (—).

wind-fields are computed externally with TurbSim [25] whereas the waves are calculated within FAST itself. As a new type of foundation is implemented, the eigenmodes of the tower change. To calculate the eigenmodes, the application BModes of the NREL [26] is used together with a sixth degree best fit polynomial approach.

The verification is focused on the differences between rigid foundations and the soil-structure interaction. To exclude the influences of the overall aero-hydro-servo-elastic simulation code FAST and its implementation, the coupling of FAST and BModes has to be tested primarily. Therefore, test cases with rigid foundation are conducted firstly. These calculations assure that possible differences are results of the soil-structure interaction and not due to slightly deviating input values, a different calculation method of the tower eigenmodes and the wind field or the FAST code itself.

The best possibility of verifying aero-hydro-servo-elastic simulation codes are the offshore code-comparison tasks OC3 [2] and OC4 [3]. Therefore, the results of FAST with rigid foundations are compared with OC3 in case of the monopile and with OC4 for the jacket. For both configurations one load case is chosen to show the good accordance of the FAST results with different codes.

For the monopile OC3 load case 5.3 is selected. For this load case all degrees of freedom are enabled. A turbulent wind-field with a mean hub wind speed of  $V_{hub} = 18.0$  m/s and irregular waves with a significant wave height  $H_s = 6$  m and a peak-spectral period  $T_p = 10$  s are applied. The corresponding OC4 load case 5.7 with a turbulent wind-field with  $V_{hub} = 18.0$  m/s and irregular waves with a significant wave height  $H_s = 6$  m and a peak-spectral period  $T_p = 10$  s is used for the jacket tests. For detailed descriptions of the load cases it is referred to Jonkman et al. [2] and Vorpahl and Popko [27]. Details on modeling parameters of FAST and differences between

the original load cases and the applied load cases like a lack of wave-stretching were described by Barahona et al. [24].

Fig. 2(a)–(c) shows the power spectral densities for the generator power, the base overturning moment and the flapwise bending moment at 50% of the span of blade one for the monopile in load case 5.3. It has to be highlighted, that the overall agreement between the different codes is very good and the FAST results always follow the trend of the other codes.

The results for the jacket and load case 5.7 are illustrated in Fig. 3. All power spectral densities are in good agreement with the other codes of OC4. Especially for lower frequencies the congruence is quite exact. For higher frequencies all codes show some differences, but as they occur at higher frequencies these discrepancies do not present a problem. Furthermore, it is a general problem that the agreements between lower frequencies are much better than at higher frequencies. The peaks around 0 Hz of the OC4 results, that are out of the y-axis scale, are a consequence of the non-zero mean values of the data in OC4. Together with a smoothing of the spectra this leads to the peaks close to 0 Hz. These peaks do not occur in all other results as corresponding signals are zero mean.

Although, there are discrepancies among the reported results, all these remain bounded by a well defined margin and FAST shows a good agreement with the general characteristics previously documented. Therefore, the following calculations concerning the new soil-structure interaction are feasible. Before analyzing the outcomes of the soil-structure interaction, the impact of changed mode shapes of the tower is investigated. This has to be done for two reasons: firstly, the tower eigenmodes are calculated differently in the proposed approach and by the NREL. Here BModes is used whereas the NREL calculates the mode shapes with ADAMS.

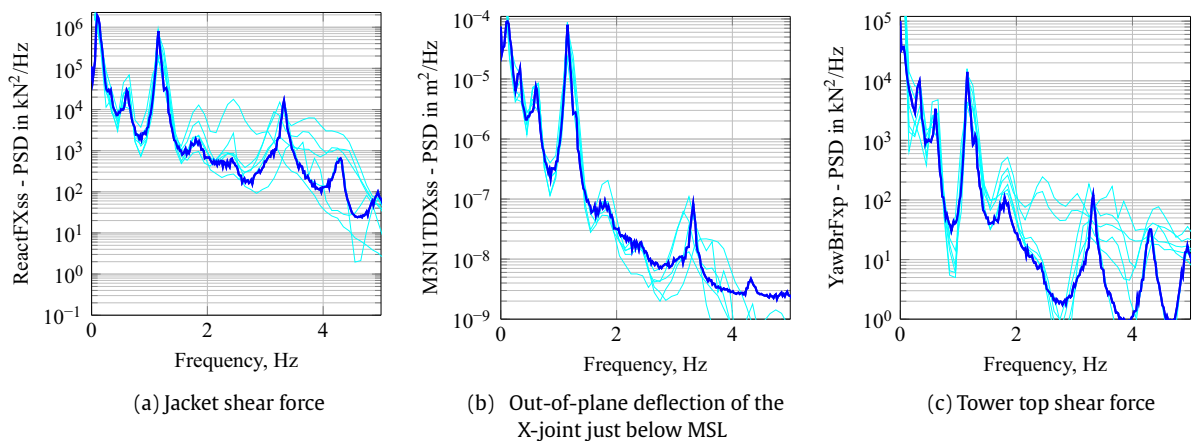


Fig. 3. Power spectral densities from load case 5.7 for OC4-jacket of FAST (—) and others (—).

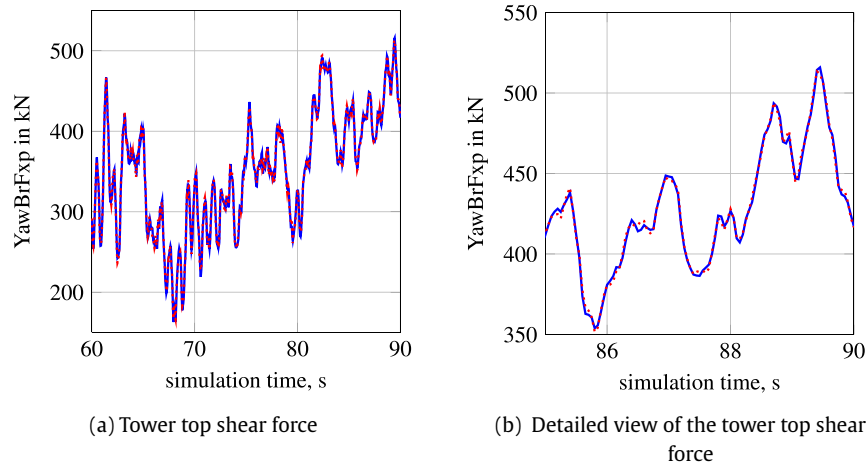


Fig. 4. Time plots from load case 5.7 for the OC4-jacket with tower mode shapes calculated originally by the NREL (—) and with BModes (- - -).

Secondly, the tower mode shapes change when the foundation is modified. Therefore, the influence of slightly different eigenmodes has to be investigated. In FAST only the first two side-to-side and fore-aft mode shapes are considered in the structural model of the tower. The first eigenmodes are nearly the same independent of the foundation type and the calculation type. The second mode shapes show partly significant differences. It has to be mentioned that only one type of soil was examined and this was the soil of OC3 [2]. For very soft soil conditions it can be assumed, that the differences become more relevant. However, for these inputs there are no significant changes in the overall results, because the influence of the second mode shapes of the tower is quite small. A detailed examination of the effect of the soil properties on mode shapes of the tower is not regarded here. The negligible variation of the results for this type of soil is shown in Fig. 4(a) using the example of the tower top shear force in load case 5.7. The OC4 jacket is used with the originally calculated tower mode shapes by NREL with ADAMS and with the new calculated modes shapes with BModes. In Fig. 4(b) a scaled up version can be seen, where there are nearly no differences. If at all there are small high-frequency changes correlated to the second tower mode shapes. In case of comparing results of soil-structure calculations with original NREL tower mode shapes to results with the new calculated ones the differences are similarly small which is why no further details are given.

State-of-the-art is to model the foundation of offshore wind turbines as rigid. This is an oversimplification for some applications. Therefore, there have been already some investigations of flexible foundations for monopiles in OC3 for some codes [2]. However, until now the FAST code is not capable of simulating flexible foundations. This is the starting point of the present work. The new soil-structure feature removes the drawback of a rigid foundation of FAST. This improvement of the simulation code FAST offers the opportunity to model offshore wind turbines more realistic and accurate. The following two examples illustrate the potential of this approach.

### 3.1. Monopile foundation

Results of FAST with flexible foundation are presented for the OC3 monopile in this subsection. These outcomes are compared with the results of OC3 to validate the new soil-structure interaction for FAST. Furthermore, a very rudimentary approach of modeling flexible foundations is considered as well. It is the approach of an apparent fixity length. For this method the monopile

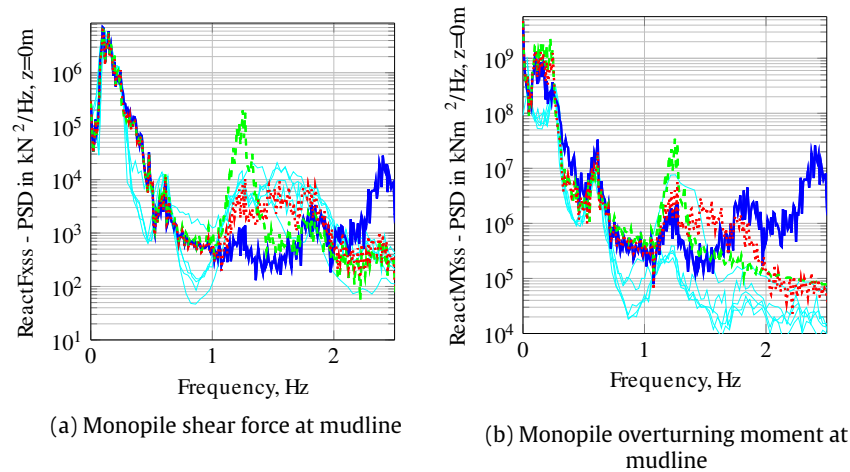
remains clamped; it is not clamped at mudline, but at a fictive point below the mudline in order to fake a flexible foundation. For the length of the pile below the mudline a value of four times the diameter of the pile is applied for the monopile according to [4].

Two different load cases are analyzed. Both are taken from the OC3 report. The first load case focuses on the substructure by disabling the degrees of freedom of the drivetrain and the blades. Furthermore, there is no wind and the air density is zero. Only wave loads are applied with an irregular wave spectrum with a significant wave height  $H_s = 6$  m and a peak-spectral period  $T_p = 10$  s. This represents load case 4.2 of the OC3 project. The second load case is load case 5.2 with turbulent wind conditions and irregular waves. It is similar to 5.3, but with  $V_{hub} = 11.4$  m/s. The consideration of these two different load cases allows to analyze more easily the influences of the soil-structure interaction. As in load case 4.2 the degrees of freedom of the blades are disabled and the air density is zero, no aerodynamic damping occurs and there is no coupling of the blades and the substructure. That is why, it is beneficial to consider both load cases.

Fig. 5 shows the power spectral densities of load case 5.2 for the monopile shear force and bending moment at mudline. It can be seen that on the whole the results of the new soil-structure interaction model correspond very well with the results of OC3, especially in the case of the shear force. The second natural frequencies of the support structure, which are at about 2.4 Hz for the rigid foundation, are shifted to about 1.5 Hz for the flexible foundation. The peak of the second eigenfrequencies of the support structure interferes with the peak of edgewise blade mode shapes at about 1.2 Hz and the second asymmetric modes at about 1.7 Hz. This leads to a blurred peak between 1.2 Hz and 1.8 Hz. In contrast to this, the apparent fixity length solution shows a distinct peak at 1.2 Hz. This is a result of an overestimation of the flexible foundation. In this case the second eigenfrequencies of the support structure are shifted even further to 1.2 Hz and superpose with the edgewise blade mode shapes. This result emphasizes the importance of a good estimation of the flexibility of the foundation. As shown, this estimation can be provided by this soil-structure interaction approach. Hence, the present work enhances the state-of-the-art modeling of off-shore wind turbines.

As already mentioned, the analysis of an easier load case without air, wind or blade-modes can be valuable. Hence, Fig. 6 shows the monopile shear force at mudline. It is quite noticeable that the results show less congruence. This was already investigated in the OC3 project. Hence, there has to be future research on the influence

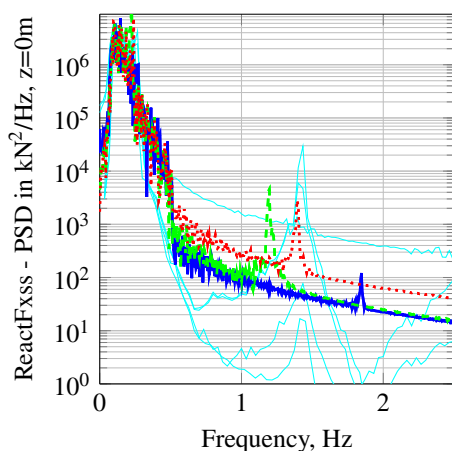




**Fig. 5.** Power spectral densities from load case 5.2 for OC3-monopile with different foundations: clamped (—), apparent length (—), new soil-structure interaction (- - -), others of OC3 (—).

of aerodynamic damping on the power spectral densities of shear forces and overturning moments that are calculated with different simulation codes. Nevertheless, the shift in the second natural frequencies of the substructure can be identified more directly. As no other modes interfere with the support structure mode shapes, the power spectral densities only show peaks of the mode shapes of the support structure. That is why, it becomes clear that FAST with the new soil-structure interaction predicts the same reduction of second natural frequencies than other codes. The apparent fixity length approach overestimates this shift. This leads to the distinctive peaks in Fig. 5 at about 1.2 Hz and 1.4 Hz for the apparent fixity length and new approach respectively. A shift of the first natural frequency of the substructure, as predicted in OC3, cannot be found as the differences are much smaller than for the second frequency. A direct calculation of natural frequencies which would probably allow a detection of this shift is not yet available for FAST.

Overall the new soil-structure interaction is definitely in good congruence with other codes and enables FAST to calculate flexible foundations easily with nearly no additional computational cost. Furthermore, the soil-structure interaction is not limited to monopile. Therefore, results of a jacket substructure with flexible foundation are presented in the next subsection.



**Fig. 6.** Power spectral density of the shear force at mudline from load case 4.2 for OC3-monopile with different foundations: clamped (—), apparent length (—), new soil-structure interaction (- - -), others of OC3 (—).

### 3.2. Jacket with pile foundation

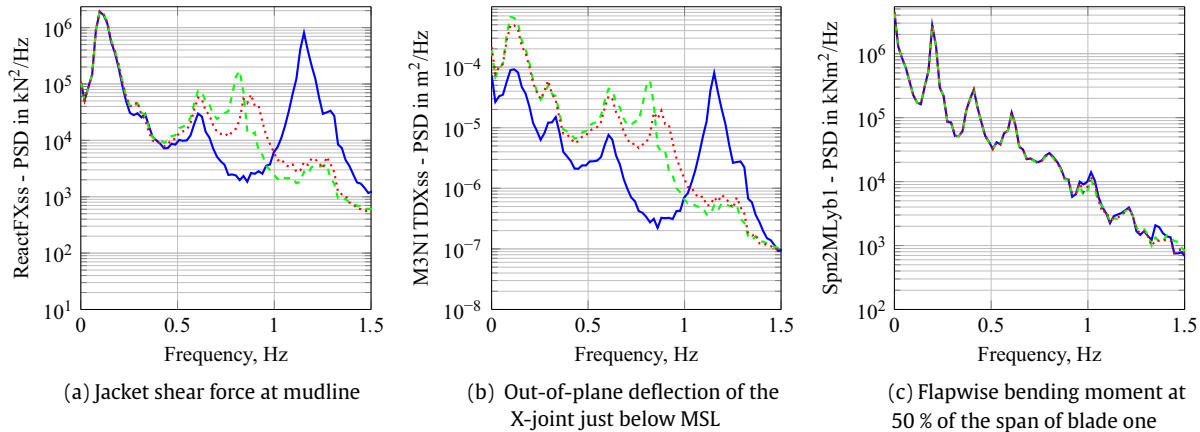
Monopiles are typically used for water depths less than 30m. As many sites of wind turbines are in deeper water conditions other types of support structures come in focus of research. However, flexible foundations have only been studied for monopiles so far. The new approach is not limited to monopiles. Therefore, this subsection presents results of calculations with the OC4 jacket and a flexible foundation. The outcomes are compared with the rigid foundation and again with the rudimentary approach of an apparent fixity length. The value of the apparent fixity length is chosen to be six times the diameter as it has to be greater for substructures like jackets or tripods compared with monopiles [4]. A comparison to other codes is not possible as there no such results available to the authors' knowledge. This lack of documented data results from the limitation to monopiles of current approaches. As the present approach is not limited to any type of foundation, it is now possible to produce results for jackets with flexible foundations. Given that the results for the monopile are in good agreement with other codes and the FAST-code is validated for jackets with rigid foundations it can be assumed that results for the jacket are generally valid as well.

For the analysis of the flexible jacket two load cases are considered. One load case with all degrees of freedom enabled and one which focuses on the substructure. The major parameters are summarized in Table 2. For further details it is referred to [27,24].

At first, the results of the fully enabled wind turbine with turbulent wind and irregular waves are presented. Fig. 7 shows three different power spectral densities for this load case. The new flexible foundation is compared with the rigid foundation and an apparent length version. Fig. 7(a) indicates clearly the shift of the second natural frequencies of the support structure from about 1.2 Hz and 1.3 Hz to about 0.9 Hz. The lower one is the fore-aft mode and the higher one the side-to-side mode. The shift for the apparent length version is slightly higher. An apparent length of six times the diameter seems to overestimate the effect of a flexible foundation for a jacket structure for this type of soil and this penetration depth, as it was already the case for the monopile. Another effect of the flexible foundation can be identified in Fig. 7(b). In addition to the shift of natural frequencies of the substructure all values of the out-of-plane deflection of the X-joint just below mean sea level are higher for the flexible foundation. For the exact position of the X-joint it is referred to [22]. The amplitude of oscillation is higher for a flexible foundation over all frequencies. This effect is forecast by the apparent length approach as well. Furthermore, a small

**Table 2**  
OC4 load cases applied on flexible jacket substructure.

Load case	Enabled DoFs	Wind conditions	Wave conditions
4.5	Substructure, tower	$\rho_{air} = 0 \text{ kg/m}^2$	Irregular: $H_s = 6 \text{ m}$ , $T_p = 10 \text{ s}$ .
5.7	All	Turbulent: $V_{hub} = 18 \text{ m/s}$ $I_{ref} = 0.14$	Irregular: $H_s = 6 \text{ m}$ , $T_p = 10 \text{ s}$ .



**Fig. 7.** Power spectral densities from load case 5.7 for OC4-jacket with different foundations: clamped (—), apparent length (---), new soil-structure interaction (····).

but recognizable change of the first natural frequencies of the support structure is shown. Fig. 7(c) clarifies that there is no significant impact of the soil-structure interaction on the blades.

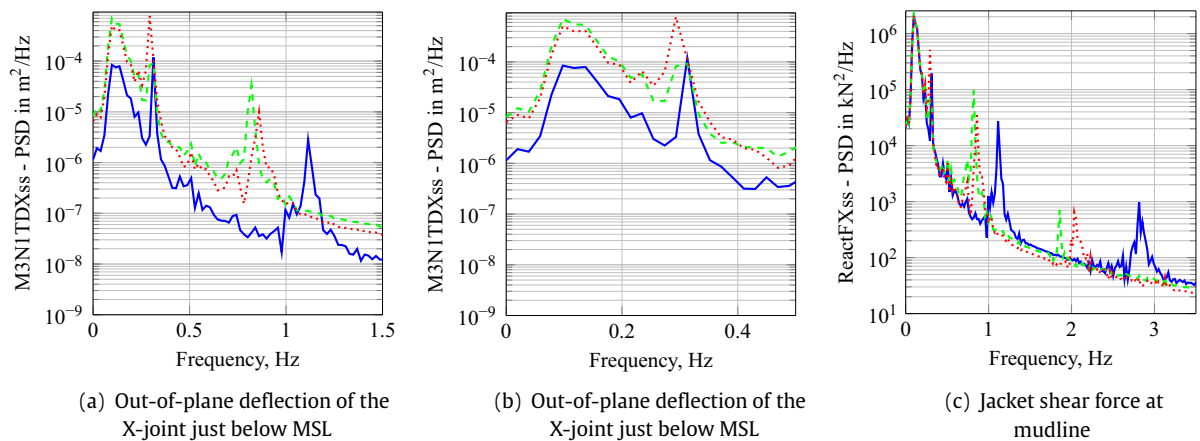
Load case 4.5 focuses on the substructure and excludes aerodynamic damping. Therefore, some phenomena can be identified more easily. Fig. 8 shows relevant power spectral densities. The out-of-plane displacement in Fig. 8(a) clearly shows the shift in the second natural frequencies and the higher values over all frequencies. A shift in the first natural frequency is slightly visible, too. Therefore, Fig. 8(b) displays the same parameter but a smaller range of frequencies. Now, it has become apparent that the first eigenfrequencies is reduced from about 0.31 Hz to about 0.29 Hz. Fig. 8(c) shows the shear force at mudline up to higher frequencies, which offers the possibility to analyze higher substructure modes as well. In case of the rigid foundation, there is another natural frequency at about 2.8 Hz. With the new flexible approach this is shifted by about 30%. However, it remains questionable whether the shift in the higher frequencies is of great

importance. It can be seen in Fig. 8(c) that the peaks of the higher natural frequencies are less distinct especially for the new soil-structure interaction approach. This follows from the much higher displacements over all frequencies that lead to more hydrodynamic damping.

**4. Benefits and limits of the approach**

A new soil-structure interaction approach has been derived and implemented in FAST. Afterwards, two examples for different types of foundations have been presented to demonstrate the benefits of this method. In this section the benefits, but also the limitations of the approach are summarized and clarified.

The major advantage of the present work is that flexible foundations can be modeled more accurately. No clamped connection to the seabed has to be assumed anymore. This fact leads to three main improvements. Firstly, a shift of the eigenfrequencies of the support structure to more realistic values can be observed. Secondly, this



**Fig. 8.** Power spectral densities from load case 4.5 for OC4-jacket with different foundations: clamped (—), apparent length (---), new soil-structure interaction (····).

shift results in changed interactions between different eigenmodes. The resulting forces and moments can be influenced by these interactions in both directions dependent on whether the interactions are intensified or weakened. Thirdly, higher, more realistic overall deflections can be achieved.

However, there have been different approaches to model soil-structure interaction beforehand. But, the proposed approach does not rely on a particular foundation type, because it needs condensed mass and stiffness information at the interface between substructure and foundation. Examples for monopiles and jackets with piles have been given. Certainly, nowadays pile foundations are state-of-the-art. Nevertheless, this approach is not restricted to piles and can be used for buckets or other foundation types with considerable soil-structure interaction behavior as well. Moreover, it does not add necessarily DOFs to the structural model of the substructure. However, it might be appropriate to increase the number of DOFs to regard the full modal behavior of the substructure with soil-structure interaction. The simulation of the soil-structure interaction does not increase the computing time significantly and is convenient for simulations with high demands on numerical efficiency.

Another advantage is the independence of the approach of the reduction technique used to evaluate the mass and stiffness matrices. Different numerical models or even experimental data can be used as possible input matrices. However, these condensed mass and stiffness matrices represent the main limitation of the method as well. The proposed method is limited to linear or at least linearized soil-structure interaction. Thus, if the nonlinear behavior or different operating points are in the focus of the analysis, an extension of the current approach might be more suitable. Furthermore, a specific handling of damping has not been discussed, but could also be included in further analyses.

## 5. Conclusion and outlook

An approach that allows a numerically efficient implementation of soil-structure interaction in simulations of offshore wind energy converters has been proposed. Two test cases including a monopile foundation and a jacket substructure with pile foundation have been analyzed and compared to the results of the OC3 and OC4 projects. The results are in good accordance with previous studies. For jacket substructures, which have not been analyzed before, valid results were achieved. It is apparent that the consideration of even simple soil-structure interaction in time domain simulations enhances the results, while the computational overhead compared to a clamped structure is quite low. This consideration is even more relevant, as the significant shift in substructure eigenvalues, which has been observed, leads to modified interactions between different modes.

While the approach has been implemented in the open source simulation code FAST, it might be adapted to other codes as well. Furthermore, it can be easily adjusted to other types of foundations and is not restricted to piles. In addition, it is possible to improve the calculation of the soil matrices by replacing the Guyan reduction [18] with a more accurate reduction method (which adds presumably more DOFs to the model). The neutral-deflection point of the soil has been used here to generate the linearized system matrices. Other more sophisticated soil-models, which incorporate for example the operation point of the turbine and regard load dependent stiffnesses will be enhancing as well.

## Acknowledgements

We gratefully acknowledge the financial support of the German Federal Ministry for Economic Affairs and Energy (research

project GIGAWIND LIFE, FKZ 0325575A) and the European Commission (research projects IRPWIND and INNWIND.EU, funded from the European Union's Seventh Framework Programme for research, technological development and demonstration under grant agreement numbers 609795 and 308974) that enabled this work.

## Appendix A. Supplementary data

Supplementary data associated with this article can be found, in the online version, at <http://dx.doi.org/10.1016/j.apor.2015.12.001>.

## References

- [1] International Electrotechnical Commission. Wind turbines – part 3: design requirements for offshore wind turbines; 2009. Standard IEC-61400-3:2009, EN 61400-3:2009.
- [2] Jonkman J, Musial W. Offshore Code Comparison Collaboration (OC3) for IEA Task 23 Offshore Wind Technology and Deployment, Tech. Rep. NREL/TP-5000-48191. National Renewable Energy Laboratory; 2010.
- [3] Popko W, Vorpahl F, Zuga A, Kohlmeier M, Jonkman J, Robertson A, et al. Offshore Code Comparison Collaboration Continuation (OC4), phase I - results of coupled simulations of an offshore wind turbine with jacket support structure. *J Ocean Wind Energy* 2014;1(1):1–11.
- [4] Zaaier M. Foundation modelling to assess dynamic behaviour of offshore wind turbines. *Appl Ocean Res* 2006;(28):45–57, <http://dx.doi.org/10.1016/j.apor.2006.03.004>.
- [5] Pinto F, Prato CA. Three-dimensional indirect boundary element method formulation for dynamic analysis of frames buried in semiinfinite elastic media. *J Eng Mech* 2006;132(9):967–78, [http://dx.doi.org/10.1061/\(ASCE\)0733-9399\(2006\)132:9\(967\)](http://dx.doi.org/10.1061/(ASCE)0733-9399(2006)132:9(967)).
- [6] Bienen B, Cassidy M. Advances in the three-dimensional fluid-structure-soil interaction analysis of offshore jack-up structures. *Mar Struct* 2006;19(2–3):110–40, <http://dx.doi.org/10.1016/j.marstruc.2006.09.002>.
- [7] Bhattacharya S, Adhikari S. Experimental validation of soil-structure interaction of offshore wind turbines. *Soil Dyn Earthq Eng* 2011;31(5–6):805–16, <http://dx.doi.org/10.1016/j.soildyn.2011.01.004>.
- [8] AlHamaydeh M, Hussain S. Optimized frequency-based foundation design for wind turbine towers utilizing soil-structure interaction. *J Franklin Inst* 2011;348(7):1470–87, <http://dx.doi.org/10.1016/j.jfranklin.2010.04.013>.
- [9] Harte M, Basu B, Nielsen S. Dynamic analysis of wind turbines including soil-structure interaction. *Eng Struct* 2012;45:509–18, <http://dx.doi.org/10.1016/j.engstruct.2012.06.041>.
- [10] Bisoi S, Haldar S. Dynamic analysis of offshore wind turbine in clay considering soil-monopile-tower interaction. *Soil Dyn Earthq Eng* 2014;63:19–35, <http://dx.doi.org/10.1016/j.soildyn.2014.03.006>.
- [11] Damgaard M, Andersen L, Ibsen L. Computationally efficient modelling of dynamic soil-structure interaction of offshore wind turbines on gravity footings. *Renew Energy* 2014;68:289–303, <http://dx.doi.org/10.1016/j.renene.2014.02.008>.
- [12] Damgaard M, Zania V, Andersen L, Ibsen L. Effects of soil-structure interaction on real time dynamic response of offshore wind turbines on monopiles. *Eng Struct* 2014;75:388–401, <http://dx.doi.org/10.1016/j.engstruct.2014.06.006>.
- [13] Craig Jr RR, Bampton MCC. Coupling of substructures for dynamic analyses. *AIAA J* 1968;6(7):1313–9, <http://dx.doi.org/10.2514/3.4741>.
- [14] Damiani R, Jonkman J, Robertson A, Song H. Assessing the importance of nonlinearities in the development of a substructure model for the wind turbine CAE tool FAST. In: 32nd international conference on ocean, offshore and Arctic engineering. 2013. p. 1–16.
- [15] Song H, Damiani R, Robertson A, Jonkman J. A new structural-dynamics module for offshore multielement substructures within the wind turbine computer-aided engineering tool FAST. In: International ocean, offshore and polar engineering conference, vol. 23. 2013.
- [16] Damiani R, Jonkman J, Hayman G. *SubDyn User's Guide and Theory Manual*; 2015.
- [17] American Petroleum Institute. *Recommended Practice for Planning, Designing and Constructing Fixed Offshore Platforms - Working Stress Design, Recommended Practice RP 2A-WSD*; 2002.
- [18] Guyan RJ. Reduction of stiffness and mass matrices. *AIAA J* 1965;3(2):380, <http://dx.doi.org/10.2514/3.2874>.
- [19] Georgiadis M, Saflekou S. Piles under axial and torsional loads. *Comput Geotech* 1990;9:291–305, [http://dx.doi.org/10.1016/0266-352X\(90\)90043-U](http://dx.doi.org/10.1016/0266-352X(90)90043-U).
- [20] Germanischer Lloyd. *Guideline for the Certification of Offshore Wind Turbines. Offshore Standard*; 2012.
- [21] Jonkman J, Butterfield S, Musial W, Scott G. Definition of a 5-MW Reference Wind Turbine for Offshore System Development, Tech. Rep. NREL/TP-500-38060. National Renewable Energy Laboratory; 2009.

- [22] Vorpahl F, Popko W, Kaufer D. Description of a basic model of the 'UpWind reference jacket' for code comparison in the OC4 project under IEA Wind Annex 30, Tech. rep. Fraunhofer IWES; 2013.
- [23] Jonkman J. The new modularization framework for the FAST wind turbine CAE tool. In: 51st AIAA aerospace sciences meeting, including the new horizons forum and aerospace exposition, no. NREL/CP-5000-57228. 2013.
- [24] Barahona B, Jonkman J, Damiani R, Robertson A, Hayman G. Verification of the new FAST v8 capabilities for the modeling of fixed-bottom offshore wind turbines. In: 33rd wind energy symposium. 2015.
- [25] Jonkman J, Kilcher L. TurbSim User's Guide: Version 1.06.00, Tech. rep. National Renewable Energy Laboratory; 2012.
- [26] Bir GS. User's Guide to BModes (Software for Computing Rotating Beam Coupled Modes), Tech. Rep. NREL/TP-500-39133. National Renewable Energy Laboratory; 2007.
- [27] Vorpahl F, Popko W. Description of the Load Cases and Output Sensors to be Simulated in the OC4 Project under IEA Wind Annex 30, Tech. rep., Fraunhofer IWES; 2013.

### 3 Load set reduction for the fatigue assessment of jacket substructure for offshore wind turbines

This work comprises a study on load set reduction potentials in fatigue limit state and is published in *Renewable Energy*, Vol. 118, 2018, pp. 99–112 (DOI: 10.1016/j.renene.2017.10.097).

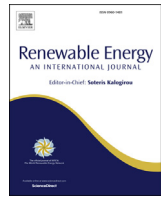
#### Author contributions

Jan Häfele is the corresponding author of the publication and the main author of section 1 (Introduction), section 3 (Simulation prerequisites), section 4 (Fatigue study), section 5 (Benefits and limits of the approach), and section 6 (Conclusion and outlook).

Clemens Hübler is the main author of section 2 (Environmental conditions).

Cristian Guillermo Gebhardt gave technical and editorial suggestions for improvement of the entire publication.

Raimund Rolfes gave technical and editorial suggestions for improvement of the entire publication and performed the final proofreading.



# A comprehensive fatigue load set reduction study for offshore wind turbines with jacket substructures



Jan Häfele<sup>\*</sup>, Clemens Hübler, Cristian Guillermo Gebhardt, Raimund Rolfe

*Institute of Structural Analysis, Leibniz Universität Hannover, Appelstr. 9a, D-30167, Hannover, Germany*

## ARTICLE INFO

### Article history:

Received 1 June 2017

Received in revised form

15 September 2017

Accepted 27 October 2017

Available online 31 October 2017

### Keywords:

Offshore wind energy

Fatigue limit state

Load set reduction

FINO3

Jacket substructures

Lattice substructures

## ABSTRACT

Designing jacket substructures for offshore wind turbines demands numerous time domain simulations to face different combinations of wind, wave, and current states. Regarding sophisticated design methods incorporating structural optimization algorithms, a load set reduction is highly desirable. To obtain knowledge about the required size of the design load set, a study on fatigue limit state load sets is conducted, which addresses mainly two aspects. The first one is a statistical evaluation of random subsets derived from probabilistic load sets with realistic environmental data obtained from the research platform FINO3. A full set comprising 2048 load simulations is gradually reduced to subsets and the results are compared to each other. The second aspect is a systematic load set reduction with the assumption of unidirectional wind, waves, and current. Firstly, critical directions are determined. Then, unidirectional load sets are systematically reduced. The corresponding damages are compared to those obtained from probabilistic load sets for eight test structures. It is shown that the omission of wind-, wave-, and current-misalignment does not necessarily imply an excessive simplification, if considered wisely. The outcome of this study can be used to decrease the numerical effort of the jacket design process and the leveled costs of energy.

© 2017 Elsevier Ltd. All rights reserved.

## 1. Introduction

On the way to high-power offshore wind turbines installed in deep water sites, the substructure technology is a key factor for reducing leveled costs of energy. Although monopile diameters are still growing to values that were not expected a decade ago and this concept has been exhausted over its forecasted limits a couple of times, jacket substructures are supposed to fill the gap between sea bed and tower foot for the upcoming turbine generation with more than 10 MW. For instance, the Innwind.EU project suggests several bottom-mounted substructure concepts for the DTU 10 MW reference turbine [1–3] where all of them are jacket structures [4–6]. Due to more sophisticated production and installation procedures, the capital expenses for these truss-like structures are relatively high nowadays. However, as the topology is more complex and the tubes dimensions vary, there is a significant cost reduction potential. From the design point of view, an optimization approach is an appropriate solution for this purpose and there are

recent approaches in literature that try to minimize the costs of the structure or a related measure [7–9]. All approaches close to practical applications have in common that they take ultimate and fatigue limit state constraints into account. The first can usually be covered by a set of expected extreme loads. For instance, this has already been shown for monopile substructures in Ref. [10]. In case of fatigue limit state design, numerous combinations of environmental conditions appearing with occurrence probabilities, that have been determined in preliminary measurements, or by given probability distributions, are required. Therefore, a reduction of fatigue limit state load sets – comprising commonly a different number of DLC 1.2 (production) and DLC 6.4 (idling) load cases according to [11] – increases the number of evaluable solutions in every design process and will directly contribute to the reduction of leveled costs of energy.

Several authors have tried to determine the impact of varying load conditions in fatigue calculations for wind turbines. Toft et al. [12] analyzed onshore wind turbines with respect to reliability and concluded that the uncertainty in damage equivalent loads is up to 13% only due to changing wind climate parameters. Zwick and Muskulus [13] released a study based on the OC4 jacket for the NREL 5 MW turbine [14] where the impact of the variability in the

<sup>\*</sup> Corresponding author.

E-mail address: [j.haeefe@isd.uni-hannover.de](mailto:j.haeefe@isd.uni-hannover.de) (J. Häfele).



Symbols			
$\Gamma$	Gamma-function	$D_L$	Leg diameter (jacket model)
$\alpha$	Statistical shape parameter ( $\beta$ -distribution)	$E$	Young's modulus (jacket model)
$\beta$	Statistical shape parameter (Gumbel and $\beta$ -distribution)	$G$	Shear modulus (jacket model)
$\beta_b$	Ratio of bottom brace-to-leg diameter (jacket model)	$H_s$	Significant wave height
$\beta_t$	Ratio of top brace-to-leg diameter (jacket model)	$L$	Entire jacket length (jacket model)
$\gamma_b$	Ratio of bottom leg radius to leg thickness (jacket model)	$L_{MSL}$	TP elevation over mean sea level (jacket model)
$\gamma_t$	Ratio of top leg radius to leg thickness (jacket model)	$L_{OSG}$	Lowest leg segment length (jacket model)
$\theta$	Statistical scale parameter ( $\gamma$ -distribution)	$L_{TP}$	Highest leg segment length (jacket model)
$\theta_{wave}$	Wave direction (north: $0^\circ$ , west: $90^\circ$ )	$N_L$	Number of legs (jacket model)
$\theta_{wind}$	Wind direction (north: $0^\circ$ , west: $90^\circ$ )	$N_X$	Number of tiers/bays (jacket model)
$\lambda$	Statistical scale parameter (Weibull distribution)	$P$	Probability function
$\mu$	Mean, statistical location parameter (Gumbel, Log-normal distribution)	$R_{Foot}$	Foot radius (jacket model)
$\xi$	Head-to-foot radius ratio (jacket model)	$T_P$	Wave peak period
$\rho$	Density (jacket model)	$f$	Probability density function
$\sigma$	Standard deviation, statistical shape parameter (Log-normal distribution)	$k$	Statistical shape parameter ( $\gamma$ -, Weibull distribution)
$\tau_b$	Ratio of bottom brace to leg thickness (jacket model)	$p$	Mixing parameter (for bi-modal distributions)
$\tau_t$	Ratio of top brace to leg thickness (jacket model)	$q$	Ratio of two consecutive tier lengths (jacket model)
		$u_w$	Near-surface current speed
		$v_s$	Wind speed
		$x$	Random variable
		$x_{MB}$	Mud brace flag (jacket model)
		$z$	Local depth below sea water level

stochastic representation of turbulent wind fields and irregular waves was investigated. It shows that – neglecting the scatter in some environmental conditions like wind and wave directions – there might be an underestimation of up to 29% for the minimum joint lifetime applying an assessment according to state-of-the-art procedures. Based on this knowledge, a proposal for a simplified fatigue load assessment of jacket substructures for offshore wind turbines was made in Ref. [15] where statistical regression methods are applied. The outcome is that a massive load set reduction is possible with only a small maximum error (only seven geometrical variations of the OC4 jacket were regarded due to limited numerical capacity). However, it has to be mentioned that this reduction is based on environmental conditions that were derived from the UpWind design basis [16] with unidirectional wind and waves and mean values for environmental conditions in each wind speed bin and further simplifications. Beyond that, the present study addresses the following questions:

1. What is the amount of uncertainty in fatigue damage assessment of jacket substructures for offshore wind turbines considering realistic environmental conditions?
2. How many design load cases per load set are at least required to cover the main environmental fatigue contributions with a specific demand for certainty?
3. Do state-of-the-art approaches describe appropriate load assumptions for fatigue assessment?
4. How should improved approaches covering main fatigue contributions look like?

To answer these questions, a numerical analysis based on time domain simulations is conducted in this work. Based on real environment data with high relevance for offshore wind energy applications that has been measured at the research platform FINO3, probability distributions for occurring wind speeds, wave heights and periods, and wind and wave directions are derived and illustrated. This is the topic of the next section. Subsequently, eight representative jacket designs are defined for the following fatigue

study which is split into two conceptual parts. The first one addresses mainly the effect of uncertainty that arises from the random reduction of design load sets. For this purpose, a comprehensive load set comprising 2048 cases linked to the probabilistic load distributions is specified and random representations of 10 min length each are simulated for two of the eight test jackets. A statistical evaluation is performed for both structures. In the next part of the study, it is analyzed how a reduction that maintains statistical properties of the initial load set can be performed without adding too much uncertainty to the results. Multiple design load sets, where unidirectional wind, waves, and current are presumed, are compared to the load set based on realistic environmental data for all test structures. The work ends with a discussion of benefits and limits of the approach and a conclusion.

## 2. Environmental conditions

Environmental conditions like wind or wave states at different sites for offshore wind turbines can deviate significantly. As fatigue loads of jacket substructures are affected, a precise characterization of the conditions is essential for a substantiated design or optimization process. It is highly desirable to use measured data in order to reach the highest possible level of significance for this purpose. Current standards [11] recommend to use data of the precise site of the offshore wind farm. However, for research purposes this data is rarely available. Even for industrial applications, there is not always data for all decisive environmental conditions, the data quality is poor, or long-term data is missing. This lack of data is one reason why there have been various research projects about the characterization of environmental conditions at specific sites or entire areas, publishing the derived statistical distributions as references. Examples are the UpWind design basis [16], the works of Stewart et al. [17], Stewart [18], or the PSA-OWT project [19]. However, all reference conditions have their drawbacks in the present context. The design basis of Stewart et al. [18] is for sites off the coasts of the United States of America. These sites are deep water sites and only suitable for floating structures but not for jacket substructures.

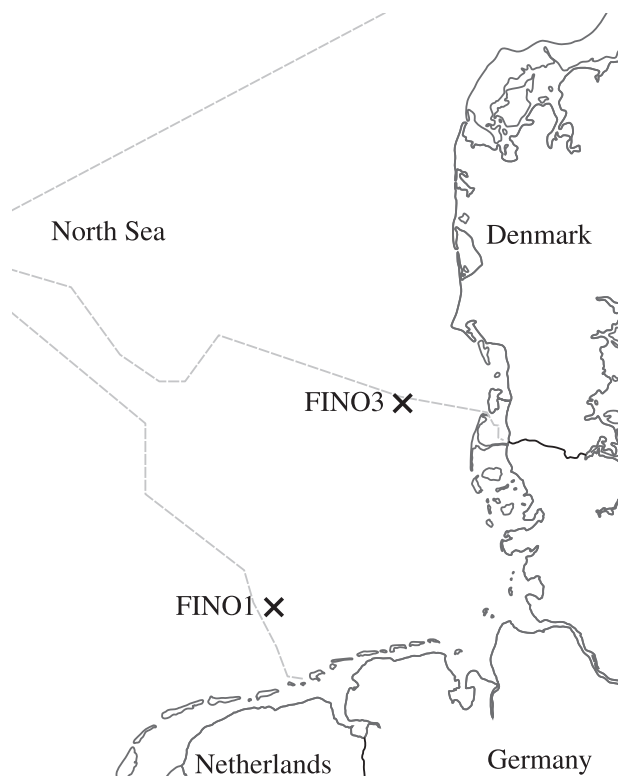


Fig. 1. Location of FINO3 and FINO1 in the German North Sea (c.f. [20]).

Furthermore, the wind speeds are measured fairly close to the water surface and not at hub height. Wind speeds at hub height are extrapolated, but this procedure leads to increased uncertainties. The UpWind design basis uses data of sites in the North Sea where most offshore wind turbines are located. At a water depth of 50 m, the environmental conditions of different sites are combined with the main part taken from a site with a water depth of 25 m. Additionally, the wind speed is given at a reference height of 10 m but not at hub height. Thus, the same problem of an increased uncertainty for the wind speed at hub height exists. And lastly, the conditional occurrence of different parameters (e.g. the wave height  $H_s$  depends on the wind speed  $v_s$ ) is only given in the form of scatter plots and raw data is not available. The PSA-OWT project uses data of the research platform FINO1 in the North Sea. The great advantage in this case is that the wind speed is measured at hub height and not close to the water surface. However, the use of a mast with a height of up to 100 m leads to shadow effects. If the wind direction is unfavorable, neither the wind speed nor the turbulence is measured correctly. These drawbacks show that an additional environmental design basis is valuable.

In this work, conditional probability distributions are directly derived for different environmental conditions using raw data of a second measurement mast in the North Sea. FINO3 is a research platform being funded under the “Wind Energy Initiative” of the German Federal Ministry for Economic Affairs and Energy and “Projektträger Jülich”<sup>1</sup> located in the North Sea, 80 km west of the island Sylt near to the wind farm DanTysk (see Fig. 1). For periods of 10 min, maximum, minimum, mean, and standard deviation values of all signals are available. The sampling frequency is 1 Hz. The wind speed is measured at different heights between 30 m and 100 m

above mean sea level (allowing the analysis of shear effects). Here, the data of three equally distributed cup anemometers (Vector - A100L2) at a height of 90 m is utilized. The use of three sensors around the mast ( $105^\circ$ ,  $225^\circ$  and  $345^\circ$ ) helps to compensate shadows effects due to wind direction changes. The wind direction is measured at a height of 100 m (at  $105^\circ$ ) with a wind vane (Vector - W200P). The wave conditions are mainly measured with a wave buoy (Datawell - MkIII) in the immediate vicinity to the research platform. Mean values of significant wave heights, wave directions and wave peak periods are measured every 30 min. Additionally available long-range measurements obtained by radar measuring are not used in this study. For further data like the speed and direction of the sea current, the water level, air pressure and temperature, and other quantities, only mean values are considered in this study or the additional information is completely neglected. Nevertheless, this additional data might be helpful for forthcoming studies to characterize the environmental conditions even more precisely, and is addressed for example in Hübler et al. [21]. The main advantages are the availability of wind data at hub height and the great amount of additional conditions that are continuously measured as well. However, the fact that the platform exists and measures only since 2009 depicts a problem: The measurement length of six years is scarce for long-term predictions. Therefore, further data of the FINO1 platform (measuring since 2003), located in the North Sea as well, is used for comparisons in this study. In contrast to FINO3 data, data of FINO1 has already been exploited frequently in literature, for example by Ernst and Seume [22] or Schmidt et al. [23].

### 2.1. Dependencies and distribution fitting for FINO3 data

In this work, raw data of the measurement platforms FINO3 and FINO1 (for comparison purposes only) is used to characterize environmental conditions of offshore wind farms. Some information concerning the raw data is given in Table 2. Post-processing is applied to eliminate sensor failures (missing data) and to identify measurement failures (outliers). In order not to introduce any bias, missing data is not interpolated, but just left out. This procedure is feasible for a sufficient data base and proper signal quality. For the wind speed, data of the anemometer in front of the measuring mast is selected by synchronizing it with the wind direction data. For wave parameters, it can be assumed that conditions remain stationary for a duration of about 3 h [24]. Therefore, for all wave parameters 3 h mean values are calculated using the 30 min raw data. Subsequently, various statistical distributions are fitted using a maximum likelihood estimation. The tested distributions are summarized in Table 1. Some histograms feature several distinct peaks. If this is the case, multi-modal distributions are fitted as well. However, as a multi-modal distribution fit is more precise due to the higher amount of degrees of freedom, it has to be chosen with care. It is only recommendable if several peaks are visible.

Environmental conditions cannot be regarded as independent. Hence, dependencies have to be defined. Here, the following ones are defined, though different dependencies are possible as well (see Ref. [18]). In general, the correlation is of main interest whereas determination of cause and effect are secondary:

- The wind speed ( $v_s$ ) is regarded as independent,
- the wind direction ( $\theta_{wind}$ ) is a function of the wind speed,
- the significant wave height ( $H_s$ ) is conditioned by the wind speed,
- the wave peak period ( $T_p$ ) depends on the parameter wave height,
- the wave direction ( $\theta_{wave}$ ) is a function of the wave height and the wind direction, both depending on the wind speed itself.

<sup>1</sup> The FINO3 measurement data is freely accessible online. See [www.fino3.de/en/](http://www.fino3.de/en/) for details.



**Table 1**  
Statistical distributions tested in this work, where  $\Gamma$  Gamma-function is the gamma-function. For multi-modal distributions, only one example is given, and non-parametric distributions are not included.

Distribution	Statistical parameters	Probability density function
Normal distribution	$\mu, \sigma$	$f(x   \mu, \sigma) = \frac{1}{\sqrt{2\sigma^2\pi}} e^{-\frac{(x-\mu)^2}{2\sigma^2}}$
Gumbel distribution	$\mu, \beta$	$f(x \mu, \beta) = \frac{1}{\beta} e^{-\frac{x-\mu}{\beta} + e^{-\frac{x-\mu}{\beta}}}$
$\beta$ -distribution	$\alpha, \beta$	$f(x \alpha, \beta) = \frac{x^{\alpha-1}(1-x)^{\beta-1}}{\frac{\Gamma(\alpha)\Gamma(\beta)}{\Gamma(\alpha+\beta)}}$
$\gamma$ -distribution	$k, \theta$	$f(x k, \theta) = \frac{1}{\Gamma(k)\theta^k} x^{k-1} e^{-\frac{x}{\theta}}$
Weibull distribution	$k, \lambda$	$f(x k, \lambda) = \begin{cases} \frac{k}{\lambda} \left(\frac{x}{\lambda}\right)^{k-1} e^{-\left(\frac{x}{\lambda}\right)^k} & \text{for } x \geq 0 \\ 0 & \text{for } x < 0 \end{cases}$
Log-normal distribution	$\mu, \sigma$	$f(x \mu, \sigma) = \frac{1}{x\sigma\sqrt{2\pi}} e^{-\frac{(\ln(x)-\mu)^2}{2\sigma^2}}$
Bi-modal log-normal distr.	$\mu_1, \mu_2, \sigma_1, \sigma_2, p$	$f(x \mu_1, \mu_2, \sigma_1, \sigma_2, p) = \frac{p}{x\sigma_1\sqrt{2\pi}} e^{-\frac{(\ln(x)-\mu_1)^2}{2\sigma_1^2}} + \frac{1-p}{x\sigma_2\sqrt{2\pi}} e^{-\frac{(\ln(x)-\mu_2)^2}{2\sigma_2^2}}$

It was shown in Ref. [25] that these parameters are most influential regarding jacket substructures. To incorporate dependencies in the statistical distributions, the data of the dependent parameters is separated in bins of the independent parameters. For example, the wave height is fitted in several wind speed bins of  $2 \text{ ms}^{-1}$  (e.g.  $P(H_s) = P(H_s | 12 \text{ ms}^{-1} \leq v_s < 14 \text{ ms}^{-1})$  where  $P$  is the probability function). The bin widths and bin ranges (indicating the covered conditions) for the different dependent parameters are summarized in Table 3.

After fitting the statistical distributions summarized in Table 1 to the data, the one matching the data best is chosen based on visual inspections and objective criteria using Kolmogorov-Smirnov tests (KS-tests) and chi-squared tests ( $\chi^2$ -tests). The same type of distribution is chosen for all bins of one parameter, even if different ones match the data best in different bins. This decision was made, as it is assumed that the same parameter follows more or less one distribution. The selection is based only on bins with 50 or more data points. Therefore, bins for high wind speeds are neglected, as too few data points are available. If several distributions fit the data equally well, FINO1 data is used as a comparison to find the most suitable solution.

The directional parameters ( $\theta_{wind}$  and  $\theta_{wave}$ ) are treated in a different way, as they cannot be fitted with classical, parametric distributions due to several peaks and a continuous distribution ( $0^\circ = 360^\circ$ ). For these parameters, a non-parametric kernel density estimation is used.

**Table 2**  
Information concerning the raw input data of the environmental conditions.

Parameter	Data points	Mean	Minimum	Maximum	5th percentile	95th percentile
Wind speed	353 000	9.9 $\text{ms}^{-1}$	0.2 $\text{ms}^{-1}$	36.3 $\text{ms}^{-1}$	2.9 $\text{ms}^{-1}$	18.0 $\text{ms}^{-1}$
Wind direction	333 000	208°	0°	360°	38°	335°
Sig. wave height	106 000	1.6 m	0.0 m	8.9 m	0.5 m	3.3 m
Wave peak period	106 000	7.4 s	1.7 s	28.6 s	4.0 s	12.5 s
Wave direction	106 000	251°	0°	360°	68°	339°

**Table 3**  
Bin widths and statistical distributions for different dependent parameters.

Parameter	Dependencies	Bin widths	Bin ranges	Statistical distribution
Wind speed				Weibull
Wind direction	Wind speed	2 $\text{ms}^{-1}$	0–34 $\text{ms}^{-1}$	Nonparametric
Sig. wave height	Wind speed	2 $\text{ms}^{-1}$	0–28 $\text{ms}^{-1}$	Gumbel
Wave peak period	Wave height	0.5 m	0–7 m	Bi-modal log-normal
Wave direction	Wave height	1.0 m	0–7 m	Nonparametric
	Wind direction	36°	0–360°	

2.2. Conditional probability distributions

The selected distributions for the five parameters ( $v_s$ ,  $\theta_{wind}$ ,  $H_s$ ,  $T_p$  and  $\theta_{wave}$ ) are summarized in Table 3. As the statistical parameters are varying in different bins and partly non-parametric distributions are used, only for the Weibull-distribution of the wind speed the parameters can be stated here:  $k = 2.32$  and  $\lambda = 10.94$ .

Fig. 2 shows some examples of statistical distributions determined. The bi-modal shape in Fig. 2(a) shall be highlighted just like the non-parametric fit for the wind direction in Fig. 2(b). Fig. 2(c) and (d) illustrate the problem that in some cases, varying distributions fit the data best in different bins by showing the fit of a Gumbel distribution and a Weibull distribution.

2.3. Further assumptions

There are some parameters and environmental conditions that cannot be estimated from the available data set due to different reasons. Therefore, the following points have been presumed for all simulations:

- FAST requires a turbulent wind field that has to be created externally prior to all simulations. For this purpose, a Kaimal model is used with mean values for turbulence intensity and power law exponent (gained from FINO3 data) in each wind speed bin. The data is created with TurbSim.

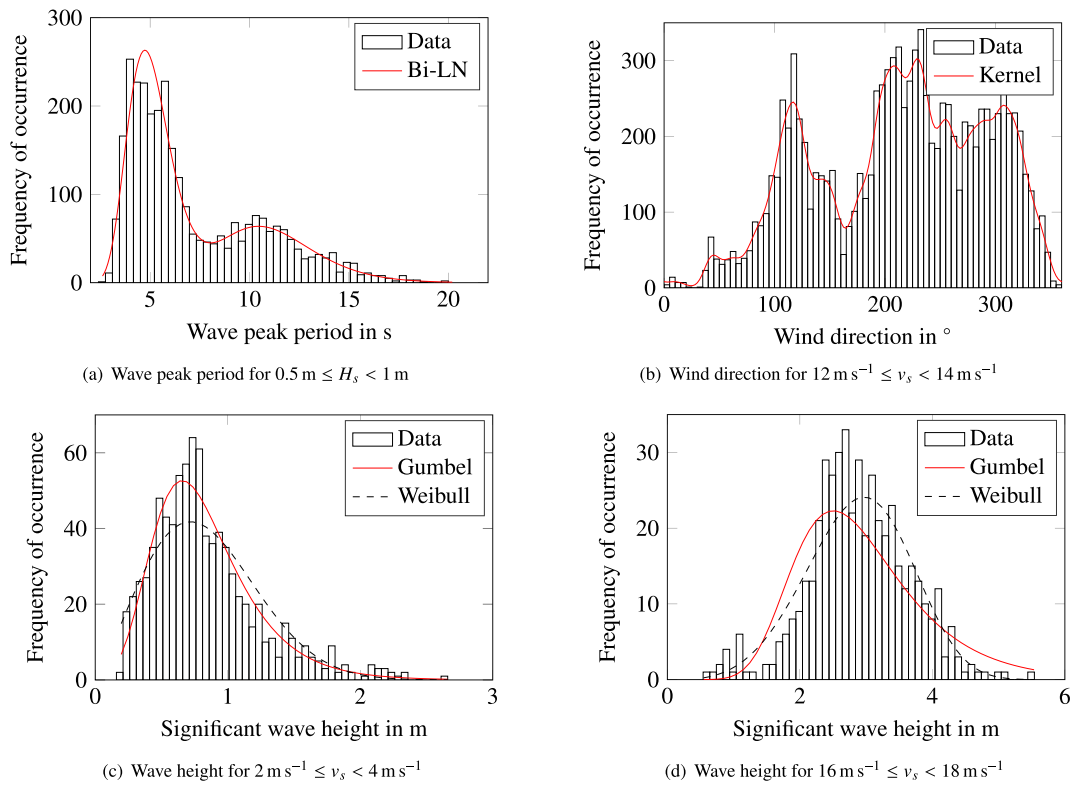


Fig. 2. Cumulative distribution plots for different environmental conditions.

- A Pierson-Moskowitz spectrum is used for the generation of irregular wave kinematics.
- There are 10 different random representations for all turbulent wind fields and irregular wave kinematic signals.
- Although the real water depth at the site of FINO3 is 22 m, the design water depth is assumed as 50 m. The same procedure was performed in Ref. [16] where the environmental data of the K13 shallow water site was transferred to the K13 deep water site.
- The near-surface current speed  $u_w(z)$  is modeled according to the following power law (which is suggested in Ref. [11]):

$$u_w(z) = u_w(0 \text{ m}) \left( 1 + \frac{z}{20 \text{ m}} \right) \quad (1)$$

$u_w(0 \text{ m})$  was identified as  $0.42 \text{ ms}^{-1}$  for the FINO3 site.  $z$  is the local depth below the sea water level, downwards negative.

- The near-surface current direction is assumed to be aligned with the wind direction (which is suggested in Ref. [11], too).
- Sub-surface current, second-order and breaking waves, and wave spreading effects are not considered in this study. Several studies [26–28] showed that it is worth regarding several of these additional phenomena, but due to demands for numerical efficiency and missing data, it was decided to disregard them.
- The soil properties of the OC3 phase II model (monopile) [29] are adopted for all simulations.
- Marine growth is considered with a density of  $1400 \text{ kg m}^{-3}$  and thicknesses of 100 mm above and 50 mm below 40 m water depth with respect to mean sea level, respectively. This assumption is adopted from the UpWind design basis [16].
- Degradation effects like scour or corrosion are not considered, though the impact might not to be insignificant (see Ref. [30]).
- The yaw error of the rotor is considered with a mean value of  $8^\circ$  and a standard deviation of  $1^\circ$  (according to [31]).

### 3. Simulation prerequisites

#### 3.1. Reference turbine

The NREL 5 MW reference wind turbine [14] is used for the following study which has a hub height of 90.15 m above mean sea level. The turbine power is pitch-controlled with a rated wind speed of  $11.4 \text{ ms}^{-1}$ , while cut-in and cut-out speeds are  $3 \text{ ms}^{-1}$  and  $25 \text{ ms}^{-1}$ , respectively. From rated to cut-off wind speed, the nominal speed of the rotor is 12.1 rpm, corresponding to a 1P-excitation frequency of 0.2 Hz and a 3P-excitation frequency of 0.6 Hz.

#### 3.2. Test jackets

The entire study bases on the parameterizable jacket model defined in Ref. [9]. The advantage of utilizing this model is that both topology and geometry of the structure can be varied, not only tube dimensions. According to the state of the art, mainly three-legged and four-legged jacket structures are supposed to be appropriate substructures for the given application. There are indeed concepts for structures with more than four legs, but current research and industrial experience has revealed that the additional number of legs does not overcome the increased production costs related to this concept. Therefore, it has been decided to consider only three- and four-legged designs in this study. The parameters of all eight test jackets, denoted from (1) to (8), are summarized in Table 4. Probably the most regarded jacket structure for offshore wind turbines in literature is the OC4 jacket which is an adaption of the four-legged reference jacket from the UpWind project [32]. The topology of the OC4 jacket has been transferred to jacket (1), see Fig. 3(a). In order to obtain a comparable three-legged design, jacket (2), which is shown in Fig. 3(b), features a similar structure with only three legs, but same the foot radius. Jacket (3) is a four-

**Table 4**  
Jacket model parameter values for test jackets according to jacket model definition in Ref. [9].

Jacket model parameter	(1)	(2)	(3)	(4)	(5)	(6)	(7)	(8)
Number of legs $N_L$	4	3	4	4	3	4	3	4
Number of tiers/bays $N_X$	4	4	3	4	3	3	4	5
Foot radius $R_{Foot}$ in m	8.49	8.49	10.19	7.64	12.73	8.49	10.19	8.49
Head-to-foot radius ratio $\xi$	0.67	0.67	0.53	0.73	0.67	0.73	0.67	0.60
Leg diameter $D_L$ in m	1.20	1.20	1.20	1.44	1.44	1.08	1.32	1.20
Ratio of bottom brace-to-leg diameter $\beta_b$	0.67	0.67	0.67	0.67	0.80	0.53	0.73	0.60
Ratio of top brace-to-leg diameter $\beta_t$	0.67	0.67	0.67	0.67	0.80	0.53	0.73	0.60
Ratio of bottom leg radius to leg thickness $\gamma_b$	15.0	15.0	15.0	15.0	18.0	12.0	13.5	16.5
Ratio of top leg radius to leg thickness $\gamma_t$	15.0	15.0	15.0	15.0	18.0	12.0	13.5	16.5
Ratio of bottom brace to leg thickness $\tau_b$	0.50	0.50	0.50	0.50	0.60	0.75	0.60	0.40
Ratio of top brace to leg thickness $\tau_t$	0.50	0.50	0.50	0.50	0.60	0.75	0.60	0.40
Entire jacket length $L$ in m					70.0			
TP elevation over mean sea level $L_{MSL}$ in m					20.0			
Lowest leg segment length $L_{OSG}$ in m					5.0			
TP length $L_{TP}$ in m					4.0			
Ratio of two consecutive tier lengths $q$					0.8			
Mud brace flag $x_{MB}$					true			
Young's modulus $E$ in $\text{Nm}^{-2}$					$2.1 \times 10^{11}$			
Shear modulus $G$ in $\text{Nm}^{-2}$					$8.1 \times 10^{10}$			
Density $\rho$ in $\text{kg m}^{-3}$					7850.0			

legged structure with bigger foot radius, but only three brace levels, while jacket (4) has a smaller foot radius, but larger leg diameter. Jacket (5) is a three-legged design with only three brace levels, but bigger foot radius and tube dimensions. The four-legged design (6) has only three tiers and small diameters, but large thicknesses of tubes. Structure (7) is an adaption of (2) with slightly different topology and geometry. Jacket (8) is the only one in the study with five brace levels which allows slightly smaller tube dimensions. In comparison to most state-of-the-art jacket structures, the proposed jacket model features a concept without prefabricated joints and no joint cans. However, the tube diameters and thicknesses do not vary from bottom to top, because  $\beta_b$  and  $\beta_t$ ,  $\gamma_b$  and  $\gamma_t$ , and  $\tau_b$  and  $\tau_t$  have identical values in all regarded designs.

The transition piece of both test jackets is supposed to be a concentrated mass point with a mass of 660 t, rigidly connected to the uppermost joints of the jacket structure. No structural appurtenances like ladders, boat landings, sacrificial anodes, or J-tubes

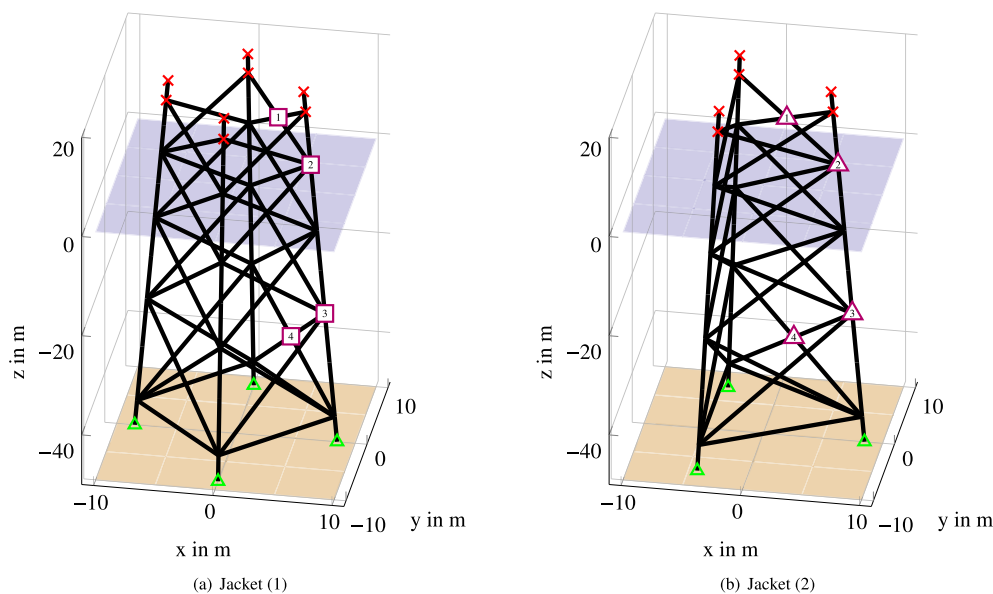
are considered in the structural model.

### 3.3. Foundation

The soil properties are adopted from the UpWind reference jacket. In order to consider soil-structure interaction, the approach proposed in Ref. [33] is employed. Zero-deflection both in translational and rotational directions is considered as operational point for the derivation of all  $p$ - $y$ - and  $T$ - $z$  curves that have been calculated according to the equations of API RP 2A-WSD [34].

### 3.4. Time domain simulation

For this study, all time domain simulations are performed with the aero-hydro-servo-elastic simulation code FAST in the version v8.15.00bjj. The substructure is represented by a linear finite element model with Timoshenko beam elements. The resulting



**Fig. 3.** Topology of test jackets (1) and (2) used for reduction study.  $\times$  indicates interface and  $\triangle$  base joints. Damage assessment is performed at positions  $\square/\triangle$  on the uppermost X-joint tier, at  $\square/\triangle$  on the uppermost K-joint tier, at  $\square/\triangle$  on the lowermost K-joint tier, and at  $\square/\triangle$  on the lowermost X-joint tier.

mass and stiffness matrices are reduced with a component mode synthesis to a system with eight degrees of freedom in order to disregard modes with higher frequencies and save computational effort. A linear-viscous modal damping of 2% is considered. However, this procedure neglects local vibration effects of braces due to numerical limitations, though the consideration might impact the fatigue behavior of the structure [35]. Joint stiffnesses are neglected as well though the impact might be non-negligible [36]. The regarded length for all time domain simulations is 780 s. Although all initial states for the integration of the differential equations are set to the quasi-static states, the first 180s are discarded from the results to overcome a possible influence of transient decay on the fatigue damage results. The equations of motions are solved by a fourth-order Adams-Bashforth-Moulton method with a time step of 0.005s and one correction step.

### 3.5. Fatigue assessment

All hot spot fatigue damages are calculated according to an S-N-curve approach defined by DNV GL RP-0005 [37]. For this purpose, stress values at eight circumferential points around each hot spot of are evaluated in every time step of the simulation output and multiplied by stress concentration factors according to [38] that depend on the joint type and geometry. Then, stress cycles are evaluated by a Rainflow counting algorithm and assessed according to linear damage accumulation. The critical hot spot of every joint is supposed to be located in the point with the maximum damage after the entire calculation procedure (see Ref. [39]). A fatigue damage factor is not considered in this study, as no design lifetimes are calculated. It has been presumed that tubular joints are not prefabricated. Thus, one-sided welds must be considered. In this case, an S-N-curve with an endurance stress limit of  $52.63 \times 10^6 \text{ Nm}^{-2}$  at  $10^7$  cycles and slopes of 3 and 5 before and after endurance limit, respectively, is selected.

## 4. Fatigue study

Starting from a load set with sufficient size (“full load set”), the goal is an evaluation of damage-equivalent subsets. However, a reduction is associated with uncertainty. To overcome this, results are treated in a statistical manner.

The study addresses two main aspects of fatigue assessment and is therefore conceptually divided into two parts. The first one analyses the level of uncertainty that arises from probabilistic distributions of environmental parameters. For this purpose, the full load set with 2048 design load cases for test jackets (1) and (2) is

regarded. This number was selected, as it is divisible without remainder by many whole-number integrals of 2. A random selection of load cases from the full load set is performed to show the impact of load set size on the degree of uncertainty. The second one compares load sets with unidirectional wind, waves, and current to load sets obtained with probabilistic distributions. In the final analysis, the outcome is used to define a reduced load set which is verified for all eight test jackets (1) to (8). The flow chart in Fig. 4 illustrates the partition of the study graphically.

### 4.1. Full load set

The full load set comprises 2048 design load cases where the environmental conditions occur according to the probability distributions that have been derived in section 2. To conduct all time domain simulations in an adequate amount of time, the scientific computing cluster system of Leibniz Universität Hannover has been utilized: Using 64 nodes simultaneously, where each has two Intel Haswell Xeon E5-2630 CPUs with eight cores (therefore 16 cores per node) running with at least 2.4GHz and an estimated duration of 10 h per design load case, the entire study can be performed theoretically in less than one day per test jacket. However, practical implementation issues and limitations lead to a realistic duration of about three days for the entire study which still outperforms expected durations for calculations on common state-of-the-art workstations roughly by a power of ten. The calculated fatigue damages for all evaluated X- and K-joints are shown in Fig. 5.

Generally, all trends are roughly driven by the characteristic of rotor trust in dependency of the wind speed and the effect of the tendency to increasing wave loading for higher wind speeds. Two trends can be derived from the diagrams: Firstly, the absolute damage values per load case decrease from the lower joints to the upper ones in average. And secondly, X-joints are far more prone to fatigue than K-joints, in terms of numbers by some powers of ten. On average, the damage per load case is higher for the three-legged jacket compared to the four-legged design. Scatter is significantly higher for locations with lower damage values, in particular in case of all K-joints. Regarding all diagrams, a resonance effect in the  $8 \text{ ms}^{-1}$  wind speed bin is obvious for the four-legged design, as the damages per load case are significantly higher than in the adjacent bins, best visible in case of the uppermost X-joints (see Fig. 5(a) and (g)). It is supposed that in this case, the first bending eigenfrequency is nearly equal to the 3P-excitation frequency of the rotor. A similar phenomenon was discovered by Stewart [18]. The resonance does not appear so plainly in the results of the three-

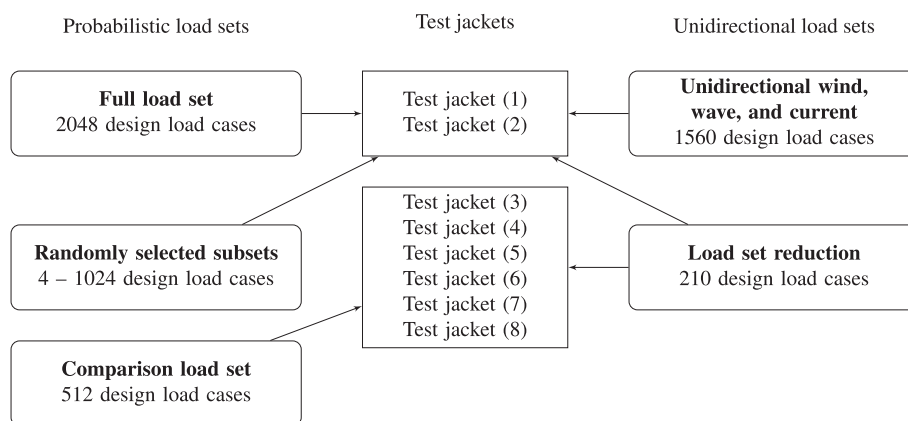
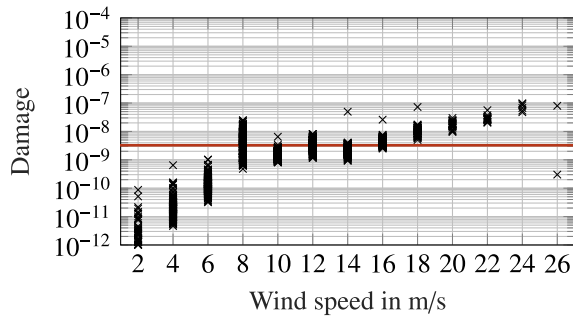
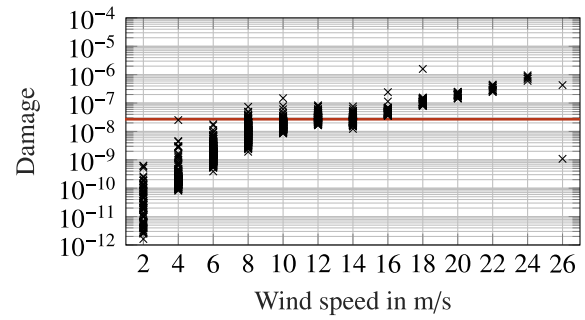


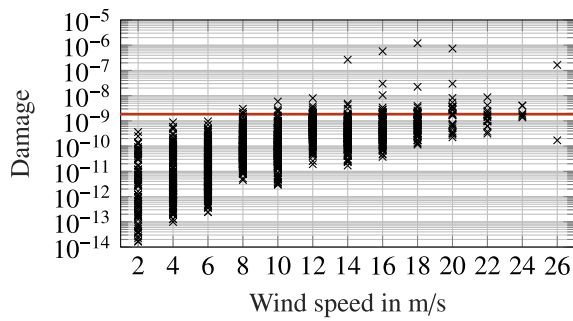
Fig. 4. Flowchart of fatigue reduction study.



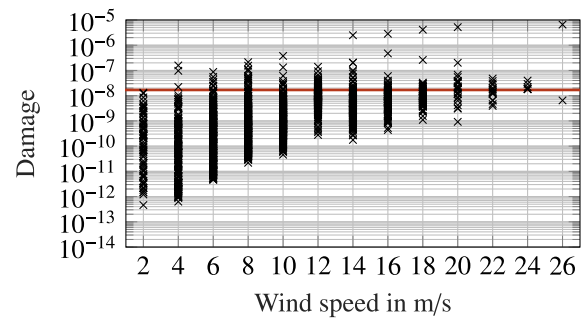
(a) Structure (1), uppermost X-joint (position 1)



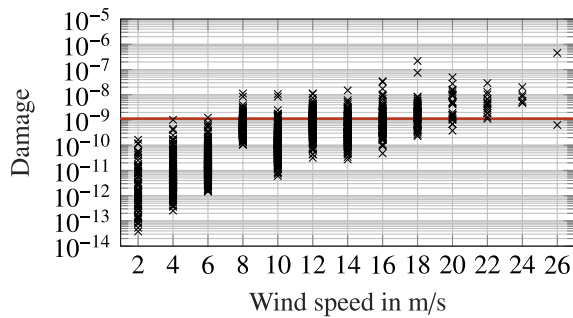
(b) Structure (2), uppermost X-joint (position 2)



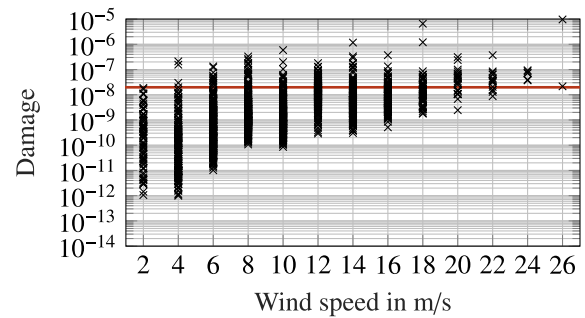
(c) Structure (1), uppermost K-joint (position 2)



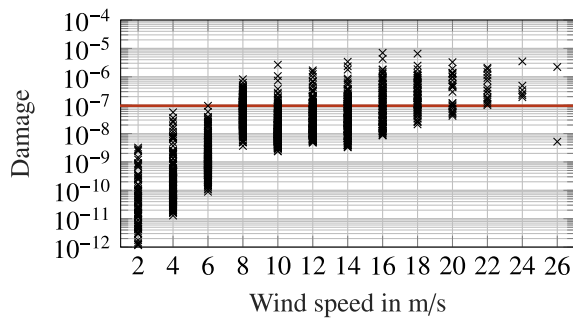
(d) Structure (2), uppermost K-joint (position 3)



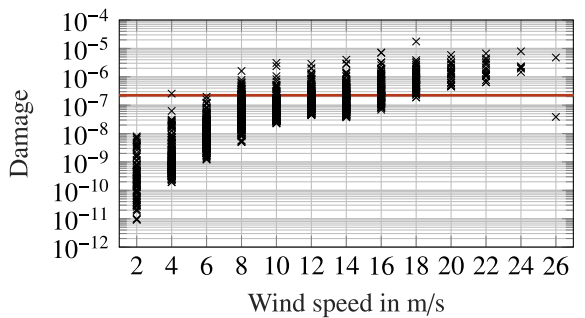
(e) Structure (1), lowermost K-joint (position 3)



(f) Structure (2), lowermost K-joint (position 4)



(g) Structure (1), lowermost X-joint (position 4)



(h) Structure (2), lowermost X-joint (position 5)

**Fig. 5.** Damage assessment of full load set at all regarded joints of structures (1) and (2). Each  $\times$  depicts the damage of a single load case in the corresponding wind speed bin according to the fatigue assessment procedure described in section 3.5. The mean joint damage is illustrated by  $\text{—}$ .

legged design. While some effects are supposed to appear more or less for every jacket design, especially the general characteristic of mean damage per load case, others will have different impact or even vanish. These are mainly two: On the one hand, the critical resonance frequency will shift for harder or softer designs and

therefore the corresponding wind speed bin (also dependent on the pitch controller) which is illustrated by the comparison between four- and three-legged jacket in this study. On the other hand, the influence of wave loading will generally increase for larger tube diameters.

**Table 5**  
 Statistical evaluation of randomly selected subsets at regarded X-joints of jackets (1) and (2) (10 000 random evaluations for each load set size).

Position	Load set Size	Damage per load case			Percentiles						
		Mean	Median	Std. dev.	0,5th	2,5th	5th	95th	97,5th	99,5th	
□	2048	0.31	0.31	0.01	0.30	0.30	0.30	0.32	0.33	0.33	×10 <sup>-8</sup>
	1024	0.31	0.31	0.01	0.29	0.29	0.30	0.33	0.33	0.34	
	512	0.33	0.32	0.01	0.29	0.30	0.30	0.35	0.36	0.36	
	256	0.31	0.31	0.02	0.27	0.28	0.29	0.34	0.35	0.37	
	128	0.29	0.29	0.02	0.25	0.25	0.26	0.33	0.34	0.37	
	64	0.32	0.31	0.03	0.25	0.26	0.27	0.38	0.40	0.44	
	32	0.24	0.23	0.04	0.17	0.18	0.19	0.31	0.33	0.44	
	16	0.28	0.27	0.07	0.18	0.20	0.21	0.39	0.45	0.68	
	8	0.15	0.14	0.07	0.07	0.08	0.09	0.25	0.30	0.65	
4	0.24	0.21	0.10	0.09	0.11	0.12	0.44	0.51	0.67		
△	2048	2.69	2.68	0.08	2.55	2.57	2.58	2.84	2.87	2.94	×10 <sup>-8</sup>
	1024	2.70	2.67	0.11	2.52	2.55	2.56	2.91	2.95	3.09	
	512	2.81	2.77	0.16	2.57	2.61	2.63	3.11	3.20	3.39	
	256	2.72	2.66	0.22	2.46	2.50	2.52	3.25	3.32	3.78	
	128	2.48	2.41	0.30	2.19	2.24	2.26	3.46	3.58	3.72	
	64	2.75	2.67	0.43	2.34	2.40	2.44	3.03	4.85	5.15	
	32	1.90	1.82	0.57	1.53	1.59	1.62	2.17	2.35	6.51	
	16	2.42	2.24	1.18	1.82	1.90	1.94	2.77	3.16	11.59	
	8	1.08	1.04	0.23	0.72	0.77	0.81	1.51	1.65	1.94	
4	1.50	1.44	0.38	0.90	1.00	1.05	2.16	2.43	2.96		
□	2048	0.95	0.95	0.07	0.79	0.82	0.84	1.07	1.10	1.15	×10 <sup>-7</sup>
	1024	0.95	0.95	0.10	0.74	0.78	0.80	1.12	1.16	1.23	
	512	0.98	0.97	0.14	0.68	0.74	0.77	1.23	1.29	1.40	
	256	0.94	0.92	0.20	0.56	0.63	0.67	1.31	1.39	1.58	
	128	0.93	0.88	0.28	0.47	0.54	0.58	1.47	1.61	1.89	
	64	0.99	0.90	0.38	0.40	0.48	0.52	1.77	1.99	2.43	
	32	0.78	0.64	0.50	0.24	0.29	0.32	1.77	2.45	3.02	
	16	0.98	0.72	0.84	0.20	0.27	0.31	2.54	4.16	5.09	
	8	0.41	0.27	0.56	0.05	0.07	0.08	1.15	2.16	4.38	
4	0.50	0.34	0.66	0.06	0.08	0.10	1.39	2.16	4.48		
△	2048	2.18	2.17	0.12	1.90	1.95	1.98	2.39	2.44	2.55	×10 <sup>-7</sup>
	1024	2.19	2.17	0.18	1.80	1.88	1.92	2.50	2.57	2.72	
	512	2.25	2.23	0.25	1.74	1.83	1.88	2.71	2.82	3.05	
	256	2.17	2.11	0.36	1.52	1.62	1.69	2.84	3.03	3.42	
	128	2.11	2.02	0.49	1.28	1.42	1.50	3.08	3.40	3.96	
	64	2.29	2.16	0.72	1.16	1.35	1.45	3.54	4.39	5.41	
	32	1.67	1.46	0.88	0.72	0.83	0.89	3.10	3.72	6.91	
	16	2.15	1.75	1.61	0.73	0.86	0.95	4.13	5.80	12.49	
	8	0.88	0.67	0.77	0.23	0.27	0.31	2.12	3.73	5.27	
4	1.04	0.77	0.94	0.28	0.34	0.38	2.53	3.56	7.33		

4.2. Randomly selected subsets

A high number of load sets is often undesirable, for example in predesign procedures or optimization approaches where a lot of test samples have to be evaluated. The question to be answered in the following is: Which load set size is required to reach a certain level of accurateness in fatigue damage evaluation?

To address this point, the full load set has been reduced by a random selection of subsets that maintains the probability distribution of wind speed occurrence. For example, if the initial load set is supposed to have each of the 512 design load cases in four different wind speed bins, the reduced load set with a load set size of 1024 depicts one with each 256 randomly selected design load cases from each bin and so forth. This procedure has been performed for reduction sizes from 1024 down to 4 (unique) load cases (for the full load set described in section 4.1). The corresponding results are illustrated for all X-joints in Table 5 and for all K-joints in Table 6. As this procedure depends on randomness, the results show mean, median, standard deviation, and different percentiles related to confidence intervals of 90, 95, and 99%. 10 000 random representations are the basis for each reduced load set. The random selection of design load cases for each subset is underlied by a bootstrapping procedure (“sampling with replacement”).

At the first glance, the trend of results is as expected. The

uncertainty increases with decreasing load set size (both visible in standard deviation and percentile values). One main demand on a reduced load set is that it maintains the mean values and this is in valid for load set sizes down to 64 at all regarded joint positions in a great measure. However, the scatter is distinctly higher for all regarded K-joints due to wide spreading results. For a reduced load set size of 64 and the four-legged jacket, 99% of all damages at the lowest X-joint position □ are in a range from 46% to 157% of the full load set mean value which is a quite good outcome keeping in mind that this reduction is 32 times more efficient. However, the range increases to 2% at the lower boundary and 1538% at the upper boundary regarding the upper K-joint position △ with the same reduction factor. The occurring K-joint damages are significantly lower than the X-joint damages. The reason why the reduction works commonly better for the latter positions is that the impact of extreme design load cases in a load set is less. In this respect, it is beneficial that these positions are design driving.

Considering that the main damage occurs at the X-joint positions, the reduction of load set size is in general easily conceivable. Even in case of high significance levels, the scatter does not increase in the same order of reduction factors. It is straightforward to use an appropriate load set size with the knowledge of uncertainty that is given by Tables 5 and 6



**Table 6**

Statistical evaluation of randomly selected subsets at regarded K-joints of jackets (1) and (2) (10 000 random evaluations for each load set size).

Position	Load set	Damage per load case			Percentiles						
	Size	Mean	Median	Std. dev.	0,5th	2,5th	5th	95th	97,5th	99,5th	
□	2048	1.30	1.22	0.62	0.25	0.35	0.50	2.48	2.76	3.29	$\times 10^{-9}$
	1024	1.39	1.34	0.88	0.18	0.20	0.23	3.10	3.43	4.47	
	512	1.53	1.41	1.29	0.16	0.18	0.19	3.94	4.91	6.20	
	256	1.46	0.26	1.94	0.14	0.15	0.16	4.98	5.98	9.61	
	128	1.59	0.23	2.87	0.12	0.14	0.15	9.57	9.65	14.07	
	64	1.71	0.23	4.26	0.11	0.13	0.14	11.71	18.98	19.22	
	32	1.11	0.17	5.05	0.08	0.09	0.10	1.06	18.17	37.85	
	16	1.90	0.20	10.06	0.08	0.10	0.11	1.48	16.91	75.56	
	8	0.34	0.14	2.44	0.03	0.04	0.05	0.38	0.56	33.40	
	4	0.24	0.21	0.19	0.02	0.05	0.06	0.52	0.66	1.18	
△	2048	9.10	9.11	2.48	3.50	4.61	5.24	13.28	14.36	16.28	$\times 10^{-9}$
	1024	9.98	9.81	3.55	2.85	3.26	3.74	15.85	17.30	21.07	
	512	13.41	15.52	6.34	2.46	2.85	3.06	22.47	24.29	29.36	
	256	9.55	4.25	8.59	2.05	2.28	2.44	26.19	29.05	42.04	
	128	10.73	3.95	13.74	1.78	2.00	2.16	42.28	43.11	56.54	
	64	11.09	3.65	20.32	1.59	1.84	1.99	66.80	82.73	84.99	
	32	8.91	2.89	22.63	1.10	1.31	1.46	78.50	90.60	130.83	
	16	11.76	3.13	39.52	1.07	1.34	1.51	24.63	158.35	260.24	
	8	5.14	1.94	22.31	0.35	0.54	0.70	13.98	24.20	188.72	
	4	4.82	2.79	7.41	0.33	0.62	0.80	13.85	23.33	42.63	
□	2048	0.84	0.83	0.19	0.46	0.49	0.51	1.16	1.21	1.33	$\times 10^{-9}$
	1024	0.84	0.90	0.27	0.42	0.45	0.47	1.26	1.38	1.54	
	512	1.07	1.27	0.49	0.40	0.44	0.46	1.85	1.91	2.28	
	256	0.64	0.54	0.30	0.35	0.38	0.40	1.37	1.44	1.70	
	128	0.65	0.52	0.43	0.30	0.33	0.35	2.07	2.20	2.41	
	64	0.72	0.55	0.65	0.27	0.31	0.33	1.51	3.76	4.11	
	32	0.56	0.37	0.90	0.17	0.20	0.22	1.18	2.52	7.18	
	16	0.77	0.43	1.72	0.17	0.20	0.23	1.55	4.86	14.01	
	8	0.31	0.25	0.25	0.06	0.08	0.10	0.69	1.01	1.87	
	4	0.47	0.37	0.40	0.08	0.11	0.13	1.00	1.41	2.91	
△	2048	15.93	15.87	4.59	7.13	7.74	8.16	23.89	25.68	29.64	$\times 10^{-9}$
	1024	16.13	16.68	6.55	6.62	7.12	7.40	26.84	30.31	36.78	
	512	20.91	24.95	11.29	5.98	6.65	7.03	40.16	41.28	53.03	
	256	11.81	8.72	8.95	5.06	5.61	5.93	33.92	35.34	57.44	
	128	11.95	8.28	12.59	4.18	4.82	5.17	57.02	59.41	62.97	
	64	12.46	8.31	17.53	3.57	4.24	4.67	25.47	107.45	112.97	
	32	11.99	6.36	27.26	2.11	2.62	3.00	30.74	43.54	213.20	
	16	16.90	6.72	52.68	1.83	2.39	2.81	38.98	80.01	417.80	
	8	7.13	3.55	13.16	0.52	0.82	1.04	24.04	37.02	125.29	
	4	8.39	4.92	12.31	0.49	0.88	1.18	25.05	39.20	72.06	

#### 4.3. Load set with unidirectional wind, wave, and current

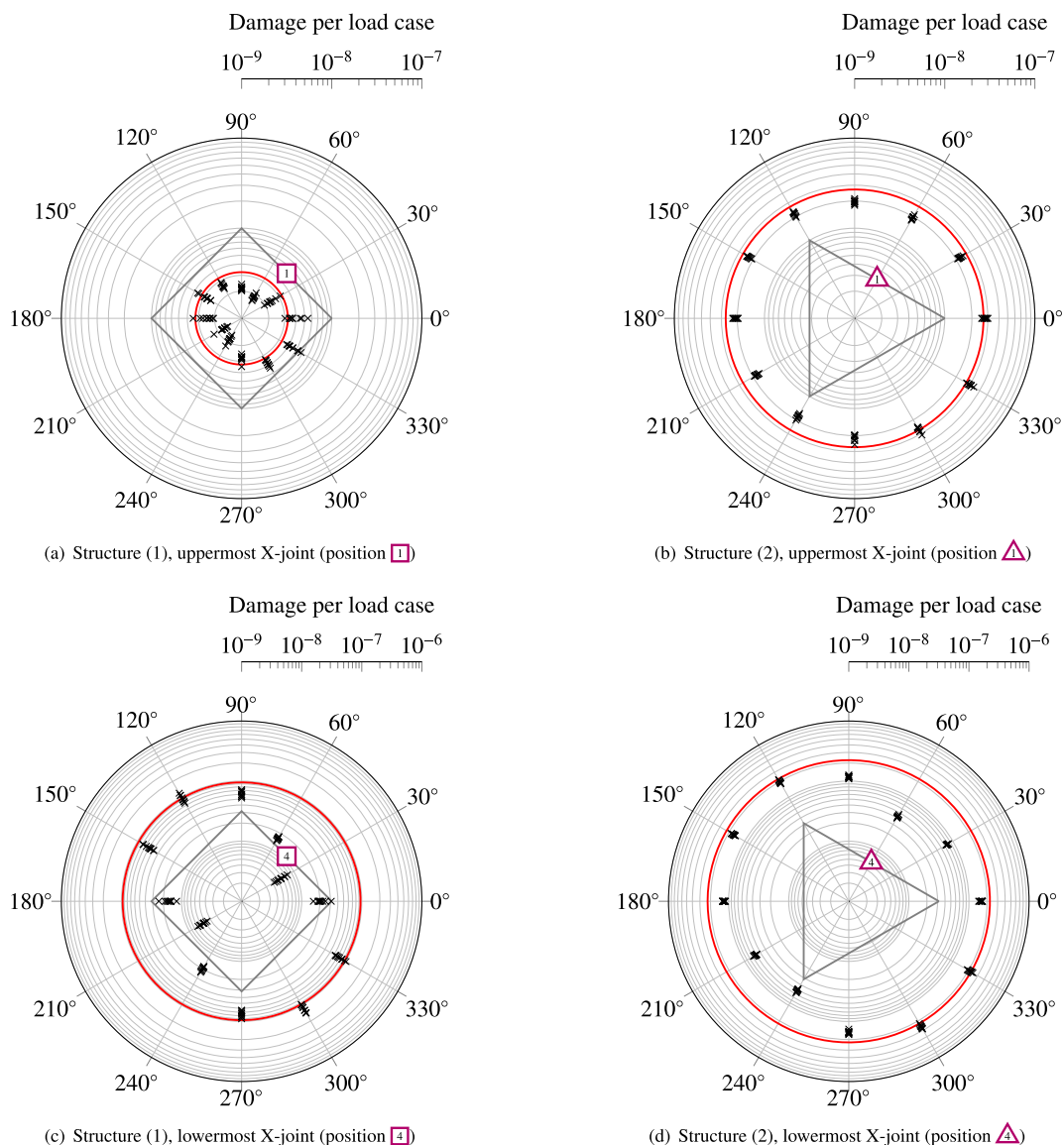
In time domain simulations for offshore wind turbines, the assumption of unidirectional wind, waves, and current is common practice. To prove this approach with respect to reliability of results, a new load set with the following properties is defined:

- Wind, wave, and current direction are assumed to be unidirectional. 12 directions are regarded for every structure from  $0^\circ$  to  $360^\circ$  in  $30^\circ$  steps.
- Each direction comprises 13 equidistant wind speed bins from  $2 \text{ ms}^{-1}$  to  $26 \text{ ms}^{-1}$ . An occurrence probability of each bin is calculated from the wind speed distribution and applied for the final fatigue assessment.
- 10 random representations of turbulent wind fields and wave kinematics are used for each combination of wind speed bin and direction.
- Wind speed dependent mean values of significant wave heights and peak periods are utilized.
- The yaw error is fixed to  $8^\circ$ .

Hence, all combinations result in  $12 \times 13 \times 10 = 1560$  simulations per jacket. The results are calculated for jackets (1) and (2) (3120 simulations in total) and illustrated in Fig. 6. The polar plots show the value of damage per load case dependent on the direction

of (aligned) wind, waves, and current. For comparison purposes, the mean damage value of the full load set is illustrated as a circle, too.

The diagrams show that the uncertainty due to stochastic representation of turbulent wind fields and wave kinematics is much lower than the uncertainty due to spreading environmental conditions (in contrast to common assumptions in literature). Compared to the probabilistic load set, the load set with unidirectional load set underestimates the occurring damages substantially for most directions. It is supposed that there are some reasons for this phenomenon. Mean values for wave conditions are presumed for the present load set. However, a linear change of significant wave height or period is related to a nonlinear damage amplification and the load cases with severe sea states have a quite low occurrence rate which is related to the wind speed distribution. In addition, the critical excitation direction concerning fatigue is the one perpendicular to the rotor symmetry axis (side-side), because aerodynamic damping affects mainly fore-aft motion. The unidirectional load set does not consider wind-/wave-/current-misalignment and only comprises load cases with wave and current heading parallel to the wind field direction. However, excitation directions aligned parallel to the regarded X-joint tier ( $-45^\circ = 315^\circ$  in case of four-legged jacket (1) and  $-30^\circ = 330^\circ$  in case of three-legged jacket (2)) result in damage values similar to the mean value obtained by the probabilistic load set. Therefore, it is worth analyzing this for all eight test jackets in the subsequent



**Fig. 6.** Damage assessment of unidirectional load set at regarded X-joints. Each × depicts the damage of a single load case in the corresponding wind speed and direction bin. The mean joint damage is illustrated by —, the contour of the corresponding jacket by —.

reduction study.

#### 4.4. Load set reduction

Based on the obtained knowledge, a new load set with a high degree of reduction is defined where noncritical directions and wind speed bins with either low damage values ( $2 \text{ ms}^{-1}$ ) or low occurrence probability ( $24 \text{ ms}^{-1}$ ,  $26 \text{ ms}^{-1}$ ) are neglected. Moreover, the number of stochastic representations for each combination of wind speed bin and direction is reduced to 3. The summary of differences compared to the load set defined in subsection 4.3 is:

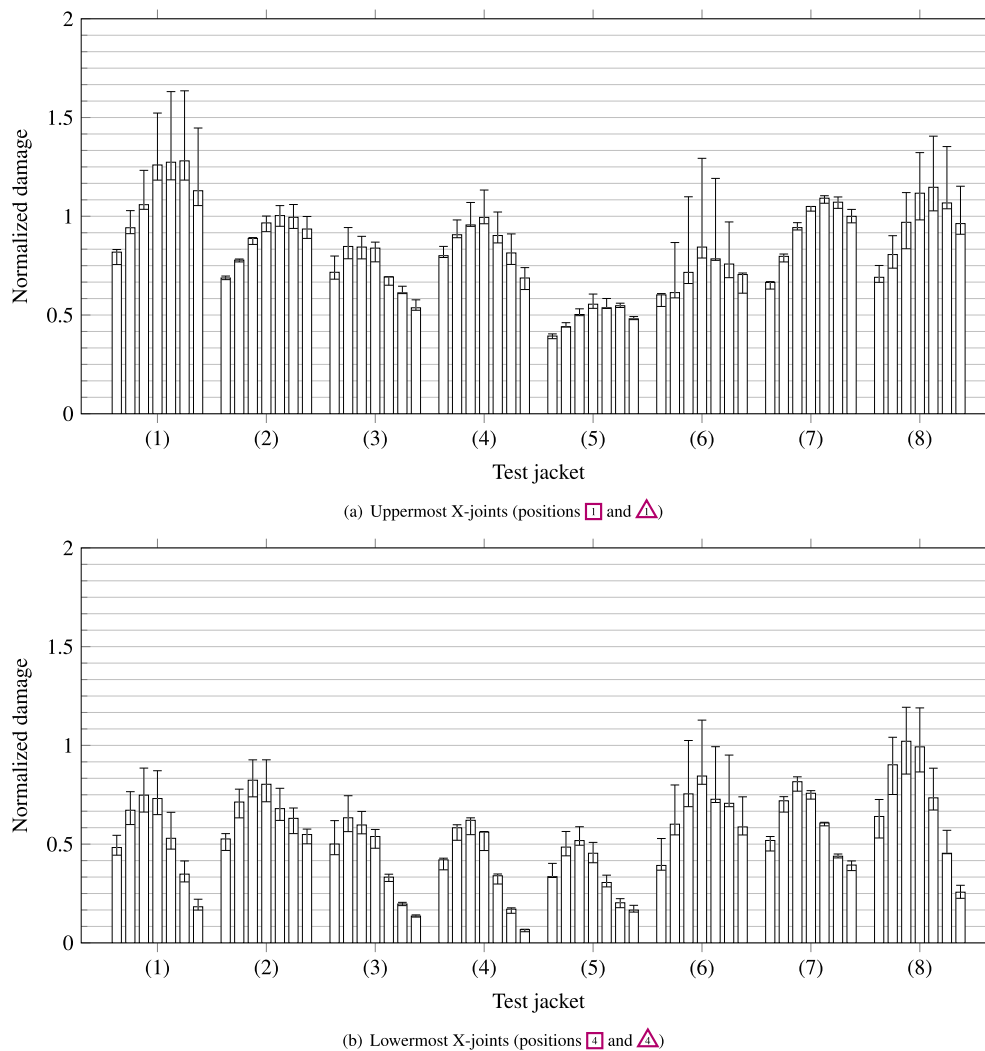
- 7 directions of wind, waves, and current are regarded for every structure from  $270^\circ$  to  $360^\circ$  in  $15^\circ$  steps.
- Each direction comprises 10 equidistant wind speed bins from  $4 \text{ ms}^{-1}$ – $22 \text{ ms}^{-1}$ . An occurrence probability of each bin is calculated from the wind speed distribution and applied for the final fatigue assessment.

- 3 random representations of turbulent wind fields and wave kinematics are used for each combination of wind speed bin and direction.

The size of this load set is  $7 \times 10 \times 3 = 210$  which enables the calculations for all eight test jackets (1) to (2) as defined in Table 4, requiring 1680 simulations. The results are compared to a reduced probabilistic load set with 512 samples for each test jacket (4096 simulations in total, where  $2 \times 512 = 1024$  have already been calculated for the full load set, therefore 3072 additional simulations). The normalized median damage values (with respect to the probabilistic load set) obtained by this load set are illustrated in Fig. 7 for the uppermost and lowermost X-joint layers and all eight test jackets. All direction bins are shown from left to right. Error bars show the minimum and maximum values, too.

From the results, it can be stated that the occurring damage values are generally in the same dimensions as the mean damages. There is no test structure where the normalized damage is below a value of 0.5. Therefore, it is imaginable to utilize this reduced load





**Fig. 7.** Normalized damages with reduced, unidirectional load set for test jackets (1) to (8) compared to mean damage obtained by reduced probabilistic load set with 512 design load cases. Each bar represents the median damage value in the corresponding direction bins from 270° to 360° in 15° steps, error bars show minimum and maximum values. Value of 1 means that the damage value is equal to the mean damage.

set for damage estimation by applying a safety factor in the dimension of 2. It is noticeable that the uppermost X-joint position, shown in Fig. 7(a), is related to higher normalized fatigue damages, where the values tend to be slightly overestimated for some structures, than the lowermost position in Fig. 7(b), for instance jackets (1), (7), and (8). Jacket (5) is the one where the damages are underestimated for both regarded joints. In general, it can be adhered to the assumption unidirectional load sets are significant for jacket substructures concerning fatigue limit state, when considering a safety factor.

## 5. Benefits and limits of the approach

The present work compares different methods to reduce fatigue limit state design load sets for time domain simulations of offshore wind turbine jacket substructures. Previous approaches in literature addressing this topic consider the environmental impact on the turbine mainly by variations of wind speed and different stochastic representations of turbulent wind fields or wave kinematics. However, though this procedure is straightforward at first sight, several environmental influence quantities are often disregarded. In this work, measured data from the research platform

FINO3 is the basis for a comprehensive fatigue study on jackets involving the effects of wind, waves, and current (each including kinematics and directions). Results are computed for eight artificial test structures very close to real applications. Though the comprehensive fatigue assessment is only performed for two jackets, this study is the first one that considers the impact of realistic environmental conditions on fatigue of multiple jacket structures. With 11 968 full-coupled simulations in total, the present work depicts a comprehensive study on fatigue of jacket substructures.

Of course, this study has still shortcomings due to limited numerical capacity or imprecise knowledge about some environmental conditions. Firstly, the study's main limitation is that the demand on numerical capacity is indeed very high. Therefore, the full load set was only applied to two test structures. In order to obtain knowledge about multiple structures, a reduced load set was defined. However, this load set depicts a simplification of the environmental conditions. Secondly, some limitations arise from partly conservative load assumptions. The environmental data was extrapolated from a water depth of 22 m to 50 m. Wind speeds are binned and the turbulence intensity is set to the mean value for each bin, because the wind data has to be calculated prior to all

simulations. The near-surface current has been modeled according to a power law and assumed to be aligned with wind direction. It is to be analyzed whether all these shortcomings weaken the general statement of the reduction study.

## 6. Conclusion

The fatigue limit state design directs the design of jacket substructures. Therefore, it is worth reconsidering the general methodology that leads to the corresponding design load sets. The core innovation of this work is the utilization of comprehensive environmental data as a basis for a structural fatigue assessment of jacket substructures for offshore wind turbines. In this article, four leading questions have been pretended to address recent topics in literature and there is an answer to all of them. Firstly, it can be concluded that there is a high scatter of damage values in each wind speed bin of the full load set results which is significantly higher than the scatter arising from different random representations of turbulent wind fields or wave kinematics. For this reason, it is necessary to face the effect of uncertainty in the damage calculation. In this context, there exist several approaches. A conservative one might be to apply (constant) safety factors to the calculated damages which is a state-of-the-art procedure. Secondly, with regard to numerical efficiency, there is a lot of improvement potential as shown in the reduction study. When considering only a partial quantity of the full load set as design basis, it is still possible to predict percentiles of the mean damage per load case for a given level of significance. One finding in this study is that the estimation mistake increases much slower than the level of reduction. Hence, a quite high quantity of reduction is imaginable for these load sets. Thirdly, the approach of unidirectional wind and waves (and current, if considered), which depicts a state-of-the-art technique in load preestimation, has been proven to be an approach that tends to underestimate the occurring structural damages for many directions. This might cause massive miscalculations, if wrong directions are considered. This leads to the answer of the fourth question: An efficient load set must discard design load cases that have no significant effect on the damage assembly, when knowing the probability distributions of environmental conditions. In this study, this was addressed by a reduced load set which showed that unidirectional load sets depict a significant reduction for jacket substructures with regard to fatigue limit state. An efficient load set reduction can decrease the levelized costs of energy significantly, because it increases the number of possible design iterations in the design process and leads to less expensive structures. Further studies will have to address the issue that damage characteristics might change for many different structural designs. It is imaginable that a lot of numerical capacity will be required for this purpose.

## Acknowledgements

We gratefully acknowledge the financial support of the German Federal Ministry for Economic Affairs and Energy (research project Gigawind life, FKZ 0325575A), the Lower Saxony Ministry of Science and Culture (research project ventus efficiens, FKZ ZN3024) and the European Commission (research project IRPWind, funded from the European Union's Seventh Framework Programme for research, technological development, and demonstration under grant agreement number 609795) that enabled this work.

This work was supported by the compute cluster which is funded by the Leibniz Universität Hannover, the Lower Saxony Ministry of Science and Culture (MWK), and the German Research

Foundation (DFG).

## References

- [1] C. Bak, R. Bitsche, A. Yde, T. Kim, M.H. Hansen, F. Zahle, M. Gaunaa, J. Blasques, M. Døssing, J.-J. Wedel Heinen, T. Behrens, Light Rotor: the DTU 10-MW reference wind turbine, in: EWEA 2012 – European Wind Energy Conference & Exhibition, Copenhagen, 2012.
- [2] C. Bak, F. Zahle, R. Bitsche, T. Kim, A. Yde, L.C. Henriksen, M.H. Hansen, J. Blasques, M. Gaunaa, A. Natarajan, The DTU 10-MW reference wind turbine, in: Danish Wind Power Research, Fredericia, 2013.
- [3] F. Zahle, C. Bak, R. Bitsche, T. Kim, M.H. Hansen, A. Yde, Towards an integrated design complex for wind turbines, in: The 2nd NREL Wind Energy Systems Engineering Workshop, Broomfield, CO, 2013.
- [4] T. von Borstel, Design Report Reference Jacket, Tech. Rep. INNWIND.EU Deliverable D4.3.1, 2013.
- [5] M. Stolpe, W.N. Wandji, A. Natarajan, R. Shirzadeh, M. Kühn, D. Kaufer, Innovative Design of a 10MW Steel-type Jacket, Tech. Rep. INNWIND.EU Deliverable D4.3.4, 2016.
- [6] J. Häfele, C.G. Gebhardt, R. Rolfes, Innovative Design of a Hybrid-type Jacket for 10MW Turbines, Tech. Rep. INNWIND.EU Deliverable D4.3.5, 2016.
- [7] S. Schaffhirt, D. Zwick, M. Muskulus, Reanalysis of jacket support structure for computer-aided optimization of offshore wind turbines with a genetic algorithm, *J. Ocean Wind Energy* 1 (4) (2014) 209–216.
- [8] J. Oest, R. Sørensen, L.C.T. Overgaard, E. Lund, Structural optimization with fatigue and ultimate limit constraints of jacket structures for large offshore wind turbines, *Struct. Multidiscip. Optim.* 55 (2016) 779–793, <https://doi.org/10.1007/s00158-016-1527-x>.
- [9] J. Häfele, R. Rolfes, Approaching the ideal design of jacket substructures for offshore wind turbines with a Particle Swarm Optimization algorithm, in: Proceedings of the Twenty-sixth (2016) International Offshore and Polar Engineering Conference, Rhodes, Greece, 2016, pp. 156–163.
- [10] A. Morató, S. Sriramula, N. Krishnan, J. Nichols, Ultimate loads and response analysis of a monopile supported offshore wind turbine using fully coupled simulation, *Renew. Energy* 101 (2017) 126–143, <https://doi.org/10.1016/j.renene.2016.08.056>.
- [11] International Electrotechnical Commission, Wind Turbines – Part 3: Design Requirements for Offshore Wind Turbines, Norm IEC-61400-3:2009, EN 61400-3:2009, 2009.
- [12] H.S. Toft, L. Svenningsen, J.D. Sørensen, W. Moser, M.L. Thøgersen, Uncertainty in wind climate parameters and their influence on wind turbine fatigue loads, *Renew. Energy* 90 (2016) 352–361, <https://doi.org/10.1016/j.renene.2016.01.010>.
- [13] D. Zwick, M. Muskulus, The simulation error caused by input loading variability in offshore wind turbine structural analysis, *Wind Energy* 18 (8) (2015) 1421–1432, <https://doi.org/10.1002/we.1767>.
- [14] J.M. Jonkman, S. Butterfield, W. Musial, G. Scott, Definition of a 5-MW Reference Wind Turbine for Offshore System Development, Technical Report NREL/TP-500-38060, National Renewable Energy Laboratory, Golden, CO, 2009.
- [15] D. Zwick, M. Muskulus, Simplified fatigue load assessment in offshore wind turbine structural analysis, *Wind Energy* 19 (2) (2016) 265–278, <https://doi.org/10.1002/we.1831>.
- [16] T. Fischer, W. de Vries, B. Schmidt, Upwind Design Basis, Tech. rep., 2010.
- [17] G.M. Stewart, A. Robertson, J. Jonkman, M.A. Lackner, The creation of a comprehensive metocean data set for offshore wind turbine simulations, *Wind Energy* 19 (6) (2015) 1151–1159, <https://doi.org/10.1002/we.1881>.
- [18] G.M. Stewart, Design Load Analysis of Two Floating Offshore Wind Turbine Concepts, Ph.D. thesis, University of Massachusetts, 2016.
- [19] M. Hansen, B. Schmidt, B. Ernst, J. Seume, M. Wilms, A. Hildebrandt, T. Schlurmann, M. Achmus, K. Schmoor, P. Schaumann, S. Kelma, J. Goretzka, R. Rolfes, L. Lohaus, M. Werner, G. Poll, R. Böttcher, M. Wehner, F. Fuchs, S. Brenner, Probabilistic Safety Assessment of Offshore Wind Turbines, Tech. rep., Leibniz Universität Hannover, 2015.
- [20] NordNordWest/Wikipedia, Location Map of the North Sea, Online and published under CC-BY-SA-3.0-DE (<https://creativecommons.org/licenses/by-sa/3.0/de/legalcode>), 2010, [commons.wikimedia.org/wiki/File:North\\_Sea\\_location\\_map.svg](https://commons.wikimedia.org/wiki/File:North_Sea_location_map.svg). (Accessed 9 January 2017).
- [21] C. Hübler, C. G. Gebhardt, R. Rolfes, Development of a Comprehensive Data Basis of Scattering Environmental Conditions and Simulation Constraints for Offshore Wind Turbines, (Wind Energy Science Discussion).
- [22] B. Ernst, J.R. Seume, Investigation of site-specific wind field parameters and their effect on loads of offshore wind turbines, *Energies* 5 (10) (2012) 3835–3855, <https://doi.org/10.3390/en5103835>.
- [23] B. Schmidt, M. Hansen, S. Marx, Directional dependence of extreme load parameters for offshore wind turbines, in: Proceedings of the Twenty-fifth (2015) International Offshore and Polar Engineering Conference, Kona, HI, 2015, pp. 21–26.
- [24] Germanischer Lloyd, Guideline for the Certification of Offshore Wind Turbines, Offshore Standard, 2012.
- [25] C. Hübler, C.G. Gebhardt, R. Rolfes, Hierarchical four-step global sensitivity analysis of offshore wind turbines based on aeroelastic time domain simulations, *Renew. Energy* 111 (2017) 878–891, <https://doi.org/10.1016/j.renene.2017.05.013>.

- [26] P. Schaumann, C. Böker, Influence of wave spreading in short-term sea states on the fatigue of offshore support structures at the example of the FINO1-research platform, *DEWI Mag.* 30 (2007) 51–57.
- [27] A. Natarajan, in: *Impact of Model Uncertainties on the Design Loads of Large Wind Turbine Jacket Foundations*, Offshore, Amsterdam, 2011.
- [28] A. Hildebrandt, *Hydrodynamics of Breaking Waves on Offshore Wind Turbine Structures*, Ph.D. thesis, Leibniz Universität Hannover, 2013.
- [29] J.M. Jonkman, W. Musial, *Offshore Code Comparison Collaboration (OC3) for IEA Task 23 Offshore Wind Technology and Deployment*, Technical Report NREL/TP-5000-48191, National Renewable Energy Laboratory, Golden, CO, 2010.
- [30] W. Dong, T. Moan, Z. Gao, Fatigue reliability analysis of the jacket support structure for offshore wind turbine considering the effect of corrosion and inspection, *Reliab. Eng. Syst. Saf.* 106 (2012) 11–27, <https://doi.org/10.1016/j.res.2012.06.011>.
- [31] H.F. Veldkamp, *Chances in Wind Energy – a Probabilistic Approach to Wind Turbine Fatigue Design*, Ph.D. thesis, Delft University of Technology, 2006.
- [32] N.K. Vemula, T. Fischer, W. de Vries, A. Cordle, B. Schmidt, *Design Solution for the Upwind Reference Offshore Support Structure*, Tech. Rep. Upwind deliverable report D4.2.5, 2010.
- [33] J. Häfele, C. Hübler, C.G. Gebhardt, R. Rolfes, An improved two-step soil-structure interaction modeling method for dynamical analyses of offshore wind turbines, *Appl. Ocean Res.* 55 (2016) 141–150, <https://doi.org/10.1016/j.apor.2015.12.001>.
- [34] American Petroleum Institute, *Recommended Practice for Planning, Designing and Constructing Fixed Offshore Platforms – Working Stress Design*, Recommended Practice RP 2A-WSD, 2002.
- [35] W. Popko, F. Vorpahl, A. Panagiotis, Investigation of local vibration phenomena of a jacket sub-structure caused by coupling with other components of an offshore wind turbine, *J. Ocean Wind Energy* 1 (2014) 111–118.
- [36] W. Popko, S. Georgiadou, E. Loukogeorgaki, F. Vorpahl, Influence of joint flexibility on local dynamics of a jacket support structure, *J. Ocean Wind Energy* 3 (1) (2016) 1–9, <https://doi.org/10.17736/jowe.2016.jcr45>.
- [37] DNV GL AS, *RP-C203: Fatigue Design of Offshore Steel Structures*, Recommended Practice DNVGL-RP-0005:2014-06, 2014.
- [38] M. Efthymiou, S. Durkin, Stress concentrations in t/y and gap/overlap k-joints, in: *Proceedings of the 4th International Conference on Behaviour of Offshore Structures*, Delft, 1985, pp. 429–441.
- [39] B.H. Hammerstad, M. Schafhirt, Sebastianand Muskulus, On fatigue damage assessment for offshore support structures with tubular joints, *Energy Procedia* 94 (2016) 339–346.

## 4 Accurate and numerically efficient formulation of the jacket optimization problem

The research article proposes a jacket model along with models for costs and structural code checks. It is published in *Wind Energy Science*, Vol. 3, 2018, pp. 553–572 (DOI: 10.5194/wes-3-553-2018).

### Author contributions

Jan Häfele is the corresponding author of the publication and the main author of all sections.

Rick Damiani gave technical and editorial suggestions for improvement of the entire publication, in particular concerning all topics related to jacket substructures.

Ryan King gave technical and editorial suggestions for improvement of the entire publication, in particular concerning surrogate modeling.

Cristian Guillermo Gebhardt gave technical and editorial suggestions for improvement of the entire publication.

Raimund Rolfes gave technical and editorial suggestions for improvement of the entire publication and performed the final proofreading.



# A systematic approach to offshore wind turbine jacket predesign and optimization: geometry, cost, and surrogate structural code check models

Jan Häfele<sup>1</sup>, Rick R. Damiani<sup>2</sup>, Ryan N. King<sup>2</sup>, Cristian G. Gebhardt<sup>1</sup>, and Raimund Rolfes<sup>1</sup>

<sup>1</sup>Leibniz Universität Hannover, Institute of Structural Analysis, Appelstr. 9a, 30167 Hanover, Germany

<sup>2</sup>National Renewable Energy Laboratory, 15013 Denver West Parkway, Golden, CO 80401, USA

**Correspondence:** Jan Häfele (j.haeefe@isd.uni-hannover.de)

Received: 6 May 2018 – Discussion started: 18 May 2018

Revised: 23 July 2018 – Accepted: 6 August 2018 – Published: 23 August 2018

**Abstract.** The main obstacles in preliminary design studies or optimization of jacket substructures for offshore wind turbines are high numerical expenses for structural code checks and simplistic cost assumptions. In order to create a basis for fast design evaluations, this work provides the following: first, a jacket model is proposed that covers topology and tube sizing with a limited set of design variables. Second, a cost model is proposed that goes beyond the simple and common mass-dependent approach. And third, the issue of numerical efficiency is addressed by surrogate models for both fatigue and ultimate limit state code checks. In addition, this work shows an example utilizing all models. The outcome can be utilized for preliminary design studies and jacket optimization schemes. It is suitable for scientific and industrial applications.

**Copyright statement.** The U.S. government retains, and the publisher, by accepting the article for publication, acknowledges that the U.S. government retains a nonexclusive, paid-up, irrevocable, worldwide license to publish or reproduce the published form of this work, or allow others to do so, for U.S. government purposes.

## 1 Introduction

In the oil and gas industry, the jacket substructure is well established due to a good trade-off between cost efficiency and reliability. It has been considered for offshore wind turbine substructures for several years and has already had some successful applications in Europe and the United States. Smith et al. (2015) showed that among all wind farms announced to be built from the second quarter of 2015 until 2020, 16 % of the substructures are jackets, whereas this share was only 10 % for wind farms built before 2015 (see Fig. 1 for the market shares of offshore wind turbine substructures in the past and present). Despite potential advantages, the market is still strongly dominated by monopiles (Ho et al., 2016), as financial aspects and significantly lower uncertainty play an important role from an economical point

of view (BVGassociates, 2012). However, the development of new turbines with higher rated power in combination with the need for deeper water installations might be a catalyst for a technological leap toward jacket substructures. Damiani et al. (2016) calculated that for water depths deeper than 40 m jackets promise lower costs than monopiles, considering six offshore sites along the US Eastern Seaboard and the Gulf of Mexico. The break-even point or water depth at which the jacket technology becomes truly competitive is, however, dependent on the costs of the vessels used to transport and install the structures. State-of-the-art jackets can still benefit from design studies and structural optimization to render lower costs to the project (BVGassociates, 2013), which is addressed by current research. The accumulation of publications dealing with this topic in the recent past is a confirmation of this statement. Chew et al. (2016) and Oest et al. (2016) performed structural optimization of jacket substructures with simulation-based approaches using gradient-based algorithms. The basis for these papers was the structure defined in the first phase of the Offshore Code Comparison Collaboration Continuation (OC4) project (Popko et al., 2014). Damiani et al. (2017) studied the impact of environmental

and turbine parameters on the costs or mass of jackets, considering 81 different structures. Hübler et al. (2017b) analyzed the effect of variations in jacket design on the economic viability. AlHamaydeh et al. (2017) and Kaveh and Sabeti (2018) used meta-heuristic algorithms for the optimization of jacket substructures but without realistic – in particular, fatigue limit state – load assumptions. Stolpe and Sandal (2018) introduced discrete variables in the jacket optimization problem formulation to account for the fact that steel tubes are only available in fixed dimensions.

From a global perspective, the main obstacles that lead to nonoptimal structures are both the dependence on expert knowledge and the large computational cost associated with the optimization of a complex structure. Many design assessments or optimization approaches addressing this problem fail (because they lead to either unrealistic or impractical design) for the following simple reasons.

- *Design variables.* Most approaches do not consider the structural topology, but only the sizing of predefined members. Involving topological parameters, which may be real or discrete, as design variables is mandatory for a proper design that makes use of a mixed-integer formulation.
- *Cost assumptions.* Often, the mass of the entire jacket is used as an objective function in optimization approaches. But obviously, the cost breakdown for a welded structure includes many items that do not depend on the mass of the structure. Moreover, other expenses such as transport and installation costs should not be ignored.
- *Load assumptions.* The assumption of simplified environmental states (for instance, the omission of wind-wave misalignment) is the state of the art in many jacket design procedures because it relaxes the computational demand and fills any existing gap in the knowledge of the actual metocean conditions.
- *Structural code checks.* A realistic jacket design involves structural design code checks for fatigue and ultimate limit state based on time domain simulations. Many approaches miss either one or both of them, most likely because the computational implementation is resource intensive.
- *Simulation approaches.* Design iterations cause changes in the structural behavior. A coupled simulation or at least a rigorous approach addressing this aspect is mandatory. However, it is often seen that sequential approaches are applied when decoupled loads are exchanged at the interface between substructure and turbine tower, even in the case of fatigue assessment.

One possible approach to address some of these issues was the jacket sizing tool proposed by Damiani and Song (2013),

which enables conceptual design by considering preliminary load assumptions. It, however, lacked extensions to full dynamics simulations and fatigue limit states. Wind turbine cost models are available (Fingersh et al., 2006; National Wind Technology Center Information Portal, 2014) and were used for the definition of wind turbine optimization objectives and constraints (Ning et al., 2013), but without explicit or detailed cost formulations for jacket substructures. The goal of the current work is to provide a basic jacket model that can be efficiently used in conceptual studies and optimization approaches by providing a basis for more realistic designs and mainly using mathematically manageable equations. Or, in other words, the main innovation of this study is a basic jacket model that prevents the issues stated above. The first part of this study addresses the first two points described above. The last three points are handled in the second part, as they involve a completely different field. This paper is structured as follows: Sect. 2 explains the utilized jacket model with the assumptions made for the structural details. In Sect. 3, a simple cost model is proposed, which covers cost contributions from materials, fabrication, transition piece, coating, and transport and installation (including foundation). In Sect. 4, load sets are defined for both fatigue and ultimate limit state load cases and a design of experiments is created to fit appropriate surrogate models. The paper concludes with remarks on the benefits of the jacket model, its limitations, and a brief outlook on further work based on this model.

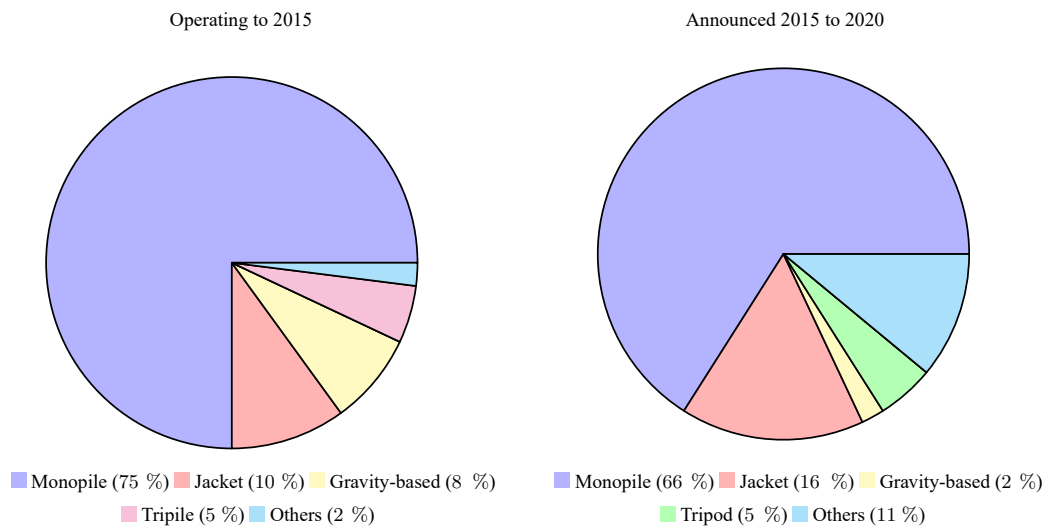
## 2 Jacket model

The previous section summarized some issues leading to certain requirements of a simple jacket model.

- The set of design variables must be as comprehensive as necessary to accurately model the fundamental topology, physics, and dynamics of a typical jacket but as small as possible for ease of computation, too.
- The design variables must cover both topological and geometrical parameters.
- Structural details with little bearing on the mechanical behavior shall be disregarded.
- The cost model formulation shall only depend on the parameters of the jacket model.
- The structure shall be manufacturable, transportable, and installable.
- The structure shall be easily transferable to common design tools (mostly based on finite-element formulations).

A concept matching all of these points was initially described by Häfele and Rolfes (2016) and is extended in this section.





**Figure 1.** Share of utilized substructures among operating turbines in 2015 and from 2015 to 2020 according to Smith et al. (2015).

First, the topology is defined; then the tube dimensions and material properties are derived.

### 2.1 Topology

The main presumption is that the jacket model need not be limited to a certain number of legs or brace layers (bays), but instead allows for different topologies. As foot and head girth are measures related to four-legged structures, a general formulation in terms of foot (on the ground layer) and head (on the same layer as the transition piece) circles with foot and head radii  $R_{Foot}$  and  $R_{Head}$ , respectively, is introduced. In order to prevent obtaining structures with a funnel shape, a parameter,  $\xi$ , is introduced, which relates the two radii (and can be set to a value less than or equal to 1). The two circles depict the bottom and top of a frustum of length,  $L$  (see Fig. 2a). The  $N_L$  legs can then be constructed as straight lines on the surface of the cone, equidistantly distributed. This is illustrated for a four-legged jacket in Fig. 2b. However, this procedure is applicable to every number of legs that is greater than or equal to three. With these variables, the angle enclosed by two legs can be found according to the following equation:

$$\vartheta = \frac{2\pi}{N_L}. \tag{1}$$

The spatial batter angle,  $\Phi_s$ , is the inclination angle of each leg with respect to the symmetry axis of the frustum (sometimes denoted as the three-dimensional batter angle):

$$\Phi_s = \arctan\left(\frac{R_{foot}(1-\xi)}{L}\right). \tag{2}$$

The planar batter angle,  $\Phi_p$ , is the inclination angle projected to a vertical–horizontal layer through the symmetry axis of

the frustum (sometimes denoted as the two-dimensional batter angle):

$$\Phi_p = \arctan\left(\frac{R_{foot}(1-\xi)\sin\left(\frac{\vartheta}{2}\right)}{L}\right). \tag{3}$$

The parameter,  $N_X$ , defines the number of bays. A bay is one part of the jacket that is delimited by  $N_L$  double-K joints at the lower side and  $N_L$  double-K joints at the upper side and comprises all structural elements in between, in particular  $N_X$  X joints. The  $i$ th bay is denoted with  $i$ , where

$$i \in \mathbb{N}^{[1, N_X]}. \tag{4}$$

The ratio,  $q$ , relates the heights of two consecutive bays,  $L_{i+1}$  and  $L_i$ , which is assumed to be constant:

$$q = \frac{L_{i+1}}{L_i}. \tag{5}$$

It has to be noted that  $L_1$  is the height of the lowest bay and  $L_{N_X}$  is the height of the highest one. Based on previous assumptions and elementary geometrical considerations, circles on every double-K joint layer can be constructed. With the height of the entire jacket,  $L$ , the distance between the ground and lowest bay,  $L_{OSG}$ , and the distance between the transition piece and highest bay,  $L_{TP}$ , the  $i$ th jacket bay height,  $L_i$ , can be calculated by

$$L_i = \frac{L - L_{OSG} - L_{TP}}{\sum_{n=1}^{N_X} q^{n-i}}. \tag{6}$$

The radius of each bay (at the lower double-K joint layer),  $R_i$ , is

$$R_i = R_{foot} - \tan(\Phi_s) \left( L_{OSG} + \sum_{n=1}^{i-1} L_n \right). \tag{7}$$

This step is shown in Fig. 2c. The distance between the lower layer of double-K joints and the layer of X joints for the  $i$ th bay,  $L_{m,i}$ , can be calculated by simple geometrical relations:

$$L_{m,i} = \frac{L_i R_i}{R_i + R_{i+1}}. \quad (8)$$

The radius of the  $i$ th X joint layer is

$$R_{m,i} = R_{\text{foot}} - \tan(\Phi_s) \left( L_{\text{OSG}} + \sum_{n=1}^{i-1} L_n + L_{m,i} \right). \quad (9)$$

The lower and upper brace-to-leg connection angles,  $\psi_{1,i}$  and  $\psi_{2,i}$ , respectively, and the brace-to-brace connection angle,  $\psi_{3,i}$ , in the  $i$ th bay are related by trigonometrical relations (see Fig. 3):

$$\psi_{1,i} = \frac{\pi}{2} - \arctan\left(\frac{R_{\text{foot}}(1-\xi)\sin\left(\frac{\vartheta}{2}\right)\cos(\Phi_p)}{L}\right) - \arctan\left(\frac{L_{m,i}}{R_i \sin\left(\frac{\vartheta}{2}\right)\cos(\Phi_p)}\right), \quad (10)$$

$$\psi_{2,i} = \frac{\pi}{2} + \arctan\left(\frac{R_{\text{foot}}(1-\xi)\sin\left(\frac{\vartheta}{2}\right)\cos(\Phi_p)}{L}\right) - \arctan\left(\frac{L_{m,i}}{R_i \sin\left(\frac{\vartheta}{2}\right)\cos(\Phi_p)}\right), \quad (11)$$

$$\psi_{3,i} = 2 \arctan\left(\frac{L_{m,i}}{R_i \sin\left(\frac{\vartheta}{2}\right)\cos(\Phi_p)}\right). \quad (12)$$

In addition,  $L_{\text{MSL}}$  is the distance between the transition piece (which is at the same height as the tower foot) and mean sea level layer or, in other words, the difference between jacket length and water depth. This information is necessary to create a mesh for the computation of hydrodynamic loads. The flag,  $x_{\text{MB}}$ , determines whether the jacket is equipped with mud braces or not. The final topology is illustrated in Fig. 2d, in this example with four legs ( $N_L = 4$ ), four bays ( $N_X = 4$ ), and a mud brace ( $x_{\text{MB}} = \text{true}$ ).

## 2.2 Tube dimensions

The proposed jacket model makes no use of prefabricated joints (as in the state of the art), and no joint cans or stiffeners (mainly to improve punching shear resistance) are used. The consequences of only single-sided welds and no stiffened joints should be considered. However, the number of (expensive) welds is reduced to a minimum, which reduces the number of degrees of freedom in a structural analysis as well. Moreover, the cost model is not burdened by possible impacts of series manufacturing for prefabricated joints. This is not far away from practical application: it was analyzed for substructures with a rated power higher than 10 MW in the research project INNWIND.EU and evaluated as the most efficient one concerning fabrication costs (Scholle et al., 2015).

Instead of regarding the diameters and thicknesses of each tube as independent variables, which would lead – depending on the structural topology – to a high number of design variables, the tube dimensions are interpolated between values at the top and the bottom of the structure. Another potential problem is that the tube dimensions, if all are regarded as independent, might lead to undesirable relations between the tube dimensions. Standards and guidelines provided by DNV GL AS (2016b, a) for the design and certification of offshore structures propose the adoption of three ratio parameters initially defined by Efthymiou (1988). However, one variable has to be independent; in our case, it is the leg diameter,  $D_L$ , which is assumed to be constant.

$\gamma_b$  and  $\gamma_t$  define the ratios between leg radii (not the diameters) and thicknesses:

$$\gamma_b = \frac{D_L}{2T_{Lb}}, \quad (13)$$

$$\gamma_t = \frac{D_L}{2T_{Lt}}, \quad (14)$$

where the index  $b$  indicates the affiliation to the lowermost (bottom) and  $t$  to the uppermost (top) tubes. The parameters  $\beta_b$  and  $\beta_t$  define the ratios of brace and leg diameter at the bottom and top, respectively:

$$\beta_b = \frac{D_{Bb}}{D_L}, \quad (15)$$

$$\beta_t = \frac{D_{Bt}}{D_L}. \quad (16)$$

The values  $\tau_b$  and  $\tau_t$  define the relations between brace and leg thicknesses at the bottom and top, respectively:

$$\tau_b = \frac{T_{Bb}}{T_{Lb}}, \quad (17)$$

$$\tau_t = \frac{T_{Bt}}{T_{Lt}}. \quad (18)$$

The final determination of the leg and brace dimensions as functions of the height elevation is illustrated in Figs. 4 and 5. The values  $\gamma_i$ ,  $\beta_i$ , and  $\tau_i$  can be calculated as follows:

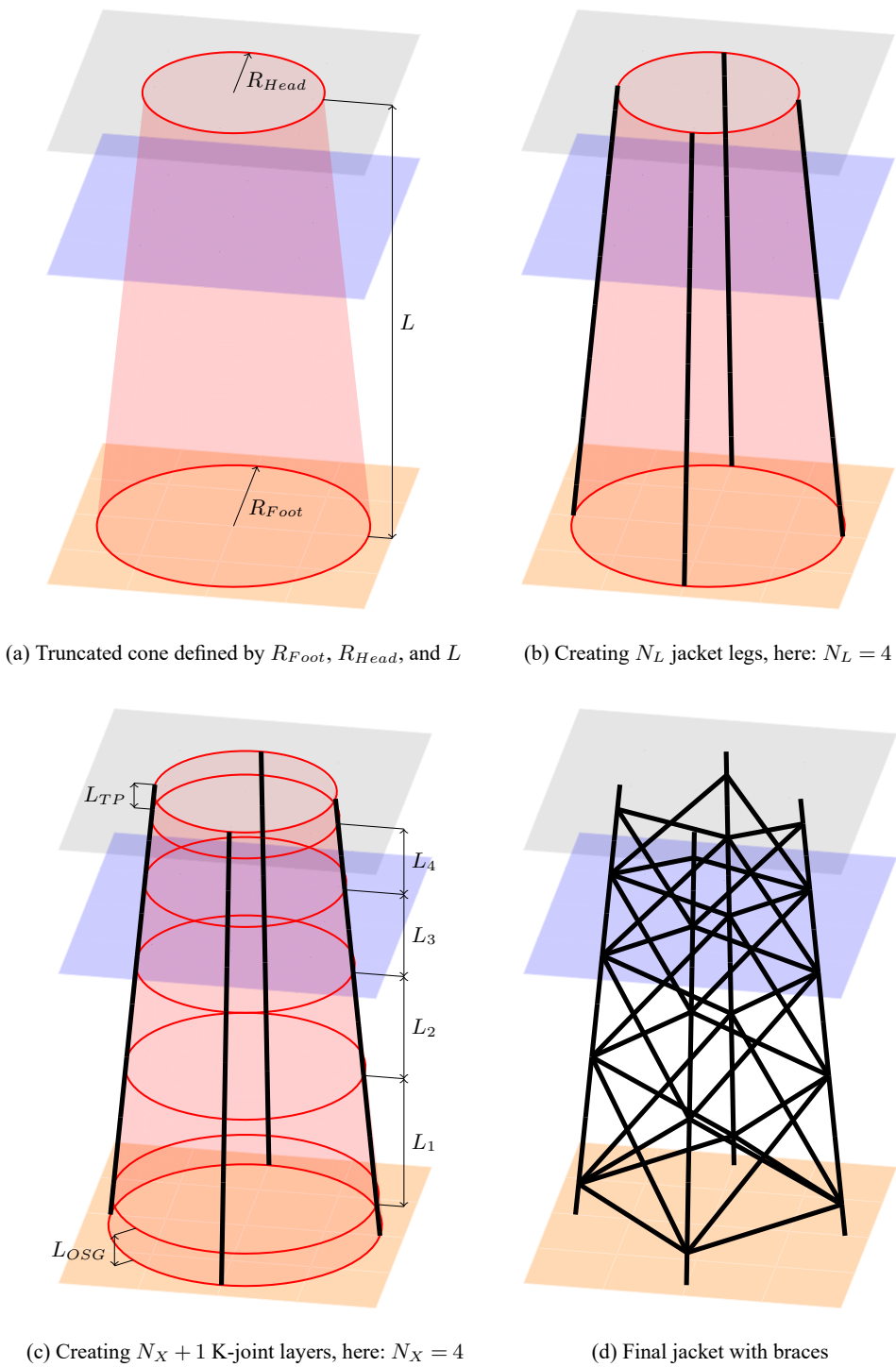
$$\gamma_i = \begin{cases} \gamma_b, & i = 1 \\ \frac{(\gamma_t - \gamma_b)(L_{\text{OSG}} + \sum_{n=1}^{i-1} L_n + L_{m,i})}{L - L_{N_X} + L_{m,N_X} - L_{\text{TP}}} + \gamma_b & \text{else,} \end{cases} \quad (19)$$

$$\beta_i = \frac{\beta_t - \beta_b}{L - L_{N_X} - L_{\text{OSG}} - L_{\text{TP}}} \sum_{n=1}^{i-1} L_n + \beta_b, \quad (20)$$

$$\tau_i = \frac{\tau_t - \tau_b}{L - L_{N_X} - L_{\text{OSG}} - L_{\text{TP}}} \sum_{n=1}^{i-1} L_n + \tau_b. \quad (21)$$

These equations depict a linear-stepwise interpolation from the values at the bottom (index  $b$ ) to the top (index  $t$ ). To allow for a smooth transition of the leg thicknesses on the height of the double-K joints, steps of  $\gamma_i$  are located on the



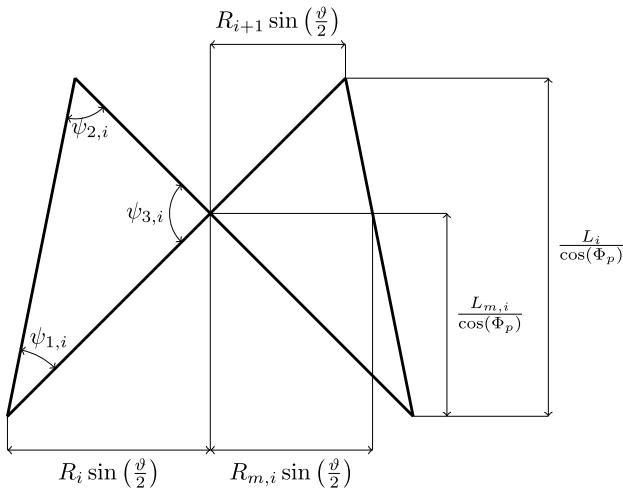


**Figure 2.** Creation of the jacket topology in four steps.

height of the X joints. Steps of  $\beta_i$  and  $\tau_i$  are located on the height of the double-K joints in order to enable the use of constant tube sizes in each bay.

### 2.3 Material properties

The entire jacket is supposed to be made of the same isotropic material, which can be described by the Young's



**Figure 3.** The  $i$ th jacket bay topology projected to the layer of X and double-K joints on one side of the structure.

modulus,  $E$ , the shear modulus,  $G$ , and the material density,  $\rho$ .

#### 2.4 Parameter summary and array of design variables

There are 20 parameters of the jacket model in total: 10 describe the topology, 7 the tube dimensions, and 3 the material properties. It can be assumed that site- and material-dependent parameters are commonly predetermined, so the number of free design variables might be smaller than 20. To ease the notation in what follows, all variables of the jacket model are assembled in the array  $\mathbf{x}$ :

$$\mathbf{x} = (N_L \ N_X \ R_{\text{foot}} \ \xi \ L \ L_{\text{MSL}} \ L_{\text{OSG}} \ L_{\text{TP}} \ x_{\text{MB}} \ q \ D_L \ \gamma_b \ \gamma_t \ \beta_b \ \beta_t \ \tau_b \ \tau_t \ E \ G \ \rho)^T. \quad (22)$$

### 3 Cost modeling

A possible approach to the jacket substructure cost calculation is to regard the total capital expenses,  $C_{\text{total}}$ , as a linear combination of multiple contributions, with each one given by a cost factor,  $c_j$ , multiplied by the corresponding unit cost  $a_j$ :

$$C_{\text{total}}(\mathbf{x}) = \sum \underbrace{a_j c_j(\mathbf{x})}_{C_j(\mathbf{x})}. \quad (23)$$

Basic factors for material, fabrication, coating, transition piece, structural appurtenances (if regarded as additional parts), and transport and installation (including costs for the pile foundation) are assumed here, acknowledging that this breakdown may look different if increasing the level of detail.

- $c_1$ : material factor
- $c_2$ : fabrication factor
- $c_3$ : coating factor
- $c_4$ : transition piece factor
- $c_5$ : transport factor
- $c_6$ : foundation and installation factor
- $c_7$ : fixed expenses factor

#### 3.1 Material expenses

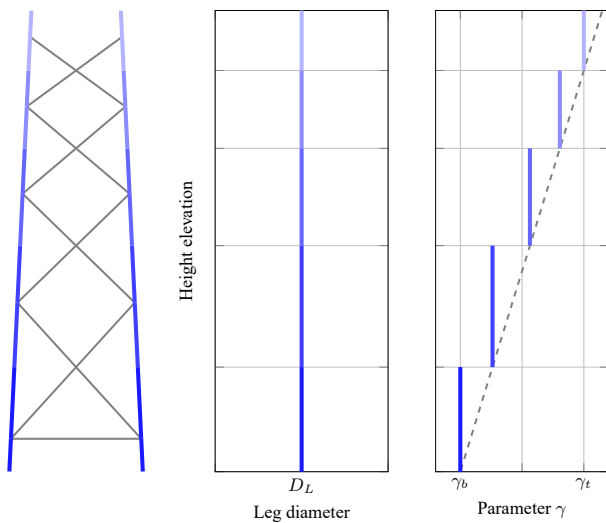
The material expenses are supposed to be proportional to the mass of the components. Therefore,  $c_1$  is the total jacket mass, which is the mass of the assembled substructure excluding the transition piece, foundation, or appurtenances of any kind and which can be obtained by evaluating structural analysis tools or by applying simple geometrical relations from the jacket topology (Fig. 3). The latter can be expressed as a sum:

$$\begin{aligned} c_1(\mathbf{x}) = & \underbrace{2\rho N_L \pi D_L^2 \sum_{i=1}^{N_X} \left( \left( \frac{\beta_i \tau_i}{2\gamma_i} + \frac{\tau_i^2}{4\gamma_i^2} \right) \sqrt{\frac{L_i^2}{\cos^2(\Phi_p)} + (R_i + R_{i+1})^2 \sin^2\left(\frac{\vartheta}{2}\right)} \right)}_{\text{Mass of all diagonal braces}} \\ & + \underbrace{x_{\text{MB}} \rho N_L \pi D_L^2 \left( \frac{\beta_b \tau_b}{2\gamma_b} + \frac{\tau_b^2}{4\gamma_b^2} \right) 2R_1 \sin\left(\frac{\vartheta}{2}\right)}_{\text{Mass of mud braces}} \\ & + \underbrace{\rho N_L \pi D_L^2 \sum_{i=1}^{N_X} \left( \left( \frac{1}{2\gamma_i} + \frac{1}{4\gamma_i^2} \right) \frac{L_{m,i}}{\cos(\Phi_s)} + \left( \frac{1}{2\gamma_{i+1}} + \frac{1}{4\gamma_{i+1}^2} \right) \frac{(L_i - L_{m,i})}{\cos(\Phi_s)} \right)}_{\text{Mass of intermediate leg elements}} \\ & + \underbrace{\rho N_L \pi D_L^2 \left( \frac{1}{2\gamma_b} + \frac{1}{4\gamma_b^2} \right) \frac{L_{\text{OSG}}}{\cos(\Phi_s)}}_{\text{Mass of intermediate lowermost elements}} \\ & + \underbrace{\rho N_L \pi D_L^2 \left( \frac{1}{2\gamma_t} + \frac{1}{4\gamma_t^2} \right) \frac{L_{\text{TP}}}{\cos(\Phi_s)}}_{\text{Mass of uppermost leg elements}}. \end{aligned} \quad (24)$$

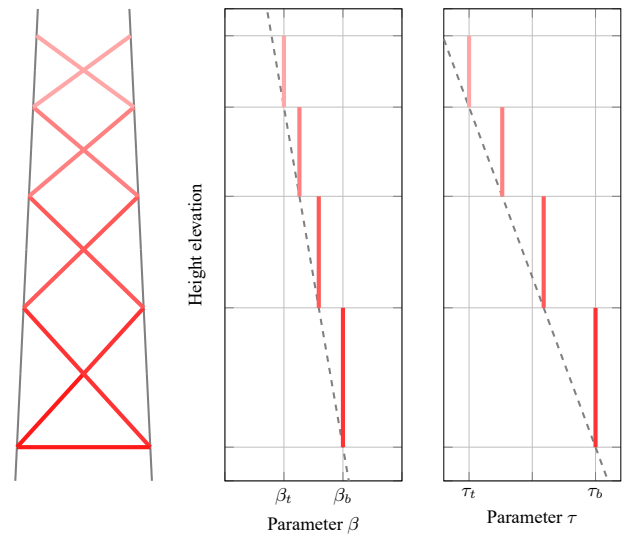
#### 3.2 Fabrication expenses

Although it can be assumed that fabrication expenses contribute significantly to the overall jacket costs, this factor is often neglected because it is difficult to measure. A common approach in practical applications is to assume a proportional relation to the cumulated weld volume. In this cost model,  $c_2$  is the cumulative volume of all structural welds. With the weld root thickness,  $t_0$  (given as 3 mm in Germanischer Lloyd, 2012) and assuming a  $45^\circ$  weld angle around the entire weld, the sectional weld area can be approximated and multiplied by the weld length, which is the perimeter of the ellipse that is projected to the connected chord surface<sup>1</sup>:

<sup>1</sup>The ellipse perimeter is approximated in a very simple way here. However, the occurring eccentricities are in a range in which this simplification causes no significant error.



**Figure 4.** Definition of leg dimensions with a dependency on the jacket height. Values are illustrated by darker coloring at the bottom and shade to lighter at the top of the structure.



**Figure 5.** Definition of brace dimensions with a dependency on the jacket height. Values are illustrated by darker coloring at the bottom and shade to lighter at the top of the structure.

thus

$$\begin{aligned}
 c_2(\mathbf{x}) = & 2N_L\pi D_L \sum_{i=1}^{N_X} \left( \beta_i \left( \frac{D_L^2 \tau_i^2}{8\gamma_i^2} + \frac{t_0 D_L \tau_i}{2\sqrt{2}\gamma_i} \right) \left( \sqrt{\frac{1}{2\sin^2(\psi_{1,i})} + \frac{1}{2}} \right. \right. \\
 & \left. \left. + \sqrt{\frac{1}{2\sin^2(\psi_{2,i})} + \frac{1}{2}} + \sqrt{\frac{1}{2\sin^2(\psi_{3,i})} + \frac{1}{2}} \right) \right) \\
 & \text{Brace-to-brace and brace-to-leg weld volume} \\
 & + 2x_{MB} N_L \pi D_L \beta_b \left( \frac{D_L^2 \tau_b^2}{8\gamma_b^2} + \frac{t_0 D_L \tau_b}{2\sqrt{2}\gamma_b} \right) \\
 & \text{Mud brace-to-leg weld volume} \\
 & + N_L \pi D_L \sum_{i=1}^{N_X} \left( \frac{D_L^2 \min\left(\frac{1}{\gamma_i^2}, \frac{1}{\gamma_{i+1}^2}\right)}{8} + \frac{D_L t_0 \min\left(\frac{1}{\gamma_i}, \frac{1}{\gamma_{i+1}}\right)}{2\sqrt{2}} \right). \quad (25) \\
 & \text{Leg-to-leg weld volume}
 \end{aligned}$$

The equation uses the perimeter of the ellipse that is projected on a plane to calculate the weld length. This is not exactly equal to the real weld length, but simplifies the equation considerably.

### 3.3 Coating expenses

Coating is necessary to protect the jacket from corrosion and causes non-negligible costs. It is assumed that the entire outer surface area of all tubes is coated after manufacturing and the

coating expenses are proportional to the outer surface area  $c_3$ :

$$\begin{aligned}
 c_3(\mathbf{x}) = & \underbrace{2N_L\pi D_L \sum_{i=1}^{N_X} \left( \beta_i \sqrt{\frac{L_i^2}{\cos^2(\Phi_p)} + (R_i + R_{i+1})^2 \sin^2\left(\frac{\vartheta}{2}\right)} \right)}_{\text{Outer surface area of all diagonal braces}} \\
 & + \underbrace{x_{MB} N_L \pi D_L \beta_b \left( 2R_1 \sin\left(\frac{\vartheta}{2}\right) \right)}_{\text{Outer surface area of mud braces}} \\
 & + \underbrace{N_L \pi D_L \frac{L}{\cos(\Phi_s)}}_{\text{Outer surface area of all legs}}. \quad (26)
 \end{aligned}$$

The equation assumes that the reduction of the entire outer surface area due to intersecting tubes is negligible.

### 3.4 Transition piece expenses

Although there are different transition piece types, a stellar-type transition piece is assumed, which connects the uppermost leg ends with straight bars to a center point. In this case, it can be assumed that the costs depend linearly, on the one hand, on the number of legs and, on the other hand, on the head radius; thus the factor  $c_4$  reads

$$c_4(\mathbf{x}) = N_L R_{\text{foot}} \xi. \quad (27)$$

### 3.5 Transport expenses

For a simplified cost estimation, the expenses to be raised for the transport of the structure from the port to the wind

farm site can be roughly measured in terms of a linear mass dependency, and therefore factors  $c_5$  and  $c_1$  are equal:

$$c_5(\mathbf{x}) = c_1(\mathbf{x}). \quad (28)$$

However, this value (mass after production) is supposed to be slightly different from the wrought mass that is used due to overlapping joints and material removal prior to welding. To simplify the cost calculation, it is assumed that both values are equal.

### 3.6 Foundation and installation expenses

The foundation is the structural part that provides an interface to the seabed. Both the production costs for the foundation structures, no matter of which type, and the on-site installation costs depend linearly on the number of legs in our approach. For the sake of simplicity, it is assumed that these costs do not cover costs due to modifications of the structural pile design. They are assembled in the foundation and installation expenses, and the corresponding factor  $c_6$  reads

$$c_6(\mathbf{x}) = N_L. \quad (29)$$

### 3.7 Fixed expenses

There are costs that cannot be measured in terms of any parameters of the jacket model:

$$c_7(\mathbf{x}) = 1. \quad (30)$$

These kinds of costs – in the nomenclature of this work proportional to the factor  $c_7$  – arise for every structure and are indeed very important for a cost assessment, but have a rather minor impact on design studies or optimization results, as there is no contribution to differential operators. Examples are costs for structural appurtenances, like boat landings and ladders, or production facilities and infrastructure, like scaffolds or cranes.

## 4 Surrogate models for fatigue and ultimate limit state

A general presupposition made in this work is that realistic jacket design necessitates simulation-based proofs to ensure the structural functionality in different limit states. While the proof of serviceability limit state is mostly simple in the case of relatively stiff lattice structures, for which the tubular tower dominates the modal behavior of the entire turbine, the checks for fatigue and ultimate limit state are computationally expensive. There are indeed simulation-based optimization approaches in the literature, but all with very limited design load sets and proposals trying to find efficient load sets or simplifications of load cases.

Recent work showed that Gaussian process regression (GPR) models are appropriate to predict numerically

obtained fatigue damages for two test structures from environmental state inputs (Brandt et al., 2017). It is thus straightforward to transfer the same methodology to the prediction of fatigue damages or utilization ratios due to extreme loads for varying jacket designs in the case that the load sets are given. It is also imaginable to apply a classification approach to this type of problem, with the statements “structural code check successful” or “structural code check failed” as outputs. However, this would limit the imaginable applications, so regression is applied. In the following, a brief introduction to Gaussian process regression is given. For the sake of simplicity, the output dimension of the problem is restricted to one, which is a single-output regression problem. The basis for GPR is the Bayesian regression problem:

$$y = f(\mathbf{x}) + e \quad (31)$$

with

$$e \sim \mathcal{N}\left(0, \sigma_n^2\right). \quad (32)$$

We want to make predictions,  $y^*$ , for an arbitrary set of (prediction) input variables,  $\mathbf{x}^*$ , based on information gathered from the training set, which is represented by the input matrix,  $\mathbf{X}$ , and the vector of corresponding output values,  $\mathbf{y}$ . The key assumption of Gaussian process regression is that a Gaussian distribution over  $f(\mathbf{x})$  exists; thus

$$f(\mathbf{x}) \sim \mathcal{GP}\left(m(\mathbf{x}), k(\mathbf{x}, \mathbf{x}')\right), \quad (33)$$

with

$$m(\mathbf{x}) = \mathbb{E}\left[f(\mathbf{x})\right] \quad (34)$$

and

$$k(\mathbf{x}, \mathbf{x}') = \text{cov}\left[f(\mathbf{x}), f(\mathbf{x}')\right], \quad (35)$$

which is a Mercer kernel function. Due to the marginalization property of Gaussian processes, there is a joint distribution of training and prediction sets:

$$\begin{pmatrix} \mathbf{y} \\ \mathbf{y}^* \end{pmatrix} \sim \left( \mathbf{0}, \begin{bmatrix} \mathbf{K}(\mathbf{X}, \mathbf{X}) & \mathbf{k}(\mathbf{X}, \mathbf{x}^*) \\ \mathbf{k}(\mathbf{x}^*, \mathbf{X}) & k(\mathbf{x}^*, \mathbf{x}^*) \end{bmatrix} \right). \quad (36)$$

In this equation,  $\mathbf{K}$  and  $\mathbf{k}$  were introduced to ease the notation and just represent matrices and vectors for which each element is the corresponding value of  $k$ . The mean of the joint distribution was set to zero. From this equation, the conditional posterior distribution of  $y^*$  can be obtained:

$$y^* | \mathbf{x}^* \sim \mathcal{N}\left(\mathbf{k}(\mathbf{X}, \mathbf{x}^*)^T \left(\mathbf{K}(\mathbf{X}, \mathbf{X}) + \sigma_n^2 \mathbf{I}\right)^{-1} \mathbf{y}, \mathbf{k}(\mathbf{x}^*, \mathbf{x}^*) - \mathbf{k}(\mathbf{x}^*, \mathbf{X}) \left(\mathbf{K}(\mathbf{X}, \mathbf{X}) + \sigma_n^2 \mathbf{I}\right)^{-1} \mathbf{k}(\mathbf{X}, \mathbf{x}^*)\right). \quad (37)$$

For further details, the interested reader is referred to Rasmussen and Williams (2008), which is the most comprehensive work in this field in the opinion of the authors. Due to the

probabilistic nature of these models, the computation of prediction intervals is possible. This is a substantial advantage because realistic load sets are large and thus the size of the design of experiments is limited. In addition, when the uncertainty arising from design load set assumptions is known, it can be easily considered by an appropriate choice and parameterization of the kernel function.

The prediction of values from a GPR model requires the complete input and output training to set it up. In contrast to the proposed geometry and cost assumptions, the derivation of surrogate models for fatigue and ultimate limit state depends highly on the reference turbine and the environmental conditions. The first one has been selected to be the National Renewable Energy Laboratory (NREL) 5 MW turbine, defined by Jonkman et al. (2009). The water depth at the fictive location is 50 m. In addition, the research platforms FINO3 (mainly) and FINO1 (for validation purposes) provide detailed, long-term measurements to derive the environmental conditions. Soil properties are adopted from the definition of the soil layers in the Offshore Code Comparison Collaboration (OC3) project (Jonkman and Musial, 2010). The transition piece is considered with a lumped mass of 660 t at the bottom of the tubular steel tower. There are, however, some limitations in these assumptions that cannot be suppressed. No structural appurtenances like ladders, boat landings, sacrificial anodes, or J tubes are considered in the structural model. The assumption of 50 m of water depth does not match the water depths at the FINO locations. Nevertheless, no other measurements of environmental states are available, and this assumption was also made in the design basis of the UpWind project (Fischer et al., 2010).

#### 4.1 Training and validation data sets

To obtain training data for surrogate modeling, 200 test jackets were sampled from the design space by a space-filling design of experiments with minimum correlation between all samples. Assuming that it is the state-of-the-art reference for 5 MW wind turbine jacket structures, the boundaries in Table 1 were chosen in a realistic range around the values of the OC4 jacket (Popko et al., 2014), excluding “too optimistic”<sup>2</sup> jacket designs. Although the number of samples seems to be low, it has to be considered that the number of time domain simulations depends linearly on the sample size. Moreover, Eq. (37) requires the inversion of  $\mathbf{K}(\mathbf{X}, \mathbf{X})$ , which may lead to weak numerical performance of the prediction. Furthermore, an independent validation set with 40 samples from the entire design space was generated, which was created by another space-filling design of experiments. It has to be noted that the purpose of this data set is just validation of the final parameterized models; it is not involved in the training phase and is not part of the cross-validation procedure.

<sup>2</sup>This statement means that the structural code checks allow wider ranges of the design parameters.

#### 4.2 Design load sets

In order to conduct time domain simulations, load sets for both fatigue and ultimate limit state have to be defined. For the fatigue case, broad knowledge about the required size of design load sets is already available because it was analyzed previously in a comprehensive study (Häfele et al., 2017a, b) in which both probabilistic and unidirectional load sets were investigated. However, as the GPR allows us to propagate uncertainties, it is reasonable to utilize a probabilistic load set with 128 production load cases (design load case (DLC) 1.2 and 6.4 according to IEC-61400-3; see International Electrotechnical Commission, 2009) for damage estimation (see Table 2), which is a finding of the previously mentioned study. In the extreme load case, the focus is rather on the consideration of multiple special events than on the reproduction of the long-term behavior. Table 3 features a summary of all design load cases that are to be calculated for every sample. There are 10 extreme load cases that were identified to be potentially critical. DLC 1.3 and 1.6a are production load cases with extreme turbulence and severe sea state, respectively. DLC 2.3 is a design load case for which electrical grid loss occurs during the production state. DLC 6.1a and 6.2a are events with extreme mean wind speed, the first one with an extreme sea state and the second one with an extreme yaw error. The values of the parameters in Table 3 were obtained by evaluating probability density functions of environmental parameters at the FINO locations given by Hübner et al. (2017a).

#### 4.3 Time domain simulations

As the varying jacket design changes the structural behavior of the entire turbine, only fully coupled simulations were conducted for this study, as so-called sequential or uncoupled approaches are considered not sufficiently accurate. All simulations are computed with FAST (National Wind Technology Center Information Portal, 2016) in the current version at the publication of this study and comprise 10 min time series<sup>3</sup> plus an additional 3 min time for transient decay. To account for soil–structure interaction, a reduced representation of the substructure (see Häfele et al., 2016) is considered, in which eight interior modes are the basis for the representation of the jacket with foundation. The pile foundation is considered by lumped mass and stiffness matrices at the transition between substructure and ground. These matrices are derived by a preprocessing procedure in which the piles with  $p - y$  and  $T - z$  curves according to the American Petroleum Institute (2002) are discretized with finite elements. In the fatigue limit state case, the soil is linearized in the zero-deflection operating point. The operating-point-dependent soil behavior cannot be neglected in the extreme

<sup>3</sup>For some extreme load events, this is a rather low value. However, due to limited capacity of computational resources, it was decided to choose this length for all simulations.



**Table 1.** Jacket model parameter boundaries for the design of experiments. Topological, tube sizing, and material parameters are separated in groups; single values indicate that the corresponding value is held constant.

Parameter	Description	Lower boundary	Upper boundary
$N_L$	Number of legs	3	4
$N_X$	Number of bays	3	5
$R_{\text{foot}}$	Foot radius	6.792 m	12.735 m
$\xi$	Head-to-foot radius ratio	0.533	0.733
$L$	Overall jacket length		70.0 m
$L_{\text{MSL}}$	Transition piece elevation over MSL		20.0 m
$L_{\text{OSG}}$	Lowest leg segment height		5.0 m
$L_{\text{TP}}$	Transition piece segment height		4.0 m
$q$	Ratio of two consecutive bay heights	0.640	1.200
$x_{\text{MB}}$	Mud brace flag		true
$D_L$	Leg diameter	0.960 m	1.440 m
$\gamma_b$	Leg radius-to-thickness ratio (bottom)	12.0	18.0
$\gamma_t$	Leg radius-to-thickness ratio (top)	12.0	18.0
$\beta_b$	Brace-to-leg diameter ratio (bottom)	0.533	0.800
$\beta_t$	Brace-to-leg diameter ratio (top)	0.533	0.800
$\tau_b$	Brace-to-leg thickness ratio (bottom)	0.350	0.650
$\tau_t$	Brace-to-leg thickness ratio (top)	0.350	0.650
$E$	Material Young's modulus	$2.100 \times 10^{11} \text{ N m}^{-2}$	
$G$	Material shear modulus	$8.077 \times 10^{10} \text{ N m}^{-2}$	
$\rho$	Material density	$7.850 \times 10^3 \text{ kg m}^{-3}$	

**Table 2.** Considered design load sets according to IEC-61400-3 (International Electrotechnical Commission, 2009) for the fatigue limit state (SF: partial safety factor,  $v_s$ : mean wind speed,  $P$ : probability density function, TI: turbulence intensity,  $H_s$ : significant wave height,  $T_p$ : wave peak period,  $\theta_{\text{wind}}$ : wind direction,  $\theta_{\text{wave}}$ : wave direction,  $u_w$ : near-surface current velocity,  $u_{ss}$ : subsurface current velocity, MSL: mean sea level). Yaw error is normally distributed with  $-8^\circ$  mean value and  $1^\circ$  standard deviation.

DLC	Quantity	Wind	Waves	Directionality	Current	Water level
1.2, 6.4 SF = 1.25	128	$v_s = P(v_s)$ $\text{TI} = \text{TI}(v_s)$	$H_s = P(H_s v_s)$ $T_p = P(T_p H_s)$	$\theta_{\text{wind}} = P(\theta_{\text{wind}} v_s)$ $\theta_{\text{wave}} = P(\theta_{\text{wave}} H_s, \theta_{\text{wind}})$	$u_w(0) = 0.42 \text{ m s}^{-1}$ $u_{ss}(0) = 0 \text{ m s}^{-1}$	MSL

load case and is considered by an ad hoc approach (Hübler et al., 2016).

#### 4.4 Post-processing of time domain results

Fatigue is evaluated in terms of the maximum cumulative damage that occurs in the critical joint after summing up all hot spot damages. An  $S-N$  curve approach defined by the structural code DNV GL RP-0005 (DNV GL AS, 2016a) is utilized for this purpose. Hot spot stresses are obtained by stress concentration factors. Stress cycles are evaluated by a rainflow-counting algorithm and added up according to linear damage accumulation. Fatigue checks are only performed for tubular joints corresponding to class  $T$  according to the structural code. The related  $S-N$  curve has an endurance stress limit of  $52.63 \times 10^6 \text{ N m}^{-2}$  at  $10^7$  cycles and slopes of 3 and 5 before and after endurance limit, respectively.

Ultimate limit state proofs are performed according to the structural code NORSOK N-004 (NORSOK, 2004), which

is a well-established standard for this purpose. Although the extreme load assessment involves all tubes of the jacket, the output value is only the one with the highest utilization ratio among all considered load cases, including partial safety factors. Punching shear resistance of tubular joints is not considered in the surrogate model because it is not part of the pre-design process. Steel with a yield stress of 355 MPa (S355) is considered as the material for the entire structure, excluding structural appurtenances.

#### 4.5 Derivation and parameterization of Gaussian process regression models

While the outputs of both limit state assessments are single real values, it has to be conceived that the output values are distributed differently. GPR models are mainly governed by the kernel function choice and the corresponding hyperparameters. Different kernel functions were tested with respect to the creation of appropriate surrogate models and evaluated

**Table 3.** Considered design load sets according to IEC-61400-3 (International Electrotechnical Commission, 2009) for the ultimate limit state (SF: partial safety factor,  $v_s$ : mean wind speed, TI: turbulence intensity,  $H_S$ : significant wave height,  $T_p$ : wave peak period,  $\theta_{wind}$ : wind direction,  $\theta_{wave}$ : wave direction,  $u_w$ : near-surface current velocity,  $u_{ss}$ : subsurface current velocity, MSL: mean sea level). Yaw error is constantly set to  $-8^\circ$  if not stated differently.

DLC	Quantity	Wind	Waves	Directionality	Current	Water level	Special event
1.3 SF = 1.35	1	$v_s = 15.40 \text{ m s}^{-1}$ TI = 58.10 %	$H_S = 2.04 \text{ m}$ $T_p = 7.50 \text{ s}$	$\theta_{wind} = 0^\circ$ $\theta_{wave} = 0^\circ$	$u_w(0) = 0.42 \text{ m s}^{-1}$ $u_{ss}(0) = 0 \text{ m s}^{-1}$	MSL	
1.3 SF = 1.35	1	$v_s = 15.40 \text{ m s}^{-1}$ TI = 58.10 %	$H_S = 2.04 \text{ m}$ $T_p = 7.50 \text{ s}$	$\theta_{wind} = 15^\circ$ $\theta_{wave} = 15^\circ$	$u_w(0) = 0.42 \text{ m s}^{-1}$ $u_{ss}(0) = 0 \text{ m s}^{-1}$	MSL	
1.3 SF = 1.35	1	$v_s = 17.40 \text{ m s}^{-1}$ TI = 44.22 %	$H_S = 2.50 \text{ m}$ $T_p = 7.50 \text{ s}$	$\theta_{wind} = 0^\circ$ $\theta_{wave} = 0^\circ$	$u_w(0) = 0.42 \text{ m s}^{-1}$ $u_{ss}(0) = 0 \text{ m s}^{-1}$	MSL	
1.6a SF = 1.35	1	$v_s = 11.40 \text{ m s}^{-1}$ TI = 8.09 %	$H_S = 10.60 \text{ m}$ $T_p = 15.09 \text{ s}$	$\theta_{wind} = 0^\circ$ $\theta_{wave} = 0^\circ$	$u_w(0) = 0.42 \text{ m s}^{-1}$ $u_{ss}(0) = 0 \text{ m s}^{-1}$	MSL +2.02 m	
2.3 SF = 1.1	1	$v_s = 25.00 \text{ m s}^{-1}$ TI = 8.09 %	$H_S = 4.63 \text{ m}$ $T_p = 10.47 \text{ s}$	$\theta_{wind} = 0^\circ$ $\theta_{wave} = 0^\circ$	$u_w(0) = 0.42 \text{ m s}^{-1}$ $u_{ss}(0) = 0 \text{ m s}^{-1}$	MSL	Grid loss
2.3 SF = 1.1	1	$v_s = 25.00 \text{ m s}^{-1}$ TI = 8.09 %	$H_S = 4.63 \text{ m}$ $T_p = 10.47 \text{ s}$	$\theta_{wind} = 60^\circ$ $\theta_{wave} = 60^\circ$	$u_w(0) = 0.42 \text{ m s}^{-1}$ $u_{ss}(0) = 0 \text{ m s}^{-1}$	MSL	Grid loss
6.1a SF = 1.35	1	$v_s = 42.14 \text{ m s}^{-1}$ TI = 12.47 %	$H_S = 4.63 \text{ m}$ $T_p = 10.47 \text{ s}$	$\theta_{wind} = 0^\circ$ $\theta_{wave} = 0^\circ$	$u_w(0) = 1.88 \text{ m s}^{-1}$ $u_{ss}(0) = 0.69 \text{ m s}^{-1}$	MSL +2.74 m	
6.2a SF = 1.1	1	$v_s = 42.14 \text{ m s}^{-1}$ TI = 12.47 %	$H_S = 4.63 \text{ m}$ $T_p = 10.47 \text{ s}$	$\theta_{wind} = 0^\circ$ $\theta_{wave} = 0^\circ$	$u_w(0) = 1.88 \text{ m s}^{-1}$ $u_{ss}(0) = 0.69 \text{ m s}^{-1}$	MSL +2.74 m	Yaw error $60^\circ$
6.2a SF = 1.1	1	$v_s = 42.14 \text{ m s}^{-1}$ TI = 12.47 %	$H_S = 4.63 \text{ m}$ $T_p = 10.47 \text{ s}$	$\theta_{wind} = 0^\circ$ $\theta_{wave} = 0^\circ$	$u_w(0) = 1.88 \text{ m s}^{-1}$ $u_{ss}(0) = 0.69 \text{ m s}^{-1}$	MSL +2.74 m	Yaw error $90^\circ$
6.2a SF = 1.1	1	$v_s = 42.14 \text{ m s}^{-1}$ TI = 12.47 %	$H_S = 4.63 \text{ m}$ $T_p = 10.47 \text{ s}$	$\theta_{wind} = 0^\circ$ $\theta_{wave} = 0^\circ$	$u_w(0) = 1.88 \text{ m s}^{-1}$ $u_{ss}(0) = 0.69 \text{ m s}^{-1}$	MSL +2.74 m	Yaw error $120^\circ$

in terms of cross-validations in this section. Due to the highly nonlinear character of the utilized structural codes and therefore significant variance in the model outputs, a certain extent of uncertainty has to be tolerated. For the learning procedure, the fatigue damages are logarithmized because the underlying  $S - N$  curve is also logarithmic and the range of values covers at least 4 powers of 10. For the ultimate limit state, results cover only a range from zero to about 3, and no normalization is necessary. However, to exclude severe outliers from the training set of the surrogate model for the ultimate limit state, 10 % of the samples with the highest extreme load utilization ratios are excluded.

The problem of choosing the right kernel function is discussed by many authors. In order to limit the extent of this section, the reader is referred to the works of Duvenaud (2014) and King (2016) for further details. In general, the kernel choice implies a belief about the shape or smoothness of the covariance. In this case, four commonly used stationary kernel functions are compared that represent relatively smooth approximations of the function.

The squared exponential kernel reads

$$k_{SE}(\mathbf{x}, \mathbf{x}') = \exp\left(-\frac{(\mathbf{x} - \mathbf{x}')(\mathbf{x} - \mathbf{x}')^T}{2l^2}\right). \quad (38)$$

The Matérn 3/2 kernel is

$$k_{Ma_{3/2}}(\mathbf{x}, \mathbf{x}') = \left(1 + \frac{\sqrt{3(\mathbf{x} - \mathbf{x}')(\mathbf{x} - \mathbf{x}')^T}}{l}\right) \exp\left(-\frac{\sqrt{3(\mathbf{x} - \mathbf{x}')(\mathbf{x} - \mathbf{x}')^T}}{l}\right), \quad (39)$$

the Matérn 5/2 kernel is

$$k_{Ma_{5/2}}(\mathbf{x}, \mathbf{x}') = \left(1 + \frac{\sqrt{5(\mathbf{x} - \mathbf{x}')(\mathbf{x} - \mathbf{x}')^T}}{l} + \frac{5(\mathbf{x} - \mathbf{x}')(\mathbf{x} - \mathbf{x}')^T}{3l^2}\right) \exp\left(-\frac{\sqrt{5(\mathbf{x} - \mathbf{x}')(\mathbf{x} - \mathbf{x}')^T}}{l}\right), \quad (40)$$

and the rational quadratic kernel is

$$k_{\text{RQ}}(\mathbf{x}, \mathbf{x}') = \left(1 + \frac{(\mathbf{x} - \mathbf{x}')(\mathbf{x} - \mathbf{x}')^T}{2al^2}\right)^a, \quad (41)$$

where  $l$  is a length scale and  $a$  a weighting parameter. It is best practice to choose different scales for all input parameters. This is called automatic relevance determination (Duvenaud, 2014).

The squared exponential kernel is a common choice for Gaussian processes as an “initial guess” because it is infinitely differentiable and therefore very smooth. The Matérn kernels are less smooth than the squared exponential kernel: Matérn 3/2 is once and Matérn 5/2 twice differentiable. The rational quadratic kernel is a sum of squared exponential kernels with the capability to weight between large- and small-scale variations. To figure out which kernel function is most suitable for both surrogate models, various cross-validations are performed. An  $N$ -fold cross-validation means that the training data set (which comprises 200 jacket samples in the fatigue limit state case and 180 samples in the ultimate limit state case in this study) is divided into  $N$  parts with equal size.  $N - 1$  parts are then used to train the model and the leftover is the test set, which is used to predict a vector of validation results,  $\mathbf{y}^*$ . This is repeated  $N$  times to compute the mean of the two common error measures, bias  $e_{\text{bias}}$  and mean squared error  $e_{\text{mse}}$ :

$$e_{\text{bias}} = \frac{1}{N} \sum_{n=1}^N \left( \frac{1}{M} \sum_{m=1}^M (y_{n,m}^* - y_{n,m}) \right), \quad (42)$$

$$e_{\text{mse}} = \frac{1}{N} \sum_{n=1}^N \left( \frac{1}{M} \sum_{m=1}^M (y_{n,m}^* - y_{n,m})^2 \right), \quad (43)$$

where  $y_{n,m}^*$  is the  $m$ th predicted element in the  $n$ th cross-validation set and  $y_{n,m}$  is the corresponding value in the output vector.  $M$  is the size of the cross-validation leftover. For instance, in the case of a 10-fold cross-validation,  $M$  is 20. While the mean squared error is always positive, the bias can have both positive and negative values. Table 4 shows validation results for the four kernels using leave-one-out, 10-fold, and 5-fold cross-validations. There are no values completely off and all kernel functions lead to similar results in the fatigue limit state case; the Matérn 5/2 function is eventually chosen for both surrogate models.

#### 4.6 Validation of Gaussian process regression models

Based on the kernel function selection, the surrogate models are validated with 40 samples from the design space given in Table 1. A Matérn 5/2 kernel with independent hyperparameters and a Gaussian likelihood function with  $\ln(\sqrt{\sigma_n^2}) = -2.06$ , where  $\sqrt{\sigma_n^2}$  is the mean standard deviation of logarithmized damage per load case accounting for load set reduction uncertainty evaluated from the results by

Häfele et al. (2017a, b), are chosen for the fatigue case. The ultimate limit state case does not incorporate prior knowledge of uncertainty because it is assumed that one of the considered load cases in Table 3 is the severest imaginable one. The predicted validation values for both fatigue and ultimate limit state are shown in Fig. 6. Although the drawn whiskers show quite wide prediction intervals, the mean values predict the calculated ones well in both diagrams. Therefore, it can be stated that Gaussian process regression is suitable for this task.

## 5 Example

Although the focus of this work shall not be a comprehensive design study, a short example is provided in this section, which shows how the proposed models can be used in further studies.

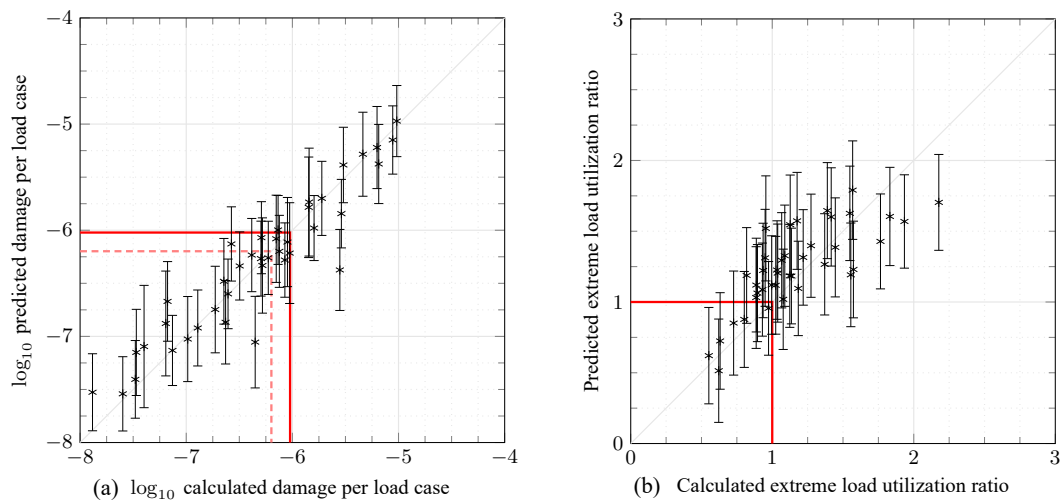
We assume that for a fixed wind farm location with 50 m of water depth, NREL 5 MW turbine, FINO3 environmental conditions, and OC3 soil properties, it has to be evaluated which of three given jacket designs is most suitable with regard to capital expenses. There is uncertainty in the capital expenditures arising from, for example, the market situation, the availability of fabrication facilities and ships, the distance of the installation site from shore, the weather situation, and the sea state. For the sake of simplicity, we assume that this uncertainty can be described in terms of normally distributed cost model parameters given as mean values and standard deviations in Table 5<sup>4</sup>. The parameter distributions indicate relatively high uncertainty, in particular in the expenses for transport and installation, which is a common experience in the wind farm planning process. There are three substructure options to be compared: the first (a), derived from the so-called OC4 jacket (Popko et al., 2014), and second (b) ones are four-legged ( $N_X = 4$ ) jackets, and the third (c) one is a three-legged ( $N_X = 3$ ) structure. All structures have a length of  $L = 70$  m with transition piece  $L_{\text{MSL}} = 20$  m above mean sea level and use steel ( $E = 2.100 \times 10^{11}$  N m<sup>-2</sup>,  $G = 8.077 \times 10^{10}$  N m<sup>-2</sup>,  $\rho = 7.850 \times 10^3$  kg m<sup>-3</sup>) as the material. The height between the ground and lowermost double-K joint layer is  $L_{\text{OSG}} = 5$  m, and the transition piece height is  $L_{\text{TP}} = 4$  m. Furthermore, all jackets have mud braces ( $x_{\text{MB}} = \text{true}$ ); the foot radii,  $R_{\text{foot}}$ , are all 8.485 m, the bay height ratio,  $q$ , is 0.8, and the head-to-foot radius ratio,  $\xi$ , is 0.67. The leg radius-to-thickness and the leg-to-brace thickness ratios are held constant at  $\gamma = \gamma_b = \gamma_t = 15.0$  and  $\tau = \tau_b = \tau_t = 0.5$ , respectively. The structures differ, except for the number of legs ( $N_L$ ), in the number of bays ( $N_X$ ) and tube dimensions ( $D_L$ ,  $\beta_b$ ,  $\beta_t$ ). The first one (a) has four bays, a leg

<sup>4</sup>The mean values are in accordance with practical experience and published information about jacket expenditures (Michels, 2014; National Wind Technology Center Information Portal, 2014). The standard deviation values reflect different dimensions of scatter in the unit costs.



**Table 4.** Cross-validation results for kernel functions applied to fatigue and ultimate limit state outputs, each case with ideal hyperparameters obtained by maximum likelihood estimation.

Limit state	Cross-validation type	Error type	Kernel function			
			$k_{SE}$	$k_{Ma_{3/2}}$	$k_{Ma_{5/2}}$	$k_{RQ}$
Fatigue	Leave-one-out	$e_{bias}$	-0.003	-0.002	-0.003	-0.002
		$e_{mse}$	0.052	0.044	0.043	0.041
	10-fold	$e_{bias}$	-0.007	-0.004	-0.003	-0.005
		$e_{mse}$	0.073	0.049	0.049	0.047
	5-fold	$e_{bias}$	0.004	-0.008	0.000	-0.012
		$e_{mse}$	0.084	0.062	0.063	0.061
Ultimate	Leave-one-out	$e_{bias}$	0.003	0.001	0.003	-0.002
		$e_{mse}$	0.057	0.053	0.054	0.057
	10-fold	$e_{bias}$	0.004	0.006	0.006	-0.002
		$e_{mse}$	0.056	0.055	0.056	0.061
	5-fold	$e_{bias}$	0.003	0.002	0.003	0.008
		$e_{mse}$	0.055	0.056	0.054	0.061



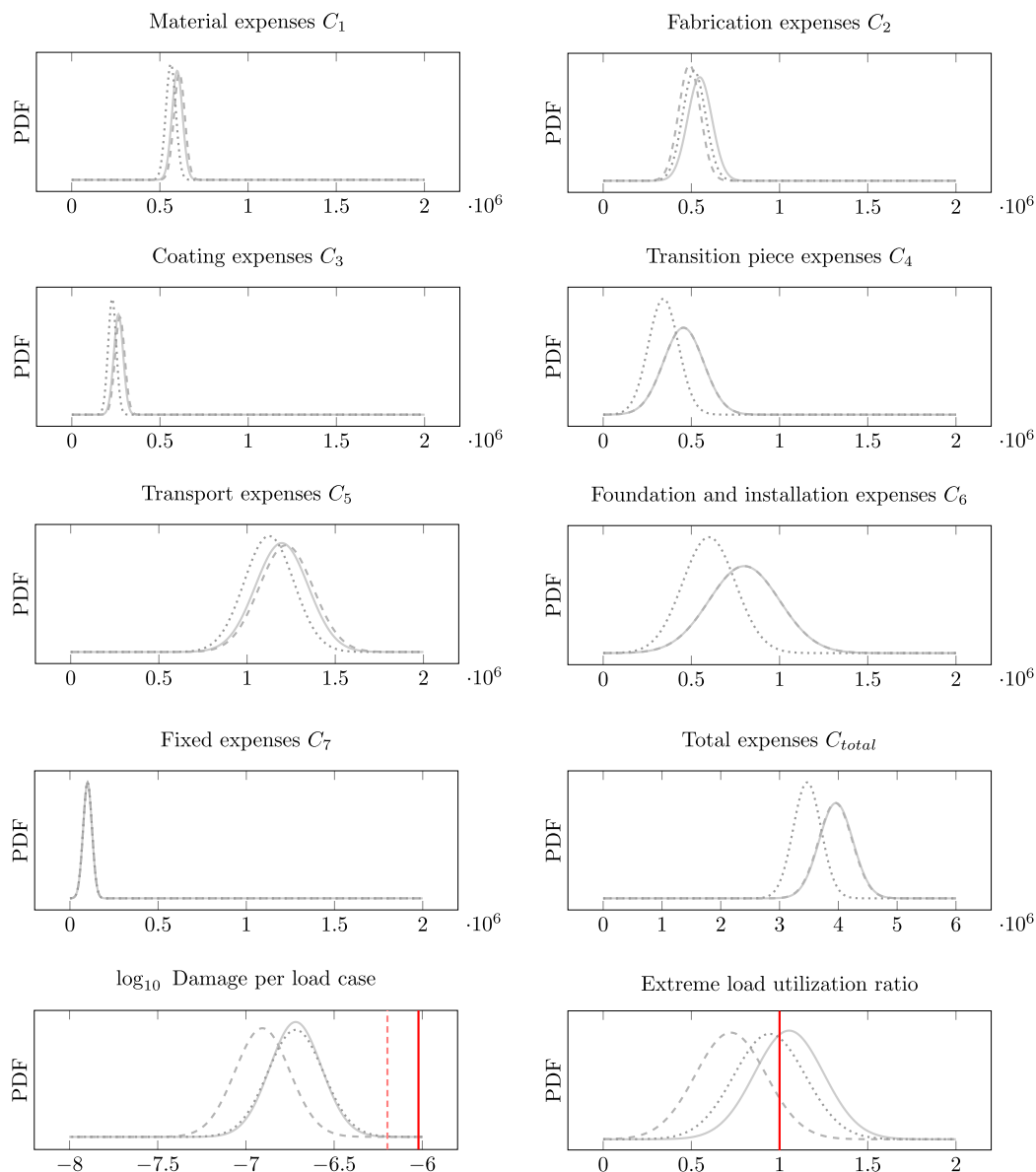
**Figure 6.** Prediction results for all samples of the validation set. Asterisks depict mean predicted damages in the first and mean extreme load utilization ratios in the second plot, and whisker ranges illustrate the 95 % significance intervals. The solid red line illustrates the critical damage related to a 20-year lifetime of the structure or a utilization ratio of 1. Moreover, the 30-year damage is illustrated with a dashed red line in the first plot.

diameter of 1.2 m, and  $\beta = \beta_b = \beta_t = 0.67$ . The second one (b) has only three bays, but higher tube diameters and thicknesses with  $D_L = 1.32$  m and constant  $\beta = \beta_b = \beta_t = 0.75$ . The third jacket (c) is the same as the first one (a), but with only three legs ( $N_L = 3$ ) and an increased leg diameter  $D_L = 1.44$  m. Thus, all structures are representative for different approaches known from practical applications and it is easily imaginable that they differ in all cost factors of the cost model except for the fixed expenses.

First, the cost contributions  $C_1 \dots C_7$  are calculated for each substructure according to the proposed cost model. Now, two helpful properties are used to evaluate the costs:

**Table 5.** Reference unit costs for the considered example, a 5 MW reference turbine in a water depth of 50 m.

Unit cost	Unit	Mean	Standard deviation
$a_1$	$kg^{-1}$	1.0	$5.0 \times 10^{-2}$
$a_2$	$m^{-3}$	$4.0 \times 10^6$	$0.5 \times 10^6$
$a_3$	$m^{-2}$	$1.0 \times 10^2$	$1.0 \times 10^1$
$a_4$	$m^{-1}$	$2.0 \times 10^4$	$5.0 \times 10^3$
$a_5$	$kg^{-1}$	2.0	$2.5 \times 10^{-1}$
$a_6$	-	$2.0 \times 10^5$	$5.0 \times 10^4$
$a_7$	-	$1.0 \times 10^5$	$2.5 \times 10^4$



**Figure 7.** Probability density functions (PDFs) of the cost contributions  $C_1 \dots C_7$ , the total expenses  $C_{total}$ , the (logarithmized) predicted damage per load case, and the predicted extreme load utilization ratio for the considered example case. Each plot shows the probability density depending on cost, damage exponent, and utilization ratio. Structure (1) is illustrated by the solid gray line, structure (2) by the dashed gray line, and structure (3) by the dotted gray line. The solid red line illustrates the critical damage related to a 20-year lifetime of the structure or a utilization ratio of 1. Moreover, the 30-year damage is illustrated with the dashed red line.

1. the total costs of each substructure,  $C_{total}$ , which are a linear combination of the single contributions,  $C_1 \dots C_7$ , and
2. the sum of normal distributions is again normally distributed.

Figure 7 shows the resulting probability density functions of all cost contributions and the total expenses when the normally distributed unit costs in Table 5 are combined with the proposed cost model. The three-leg design (c) is the cheapest

among the considered structures because the tube dimension increase of 20% (all tube sizing parameters depend linearly on the leg diameter) is overcompensated for by the reduction in jacket legs, which shows in the factor mass, resulting in significantly lower costs. The structures (a) and (b) show stronger similarities in all cost contributions, adding up to nearly equal total expenses.

However, the cost assessment is not meaningful without consideration of structural code checks. The surrogate models for fatigue and ultimate limit state are utilized for pre-

diction and also shown in Fig. 7. Structure (a) takes a mean damage of  $10^{-6.72}$  per load case, structure (b)  $10^{-6.91}$ , and structure (c)  $10^{-6.72}$ , all with similar variance. Linear damage accumulation (implying that the lifetime is reached at a cumulated damage of 1) and a simulation time per load case of 10 min yields lifetimes of approximately 100, 155, and 100 years for the three structures, considering a fatigue safety factor of 1.25. The same procedure is applied to ultimate limit state assessment and mean tube utilization ratios of 1.05, 0.72, and 0.94 are obtained in the critical load case for the structures (a), (b), and (c), respectively. Therefore, although all structures are quite close to an ideal utilization ratio, the second structure has the highest capacity concerning extreme loads.

Although only three designs were considered in this example, it is conceivable that three-legged structures are truly competitive with respect to the given boundaries because the design of structure (c) is related to the lowest capital expenses and has sufficient load capacities in the fatigue and ultimate limit state. According to the proposed cost model, the cost saving arises mainly from two contributions, namely transition piece expenses and foundation and installation expenses, both depending linearly on the number of jacket legs. This is in agreement with experiences from practical applications because three-legged structures have recently increased in importance, which is visible in the number of offshore installations for turbines with intermediate rated power. Comparing structure (a) and (b), the cost differences are marginal, while structure (b) turns out to be much better in terms of structural properties, which is visible in a higher lifetime and a lower extreme load utilization ratio. Therefore, it can be stated that the number of jacket legs and the leg diameter (in the case of dependent brace dimensions) are key parameters in the first phase of jacket design. A quantitative sensitivity analysis of the remaining parameters has to be conducted in forthcoming studies.

It can be imagined that the approach is easily usable for far more complex studies in which the number of design samples is much higher than in the present example because the entire procedure, which usually requires enormous numerical capacity, was solved in a negligible amount of time. It was already discussed that every jacket design requires a high number of time domain simulations to perform structural code checks. Therefore, the proposed methodology is appropriate to assess the topology and dimensions of a substructure, while structural details still have to be determined with high-fidelity models.

Moreover, the example shows that uncertainty can be easily incorporated in the design assessment using the proposed models for capital expenses and structural code checks. This may lead to probabilistic studies or robust jacket design.

## 6 Limitations

The models established in this work provide the groundwork to regard the jacket design process from a scientific point of view, not from an application-oriented design perspective, which depends highly on (human) expert knowledge. This aspect is emphasized strongly at this point because the outcome from studies based on these models will most likely not represent the geometry of the final structure, but an initial or conceptual design approach suitable for implementations with high numerical demands. Therefore, although the proposed models provide a comprehensive basis for design evaluations or optimization, they have to be used with caution. There is still a distinct amount of uncertainty in the surrogate model outputs, which arises from different sources, such as load set reductions, relatively small training sets (due to limited numerical capacity), or nonlinearities in physical models or structural code checks.

In addition, it has to be mentioned that though the methods are probably applicable to other turbines as well, the numerical parameters and results in the considered example are only valid for a jacket substructure at a given (fictive) offshore location with a 50 m water depth, FINO3 environmental conditions, and the NREL 5 MW turbine. An adaption to different boundaries requires a reestimation of the parameters.

## 7 Conclusions

The objective of this work was to provide a minimal but comprehensive approach to conceptual studies on jacket substructures for wind turbines. For this purpose, a geometry model was defined. A completely analytical cost model was derived afterwards. The issue of computationally expensive structural code checks was faced by surrogate modeling, namely Gaussian process regression models. Finally, an example was considered to show the capabilities of the developed models in which three artificial structures were analyzed. It was shown that different jacket design approaches (varying in topology and tube dimensions) may be appropriate solutions for a given wind turbine and environmental conditions. The present work improves the state of the art by combining a jacket model with topological design variables, more realistic cost and load assumptions, structural design code checks, and coupled time domain simulations in one approach.

Deliberately, this paper does not provide too extensive numerical results for applied science. The proposed models and equations are to be used for more realistic design studies on latticed substructures for offshore wind farms. Therefore, the path can continue in two ways: first, design studies not focused on structural aspects can benefit from these models because they do not require too much knowledge about physical details. But second and intentionally, this work contributes a substantial improvement to jacket optimization approaches, yet mostly focuses on tube dimensioning and of-

ten neglects structural topology aspects, a correct cost assessment, or realistic structural code checks. In particular, the utilization of surrogate modeling is very promising when dealing with meta-heuristic algorithms like evolutionary or swarm-based approaches applied to the jacket optimization problem because the related numerical expenses are significantly lower compared to approaches based on time domain simulations. This may lead to much more detailed analyses of the optimization procedure from the mathematical point of view because approaches known from the literature are focused on technical aspects. Questions to be answered in this

context are, for instance, how the constraints can be handled efficiently or which algorithm is most suitable for the jacket optimization problem.

**Code and data availability.** The results of training and validation sets, including fatigue and ultimate limit state code checks, are provided and available for research purposes. To set up Gaussian process regression models, we use and recommend using GPML, which can be run with Octave, MATLAB, or Python. GPML is freely available at <http://www.gaussianprocess.org/gpml/code/matlab/doc/> (GPML, 2018).

**Appendix A: Nomenclature**

DLC	Design load case
$\mathbb{E}$	Expected value
$\mathcal{GP}(m, k)$	Gaussian process with mean function $m$ and covariance function $k$
GPR	Gaussian process regression
MSL	Mean sea level
$\mathbb{N}$	Set of natural numbers
$\mathcal{N}(\mu, \sigma^2)$	Normally distributed number with mean $\mu$ and variance $\sigma^2$
SF	Partial safety factor
TI	Turbulence intensity
$\Phi_p$	Planar (two-dimensional) batter angle
$\Phi_s$	Spatial (three-dimensional) batter angle
$\beta_b$	Brace-to-leg diameter ratio at bottom (jacket model parameter)
$\beta_i$	Brace-to-leg diameter ratio in the $i$ th bay
$\beta_t$	Brace-to-leg diameter ratio at top (jacket model parameter)
$\gamma_b$	Leg radius-to-thickness ratio at bottom (jacket model parameter)
$\gamma_i$	Leg radius-to-thickness ratio in the $i$ th bay
$\gamma_t$	Leg radius-to-thickness ratio at top (jacket model parameter)
$\theta_{\text{wave}}$	Wave direction
$\theta_{\text{wind}}$	Wind direction
$\xi$	Head-to-foot radius ratio (jacket model parameter)
$\rho$	Material density (jacket model parameter)
$\sigma_n^2$	Gaussian input noise variance
$\vartheta$	Angle enclosed by two jacket legs
$\tau_b$	Brace-to-leg thickness ratio at bottom (jacket model parameter)
$\tau_i$	Brace-to-leg thickness ratio in the $i$ th bay
$\tau_t$	Brace-to-leg thickness ratio at top (jacket model parameter)
$\psi_{1,i}$	Lower brace-to-leg connection angle in the $i$ th bay
$\psi_{2,i}$	Upper brace-to-leg connection angle in the $i$ th bay
$\psi_{3,i}$	Brace-to-brace connection angle in the $i$ th bay
$C_j$	Expenses related to $j$ th cost factor
$C_{\text{total}}$	Total capital expenses
$D_{\text{Bb}}$	Bottom brace diameter
$D_{\text{Bt}}$	Top brace diameter
$D_L$	Leg diameter (jacket model parameter)
$E$	Material Young's modulus (jacket model parameter)
$G$	Material shear modulus (jacket model parameter)
$H_s$	Significant wave height
$\mathbf{I}$	Identity martrix
$\mathbf{K}$	Kernel function matrix
$L$	Overall jacket length (jacket model parameter)
$L_{\text{MSL}}$	Transition piece elevation over MSL (jacket model parameter)
$L_{\text{OSG}}$	Lowest leg segment height (jacket model parameter)
$L_{\text{TP}}$	Transition piece segment height (jacket model parameter)
$L_i$	$i$ th jacket bay height
$L_{m,i}$	Distance between the lower layer of K joints and the layer of X joints of the $i$ th bay
$M$	Size of the cross-validation leftover
$N$	Number of cross-validation bins
$N_L$	Number of legs (jacket model parameter)
$N_X$	Number of bays (jacket model parameter)
$P$	Probability density function
$R_{\text{Foot}}$	Foot radius (jacket model parameter)

$R_{\text{Head}}$	Head radius
$R_i$	$i$ th jacket bay radius at lower K joint layer
$R_{m,i}$	Radius of the $i$ th X joint layer
$T_{\text{Bb}}$	Bottom brace thickness
$T_{\text{Bt}}$	Top brace thickness
$T_{\text{Lb}}$	Bottom leg thickness
$T_{\text{Lt}}$	Top leg thickness
$T_p$	Wave peak period
$\mathbf{X}$	Matrix of training inputs (one sample per row)
$a$	Kernel weighting parameter
$a_j$	$j$ th unit cost
$c_j$	$j$ th cost factor
$e$	Noise
$e^{\text{bias}}$	Bias error
$e^{\text{mse}}$	Mean squared error
$f$	Function value
$\mathbf{k}$	Kernel function vector
$k$	Covariance (kernel) function
$k_{\text{Ma}3/2}$	Matérn 3/2 kernel function
$k_{\text{Ma}5/2}$	Matérn 5/2 kernel function
$k_{\text{RQ}}$	Rational quadratic kernel function
$k_{\text{SE}}$	Squared exponential kernel function
$l$	Kernel length-scale parameter
$m$	Mean function
$q$	Ratio of two consecutive bay heights (jacket model parameter)
$u_{\text{ss}}$	Subsurface current velocity
$u_{\text{w}}$	Near-surface current velocity
$v_s$	Mean wind speed
$\mathbf{x}$	Array of design variables/vector of training
$\mathbf{x}^*$	Array of prediction inputs
$x_{\text{MB}}$	Mud brace flag (jacket model parameter)
$\mathbf{y}$	Vector of training outputs (one sample per row)
$y$	General regression output value
$y^*$	Prediction value

**The Supplement related to this article is available online at <https://doi.org/10.5194/wes-3-553-2018-supplement>.**

**Competing interests.** The author declares that there is no conflict of interest.

**Disclaimer.** The views expressed in the article do not necessarily represent the views of the U.S. Department of Energy or the U.S. government.

**Acknowledgements.** This work was supported by the compute cluster, which is funded by the Leibniz Universität Hannover, the Lower Saxony Ministry of Science and Culture (MWK), and the German Research Foundation (DFG).

Cordial thanks are given to Jason Jonkman, Amy Robertson, and Katherine Dykes from the National Renewable Energy Laboratory, who supported this work with many valuable remarks and suggestions, and Manuela Böhm from Leibniz Universität Hannover for supporting the numerical simulation work.

The Alliance for Sustainable Energy, LLC (Alliance) is the manager and operator of the National Renewable Energy Laboratory (NREL). NREL is a national laboratory of the U.S. Department of Energy, Office of Energy Efficiency and Renewable Energy. This work was authored by the Alliance and supported by the U.S. Department of Energy under contract no. DE-AC36-08GO28308. Funding was provided by the U.S. Department of Energy Office of Energy Efficiency and Renewable Energy, Wind Energy Technologies Office.

The publication of this article was funded by the open-access fund of Leibniz Universität Hannover.

Edited by: Athanasios Kolios

Reviewed by: two anonymous referees

## References

- AlHamaydeh, M., Barakat, S., and Nasif, O.: Optimization of Support Structures for Offshore Wind Turbines Using Genetic Algorithm with Domain-Trimming, *Math. Probl. Eng.*, 2017, 1–14, <https://doi.org/10.1155/2017/5978375>, 2017.
- American Petroleum Institute: Recommended Practice for Planning, Designing and Constructing Fixed Offshore Platforms – Working Stress Design, Recommended Practice RP 2A-WSD, 2002.
- Brandt, S., Broggi, M., Häfele, J., Gebhardt, C. G., Rolfes, R., and Beer, M.: Meta-models for fatigue damage estimation of offshore wind turbines jacket substructures, *Procedia Engineer.*, 199, 1158–1163, <https://doi.org/10.1016/j.proeng.2017.09.292>, 2017.
- BVGassociates: Offshore wind cost reduction pathways – Technology work stream, Tech. rep., 2012.
- BVGassociates: Offshore wind: Industry’s journey to GBP 100/MWh – Cost breakdown and technology transition from 2013 to 2020, Tech. rep., 2013.
- Chew, K.-H., Tai, K., Ng, E., and Muskulus, M.: Analytical gradient-based optimization of offshore wind turbine substructures under fatigue and extreme loads, *Mar. Struct.*, 47, 23–41, <https://doi.org/10.1016/j.marstruc.2016.03.002>, 2016.
- Damiani, R. and Song, H.: A Jacket Sizing Tool for Offshore Wind Turbines within the Systems Engineering Initiative, in: *Offshore Technology Conference*, 6–9 May 2013, Houston, TX, USA, <https://doi.org/10.4043/24140-MS>, 2013.
- Damiani, R., Dykes, K., and Scott, G.: A comparison study of offshore wind support structures with monopiles and jackets for U.S. waters, *J. Phys. Conf. Ser.*, 753, 092003, <https://doi.org/10.1088/1742-6596/753/9/092003>, 2016.
- Damiani, R., Ning, A., Maples, B., Smith, A., and Dykes, K.: Scenario analysis for techno-economic model development of U.S. offshore wind support structures: Scenario analysis for techno-economic model development of U.S. offshore wind support structures, *Wind Energy*, 20, 731–747, <https://doi.org/10.1002/we.2021>, 2017.
- DNV GL AS: Fatigue design of offshore steel structures, Recommended Practice DNVGL-RP-C203, 2016a.
- DNV GL AS: Support structures for wind turbines, Offshore Standard DNVGL-ST-126, 2016b.
- Duvenaud, D. K.: Automatic Model Construction with Gaussian Processes, PhD thesis, University of Cambridge, Cambridge, UK, 2014.
- Efthymiou, M.: Development of SCF formulae and generalised influence functions for use in fatigue analysis, in: *Proceedings of the Conference on Recent Developments in Tubular Joints Technology*, 1–13, Surrey, 1988.
- Fingersh, L., Hand, M., and Laxson, A.: Wind Turbine Design Cost and Scaling Model, Technical Report NREL/TP-500-40566, Golden, CO, USA, 2006.
- Fischer, T., de Vries, W., and Schmidt, B.: Upwind Design Basis, Tech. rep., 2010.
- Germanischer Lloyd: Guideline for the Certification of Offshore Wind Turbines, Offshore Standard, 3–35, 2012.
- GPML: Gaussian process regression models, available at: <http://www.gaussianprocess.org/gpml/code/matlab/doc/>, last access: 13 August 2018.
- Häfele, J. and Rolfes, R.: Approaching the ideal design of jacket substructures for offshore wind turbines with a Particle Swarm Optimization algorithm, in: *Proceedings of the Twenty-sixth (2016) International Offshore and Polar Engineering Conference*, Rhodes, Greece, 156–163, 2016.
- Häfele, J., Hübler, C., Gebhardt, C. G., and Rolfes, R.: An improved two-step soil-structure interaction modeling method for dynamical analyses of offshore wind turbines, *Appl. Ocean Res.*, 55, 141–150, <https://doi.org/10.1016/j.apor.2015.12.001>, 2016.
- Häfele, J., Hübler, C., Gebhardt, C. G., and Rolfes, R.: A comprehensive fatigue load set reduction study for offshore wind turbines with jacket substructures, *Renew. Energ.*, 118, 99–112, <https://doi.org/10.1016/j.renene.2017.10.097>, 2017a.
- Häfele, J., Hübler, C., Gebhardt, C. G., and Rolfes, R.: Efficient Fatigue Limit State Design Load Sets for Jacket Substructures Considering Probability Distributions of Environmental States, in: *Proceedings of the Twenty-seventh (2017) International Off-*



- shore and Polar Engineering Conference, San Francisco, CA, USA, 167–173, 2017b.
- Ho, A., Mbistrova, A., and Corbetta, G.: The European offshore wind industry – key trends and statistics 2015, Tech. rep., 2016.
- Hübler, C., Häfele, J., Ehrmann, A., and Rolfes, R.: Effective consideration of soil characteristics in time domain simulations of bottom fixed offshore wind turbines, in: Proceedings of the Twenty-sixth (2016) International Offshore and Polar Engineering Conference, Rhodes, Greece, 127–134, 2016.
- Hübler, C., Gebhardt, C. G., and Rolfes, R.: Development of a comprehensive database of scattering environmental conditions and simulation constraints for offshore wind turbines, *Wind Energ. Sci.*, 2, 491–505, <https://doi.org/10.5194/wes-2-491-2017>, 2017a.
- Hübler, C., Piel, J.-H., Breitner, M. H., and Rolfes, R.: How Do Structural Designs Affect the Economic Viability of Offshore Wind Turbines? An Interdisciplinary Simulation Approach, in: Conference: International Conference on Operations Research, Berlin, Germany, 2017b.
- International Electrotechnical Commission: Wind turbines – Part 3: Design requirements for offshore wind turbines, Tech. Rep. IEC-61400-3:2009, EN 61400-3:2009, 2009.
- Jonkman, J. M. and Musial, W.: Offshore Code Comparison Collaboration (OC3) for IEA Task 23 Offshore Wind Technology and Deployment, Technical Report NREL/TP-5000-48191, National Renewable Energy Laboratory, Golden, CO, USA, 2010.
- Jonkman, J. M., Butterfield, S., Musial, W., and Scott, G.: Definition of a 5-MW Reference Wind Turbine for Offshore System Development, Technical Report NREL/TP-500-38060, National Renewable Energy Laboratory, Golden, CO, USA, 2009.
- Kaveh, A. and Sabeti, S.: Structural optimization of jacket supporting structures for offshore wind turbines using colliding bodies optimization algorithm, *Struct. Des. Tall. Spec.*, 27, e1494, <https://doi.org/10.1002/tal.1494>, 2018.
- King, R. N.: Learning and Optimization for Turbulent Flows, PhD thesis, University of Colorado, Boulder, CO, USA, 2016.
- Michels, G.: Mass Production of Offshore Wind-Jackets requires new Industrial Solutions, in: Nationale Staalbouwdag, Katwijk, the Netherlands, 2014.
- National Wind Technology Center Information Portal: Plant\_CostsSE, available at: [https://nwtc.nrel.gov/Plant\\_CostsSE](https://nwtc.nrel.gov/Plant_CostsSE) (last access: 23 July 2018), 2014.
- National Wind Technology Center Information Portal: FAST v8, available at: <https://nwtc.nrel.gov/FAST8> (last access: 23 July 2018), 2016.
- Ning, A., Damiani, R., and Moriarty, P.: Objectives and Constraints for Wind Turbine Optimization, in: 51st AIAA Aerospace Sciences Meeting, Grapevine, TX, USA, <https://doi.org/10.2514/6.2013-201>, 2013.
- NORSOK: Design of steel structures, Standard N-004 Rev. 2, 2004.
- Oest, J., Sørensen, R., T. Overgaard, L. C., and Lund, E.: Structural optimization with fatigue and ultimate limit constraints of jacket structures for large offshore wind turbines, *Struct. Multidiscip. O.*, 55, 779–793, <https://doi.org/10.1007/s00158-016-1527-x>, 2016.
- Popko, W., Vorpahl, F., Zuga, A., Kohlmeier, M., Jonkman, J., Robertson, A., Larsen, T. J., Yde, A., Saeterstro, K., Okstad, K. M., Nichols, J., Nygaard, T. A., Gao, Z., Manolas, D., Kim, K., Yu, Q., Shi, W., Park, H., Vasquez-Rojas, A., Dubois, J., Kaufer, D., Thomassen, P., de Ruiter, M. J., Peeringa, J. M., Zhiwen, H., and von Waaden, H.: Offshore Code Comparison Collaboration Continuation (OC4), Phase I – Results of Coupled Simulations of an Offshore Wind Turbine with Jacket Support Structure, *Journal of Ocean and Wind Energy*, 1, 1–11, 2014.
- Rasmussen, C. E. and Williams, C. K. I.: Gaussian processes for machine learning, MIT Press, Cambridge, MA, USA, 3rd print edn., 2008.
- Scholle, N., Radulović, L., Nijssen, R., Ibsen, L. B., Kohlmeier, M., Foglia, A., Natarajan, A., Thiel, J., Kuhnle, B., Kraft, M., Kühn, M., Brosche, P., and Kaufer, D.: Innovations on component level (final report), INNWIND.EU Deliverable D4.1.3, 2015.
- Smith, A., Stehly, T., and Musial, W.: 2014–2015 Offshore Wind Technologies Market Report, Technical Report NREL/TP-5000-64283, National Renewable Energy Laboratory, Golden, CO, USA, 2015.
- Stolpe, M. and Sandal, K.: Structural optimization with several discrete design variables per part by outer approximation, *Struct. Multidiscip. O.*, 57, 2061–2073, <https://doi.org/10.1007/s00158-018-1941-3>, 2018.



## 5 Evaluation of optimal designs for offshore wind turbine jacket substructures

This work merges the proposed methods to a holistic optimization approach and published in Wind Energy Science, Vol. 4, 2019, pp. 23–40 (DOI: 10.5194/wes-2018-58).

### Author contributions

Jan Häfele is the corresponding author of the publication and the main author of all sections.

Cristian Guillermo Gebhardt gave technical and editorial suggestions for improvement of the entire publication.

Raimund Rolfes gave technical and editorial suggestions for improvement of the entire publication and performed the final proofreading.



# A comparison study on jacket substructures for offshore wind turbines based on optimization

Jan Häfele, Cristian G. Gebhardt, and Raimund Rolfes

Leibniz Universität Hannover/ForWind, Institute of Structural Analysis, Appelstr. 9a,  
30167 Hanover, Germany

**Correspondence:** Jan Häfele (j.haeefe@isd.uni-hannover.de)

Received: 28 August 2018 – Discussion started: 17 September 2018

Revised: 26 December 2018 – Accepted: 6 January 2019 – Published: 22 January 2019

**Abstract.** The structural optimization problem of jacket substructures for offshore wind turbines is commonly regarded as a pure tube dimensioning problem, minimizing the entire mass of the structure. However, this approach goes along with the assumption that the given topology is fixed in any case. The present work contributes to the improvement of the state of the art by utilizing more detailed models for geometry, costs, and structural design code checks. They are assembled in an optimization scheme, in order to consider the jacket optimization problem from a different point of view that is closer to practical applications. The conventional mass objective function is replaced by a sum of various terms related to the cost of the structure. To address the issue of high demand of numerical capacity, a machine learning approach based on Gaussian process regression is applied to reduce numerical expenses and enhance the number of considered design load cases. The proposed approach is meant to provide decision guidance in the first phase of wind farm planning. A numerical example for a National Renewable Energy Laboratory (NREL) 5 MW turbine under FINO3 environmental conditions is computed by two effective optimization methods (sequential quadratic programming and an interior-point method), allowing for the estimation of characteristic design variables of a jacket substructure. In order to resolve the mixed-integer problem formulation, multiple subproblems with fixed-integer design variables are solved. The results show that three-legged jackets may be preferable to four-legged ones under the boundaries of this study. In addition, it is shown that mass-dependent cost functions can be easily improved by just considering the number of jacket legs to yield more reliable results.

## 1 Introduction

The substructure contributes significantly to the total capital expenses of offshore wind turbines and thus to the levelized costs of offshore wind energy, which are still high compared to the onshore counterpart (Mone et al., 2017). Cost breakdowns show ratios of about 20 % (such as The Crown Estate, 2012; BVGassociates, 2013) depending on rated power, water depth, and what is regarded as capital expenses. In the face of wind farms with often more than 100 turbines, it is easily conceivable that a slight cost reduction can already render substantial economic advantages to prospective projects. Structural optimization is paramount because it provides the great opportunity to tap cost-saving potential with low economic effort. Technologically, it is expected that the

jacket will supersede the mono-pile when reaching the imminent turbine generation or wind farm locations with intermediate water depths from about 40 to 60 m (see, for instance, Seidel, 2007; Damiani et al., 2016). According to current studies, there is an increasing market share of jackets (Smith et al., 2015). As it allows for many variants of structural design, the jacket structure is therefore a meaningful object of structural optimization approaches, which benefits massively from innovative design methods and tools (van Kuik et al., 2016).

It is state of the art in the field of jacket optimization to deal with optimal design in terms of a tube dimension-

ing problem, where the topology is fixed.<sup>1</sup> Structural design codes require the computation of time domain simulations to perform structural code checks for fatigue and ultimate limit state. As environmental conditions in offshore wind farm locations vary strongly, commonly thousands of simulations are necessary to cover the effect of varying wind and wave states for verification.<sup>2</sup> Therefore, numerical limitations are a great issue in state-of-the-art jacket optimization approaches. In the literature, different approaches were presented to address this issue. Schafhirt et al. (2014) proposed an optimization scheme based on a meta-heuristic genetic algorithm to guarantee global convergence. To increase the numerical efficiency, a reanalysis technique was applied. Later, an improved approach was illustrated (Schafhirt et al., 2016), where the load calculation was decoupled from the actual tube dimensioning procedure and a simplified fatigue load set (Zwick and Muskulus, 2016) was applied. Similar approaches by Chew et al. (2015, 2016) and Oest et al. (2016) applied sequential quadratic or linear programming methods, respectively, with analytically derived gradients. Other optimization approaches using meta-heuristic algorithms were reported by AlHamaydeh et al. (2017) and Kaveh and Sabeti (2018) but without comprehensive load assumptions. The problem of discrete design variables was addressed by Stolpe and Sandal (2018). Oest et al. (2018) presented a jacket optimization study, where different simulation codes were deployed to perform structural code checks. All mentioned works, except for the last one, represent tube sizing algorithms applied to the Offshore Code Comparison Collaboration Continuation (OC4) jacket substructure (Popko et al., 2014) for the National Renewable Energy Laboratory (NREL) 5 MW reference turbine (Jonkman et al., 2009),<sup>3</sup> where the initial structural topology is maintained even in the case of a strong tube diameter and wall thickness variations. Furthermore, it can be stated that all proposals share the entire mass of the jacket as an objective function to be minimized, which is meaningful in terms of tube sizing. Due to numerical limitations, the utilized load sets are altogether small, for instance with low numbers of production load cases or the omission of special extreme load events. These assumptions constitute drawbacks when considering jacket optimization as part of a decision process in early de-

sign stages, where basic properties like the numbers of legs or bays are more critical than the exact dimensions of each single tube. Therefore, an optimization scheme which addresses the early design phase is highly desirable to provide decision guidance for experienced designers. Proposals tackling this kind of problem were given by Damiani (2016) and Häfele and Rolfes (2016), where technically oriented jacket models were proposed but lacking fatigue limit state checks in the first and detailed load assumptions in the second case. Based on the latter and with improved load assumptions, a hybrid jacket for offshore wind turbines with high rated power was designed (Häfele et al., 2016). Due to innovative materials (the technology readiness level of such a structure is still low), this work lacked detailed cost assumptions. Another proposal for an integrated design approach was made by Sandal et al. (2018), considering varying bottom widths and soil properties. This work is meant as an approach for conceptual design phases. However, our conclusion on the state of the art is that an optimization approach without massive limitations is still missing.

This work is intended as a contribution to the improvement of the state of the art by considering jacket optimization in a different way. Compared to other works in this field, the focus is on

1. the incorporation of topological design variables in the optimization problem, while the dimensioning of tubes is characterized by global design variables;
2. more detailed cost assumptions;
3. more comprehensive load sets for fatigue and ultimate limit state structural design code checks;
4. a change in the exploitation of jacket optimization results. This work intends to consider jacket optimization as a part of the preliminary design phase because it is assumed that the (economically) most expensive mistakes in jacket design are made at this stage of the design process.

A basis to address these points was given by Häfele et al. (2018a), where appropriate geometry, cost, and structural code check models for fatigue and ultimate limit states were developed. In this study, these models are deployed within an optimization scheme to obtain optimal design solutions for jacket substructures. A more efficient or accurate method to solve the optimization problem is deliberately not provided in this study. The authors believe that there are numerous techniques presented in the literature that are able to solve the jacket optimization problem.

The paper is structured as follows. Sect. 2 describes the technical and mathematical problem statements. Both the objective and the constraints are presented and explained in Sect. 3. The optimization approach and methods to solve the problem are discussed in Sect. 4. Section 5 illustrates the application of the approach to a test problem, a comparison

<sup>1</sup>This work focuses on the problem of jacket optimization and disregards other substructure types. For a comprehensive overview of the structural optimization of wind turbine support structures, Muskulus and Schafhirt (2014).

<sup>2</sup>During conceptual design phases, the number of load cases is commonly reduced.

<sup>3</sup>It is worth mentioning that the Offshore Code Comparison Collaboration Continuation (OC4) jacket is actually a structurally reduced derivation of the so-called UpWind jacket (Vemula et al., 2010), which was created to ease calculations within the verification efforts in the OC4 project. Therefore, it is not guaranteed that the OC4 jacket is an appropriate comparison object, as it does not incorporate details of tubular joints.

of jackets with different topologies, performed for an NREL 5 MW turbine under FINO3 environmental conditions. This section comprises a detailed setup of the problem and a discussion of the results. The work ends with a consideration of benefits and limitations (Sect. 6) and conclusions (Sect. 7).

## 2 Problem statement

This paper presents a study on jacket substructures, based on optimization. The design of jackets is a complex task that requires profound expertise and experience. Therefore, it has to be clarified that this work does not provide a method replacing established design procedures. It is rather meant as guidance in early design phases, where it is desirable to define the basic topology and dimensions of the substructure. In industrial applications, this step is commonly highly dependent on the knowledge of experienced designers. Along with this statement, it has to be pointed out that the term “optimal solution” may indicate a solution that it is indeed optimal concerning the present problem formulation but not necessarily optimal in terms of a final design due to the following aspects.

- Although the approach deploys more detailed assumptions on the modeling of costs and environmental conditions, compared to optimization approaches known from the literature, it still incorporates simplifications, mainly for the sake of numerical efficiency.
- No sizing of each single tube is performed, for the same reason. This is a matter of subsequent design phases, and tube dimensioning approaches exist in the literature. Instead, tube dimensions are derived by global design variables.
- The design of pile foundation and transition piece is not performed in this approach. The reason is that both are considered in models of the structure and the costs but are not impacted by the selected design variables.
- Only fatigue and ultimate limit state are assumed to be design-driving constraints. Serviceability limit state, i.e., eigenfrequency constraints, is not regarded as design-driving in this work because the modal behavior of a wind turbine with jacket substructure is strongly dominated by the relatively soft tubular tower. In addition, a design leading to eigenfrequencies close to 1P or 3P excitation would probably fail due to high fatigue damage. Although the modal behavior is also impacted by the foundation, this is not significant here, as no foundation design is performed.

The overall goal of jacket optimization can be interpreted as a cost minimization problem involving certain design constraints. As stated before, it is assumed that the design-driving constraints of jackets are fatigue and extreme loads.

In other words, a set of design variables for a parameterizable structure that minimizes its costs,  $C_{\text{total}}$ , is desirable, while fatigue and ultimate limit state constraints are satisfied; i.e., the maximal normalized tubular joint fatigue damage (among all tubular joints),  $h_{\text{FLS}}$ , is less than or equal to 1,<sup>4</sup> and the extreme load utilization ratio (among all tubes),  $h_{\text{ULS}}$ , is less than or equal to 1.

The total expenses are defined as an objective function  $f(\mathbf{x})$ , which depends on an array of design variables,  $\mathbf{x}$ :

$$f(\mathbf{x}) = \log_{10}(C_{\text{total}}(\mathbf{x})). \quad (1)$$

In this equation, the cost value is logarithmized to obviate numerical issues. The constraints,  $h_1(\mathbf{x})$  and  $h_2(\mathbf{x})$ , are formulated so as to match the requirements of mathematical problem statements; thus

$$\begin{aligned} h_1(\mathbf{x}) &= h_{\text{FLS}}(\mathbf{x}) - 1, \\ h_2(\mathbf{x}) &= h_{\text{ULS}}(\mathbf{x}) - 1, \end{aligned} \quad (2)$$

depending also on the array of design variables,  $\mathbf{x}$ .

Based on the technical problem statement, we define the mathematical problem statement in terms of a nonlinear program:

$$\begin{aligned} \min f(\mathbf{x}) \\ \text{such that } \mathbf{x}_{\text{lb}} \leq \mathbf{x} \leq \mathbf{x}_{\text{ub}}, \\ h_1(\mathbf{x}) \leq 0 \text{ and } h_2(\mathbf{x}) \leq 0, \end{aligned} \quad (3)$$

where  $\mathbf{x}$  is the array or vector of design variables,  $\mathbf{x}_{\text{lb}}$  and  $\mathbf{x}_{\text{ub}}$  are the lower and upper boundaries, respectively,  $f(\mathbf{x})$  is the objective function, covering the costs related only to the substructure, and  $h_1(\mathbf{x})$  and  $h_2(\mathbf{x})$  are nonlinear constraints representing structural code checks for fatigue and ultimate limit state that are required to be satisfied for every design.

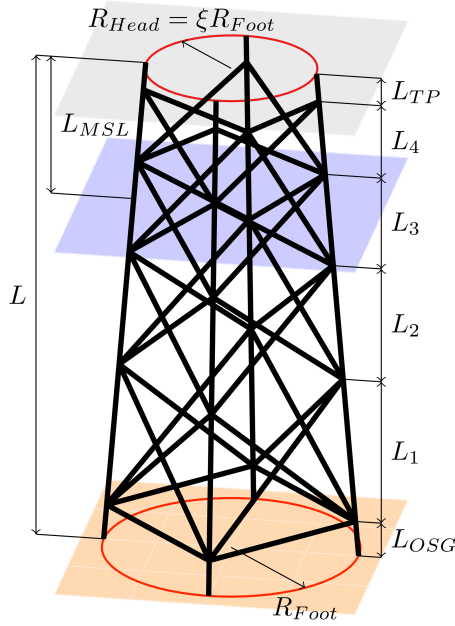
## 3 Objective and constraints

This section illustrates the jacket model, which is the basis for the optimization study. Moreover, the models for costs and structural design code checks are described, which depict the objective and constraint functions, respectively. These models were elaborated on in a previous work (Häfele et al., 2018a).

### 3.1 Jacket modeling and design variables

In this work, it is assumed that a jacket substructure can be described by 20 parameters in total, of which 10 define topology, 7 tube dimensions, and 3 material properties. Topological parameters are the number of legs,  $N_L$ , number of bays,  $N_X$  (both integer variables), foot radius,  $R_{\text{foot}}$ , head-to-foot radius ratio,  $\xi$ , jacket length,  $L$ , elevation of the transition

<sup>4</sup>All fatigue damage is normalized so that the lifetime fatigue damage corresponds to a value of 1.



**Figure 1.** Jacket geometry model with variables characterizing the topology of the structure, shown exemplarily for a jacket with four legs, four bays, and mud braces. The ground layer is illustrated by the orange surface and the mean sea level and transition piece layers by the blue and gray surfaces, respectively.

piece over mean sea level,  $L_{MSL}$ , lowermost segment height,  $L_{OSG}$ , uppermost segment height,  $L_{TP}$ , the ratio of two consecutive bay heights,  $q$ , and a boolean flag,  $x_{MB}$ , determining whether the jacket has mud braces (horizontal tubes below the lowermost layer of K joints) or not. The topology of one example with four legs ( $N_L = 4$ ), four bays ( $N_X = 4$ ), and mud braces  $x_{MB} = \text{true}$  is shown in Fig. 1. The tube sizing parameters are the leg diameter,  $D_L$ , and six dependent parameters defining relations between tube diameters and wall thicknesses at the bottom and top of the structure:  $\gamma_b$  and  $\gamma_t$  are the leg radius to thickness ratios,  $\beta_b$  and  $\beta_t$  are the brace-to-leg diameter ratios, and  $\tau_b$  and  $\tau_t$  are the brace-to-leg thickness ratios, where the indices  $b$  and  $t$  indicate values at the bottom and the top of the jacket, respectively. Using dependent parameters is beneficial because structural code checks are valid for certain ranges of these dependent variables. Furthermore, for structural analysis, the material is assumed to be isotropic and can thus be described by a Young's modulus,  $E$ , a shear modulus,  $G$ , and density,  $\rho$ .

To decrease the dimension of the problem, height measures related to the location of the wind farm ( $L$ ,  $L_{MSL}$ ,  $L_{OSG}$ ,  $L_{TP}$ ) and the material parameters ( $E$ ,  $G$ ,  $\rho$ ) are fixed. In addition, it is supposed that each design has mud braces ( $x_{MB} = \text{true}$ ). Although designs without mud braces are also imaginable, fixing this parameter is advantageous, as it is not continuous. The array of design variables therefore has a di-

mension of 12:

$$\mathbf{x} = (N_L \ N_X \ R_{foot} \ \xi \ q \ D_L \ \gamma_b \ \gamma_t \ \beta_b \ \beta_t \ \tau_b \ \tau_t)^T. \quad (4)$$

The number of design variables is not necessarily minimal, but, on the one hand, mathematically manageable and, on the other hand, meaningful from the technical point of view.

### 3.2 Cost function (objective)

The total capital expenses,  $C_{total}$ , comprise several terms,  $C_j$ , expressed as the sum of so-called factors,  $c_j$ , weighted by unit costs,  $a_j$ :<sup>5</sup>

$$C_{total}(\mathbf{x}) = \sum C_j(\mathbf{x}) = \sum a_j c_j(\mathbf{x}). \quad (5)$$

A factor may be any property of the structure describing a cost contribution that can be expressed in terms of the design variables. A pure mass-dependent cost modeling approach, as used in most optimization approaches, would involve only one factor, while no unit cost value is required for weighting. However, a realistic cost assessment involves more than only the structural mass. For example, in the case of a structure with very lightweight tubes but many bays, it can be imagined that the manufacturing costs tend to be a cost-driving factor. To consider known, important impacts on jacket capital expenses, seven factors are incorporated, namely the following:

- expenses for material,  $C_1$ , depending on the mass,  $c_1$ :

$$\begin{aligned} c_1(\mathbf{x}) = & 2\rho N_L \pi D_L^2 \sum_{i=1}^{N_X} \left( \left( \frac{\beta_i \tau_i}{2\gamma_i} + \frac{\tau_i^2}{4\gamma_i^2} \right) \right. \\ & \left. \sqrt{\frac{L_i^2}{\cos^2(\Phi_p)} + (R_i + R_{i+1})^2 \sin^2\left(\frac{\vartheta}{2}\right)} \right) \\ & + x_{MB} \rho N_L \pi D_L^2 \left( \frac{\beta_b \tau_b}{2\gamma_b} + \frac{\tau_b^2}{4\gamma_b^2} \right) 2R_1 \sin\left(\frac{\vartheta}{2}\right) \\ & + \rho N_L \pi D_L^2 \sum_{i=1}^{N_X} \left( \left( \frac{1}{2\gamma_i} + \frac{1}{4\gamma_i^2} \right) \frac{L_{m,i}}{\cos(\Phi_s)} \right. \\ & \left. + \left( \frac{1}{2\gamma_{i+1}} + \frac{1}{4\gamma_{i+1}^2} \right) \frac{(L_i - L_{m,i})}{\cos(\Phi_s)} \right) \\ & + \rho N_L \pi D_L^2 \left( \frac{1}{2\gamma_b} + \frac{1}{4\gamma_b^2} \right) \frac{L_{OSG}}{\cos(\Phi_s)} \\ & + \rho N_L \pi D_L^2 \left( \frac{1}{2\gamma_t} + \frac{1}{4\gamma_t^2} \right) \frac{L_{TP}}{\cos(\Phi_s)}; \quad (6) \end{aligned}$$

<sup>5</sup>Unit cost values are given in Sect. 5.3.

- expenses for fabrication,  $C_2$ , depending on the entire volume of welds,  $c_2$ :

$$c_2(\mathbf{x}) = 2N_L \pi D_L \sum_{i=1}^{N_X} \left( \beta_i \left( \frac{D_L^2 \tau_i^2}{8\gamma_i^2} + \frac{t_0 D_L \tau_i}{2\sqrt{2}\gamma_i} \right) \left( \sqrt{\frac{1}{2\sin^2(\psi_{1,i})} + \frac{1}{2}} + \sqrt{\frac{1}{2\sin^2(\psi_{2,i})} + \frac{1}{2}} + \sqrt{\frac{1}{2\sin^2(\psi_{3,i})} + \frac{1}{2}} \right) + 2x_{MB} N_L \pi D_L \beta_b \left( \frac{D_L^2 \tau_b^2}{8\gamma_b^2} + \frac{t_0 D_L \tau_b}{2\sqrt{2}\gamma_b} \right) + N_L \pi D_L \sum_{i=1}^{N_X} \left( \frac{D_L^2 \min\left(\frac{1}{\gamma_i^2}, \frac{1}{\gamma_{i+1}^2}\right)}{8} + \frac{D_L t_0 \min\left(\frac{1}{\gamma_i}, \frac{1}{\gamma_{i+1}}\right)}{2\sqrt{2}} \right); \quad (7)$$

- coating costs,  $C_3$ , depending on the outer surface area of all tubes,  $c_3$ :

$$c_3(\mathbf{x}) = 2N_L \pi D_L \sum_{i=1}^{N_X} \left( \beta_i \sqrt{\frac{L_i^2}{\cos^2(\Phi_p)} + (R_i + R_{i+1})^2 \sin^2\left(\frac{\vartheta}{2}\right)} + x_{MB} N_L \pi D_L \beta_b \left( 2R_1 \sin\left(\frac{\vartheta}{2}\right) \right) + N_L \pi D_L \frac{L}{\cos(\Phi_s)} \right); \quad (8)$$

- costs for the transition piece,  $C_4$ , proportional to the product of head radius and number of jacket legs,  $c_4$ :

$$c_4(\mathbf{x}) = N_L R_{\text{foot}} \xi; \quad (9)$$

- expenses for transport,  $C_5$ , expressed by the mass-dependent factor,  $c_5$ :

$$c_5(\mathbf{x}) = c_1(\mathbf{x}); \quad (10)$$

- and installation costs,  $C_6$ , modeled by a factor only depending on the number of jacket legs,  $c_6$ :

$$c_6(\mathbf{x}) = N_L. \quad (11)$$

Fixed expenses,  $C_7$ , are not dependent on any jacket parameter at all. Therefore, the factor,  $c_7$ , simply takes

$$c_7(\mathbf{x}) = 1. \quad (12)$$

In these equations,  $\vartheta$  is the angle enclosed by two jacket legs:

$$\vartheta = \frac{2\pi}{N_L}. \quad (13)$$

Bay heights,  $L_i$ , intermediate bay heights,  $L_{m,i}$ , radii,  $R_i$ , and intermediate radii,  $R_{m,i}$ , are calculated by the following equations:

$$L_i = \frac{L - L_{\text{OSG}} - L_{\text{TP}}}{\sum_{n=1}^{N_X} q^{n-i}}, \quad (14)$$

$$L_{m,i} = \frac{L_i R_i}{R_i + R_{i+1}}, \quad (15)$$

$$R_i = R_{\text{foot}} - \tan(\Phi_s) \left( L_{\text{OSG}} + \sum_{n=1}^{i-1} L_n \right), \quad (16)$$

$$R_{m,i} = R_{\text{foot}} - \tan(\Phi_s) \left( L_{\text{OSG}} + \sum_{n=1}^{i-1} L_n + L_{m,i} \right), \quad (17)$$

with the spatial batter angle,  $\Phi_s$ :

$$\Phi_s = \arctan\left(\frac{R_{\text{foot}}(1 - \xi)}{L}\right). \quad (18)$$

The interconnecting tube angles,  $\psi_{1,i}$ ,  $\psi_{2,i}$ , and  $\psi_{3,i}$ , are

$$\psi_{1,i} = \frac{\pi}{2} - \arctan\left(\frac{R_{\text{foot}}(1 - \xi) \sin\left(\frac{\vartheta}{2}\right) \cos(\Phi_p)}{L}\right) - \arctan\left(\frac{L_{m,i}}{R_i \sin\left(\frac{\vartheta}{2}\right) \cos(\Phi_p)}\right), \quad (19)$$

$$\psi_{2,i} = \frac{\pi}{2} + \arctan\left(\frac{R_{\text{foot}}(1 - \xi) \sin\left(\frac{\vartheta}{2}\right) \cos(\Phi_p)}{L}\right) - \arctan\left(\frac{L_{m,i}}{R_i \sin\left(\frac{\vartheta}{2}\right) \cos(\Phi_p)}\right), \quad (20)$$

$$\psi_{3,i} = 2 \arctan\left(\frac{L_{m,i}}{R_i \sin\left(\frac{\vartheta}{2}\right) \cos(\Phi_p)}\right), \quad (21)$$

with the planar batter angle,  $\Phi_p$ :

$$\Phi_p = \arctan\left(\frac{R_{\text{foot}}(1 - \xi) \sin\left(\frac{\vartheta}{2}\right)}{L}\right). \quad (22)$$

$\gamma_i$ ,  $\beta_i$ , and  $\tau_i$  represent the ratios of leg radius-to-thickness, brace-to-leg diameter, and brace-to-leg thickness of the  $i$ th bay, respectively, obtained by linear stepwise interpolation and counted upwards.

The cost modeling is based on several simplifications and assumptions. The mass-proportional modeling of material costs,  $C_1$ , is straightforward. Fabrication costs,  $C_2$ , mainly arise from welding and grinding processes. Although the actual manufacturing processes are quite complex, the entire



volume of welds can be regarded as a measure of the actual costs. Coating costs,  $C_3$ , are quite easy to determine by the outer surface area of all tubes, i.e., the area to be coated. There may be synergy effects when coating larger areas, but these are neglected. The expenses for the (stellar-type) transition piece,  $C_4$ , are assumed to be proportional to the head radius and the number of legs. There are more detailed approaches for this purpose, but no design of the transition piece is performed, which requires a simple approach. The determination of transport costs,  $C_5$ , is very difficult. In this work, a mass-dependent approach was selected, which is, however, a large simplification. The mass dependence reflects that barges have a limited transport capacity, which is at least to some extent mass-dependent or dependent on factors partially related to mass (like the space on the deck of the barge covered by the jacket). Installation costs,  $C_6$ , cover both the material and the manufacturing of the foundation and the installation at the wind farm location. In the case of a pile foundation, these costs are mainly governed by the number of piles, which is equal to the number of legs. The fixed expenses,  $C_7$ , are not vital for the solution of the optimization problem but are required to shift the costs to more realistic values by covering expenses for cranes, scaffolds, and so forth.

### 3.3 Structural code checks (constraints)

To check jacket designs – i.e., sets of design variables – for validity concerning fatigue and extreme load resistance, structural design code checks are performed. The standards DNV GL RP-C203 (DNV GL AS, 2016) for fatigue and NORSOK N-004 (NORSOK, 2004) for ultimate limit state checks are adopted. Both are widely accepted for practical applications and were used to design the UpWind (Vemula et al., 2010) and INNWIND.EU (von Borstel, 2013) reference jackets.

Commonly, the numerical demand of structural code checks is one of the main problems in jacket optimization. To cover the characteristics of environmental impacts on wind turbines, representative loads are to be used for the load assessment. This involves numerous load simulations to consider all load combinations that might occur, particularly in the fatigue case, where the excitation is extrapolated for the entire turbine lifetime. As not only the number of load simulations but also the duration (in the case of time domain simulations) correlates to a high demand in numerical capacity, most approaches deploy very simple load assumptions like one design load case per iteration, as already discussed. Altogether, a high numerical effort is required. Utilizing simplified load assumptions like equivalent static loads, where the substructure decoupled from the overlying structure and all interactions are neglected, depicts, however, a massive simplification in the case of a wide range of design variables. By contrast, a pure simulation-based optimization is not applicable due to the aforementioned reasons.

To face this issue, a surrogate modeling approach based on Gaussian process regression (GPR) is deployed. It was shown previously (Häfele et al., 2018a) that good regression results can be obtained by GPR for this purpose. In addition, the regression process relies on a mathematical process that can be interpreted easily and adapted to prior knowledge of the underlying physics. In the present case, the procedure is as follows: a load set with a defined number of design load cases is the basis for structural code checks. The size of the load sets and parameters of environmental and operational conditions are predetermined so as to represent the loads on the turbine adequately. With these load sets, numerical simulations are performed with the aero–hydro–servo–elastic simulation code FAST to obtain output data for the input space of the surrogate model.<sup>6</sup> As this procedure requires much computational effort, the input space is limited to 200 jacket samples (excluding validation samples) in each case as a basis for both surrogate models (fatigue and ultimate limit state),<sup>7</sup> obtained by a Latin hypercube sampling of the input space. In both cases, the results are vectors of output variables, where each element corresponds to a row in the matrix of inputs, comprising parameters of the input space. Both (input matrix and output vector) build the training data. For each new sample, the corresponding output (result of a structural code check) is evaluated by GPR.<sup>8</sup> The specific surrogate models for the considered test problems were derived in a previous work (Häfele et al., 2018a), which revealed that a Matérn 5/2 kernel function is well-suited for the present application.

#### 3.3.1 Fatigue limit state

The evaluation of fatigue limit state code checks requires many simulations considering design load cases (DLCs) 1.2 and 6.4 production load cases according to IEC 61400-3 (International Electrotechnical Commission, 2009). Under defined conditions (5 MW turbine, 50 m water depth, FINO3 environmental conditions), the required number of design load cases with respect to uncertainty was analyzed in previous papers (Häfele et al., 2017, 2018b). In these papers, a load set with 2048 design load cases was gradually reduced to smaller load sets. A reduced load set with 128 design load cases turned out to be a good compromise between accuracy, as the uncertainty arising from the load set reduction is acceptable in this case, and numerical effort, which is significantly smaller compared to the initial load set; i.e., considering two X-joint positions, the standard deviation of fatigue

<sup>6</sup>FASTv8 (National Wind Technology Center Information Portal, 2016) was used for this study.

<sup>7</sup>All parameters of these jacket samples are given in the publication where the surrogate modeling approach was reported (Häfele et al., 2018a).

<sup>8</sup>For the background theory of GPR, the reader is referred to Rasmussen and Williams (2008), which is the standard reference in this field.



damage increases by a factor of approximately 4 in the case of a 16-fold load set reduction (from 2048 to 128 design load cases). The actual fatigue assessment involves time domain simulations, an application of stress concentration factors according to Efthymiou (1988) to consider the amplification of stresses due to the geometry of tubular joints, rain flow cycle counting, and a lifetime prediction by  $S$ - $N$  curves and linear damage accumulation.<sup>9</sup> The output value  $h_{FLS}$  is the most critical fatigue damage among all damage values of the entire jacket (evaluated in eight circumferential points around each weld), normalized by the calculated damage at design lifetime. A design lifetime of 30 years is assumed, from which 25 years are the actual lifetime of the turbine and 5 years are added to consider malicious fatigue damage during the transport and installation process. Moreover, a partial safety factor of 1.25 is considered in the fatigue assessment.

### 3.3.2 Ultimate limit state

The standard IEC 61400-3 (International Electrotechnical Commission, 2009) requires several design load cases to perform structural code checks for the ultimate limit state. However, not every design load case is critical for the design of a jacket substructure. The relevant ones were analyzed and found to be DLC 1.3 (extreme turbulence during production), 1.6 (extreme sea state during production), 2.3 (grid loss fault during production), 6.1 (extreme sea state during idle), and 6.2 (extreme yaw error during idle) for a turbine with a rated power of 5 MW, under FINO3 environmental conditions and a water depth of 50 m. Extreme load parameters are derived by the block maximum method (see Agarwal and Manuel, 2010), where the environmental data are divided into many segments featuring similarly distributed data. From this data set, the maximum values are extracted. Based on these maxima, return values (as required by IEC 61400-3) of environmental states are computed. To conduct the structural code checks for the ultimate limit state, time domain simulations are performed and evaluated with respect to the extreme load of the member, where the highest utilization ratio occurs. The result  $h_{ULS}$  is a value that approaches 0 in the case of infinite extreme load resistance and 1 in the case of equal resistance and loads, implying that values greater than 1 are related to designs not fulfilling the ultimate limit state code check. The procedure considers combined loads with axial tension, axial compression, and bending, with and without hydrostatic pressure, which may lead to failure modes like material yielding, overall column buckling, local buckling, or any combination of these. A global buckling check is not performed in this study, as it is known to be uncritical for jacket substructures (Oest et al., 2016).

<sup>9</sup>It has to be stated that there are several ways to determine stress concentration factors for tubular joints. This is the approach proposed by the standard DNV GL RP-C203 (DNV GL AS, 2016).

## 4 Optimization approach and solution methods

The optimization problem incorporates a mixed-integer formulation (due to discrete numbers of legs and bays of the jacket). In order to address this issue, the mixed-integer problem is transferred to multiple continuous problems by solving solutions with a fixed number of legs and bays. As only a few combinations of these discrete variables are regarded as realistic solutions for practical applications, this procedure leads to a very limited number of subproblems but eases the mathematical optimization process significantly. Furthermore, the optimization problem is generally non-convex; i.e., a local minimum in the feasible region satisfying the constraints is not necessarily a global solution. This is addressed by repeating the optimization with multiple starting points.

The development of new or improved optimization methods to solve the numerical optimization problem is not in the scope of this work because there are methods presented in the literature that are known to be suitable for this purpose. Meta-heuristic algorithms like genetic algorithms or particle swarm optimization are not considered in this work because they are known to be slow. With regard to efficiency and accuracy, two methods are regarded as the most powerful for optimization involving nonlinear constraints: sequential quadratic programming (SQP) and interior-point (IP) methods (Nocedal and Wright, 2006). SQP methods are known to be efficient, when the numbers of constraints and design variables are of the same order of magnitude. An advantage is that these methods usually converge better when the problem is badly scaled. In theory, IP methods have better convergence properties and often outperform SQP methods on large-scale or sparse problems. In this work, both approaches are used to solve the jacket optimization problem.<sup>10</sup> They are outlined briefly in the following.

### 4.1 Sequential quadratic programming method

In principle, SQP can be seen as an adaption of Newton's method to nonlinear constrained optimization problems, computing the solution of the Karush–Kuhn–Tucker equations (necessary conditions for constrained problems). Here, a common approach is deployed, based on the works of Biggs (1975), Han (1977), and Powell (1978a, b). In the first step, the Hessian of the so-called Lagrangian (a term incorporating the objective and the sum of all constraints weighted by Lagrange multipliers) is approximated by the Broyden–Fletcher–Goldfarb–Shanno method (Fletcher, 1987). In the next step, a quadratic programming subproblem is built, where the Lagrangian is approximated by a quadratic term and linearized constraints. This subproblem can be solved by any method able to solve quadratic programs. An active-set

<sup>10</sup>The function *fmincon* in MATLAB R2017b was used for this study.

method described by Gill et al. (1981) is deployed for this task. The procedure is repeated until convergence is reached.

## 4.2 Interior-point method

IP methods are barrier methods; i.e., the objective is approximated by a term that incorporates a barrier term, expressed by a sum of logarithmized slack variables. The actual problem itself, just like in SQP, is solved as a sequence of subproblems. In this work, an approach is deployed, which may switch between line search and trust region methods to approximate the problem, depending of the success of each step. If the line search step fails, i.e., when the projected Hessian is not definitively positive, the algorithm performs a trusted region step, where the method of conjugate gradients is deployed. The algorithm is described in detail by Waltz et al. (2006).

## 5 Jacket comparison study

In this section, the proposed approach is applied to find and compare optimal jacket designs for the NREL 5 MW reference turbine (Jonkman et al., 2009). The environmental conditions are adopted from measurements recorded at the research platform FINO3 in the German North Sea.

### 5.1 Reference turbine

The NREL 5 MW reference turbine, which was published almost 1 decade ago as a proposal to establish a standardized turbine for scientific purposes, is still an object of many studies in the literature dealing with intermediate- to high-power offshore wind applications. In fact, the market already provides turbines with 8 MW and aims for even higher ratings. Choosing this reference turbine is motivated by its excellent documentation and accessibility.

The rotor has a hub height of 90 m, and the rated wind speed is  $11.4 \text{ m s}^{-1}$ , where the rotor speed is  $12.1 \text{ min}^{-1}$ . This is equal to 1P and 3P excitations of 0.2 and 0.6 Hz, respectively. The critical first fore–aft and side–side bending eigenfrequencies of the entire structure are about 0.35 Hz and do not differ very much when considering only reasonable structural designs for the jacket because the modal behavior is strongly driven by the relatively soft tubular tower.

### 5.2 Environmental conditions and design load sets

Due to excellent availability, the environmental data are derived from measurements taken from the offshore research platform FINO3, located in the German North Sea close to the wind farm “alpha ventus”. Compared to the environmental conditions documented in the UpWind design basis (Fischer et al., 2010), the FINO3 measurements are much more comprehensive and allow for a better estimation of probability density functions as inputs for the determination of prob-

abilistic loads (Hübler et al., 2017). The probabilistic load set, which is based on probability density functions of environmental state parameters and reduced in size compared to full load sets used by industrial wind turbine designers, was described in recent studies (Häfele et al., 2017, 2018b). However, there are two drawbacks that have to be mentioned when using this data. First, the FINO3 platform was built at a location with quite a shallow water depth of 22 m, though the jacket is supposed to be an adequate substructure for water depths above 40 m and the design water depth in this study is 50 m. Nevertheless, this procedure was also performed in the UpWind project for the design of the OC4 jacket, where the K13 deep-water site was considered. Second, the soil properties of the Offshore Code Comparison Collaboration (OC3) (Jonkman and Musial, 2010) are adopted to compute foundation inertias and stiffnesses, as these values are unknown for the FINO3 location. Moreover, it is assumed that the structural behavior of the OC4 jacket pile foundation is valid for all jacket designs, even with varying leg diameters and thicknesses.

### 5.3 Boundaries of design variables and other parameters

The boundaries are chosen conservatively by means of quite narrow design variable ranges (see Table 1), i.e., meaningful parameters that do not exhaust the possible range given by the structural code checks, in a realistic range around the values of the OC4 jacket (Popko et al., 2014). Only three- or four-legged structures with three, four, and five bays are regarded as valid solutions for this study. The fixed design variables are, if possible, adopted from the OC4 jacket, which can be seen as a kind of reference structure in this case. The material is steel (S355), with a Young’s modulus of 210 GPa, a shear modulus of 81 GPa, and a density of  $7850 \text{ kg m}^{-3}$ . According to DNV GL AS (2016), an *S-N* curve with an endurance stress limit of  $52.63 \times 10^6 \text{ N m}^{-2}$  at  $\times 10^7$  cycles and slopes of 3 and 5 before and after endurance limit (curve *T*), respectively, is applied. The cost model parameters or unit costs, respectively, are adopted from the mean values given in Häfele et al. (2018a) and set to  $a_1 = 1.0 \text{ kg}^{-1}$  (material),  $a_2 = 4.0 \times 10^6 \text{ m}^{-3}$  (fabrication),  $a_3 = 1.0 \times 10^2 \text{ m}^{-2}$  (coating),  $a_4 = 2.0 \times 10^4 \text{ m}^{-1}$  (transition piece),  $a_5 = 2.0 \text{ kg}^{-1}$  (transport),  $a_6 = 2.0 \times 10^5$  (installation), and  $a_7 = 1.0 \times 10^5$  (fixed). With these values, the cost function returns a dimensionless value, also interpretable as capital expenses in EUR.

### 5.4 Results and discussion

To resolve the mixed-integer formulation of the optimization problem into continuous problems, six subproblems with three legs and three bays ( $N_L = 3$ ,  $N_X = 3$ ), three legs and four bays ( $N_L = 3$ ,  $N_X = 4$ ), three legs and five bays ( $N_L = 3$ ,  $N_X = 5$ ), four legs and three bays ( $N_L = 4$ ,  $N_X = 3$ ), four legs and four bays ( $N_L = 4$ ,  $N_X = 4$ ), and four legs and

**Table 1.** Boundaries of jacket model parameters for design of experiments. Topological, tube sizing, and material parameters are separated into groups; single values mean that the corresponding value is held constant.

Parameter	Description	Lower boundary	Upper boundary
$N_L$	Number of legs	3	4
$N_X$	Number of bays	3	5
$R_{\text{foot}}$	Foot radius	6.792 m	12.735 m
$\xi$	Head-to-foot radius ratio	0.533	0.733
$L$	Entire jacket length	70.0 m	
$L_{\text{MSL}}$	Transition piece elevation over mean sea level	20.0 m	
$L_{\text{OSG}}$	Lowest leg segment height	5.0 m	
$L_{\text{TP}}$	Transition piece segment height	4.0 m	
$q$	Ratio of two consecutive bay heights	0.640	1.200
$x_{\text{MB}}$	Mud brace flag	true (1)	
$D_L$	Leg diameter	0.960 m	1.440 m
$\gamma_b$	Leg radius-to-thickness ratio (bottom)	12.0	18.0
$\gamma_t$	Leg radius-to-thickness ratio (top)	12.0	18.0
$\beta_b$	Brace-to-leg diameter ratio (bottom)	0.533	0.800
$\beta_t$	Brace-to-leg diameter ratio (top)	0.533	0.800
$\tau_b$	Brace-to-leg thickness ratio (bottom)	0.350	0.650
$\tau_t$	Brace-to-leg thickness ratio (top)	0.350	0.650
$E$	Material Young's modulus	$2.100 \times 10^{11} \text{ N m}^{-2}$	
$G$	Material shear modulus	$8.077 \times 10^{10} \text{ N m}^{-2}$	
$\rho$	Material density	$7.850 \times 10^3 \text{ kg m}^{-3}$	

five bays ( $N_L = 4$ ,  $N_X = 5$ ) were solved using the SQP and IP methods. Therefore, multiple solutions are discussed and compared in the following. The optimization problem is non-convex; i.e., a local minimum in the feasible region satisfying the constraints is not necessarily a global solution. In theory, both algorithms converge from remote starting points. However, to guarantee global convergence to some extent, all six combinations of fixed-integer variables were solved using 100 randomly chosen starting points. Installation costs and fixed expenses were excluded from the objective function and included again after the optimization procedure because these terms do not have an effect on the individual optimization problems.<sup>11</sup> Gradients were computed by finite differences. The optimization terminated, when the first-order optimality and feasibility measures were both less than  $1 \times 10^{-6}$ . There was no limit to the maximum number of iterations.

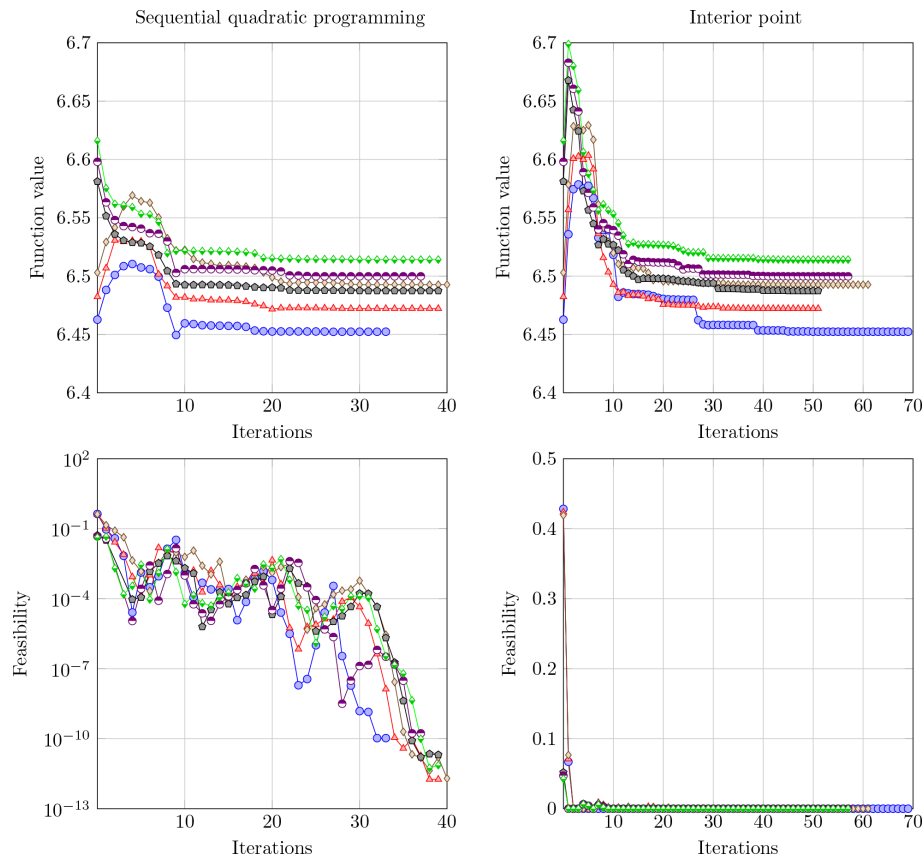
The optimal solutions of all six subproblems do not depend on the starting point when using both optimization methods because there is only one array of optimal design variables in each case. The convergence behavior of both optimization methods is illustrated in Fig. 2, where the OC4 jacket with varying numbers of legs and bays was assumed as the starting point. This structure has a foot radius,  $R_{\text{foot}}$ , of 8.79 m, a head-to-foot radius ratio,  $\xi$ , of 0.67, and a ratio of two consecutive bay heights,  $q$ , of 0.8. Moreover, it

has a leg diameter,  $D_L$ , of 1.2 m, and entirely constant tube dimensions from bottom to top, i.e., leg radius-to-thickness ratios,  $\gamma_b$  and  $\gamma_t$ , of 15, brace-to-leg diameter ratios,  $\beta_b$  and  $\beta_t$ , of 0.5, and brace-to-leg diameter ratios,  $\tau_b$  and  $\tau_t$ , of 0.5. The optimization process needed between 30 and 40 iterations using the SQP method and between 50 and 70 iterations using the IP method to converge. It is worth mentioning that the maximum constraint violation (feasibility) of the three-legged designs was higher at the beginning of the optimization process but converges stably. For the same reason, the four-legged designs have a higher improvement potential compared to the initial solution. The accuracy obtained by both methods is similar. The solutions are all feasible because they fulfill the Karush–Kuhn–Tucker conditions, and all constraint violations are around zero. Therefore, the optima are probably global optima for the given design variable boundaries.

The optimal solutions obtained by the sequential quadratic programming method are illustrated in Table 2.<sup>12</sup> Additionally, the topologies of all optimal solutions are shown in Fig. 3. With respect to the constraints and assumptions of this study (5 MW turbine, 50 m water depth, given environmental conditions and cost parameters), jackets with three legs are beneficial in terms of capital expenses. The three-legged jacket with three bays ( $N_L = 3$ ,  $N_X = 3$ ) is the best solution, i.e., is related to the lowest total expenditures, among

<sup>11</sup>The values shown in the following include all cost terms. The exclusion is only performed during optimization.

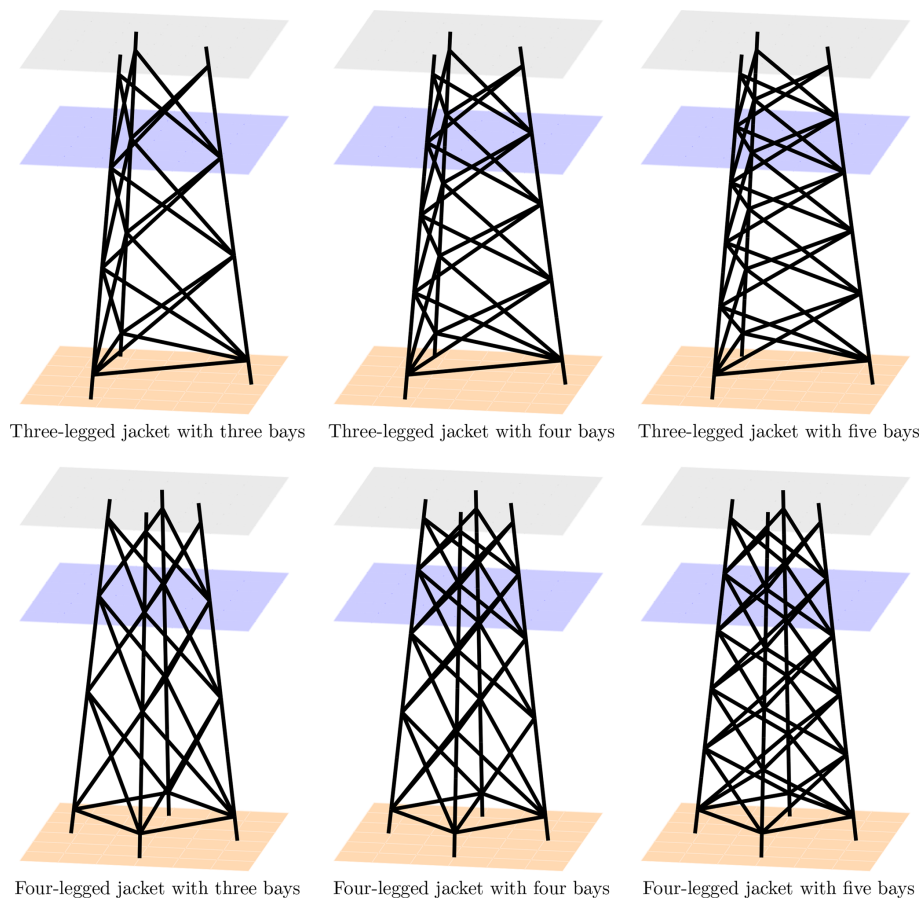
<sup>12</sup>As the accuracy of the SQP and IP methods is similar here, only results obtained by the SQP method are shown in the following.



**Figure 2.** Function and feasibility (maximum constraint violation) values during the optimization procedure of all six subproblems (blue line with circles: jacket with three legs and three bays; red line with triangles: jacket with three legs and four bays; brown line with diamonds: jacket with three legs and five bays; black line with pentagons: jacket with four legs and three bays; violet line with half-filled circles: jacket with four legs and four bays; green line with half-filled diamonds: jacket with four legs and five bays). The starting point (iteration “0”) is the OC4 jacket with a varying number of legs and bays in all cases. One iteration involves 11 evaluations of the objective function and the nonlinear constraints.

**Table 2.** Optimal solutions of design variables  $\mathbf{x}^*$  obtained by the sequential quadratic programming method for fixed values of  $N_L$  and  $N_X$ .

	Optimal solution					
	$N_L=3, N_X=3$	$N_L=3, N_X=4$	$N_L=3, N_X=5$	$N_L=4, N_X=3$	$N_L=4, N_X=4$	$N_L=4, N_X=5$
$N_L$	3	3	3	4	4	4
$N_X$	3	4	5	3	4	5
$R_{\text{foot}}$ in m	12.735	12.735	12.735	10.894	10.459	10.549
$\xi$	0.533	0.533	0.533	0.533	0.533	0.533
$q$	0.937	0.941	0.936	0.813	0.809	0.977
$D_L$ in m	1.021	1.021	1.023	0.960	0.960	0.960
$\beta_b$	0.800	0.800	0.800	0.800	0.799	0.787
$\beta_t$	0.800	0.800	0.800	0.800	0.800	0.800
$\gamma_b$	12.000	12.000	12.000	12.680	12.259	12.000
$\gamma_t$	16.165	16.029	15.928	18.000	18.000	18.000
$\tau_b$	0.513	0.505	0.493	0.497	0.493	0.478
$\tau_t$	0.472	0.466	0.454	0.383	0.387	0.383
Overall mass in t	423	444	467	412	426	439
$f(\mathbf{x}^*) = \log_{10}(C_{\text{total}}(\mathbf{x}^*))$	6.452	6.472	6.493	6.487	6.500	6.514
$h_1(\mathbf{x}^*) = h_{\text{FLS}}(\mathbf{x}^*) - 1$	$1.172 \times 10^{-10}$	$3.966 \times 10^{-11}$	$1.151 \times 10^{-10}$	$1.450 \times 10^{-10}$	$-1.056 \times 10^{-10}$	$-1.721 \times 10^{-10}$
$h_2(\mathbf{x}^*) = h_{\text{ULS}}(\mathbf{x}^*) - 1$	$7.819 \times 10^{-10}$	$2.678 \times 10^{-10}$	$1.093 \times 10^{-10}$	$3.978 \times 10^{-10}$	$3.980 \times 10^{-10}$	$5.995 \times 10^{-10}$



**Figure 3.** Topologies of optimal solutions  $\mathbf{x}^*$ . All images are displayed at the same scale. Line widths are not correlated to tube dimensions.

the considered jackets. The solutions show some interesting specialties. The foot radii,  $R_{\text{foot}}$ , are at the upper boundaries in the case of the three-legged structures, while the head-to-foot radius ratios,  $\xi$ , are at the lower boundaries. Probably this arises from the combination of cost function and non-linear constraints, where a large foot radius is quite beneficial because it generally provides a higher load capacity, while a small head radius is favorable due to lower transition piece costs. In the four-legged case, the foot radii are lower but still relatively high. In any case, it seems to be beneficial, when the ratio of two consecutive bay heights,  $q$ , is slightly below 1 (lower bays are higher than upper bays). Concerning tube dimensions, the leg diameters,  $D_L$ , are relatively small, in the case of the four-legged jackets even at the lower boundary. The structural load capacity is established by high brace diameters (represented by design variables  $\beta_b$  and  $\beta_t$ , values at the bottom and top of the structures both at upper boundaries). The brace thicknesses, represented by  $\tau_b$  and  $\tau_t$ , show intermediate values in the range of design variables, while the values for  $\tau_t$  are higher in the case of three-legged designs. Moreover, the structural resistance is strongly driven by the leg thicknesses. While the optimal values of  $\gamma_b$  are low in each case, implying high leg thicknesses

at the jacket bottom, the values of  $\gamma_t$  are much higher. The impact of all design variables on the objective function is easier to understand when the sensitivities of cost model terms to variations in design variables are considered. In Fig. 4, each subplot shows the variation in the total costs,  $C_{\text{total}}$ , and the cost function terms  $C_1$  (proportional to  $C_5$ ),  $C_2$ ,  $C_3$ , and  $C_4$  due to a 1% one-at-a-time variation in each continuous design variable in three different phases of the optimization process (initial, intermediate, and final phase). The terms  $C_6$  and  $C_7$  are not impacted by any continuous design variable and therefore not considered. For instance, a 1% increase in the foot radius,  $R_{\text{foot}}$ , causes increasing material costs of  $\Delta C_1 = 0.14\%$ , evaluated for the initial design, but increasing material costs of  $\Delta C_1 = 0.26\%$ , evaluated for the optimal design. Therefore, the sensitivity of this cost term varies during the optimization process. In contrast, the variation in transition piece expenses does not change (which is reasonable because this term only depends linearly on the number of legs,  $N_L$ , the foot radius,  $R_{\text{foot}}$ , and the head-to-foot radius ratio,  $\xi$ ). In general, Fig. 4 shows that there is no design variable with a strongly varying impact on any term of the cost function. It can also be concluded that tube sizing variables impact the costs much more strongly than topological



variables, disregarding the number of legs and bays. Among the considered design variables, the leg diameter,  $D_L$ , and leg radius-to-thickness ratios,  $\gamma_b$  and  $\gamma_t$ , are design-driving (together with the number of legs,  $N_L$ ) due to a significant impact both on the costs and on the structural code checks. In addition, an interesting specialty is featured by the cost term  $C_4$ , which is only impacted by topological design variables, more precisely the foot radius,  $R_{\text{foot}}$ , and the head-to-foot radius ratio,  $\xi$ . As a large foot radius,  $R_{\text{foot}}$ , is needed to establish structural resistance, this cost term penalizes large head-to-foot radius ratios,  $\xi$ . For this reason, this value is at the lower boundary for all design solutions.

Regarding the costs of the jackets, the best solution with three legs and three bays is related to capital expenses of  $10^{6.452} = 2\,831\,000$ . Altogether, this is a meaningful value and the designs are not far off from structural designs that are known from practical applications because it has already been reported in the literature that three-legged designs may be favorable in terms of costs (Chew et al., 2014) and three-legged structures have already been built. However, the other solutions are more expensive but not completely off. As there is some uncertainty in the unit costs, the other jackets may also be reasonable designs with slightly different boundaries. A more detailed cost breakdown is given in Fig. 5, which shows the cost contributions of all six structures and where the actual cost savings come from. The lightest structure is the four-legged jacket with three bays, while the three-legged jacket with five bays is the heaviest one, which is illustrated by the expenses for material and transport according to the cost model used for this study. Nevertheless, the mass of all structures is quite similar. Other than expected, the jacket with the lowest expenditures for manufacturing is also the four-legged one with three bays and not the three-legged jacket with three bays, which has the least number of joints. The three-legged structures benefit – from the economic point of view – mainly from lower expenses for coating, the transition piece, and, most distinctly, installation costs. In total, these contributions add up to lower costs of the three-legged jackets, except for the one with five bays ( $10^{6.493} = 3\,112\,000$ ), which is more expensive than the four-legged one with three bays ( $10^{6.487} = 3\,069\,000$ ). The most expensive jackets are the four-legged ones with four ( $10^{6.500} = 3\,162\,000$ ) and five ( $10^{6.514} = 3\,266\,000$ ) bays, where the latter is about 15 % more expensive than the best solution among the six sub-solutions. A reasonable option may also be the jacket with three legs and four bays, which features a total cost value of  $10^{6.472} = 2\,965\,000$ . In total, there is no jacket that is far too expensive compared to the others. It is indeed imaginable to find an appropriate application for each one.

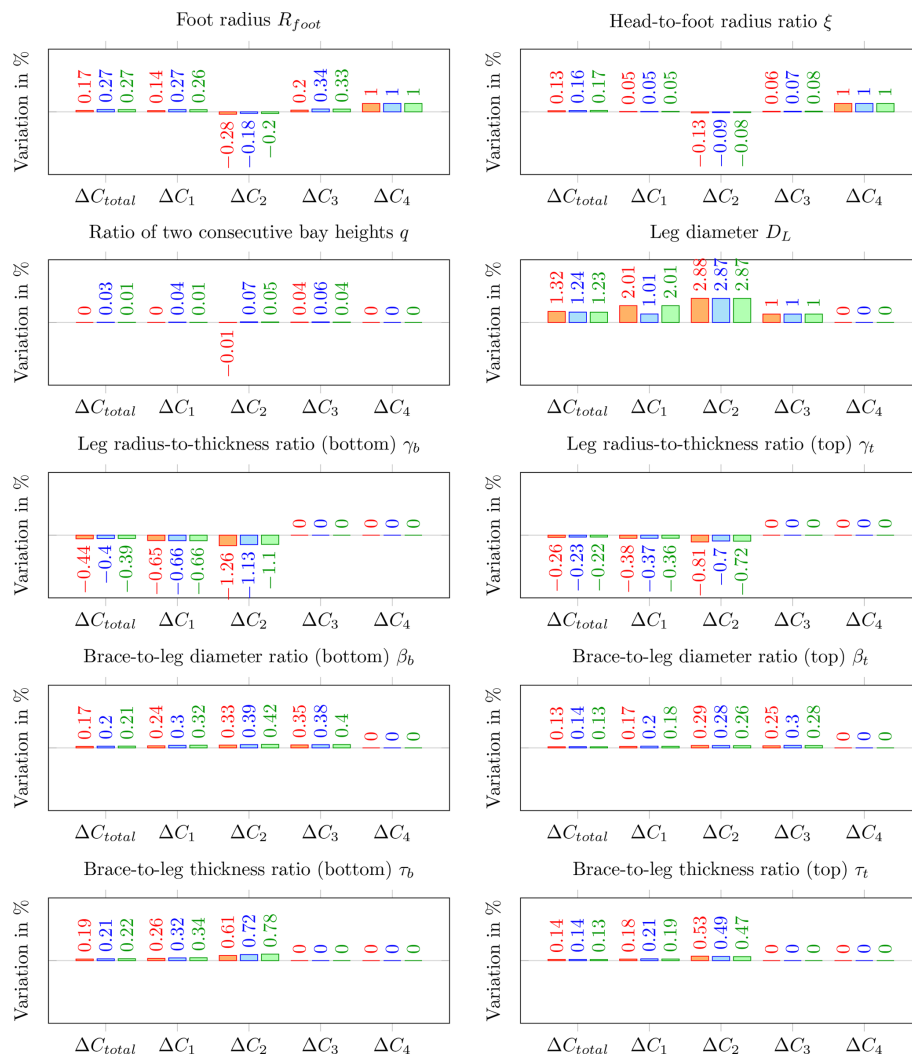
From the computational point of view, the optimization procedure based on surrogate models is very efficient. The numbers of iterations needed to find an optimal solution (from about 30 to 40 using the SQP method and from about 50 to 70 using the IP method) are related to computation

times of about 15 to 30 min on a single core of a work station with an Intel Xeon E5-2687W v3 central processing unit and 64 GB random access memory. Compared to simulation-based approaches, this can be regarded as very fast. The number of iterations may be decreased, when using analytical gradients of the objective function because using finite differences is generally more prone to numerical errors but is not vital at this level of computational expenses. It has to be pointed out that the training data set of the surrogate models required  $200 \times 128 = 25\,600$  time domain simulations in the fatigue and  $200 \times 10 = 2000$  in the ultimate limit state case, thus 27 600 simulations in total, excluding validation samples. However, for the computation of the training data, a compute cluster was utilized, which allows for the computation of many design load cases in parallel. Therefore, the presented approach based on GPR allows for outsourcing computationally expensive simulations on high-performance clusters, while the closed-loop optimization, which cannot be parallelized completely, can be run on a workstation with lower computational capacity.

The question remains what happens when some cost terms are neglected. An associated question is how the approach performs compared to a pure mass-dependent one, which can be regarded as state of the art in jacket optimization. For this purpose, all unit costs except  $a_1$  were set to zero and the optimization procedure was repeated using the sequential quadratic programming method. The results, including optimal design variables and resulting values of objective and constraint functions, are shown in Table 3. Under these assumptions, the four-legged jackets are better (in terms of minimal mass) than the three-legged ones. Interestingly, similar design variables are obtained when comparing these values to the ones obtained by the more comprehensive cost model in Table 2, particularly in the case of the three-legged jackets. The resulting objective function values are, in comparison, similar to the material costs in Fig. 5. In other words, a pure mass-dependent cost function approach yields approximately proportional costs, when the installation costs (depending on the number of legs) are considered, and similar designs. The reason for this is that all cost terms  $C_1 \dots C_5$  depend in some way on the tube dimensions and the topology does not impact the costs to a great extent, as seen in Fig. 4. Indeed, the largest proportion of costs is purely mass-dependent, as the factors  $c_1$  and  $c_5$  are the mass of the structure. Therefore, the proposed cost model can lead to more accurate results, but a mass-dependent approach would be sufficient to draw the same conclusions.

## 6 Benefits and limitations of the approach

With respect to the state of the art, the present approach can be regarded as the first one addressing the jacket optimization problem holistically, which incorporates four main improvements: a detailed geometry model with both topological and tube sizing design variables; an analytical cost model based



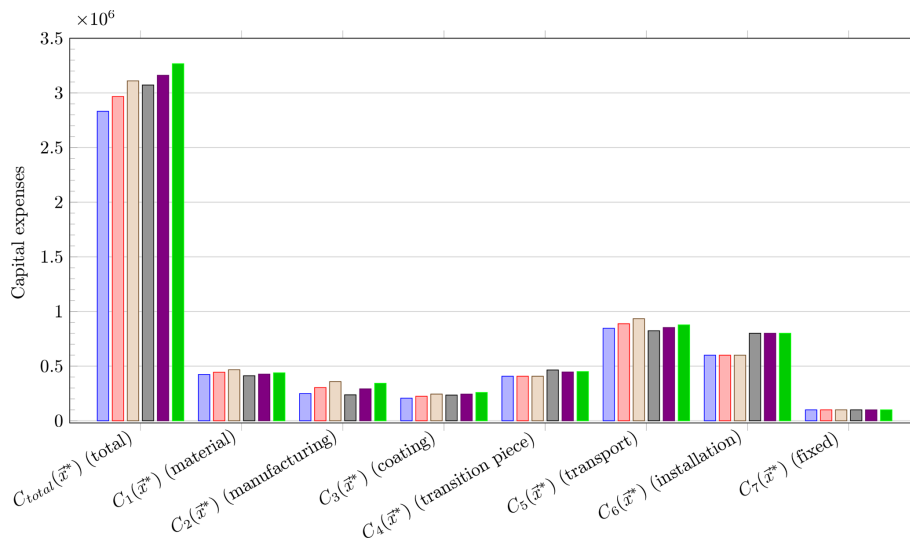
**Figure 4.** Variations in total costs,  $\Delta C_{total}$ , and cost function terms  $\Delta C_1$  (material),  $\Delta C_2$  (manufacturing),  $\Delta C_3$  (coating), and  $\Delta C_4$  (transition piece) due to 1% one-at-a-time variations in design variables (subplots) in %. Derivatives were computed for the initial design (red bars), an intermediate design after 15 iterations (blue bars), and the optimal design (green bars) of the three-legged structure with three bays ( $N_L = 3, N_X = 3$ ).

on the main jacket cost contributions; sophisticated load assumptions and assessments; and a treatment of results that considers the optimization problem to be a methodology for early design stages. All these points lead to a better understanding how to address the multidisciplinary design optimization problem and to much more reliable results.

However, some drawbacks and limitations remain, which have to be considered when dealing with the results of this study. In general, the approach is easy to use, also in industrial applications, but needs some effort in implementation. Furthermore, the present study does not incorporate a completely reliability-based design procedure, which is not beyond the means when using Gaussian process regression to perform structural code checks. However, the question of how safety factors can be replaced by a meaningful prob-

abilistic design is still a matter of research, and it is quite simple to advance the present approach to a robust one. In order to reduce the numerical cost (in particular concerning the number of time domain simulations needed to sample the input design space for surrogate modeling of structural code checks), the number of design variables is limited. The application of GPR as a machine learning approach to evaluate structural code checks performs in a numerically fast way but requires numerous time domain simulations to generate training and validation data sets. This is beneficial when dealing with numerically expensive studies (as in this case) but might lead to a numerical overhead when only considering one jacket design. Care has to be taken when transferring the results to designs with a more sophisticated geometry. Moreover, the parameterization of cost and structural





**Figure 5.** Expenses comparison of optimal solutions of three-legged jacket with three bays (blue bars), three-legged jacket with four bays (red bars), three-legged jacket with five bays (brown bars), four-legged jacket with three bays (gray bars), four-legged jacket with four bays (violet bars), and four-legged jacket with five bays (green bars).

**Table 3.** Optimal solutions of design variables  $\mathbf{x}^*$  obtained by the sequential quadratic programming method for fixed values of  $N_L$  and  $N_X$  using a pure mass-dependent objective function.

	Optimal solution					
$N_L$	3	3	3	4	4	4
$N_X$	3	4	5	3	4	5
$R_{\text{foot}}$ in m	12.735	12.735	12.735	12.735	12.735	12.735
$\xi$	0.533	0.533	0.533	0.533	0.533	0.533
$q$	1.062	0.987	0.936	1.200	1.200	1.178
$D_L$ in m	1.025	1.023	1.023	0.960	0.960	0.960
$\beta_b$	0.800	0.800	0.800	0.730	0.757	0.800
$\beta_t$	0.800	0.800	0.800	0.800	0.800	0.800
$\gamma_b$	12.000	12.000	12.000	13.194	13.318	12.000
$\gamma_t$	16.459	16.250	15.928	18.000	18.000	18.000
$\tau_b$	0.509	0.502	0.493	0.510	0.470	0.443
$\tau_t$	0.472	0.466	0.454	0.386	0.361	0.350
Overall mass in t	423	444	467	404	409	454
$f(\mathbf{x}^*) = \log_{10}(C_{\text{total}}(\mathbf{x}^*))$	5.627	5.647	5.669	5.606	5.612	5.657
$h_1(\mathbf{x}^*) = h_{\text{FLS}}(\mathbf{x}^*) - 1$	$-7.149 \times 10^{-12}$	$6.767 \times 10^{-12}$	$1.262 \times 10^{-12}$	$5.047 \times 10^{-13}$	$2.140 \times 10^{-12}$	$-1.017 \times 10^{-12}$
$h_2(\mathbf{x}^*) = h_{\text{ULS}}(\mathbf{x}^*) - 1$	$4.367 \times 10^{-11}$	$2.961 \times 10^{-11}$	$5.087 \times 10^{-12}$	$2.693 \times 10^{-12}$	$3.865 \times 10^{-12}$	$9.948 \times 10^{-13}$

code check models is site- and turbine-dependent. Therefore, the outcome of this study might not be directly transferable to other boundaries but requires recalculations. In particular, the utilized design standards and structural code checks are known to be conservative. The cost model also has shortcomings that must be mentioned. Some costs are affected by uncertain or indeterminable impacts. There is a number of examples. Transport and installation costs are strongly dependent on the availability of barges or vessels. The uncertainty in weather conditions can affect transport and installation costs. Furthermore, the design may be directly impacted

if production facilities are not available. All these effects are not considered in the cost model.

In addition, it is important to highlight again that this study does not provide a detailed design methodology but an approach to obtain preliminary decision guidance at the earliest wind farm planning stage. This is actually not a limitation but has to be considered when dealing with the results of this study. There are indeed many studies known from the literature that address the tube dimensioning problem in a larger extension. However, these approaches assume that the structural topology is always optimal, even in the case of signifi-

cant variations in tube dimensions. For instance, all optimal jackets have a larger bottom width than the OC4 jacket, while the design-driving leg diameters are relatively small. This indicates that topological design variables with minor impact on costs are useful factors to establish the structural resistance.

## 7 Conclusions

The present work began by introducing four main points to be considered in order to improve the state of the art in the field of jacket optimization. The first one, the treatment of the jacket design problem in terms of a holistic topology and tube sizing problem instead of a pure tube dimensioning problem, was addressed by a 20-parameter jacket model, of which 12 parameters are design variables. The second, important point leads to the utilization of a more complex (compared to mass-dependent) but easy to handle cost model. In order to face the challenging task of numerically efficient structural code check evaluations, a machine learning approach based on Gaussian process regression was applied as the third point. On this basis, gradient-based optimization was deployed to find optimal design solutions. Lastly, optimization results were considered differently compared to approaches presented in the literature. It was pointed out that the solution is not supposed to be the final design but a very good starting point to find an initial solution for exact tube dimensioning.

The conclusions of this work are manifold. From the numerical point of view, surrogate modeling seems – as matters stand today – to be the most promising approach enabling us to address the computationally very expensive jacket optimization problem efficiently because other approaches in the literature go along with massive simplifications, mainly in load assumptions. The optimization methods that were used to find the optimal solution seem to be appropriate for the given problem, even in terms of finding a global optimum. The present paper does not provide improvements of state-of-the-art gradient-based optimization, but active-set SQP and IP methods both converge efficiently and accurately for the given problem.

From the application-oriented point of view, it can be stated that three-legged jackets with only three bays depict the best solution (in terms of costs) for offshore turbines with about 5 MW rated power in 50 m water depth, which confirms the results from other studies in the literature. Due to the cost model, the additional load-bearing capacity gained by the extra leg of a four-legged structure cannot compensate for the higher costs arising from several cost factors directly related to the number of legs. By contrast, it is instead beneficial to increase the tube dimensions and maintain the number of structural elements at a minimum level. It was shown that the same results were obtained when using a mass-dependent cost function, also considering the number of jacket legs.

With regard to turbines with a higher rated power or installations in deeper waters, the proposed methodology might lead to the result that the best jacket solution for this case looks completely different. Before this can be analyzed, simulation tools need to be improved to enable the consideration of nonlinear effects for rotors with a very large diameter and innovative control strategies.

**Data availability.** This work is based on structural code checks computed and provided in Häfele et al. (2018a).

## Appendix A: Nomenclature

DLC	Design load case
IP	Interior-point method
SQP	Sequential quadratic programming method
$\Phi_p$	Planar (two-dimensional) batter angle
$\Phi_s$	Spatial (three-dimensional) batter angle
$\beta_b$	Brace-to-leg diameter ratio at bottom (jacket model parameter)
$\beta_i$	Brace-to-leg diameter ratio in the $i$ th bay
$\beta_t$	Brace-to-leg diameter ratio at top (jacket model parameter)
$\gamma_b$	Leg radius-to-thickness ratio at bottom (jacket model parameter)
$\gamma_i$	Leg radius-to-thickness ratio in the $i$ th bay
$\gamma_t$	Leg radius-to-thickness ratio at top (jacket model parameter)
$\xi$	Head-to-foot radius ratio (jacket model parameter)
$\rho$	Material density (jacket model parameter)
$\vartheta$	Angle enclosed by two jacket legs
$\tau_b$	Brace-to-leg thickness ratio at bottom (jacket model parameter)
$\tau_i$	Brace-to-leg thickness ratio in the $i$ th bay
$\tau_t$	Brace-to-leg thickness ratio at top (jacket model parameter)
$\psi_{1,i}$	Lower brace-to-leg connection angle in the $i$ th bay
$\psi_{2,i}$	Upper brace-to-leg connection angle in the $i$ th bay
$\psi_{3,i}$	Brace-to-brace connection angle in the $i$ th bay
$C_j$	Expenses related to $j$ th cost factor
$C_{\text{total}}$	Total capital expenses
$D_L$	Leg diameter (jacket model parameter)
$E$	Material Young's modulus (jacket model parameter)
$G$	Material shear modulus (jacket model parameter)
$L$	Overall jacket length (jacket model parameter)
$L_{\text{MSL}}$	Transition piece elevation over mean sea level (jacket model parameter)
$L_{\text{OSG}}$	Lowest leg segment height (jacket model parameter)
$L_{\text{TP}}$	Transition piece segment height (jacket model parameter)
$L_i$	$i$ th jacket bay height
$L_{m,i}$	Distance between the lower layer of K joints and the layer of X joints of the $i$ th bay
$N_L$	Number of legs (jacket model parameter)
$N_X$	Number of bays (jacket model parameter)
$R_{\text{Foot}}$	Foot radius (jacket model parameter)
$R_i$	$i$ th jacket bay radius at lower K joint layer
$R_{m,i}$	Radius of the $i$ th X joint layer
$a_j$	$j$ th unit cost
$c_j$	$j$ th cost factor
$f$	Objective function value
$h_1$	First inequality constraint value
$h_2$	Second inequality constraint value
$h_{\text{FLS}}$	Maximal normalized tubular joint fatigue damage
$h_{\text{ULS}}$	Maximal extreme load utilization ratio
$q$	Ratio of two consecutive bay heights (jacket model parameter)
$\mathbf{x}$	Array of design variables
$\mathbf{x}_{\text{lb}}$	Array of lower boundaries
$x_{\text{MB}}$	Mud brace flag (jacket model parameter)
$\mathbf{x}_{\text{ub}}$	Array of upper boundaries

**Competing interests.** The authors declare that they have no conflict of interest.

**Acknowledgements.** This work was supported by the computer cluster, which is funded by the Leibniz Universität Hannover, the Lower Saxony Ministry of Science and Culture (MWK), and the German Research Foundation (DFG).

The publication of this article was funded by the open-access fund of Leibniz Universität Hannover.

Edited by: Lars Pilgaard Mikkelsen

Reviewed by: Lars Einar S. Stiang and one anonymous referee

## References

- Agarwal, P. and Manuel, L.: Load Extrapolation Methods for Offshore Wind Turbines, in: Offshore Technology Conference, Houston, Texas, USA, <https://doi.org/10.4043/21001-MS>, 2010.
- AlHamaydeh, M., Barakat, S., and Nasif, O.: Optimization of Support Structures for Offshore Wind Turbines Using Genetic Algorithm with Domain-Trimming, *Math. Probl. Eng.*, 2017, 1–14, <https://doi.org/10.1155/2017/5978375>, 2017.
- Biggs, M. C.: Constrained minimization using recursive quadratic programming, in: Towards global optimization, North-Holland, Cagliari, Italy, 341–349, 1975.
- BVGassociates: Offshore wind: Industry's journey to GBP 100/MWh – Cost breakdown and technology transition from 2013 to 2020, Tech. rep., 2013.
- Chew, K. H., Tai, K., Ng, E. Y. K., Muskulus, M., and Zwick, D.: Offshore Wind Turbine Jacket Substructure: A Comparison Study Between Four-Legged and Three-Legged Designs, *Journal of Ocean and Wind Energy*, 1, 74–81, 2014.
- Chew, K.-H., Tai, K., Ng, E., and Muskulus, M.: Optimization of Offshore Wind Turbine Support Structures Using an Analytical Gradient-based Method, *Energy Proced.*, 80, 100–107, <https://doi.org/10.1016/j.egypro.2015.11.412>, 2015.
- Chew, K.-H., Tai, K., Ng, E., and Muskulus, M.: Analytical gradient-based optimization of offshore wind turbine substructures under fatigue and extreme loads, *Mar. Struct.*, 47, 23–41, <https://doi.org/10.1016/j.marstruc.2016.03.002>, 2016.
- Damiani, R.: JacketSE: An Offshore Wind Turbine Jacket Sizing Tool, Technical Report NREL/TP-5000-65417, National Renewable Energy Laboratory, Golden, CO, USA, 2016.
- Damiani, R., Dykes, K., and Scott, G.: A comparison study of offshore wind support structures with monopiles and jackets for U.S. waters, *J. Phys. Conf. Ser.*, 753, 092003, <https://doi.org/10.1088/1742-6596/753/9/092003>, 2016.
- DNV GL AS: Fatigue design of offshore steel structures, Recommended Practice DNVGL-RP-C203, 2016.
- Efthymiou, M.: Development of SCF formulae and generalised influence functions for use in fatigue analysis, in: Proceedings of the Conference on Recent Developments in Tubular Joints Technology, 4–5 October 1988, Surrey, UK, 1–13, 1988.
- Fischer, T., de Vries, W., and Schmidt, B.: Upwind Design Basis, Tech. rep., 2010.
- Fletcher, R.: Practical methods of optimization, Wiley, Chichester, UK, New York, USA, 2nd edn., 1987.
- Gill, P. E., Murray, W., and Wright, M. H.: Practical optimization, Academic Press, London, UK, New York, USA, 1981.
- Häfele, J. and Rolfes, R.: Approaching the ideal design of jacket substructures for offshore wind turbines with a Particle Swarm Optimization algorithm, in: Proceedings of the Twenty-sixth (2016) International Offshore and Polar Engineering Conference, 26 June–2 July 2016, Rhodes, Greece, 156–163, 2016.
- Häfele, J., Gebhardt, C. G., and Rolfes, R.: Innovative design of a hybrid-type jacket for 10MW turbines, Tech. Rep. IN-NWIND.EU Deliverable D4.3.5, 2016.
- Häfele, J., Hübler, C., Gebhardt, C. G., and Rolfes, R.: Efficient Fatigue Limit State Design Load Sets for Jacket Substructures Considering Probability Distributions of Environmental States, in: Proceedings of the Twenty-seventh (2017) International Offshore and Polar Engineering Conference, 25–30 June 2017, San Francisco, CA, 167–173, 2017.
- Häfele, J., Damiani, R. R., King, R. N., Gebhardt, C. G., and Rolfes, R.: A systematic approach to offshore wind turbine jacket predesign and optimization: geometry, cost, and surrogate structural code check models, *Wind Energ. Sci.*, 3, 553–572, <https://doi.org/10.5194/wes-3-553-2018>, 2018a.
- Häfele, J., Hübler, C., Gebhardt, C. G., and Rolfes, R.: A comprehensive fatigue load set reduction study for offshore wind turbines with jacket substructures, *Renew. Energ.*, 118, 99–112, <https://doi.org/10.1016/j.renene.2017.10.097>, 2018b.
- Han, S. P.: A globally convergent method for nonlinear programming, *J. Optimiz. Theory. App.*, 22, 297–309, <https://doi.org/10.1007/BF00932858>, 1977.
- Hübler, C., Gebhardt, C. G., and Rolfes, R.: Development of a comprehensive database of scattering environmental conditions and simulation constraints for offshore wind turbines, *Wind Energ. Sci.*, 2, 491–505, <https://doi.org/10.5194/wes-2-491-2017>, 2017.
- International Electrotechnical Commission: Wind turbines – Part 3: Design requirements for offshore wind turbines, Tech. Rep. IEC-61400-3:2009, 2009.
- Jonkman, J. and Musial, W.: Offshore Code Comparison Collaboration (OC3) for IEA Task 23 Offshore Wind Technology and Deployment, Technical Report NREL/TP-5000-48191, National Renewable Energy Laboratory, Golden, CO, USA, 2010.
- Jonkman, J., Butterfield, S., Musial, W., and Scott, G.: Definition of a 5-MW Reference Wind Turbine for Offshore System Development, Technical Report NREL/TP-500-38060, National Renewable Energy Laboratory, Golden, CO, USA, 2009.
- Kaveh, A. and Sabeti, S.: Structural optimization of jacket supporting structures for offshore wind turbines using colliding bodies optimization algorithm, *Struct. Des. Tall Spec.*, 27, e1494, <https://doi.org/10.1002/tal.1494>, 2018.
- Mone, C., Hand, M., Bolinger, M., Rand, J., Heimiller, D., and Ho, J.: 2015 Cost of Wind Energy Review, Technical Report NREL/TP-6A20-66861, National Renewable Energy Laboratory, Golden, CO, USA, 2017.
- Muskulus, M. and Schafhirt, S.: Design Optimization of Wind Turbine Structures – A Review, *Journal of Ocean and Wind Energy*, 1, 12–22, 2014.
- National Wind Technology Center Information Portal: FAST v8, available at: <https://nwtc.nrel.gov/FAST8> (last access: 28 August 2018), 2016.

- Nocedal, J. and Wright, S. J.: Numerical optimization, Springer series in operations research, Springer, New York, USA, 2nd edn., 2006.
- NORSOK: Design of steel structures, Standard N-004 Rev. 2, 2004.
- Oest, J., Sørensen, R., T. Overgaard, L. C., and Lund, E.: Structural optimization with fatigue and ultimate limit constraints of jacket structures for large offshore wind turbines, *Struct. Multidiscip. O.*, 55, 779–793, <https://doi.org/10.1007/s00158-016-1527-x>, 2016.
- Oest, J., Sandal, K., Schafhirt, S., Stieng, L. E. S., and Muskulus, M.: On gradient-based optimization of jacket structures for offshore wind turbines, *Wind Energy*, 21, 953–967, <https://doi.org/10.1002/we.2206>, 2018.
- Popko, W., Vorpahl, F., Zuga, A., Kohlmeier, M., Jonkman, J., Robertson, A., Larsen, T. J., Yde, A., Saetertro, K., Okstad, K. M., Nichols, J., Nygaard, T. A., Gao, Z., Manolas, D., Kim, K., Yu, Q., Shi, W., Park, H., Vasquez-Rojas, A., Dubois, J., Kaufer, D., Thomassen, P., de Ruyter, M. J., Peeringa, J. M., Zhiwen, H., and von Waaden, H.: Offshore Code Comparison Collaboration Continuation (OC4), Phase I – Results of Coupled Simulations of an Offshore Wind Turbine with Jacket Support Structure, *Journal of Ocean and Wind Energy*, 1, 1–11, 2014.
- Powell, M. J. D.: The Convergence of Variable Metric Methods for Nonlinearly Constrained Optimization Calculations, *Nonlinear Programming*, 3, 27–63, <https://doi.org/10.1016/B978-0-12-468660-1.50007-4>, 1978a.
- Powell, M. J. D.: A fast algorithm for nonlinearly constrained optimization calculations, in: *Numerical Analysis*, Dundee, Scotland, 630, 144–157, <https://doi.org/10.1007/BFb0067703>, 1978b.
- Rasmussen, C. E. and Williams, C. K. I.: Gaussian processes for machine learning, MIT Press, Cambridge, MA, USA, 3rd print edn., 2008.
- Sandal, K., Latini, C., Zania, V., and Stolpe, M.: Integrated optimal design of jackets and foundations, *Mar. Struct.*, 61, 398–418, <https://doi.org/10.1016/j.marstruc.2018.06.012>, 2018.
- Schafhirt, S., Zwick, D., and Muskulus, M.: Reanalysis of Jacket Support Structure for Computer-Aided Optimization of Offshore Wind Turbines with a Genetic Algorithm, *Journal of Ocean and Wind Energy*, 1, 209–216, 2014.
- Schafhirt, S., Zwick, D., and Muskulus, M.: Two-stage local optimization of lattice type support structures for offshore wind turbines, *Ocean Eng.*, 117, 163–173, <https://doi.org/10.1016/j.oceaneng.2016.03.035>, 2016.
- Seidel, M.: Jacket substructures for the REpower 5M wind turbine, in: *Conference Proceedings European Offshore Wind 2007*, Berlin, Germany, 2007.
- Smith, A., Stehly, T., and Musial, W.: 2014–2015 Offshore Wind Technologies Market Report, Technical Report NREL/TP-5000-64283, National Renewable Energy Laboratory, Golden, CO, USA, 2015.
- Stolpe, M. and Sandal, K.: Structural optimization with several discrete design variables per part by outer approximation, *Struct. Multidiscip. O.*, 57, 2061–2073, <https://doi.org/10.1007/s00158-018-1941-3>, 2018.
- The Crown Estate: Offshore Wind Cost Reduction – Pathways Study, Tech. rep., 2012.
- van Kuik, G. A. M., Peinke, J., Nijssen, R., Lekou, D., Mann, J., Sørensen, J. N., Ferreira, C., van Wingerden, J. W., Schlipf, D., Gebraad, P., Polinder, H., Abrahamsen, A., van Bussel, G. J. W., Sørensen, J. D., Tavner, P., Bottasso, C. L., Muskulus, M., Matha, D., Lindeboom, H. J., Degraer, S., Kramer, O., Lehnhoff, S., Sonnenschein, M., Sørensen, P. E., Künneke, R. W., Morthorst, P. E., and Skytte, K.: Long-term research challenges in wind energy – a research agenda by the European Academy of Wind Energy, *Wind Energ. Sci.*, 1, 1–39, <https://doi.org/10.5194/wes-1-1-2016>, 2016.
- Vemula, N., DeVries, W., Fischer, T., Cordle, A., and Schmidt, B.: Design solution for the upwind reference offshore support structure, UpWind deliverable report D4.2.6, 2010.
- von Borstel, T.: Design Report Reference Jacket, Tech. Rep. IN-NWIND.EU deliverable report D4.3.1, 2013.
- Waltz, R. A., Morales, J. L., Nocedal, J., and Orban, D.: An interior algorithm for nonlinear optimization that combines line search and trust region steps, *Math. Program.*, 107, 391–408, <https://doi.org/10.1007/s10107-004-0560-5>, 2006.
- Zwick, D. and Muskulus, M.: Simplified fatigue load assessment in offshore wind turbine structural analysis, *Wind Energy*, 19, 265–278, <https://doi.org/10.1002/we.1831>, 2016.

## 6 Conclusion

### 6.1 Summary

In the previous chapters, the thesis addressed four objectives for an improvement of state-of-the-art jacket optimization approaches, which will be summarized in the following.

#### **Improvement of offshore wind turbine time-domain simulation codes**

According to the state of the art, an onshore wind turbine, including rotor blades, hub, drivetrain, tower, and foundation can be modeled by multi-body systems with about 20 to 30 degrees of freedom, obtaining medium fidelity. As to offshore wind turbines, the structural behavior of the substructure has to be considered, too. A naive approach would be to use a finite-element discretization, which, however, results – in the case of jackets – in a structural assembly with hundreds or thousands of degrees of freedom. It is obvious that the coupling of turbine itself and the substructure would lead to a massive imbalance in model fidelity. To resolve this issue, reduction methods like the component mode synthesis are deployed, enabling a representation of the substructure with about ten degrees of freedom. However, in this case, the structural behavior of the foundation is often neglected and the substructure is assumed to be clamped at its bottom. To improve the modeling accuracy, a novel two-step approach was proposed (Häfele et al. 2016) and presented in chapter 2. In the first step, a structural foundation model was created, yielding lumped mass and stiffness matrices at the interface between substructure and foundation, obtained by an arbitrary reduction method. In the second step, the finite-element representation of the substructure was combined with these lumped matrices by adding the mass and stiffness values to the corresponding degrees of freedom. The modified system matrices of the substructure were reduced by a component mode synthesis. The great advantage of this approach is that it usually does not require additional degrees of freedom. Therefore, it increases the accuracy without harming the numerical efficiency, which is a highly desirable feature. In general, an operating point has to be defined prior to the derivation of the matrices of soil-structure interaction. It may be reasonable to consider operating point-dependent soil resistances, which is not part of this thesis, but was proposed in another work (Hübler et al. 2018b). It is also possible to use different foundation types like suction caissons. The approach was implemented in the aero-hydro-servo-elastic simulation code FAST and tested using different design load cases and two substructures, a monopile and a jacket, for the NREL 5 MW reference turbine. The results show that significant shifts in the spectra of structural responses may occur when considering foundation properties in the simulation of offshore wind turbines, in particular for the second and higher modes.

#### **Load set reduction for the fatigue assessment of jacket substructure for offshore wind turbines**

Fatigue as a design driver is a particular challenge in the design of offshore wind turbines. Due to the main excitation by turbulent wind, irregular waves, and the rotor motion, an offshore wind turbine



is exposed to high fatigue damages. For this reason, the design of a wind turbine requires a detailed load assessment, which involves the consideration of varying environmental and operational states. State-of-the-art jacket substructures are designed with load sets for fatigue limit state comprising thousands of design load cases according to standards and guidelines, mainly to account for varying combinations of wind and wave states, like wind speeds, wave heights and peak periods, or directional wind-wave misalignments. In chapter 3, it was analyzed, whether the size of load sets for fatigue limit state assessments can be reduced (Häfele et al. 2018b). For this purpose, a design basis using measurement data of the research platforms FINO3 and FINO1 (for validation purposes) was used to derive distributions of the main parameters characterizing environmental conditions in wind farms. The first step was to evaluate a three-legged and a four-legged jacket, using a probabilistic load set with 2048 design load cases, sampled by probability density functions of environmental states. It was shown that fatigue damages, even if evaluated in the same wind speed bins, may vary by several orders of magnitude. In the next step, it was evaluated, how a load set reduction impacts the fatigue assessment. In general, the scatter in the results increases with higher reduction. However, the study shows that it may be reasonable to reduce the number of load cases significantly when accepting a certain degree of uncertainty. For instance, in case of a sixteen-fold reduction from 2048 to 128 design load cases, the error due to uncertainty can be maintained (depending on the structure and the position of fatigue evaluation) at a manageable level. In a third step, load sets with unidirectional loads, representing the state of the art in some industrial and scientific applications, were analyzed and compared to stochastic load sets based on probability density functions of environmental parameters. In some cases, unidirectional loads may also yield reasonable results. However, this assumption does not generally imply significantly lower numerical costs. Although a simplified load set with unidirectional loads was defined, it can be summarized that load sets based on stochastic loads are preferable, provided that the size of the load set is not too small.

### **Accurate and numerically efficient formulation of the jacket optimization problem**

An appropriate problem formulation is the key to reasonable results that may be transferred to practical applications. This objective involves three aspects: A jacket model along with a representative set of design variables, a comprehensive objective or cost function, representing the real capital expenditures of the jacket adequately, and efficient but valid structural code checks, serving as nonlinear constraints of the problem. All three aspects were addressed in a comprehensive research paper (Häfele et al. 2018c), presented in chapter 4. Basis of this work is a jacket model incorporating both topological and tube sizing design variables. This is an important property, because state-of-the-art approaches consider the problem commonly as pure tube sizing problem with fixed topology. Therefore, this approach is suitable for analyzing different configurations. In order to keep the number of parameters or design variables constant, tube dimensions are interpolated between values given at the bottom and top of the structure. The jacket model has 20 parameters, where twelve are design variables. The proposed cost model addresses another issue in jacket optimization. Commonly, the mass of the jacket serves as objective function in the formulation of the optimization problem, which is, however, not fully related to the actual capital expenditures of the structure. Therefore, the cost function incorporates contributions of material, manufacturing, coating, transition piece, transport, installation, and fixed expenses. In fact, this is still an approximation implying simplifications, but it can be considered as a more comprehensive approach. The third aspect is very important concerning numerical efficiency. The computationally demanding evaluation of structural code checks, which bases on multiple time-domain simulations, was replaced by a surrogate modeling approach utilizing Gaussian process regression. To set up these surrogate models, still a high number of time-domain

simulations had to be performed to obtain training data. However, all time-domain simulations can easily be outsourced to parallelizable high-performance computers in this open-loop procedure, while the evaluation of the closed-loop optimization procedure does not require high numerical capacity and can be performed on local working stations. This is particularly beneficial for scientific applications, where compute clusters with very high numbers of central processing units are available. The functionality of all models was shown by a simple example, indicating the potential for optimization applications.

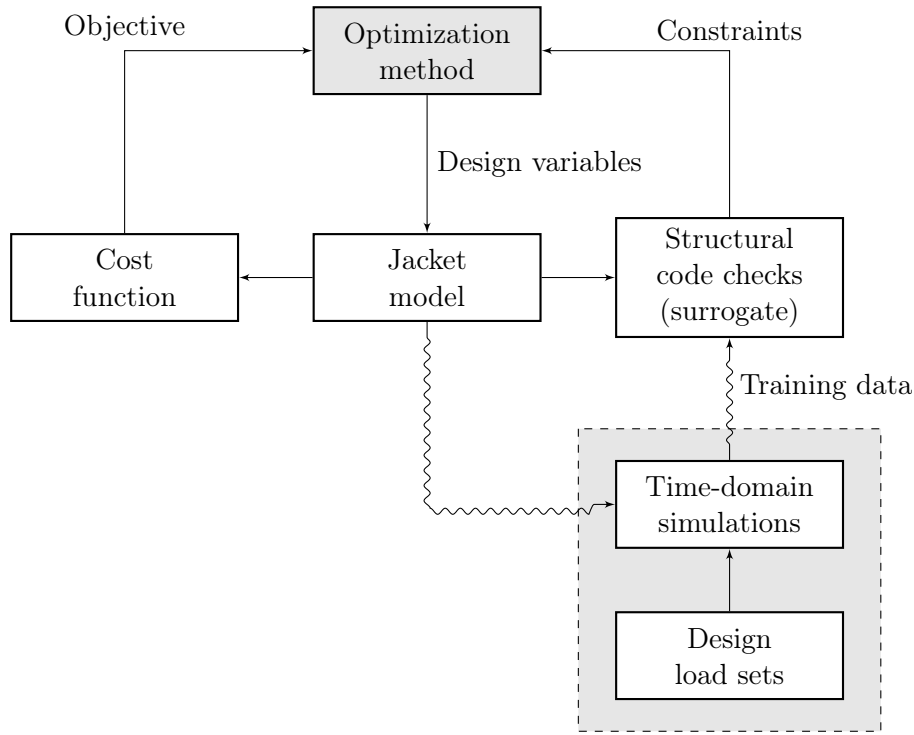
### Evaluation of optimal designs for offshore wind turbine jacket substructures

In the first three parts, models and methods improving state-of-the-art approaches in the field of jacket optimization were proposed. The fourth part combined the first three ones to a coherent optimization approach (Häfele et al. 2018a) as shown in chapter 5. In doing so, the technical problem was transferred to a nonlinear program with capital expenditures as objective function and structural code checks for fatigue and ultimate limit state, respectively, as nonlinear constraints. Exemplarily, the approach was deployed to find the optimal design solution for a jacket substructure for the NREL 5MW reference turbine, 50m water depth, and North Sea environmental conditions. The mixed-integer problem formulation was addressed by solving subproblems with fixed values of integer design variables. Two nonlinear programming optimization methods were utilized, a sequential quadratic programming and an interior-point method. Both converged quickly from remote starting points, whereby the sequential quadratic programming method required fewer iterations to converge. The suitability of gradient-based optimization for the present problem formulation can be assumed. Furthermore, it became apparent that surrogate modeling is very promising to improve the performance of jacket design optimization significantly. From the technical point of view, jackets with three legs seem economically more favorable compared to four-legged ones. For instance, the cheapest three-legged jacket substructure features about 8% lower costs than the cheapest four-legged version, under the assumptions and parameters of this study. In fact, due to limited information on real cost breakdowns, the results of such a study are not easy to validate, but agree with practical experiences. The comprehensive cost function was also compared to a pure mass-dependent approach. Interestingly, it became apparent that a mass-dependent approach yields similar results, when installation costs are considered in the objective function. Other costs are mainly – either directly or partly – proportional to the mass of the jacket.

## 6.2 Innovations

In this thesis, a novel scheme for jacket optimization was proposed. Figure 6.1 illustrates the main aspects of the approach. Compared to the optimization scheme shown in Figure 1.3, which can be considered as state of the art, the novel approach generally incorporates all elements known from other works, but additionally features several innovations:

- The application of surrogate modeling allows for a decoupled computation of time-domain simulations. This is an essential feature to accelerate jacket optimization, because the evaluation of surrogate models can be performed quickly, while the computationally intensive generation of training data for surrogate modeling is outsourced to high-performance compute clusters.



**Figure 6.1:** Scheme of the proposed approach to time-domain jacket optimization with nonlinear structural code check constraints evaluated by surrogate models.

- The cost modeling was performed in such a way as to consider realistic cost breakdowns of jacket substructures adequately, namely by incorporating capital expenditures for material, manufacturing, coating, transition piece, transport, installation, and fixed costs in a sum cost function.
- To reduce the demand for numerical capacity of time simulations, a reduced load set for fatigue limit state was proposed.
- To increase the fidelity of time-domain simulations, a soil-structure interaction approach for offshore wind turbines was developed without the need for higher numerical capacity.
- It was shown that jacket optimization is not only a tool for final, but also for preliminary design phases. For this purpose, a jacket model involving both topological and tube dimensioning design variables was implemented in the optimization scheme.

### 6.3 Concluding remarks

In the present thesis, four main topics, all with the objective of improving jacket design optimization in the context of offshore wind turbines, were addressed. These topics are (in the order of appearance in this work) improvement of time-domain simulations, load set reduction models for geometry, costs, and structural code checks, and optimal jacket designs. It was shown that each of these topics has

improvement potential concerning the global problem of optimal jacket design, which was realized to some extent by the methods proposed in this thesis.

The result of this work is not the ultimate optimal jacket design, which may be the unforeseeable result of extensive work dealing with jacket optimization. In fact, a large part of this thesis addressed the problem of optimal jacket design. However, it became apparent that there are too many factors impacting the actual structural design. In general, the optimal design is dependent on the boundary conditions of the problem, like reference turbine, environmental states, water depth, and soil properties, but also on the parameters of the cost model. These parameters are difficult to estimate from the scientific perspective and also depend on side effects subject to strong uncertainty. When considering these restrictions, it becomes clear that the result of this work is intended as a general, parameter-independent approach to the optimal design of jacket substructures for offshore wind turbines. Due to excellent accessibility and documentation, the functionality of all proposed methods was shown using the NREL 5 MW reference wind turbine. However, it can be assumed that the transfer to a different wind turbine should be easily possible. The same applies to all other boundary conditions.

When trying to classify the present approach, it is helpful to look back at the state of the art in the field of jacket optimization. Recent approaches that were reported in literature and yielded promising results interpreted the problem mainly as a pure tube dimensioning task with fixed topology. Commonly, gradient-based optimization methods are used to minimize the mass of substructures. In addition, fatigue and extreme loads are considered as constraints. Structural code checks are performed using time-domain simulations. This was identified as a main limitation, because the arising demand of high numerical capacity is usually compensated by simplified loads or incomprehensive load sets. In other words, an improvement in numerical efficiency may be related to an deterioration in accuracy. Therefore, the present approach may be classified as a holistic one, because it addresses the task in a multi-perspective way. On the one hand, the entire mathematical problem formulation was reconsidered. On the other hand, the optimization procedure was decoupled from the computationally parallelizable time-domain simulations utilizing machine learning regression methods. This leads to significant benefits in the whole optimization process, resulting in a potential increase of iterates in the design process of jacket substructures. As a consequence, costs and, eventually, levelized costs of energy can be reduced.

## 6.4 Future work

Further improvements of the approach depend on enhancements in all fields involved in the optimization framework (see Figure 6.1). While it can be assumed that the performance of optimization methods has been largely exhausted, all other points pose tasks that need to be addressed in the future. There are two key trends that may impact the results of jacket optimization distinctly in a positive way. First, it can be supposed that developments in time-domain simulation codes, with the trend to nonlinear structural analyses, may lead to generally more accurate predictions of the structural behavior in the midterm. With regard to optimization, it is important to focus on the numerical efficiency of simulations, too. The question remains, whether other than time-domain simulation techniques are able to predict structural responses that are suitable as input for appropriate structural code checks. A second trend involves probabilistic-based structural code checks. Nowadays, uncertainties are addressed by safety factors. When knowing all uncertainties in the entire design procedure, these factors can be replaced by probabilistic design assessments (Hübler et al. 2018a,c). Both factors may lead to more accurate and less conservative designs. In this thesis, possible design

---

load set reductions were analyzed. The results were quite promising, but only based on a sampling method without considering prior knowledge of occurrence of specific load events. Recent research reveals that there is even more reduction potential that can be exploited (Stieng and Muskulus 2018). Moreover, it was shown that the consideration of a more comprehensive objective function may lead to better results. The cost model that was used in this work is still quite simple and largely mass-dependent. Incorporating a more sophisticated cost model may lead to even better results. It is also imaginable to extend the jacket model in the way that it considers the topology or tube sizing in greater detail.

In addition, the approach may be coupled with state-of-the-art tube sizing approaches, too. It was discussed that the problem formulation rather addresses early design stages, while other approaches focus on design stages, where decisive topological parameters are fixed. Combining both offers further potential for cost reduction. In addition, the application of robust design methods is imaginable, in particular, because the problem involves uncertainties both in the formulations of objectives and constraints (which is similar to the point of probabilistic-based structural code checks). Future work in this field should address all these points to make use of further cost reduction potentials.

## Glossary

- alpha ventus** First German offshore wind farm in the North Sea with 12 wind turbines in the 5 MW class. 2, 3
- bracing** Structural element in a jacket substructure, intersecting diagonally with other bracings and connecting the jacket legs. 1, 7
- FAST** Aero-servo-hydro-elastic simulation code for (offshore) wind turbines with intermediate fidelity. FAST is an open-source code and freely available at no charge. 4, 5, 7, 12, 82
- FINO1** Offshore research platform, located in the North Sea close to the offshore wind farm alpha ventus. 3, 9, 83
- FINO2** Offshore research platform, located in the Baltic Sea close to the offshore wind farm Baltic 2. 9
- FINO3** Offshore research platform, located in the North Sea close to the offshore wind farm DanTysk. 9, 83
- INNWIND.EU** Research project (duration: 2012–2017), funded by the European Union and the follow-up project of the research project UpWind, focusing on beyond-state-of-the-art turbines in the range of about 10 to 20 MW rated power. 2, 8
- jacket** Truss-like, bottom-fixed offshore substructure, known from petrol industry for large offshore platforms. Commonly installed on pile foundations. 1, 2, 3, 6, 7, 8, 10, 11, 12, 13, 14, 15, 82, 83, 84, 85, 86, 87
- leg** Almost (when installed) vertical tubes building the corset of a jacket substructure. In case of a pile foundation, the number of legs is equal to the number of piles. 1, 6, 12
- levelized costs of energy** Normalized measure determining energy costs. 1, 2, 86
- monopile** Large, hollow steel pile, combining the functions of foundation and substructure for offshore wind turbines. To date, the substructure type with the most installations world-wide. 1, 2, 6, 7, 8, 11, 12, 13, 82
- OC3** *Offshore Code Comparison Collaboration*, a project under the International Energy Agency task 23, which aimed at code-to-code verifications of multiple aero-servo-hydro-elastic frameworks for simulating responses of offshore wind turbines. 5, 7, 8
- OC4** *Offshore Code Comparison Collaboration Continuation*, formed under the International Energy Agency task 30, considering simulations of offshore wind turbines with—compared to OC3—more complex substructures. 5, 7, 8, 12



**OC5** *Offshore Code Comparison Collaboration Continuation, with Correlation*, project analyzing the accuracy of different frameworks for the simulation of offshore wind turbines. Initiated under the International Energy Agency task 30, where the focus was on validations by physical measurements. 5

**substructure** Part of the support structure of an offshore wind turbine that bridges the gap between ground and tower foot. The largest part of the substructure is commonly under water. 1, 2, 3, 5, 6, 7, 8, 10, 11, 12, 13, 14, 15, 82, 83, 84, 85, 86

**support structure** Structure carrying the rotor and nacelle. Includes foundation, substructure, and tower in case of a state-of-the-art bottom-fixed offshore wind turbine. 3, 4, 8, 9, 10, 11, 12

**transition piece** Structural element connecting substructure and tower. 8, 12, 83, 85

**UpWind** Research project (duration: 2006–2011), funded by the European Union, with 40 partners and aiming to develop and verify models for components of wind turbines of about 5 to 10 MW rated power. 2, 7, 8, 9

## Bibliography

- 4C Offshore (2018). *Offshore Vessel Update 22nd February 2018*.
- AlHamaydeh, M., Barakat, S., and Nassif, O. (2015). “Optimization of quatropod jacket support structures for offshore wind turbines subject to seismic loads using genetic algorithms”. In: *Proceedings of the 5th International Conference on Computational Methods in Structural Dynamics and Earthquake Engineering*. Crete, Greece, pp. 3505–3513. DOI: 10.7712/120115.3634.1443.
- AlHamaydeh, M., Barakat, S., and Nasif, O. (2017). “Optimization of Support Structures for Offshore Wind Turbines Using Genetic Algorithm with Domain-Trimming”. In: *Mathematical Problems in Engineering 2017*, pp. 1–14. DOI: 10.1155/2017/5978375.
- American Bureau of Shipping (2010). *Guide for the Fatigue Assessment of Offshore Structures*. Recommended Practice.
- American Petroleum Institute (2002). *Recommended Practice for Planning, Designing and Constructing Fixed Offshore Platforms – Working Stress Design*. Recommended Practice RP 2A-WSD.
- Arora, J. S. (2012). *Introduction to optimum design*. Third edition. Amsterdam, Boston, Heidelberg, London, New York, Oxford, Paris, San Diego, San Francisco, Singapore, Sydney, Tokyo: Academic Press.
- Ashuri, T. (2012). “Beyond Classical Upscaling: Integrated Aeroservoelastic Design and Optimization of Large Offshore Wind Turbines”. PhD thesis. Delft University of Technology.
- Bachmann, J. and Barton, B. (2008). “Die Forschungsplattform FINO3”. In: *Stahlbau 77(9)*, pp. 685–687. DOI: 10.1002/stab.200890099.
- Bak, C., Bitsche, R., Yde, A., Kim, T., Hansen, M. H., Zahle, F., Gaunaa, M., Blasques, J., Døssing, M., Wedel Heinen, J.-J., and Behrens, T. (2012). “Light Rotor: The DTU 10-MW reference wind turbine”. In: *EWEA 2012 - European Wind Energy Conference & Exhibition*. Copenhagen, Denmark.
- Bak, C., Zahle, F., Bitsche, R., Kim, T., Yde, A., Henriksen, L. C., Hansen, M. H., Blasques, J., Gaunaa, M., and Natarajan, A. (2013). “The DTU 10-MW reference wind turbine”. In: *Danish wind power research*. Fredericia, Denmark.
- Barltrop, N. D. P., Adams, A. J., and Hallam, M. G. (1991). *Dynamics of fixed marine structures*. 3rd ed. MTD Ltd. publication 91/102. Oxford, London: Butterworth-Heinemann; Marine Technology Directorate.
- Bazeos, N., Hatzigeorgiou, G., Hondros, I., Karamaneas, H., Karabalis, D., and Beskos, D. (2002). “Static, seismic and stability analyses of a prototype wind turbine steel tower”. In: *Engineering Structures 24*, pp. 1015–1025. DOI: 10.1016/S0141-0296(02)00021-4.
- Böker, C. (2010). “Load simulation and local dynamics of support structures for offshore wind turbines”. PhD thesis. Leibniz Universität Hannover.
- Brommundt, M., Krause, L., Merz, K., and Muskulus, M. (2012). “Mooring system optimization for floating wind turbines using frequency domain analysis”. In: *Energy Procedia 24*, pp. 289–296. DOI: 10.1016/j.egypro.2012.06.111.
- BVGassociates (2012). *Offshore wind cost reduction pathways – Technology work stream*. Tech. rep.
- BVGassociates (2013). *Offshore wind: Industry’s journey to £100/MWh – Cost breakdown and technology transition from 2013 to 2020*. Tech. rep.

- Chaviaropoulos, P., Rasmussen, F., Abrahamsen, A. B., Conti, D., Natarajan, A., Roukis, G., Makris, A., Sartori, L., Bellini, F., Croce, A., Polinder, H., Kaufer, D., Armendariz, J. A., Kumar, A., Powell, D., Todd, P., and Clark, R. (2017). *PI-based assessment (application) on the results of WP2-WP4 for 20 MW wind turbines*. Tech. rep. INNWIND.EU deliverable report D1.2.5.
- Chen, J., Yang, R., Ma, R., and Li, J. (2016). “Design optimization of wind turbine tower with lattice-tubular hybrid structure using particle swarm algorithm”. In: *The Structural Design of Tall and Special Buildings* 25(15), pp. 743–758. DOI: 10.1002/ta1.1281.
- Chen Ong, M., Bachynski, E. E., and David Økland, O. (2017). “Dynamic Responses of Jacket-Type Offshore Wind Turbines Using Decoupled and Coupled Models”. In: *Journal of Offshore Mechanics and Arctic Engineering* 139(4), p. 041901. DOI: 10.1115/1.4035772.
- Chew, K. H., Muskulus, M., Zwick Daniel, D., Ng, E. Y. K., and Tai, K. (2013). “Structural Optimization and Parametric Study of Offshore Wind Turbine Jacket Substructure”. In: *International Ocean, Offshore and Polar Engineering Conference*. Vol. 23. Anchorage, AK, USA, pp. 203–210.
- Chew, K. H., Tai, K., Ng, E. Y. K., Muskulus, M., and Zwick, D. (2014). “Offshore Wind Turbine Jacket Substructure: A Comparison Study Between Four-Legged and Three-Legged Designs”. In: *Journal of Ocean and Wind Energy* 1(2), pp. 74–81.
- Chew, K.-H., Tai, K., Ng, E., and Muskulus, M. (2015). “Optimization of Offshore Wind Turbine Support Structures Using an Analytical Gradient-based Method”. In: *Energy Procedia* 80, pp. 100–107. DOI: 10.1016/j.egypro.2015.11.412.
- Chew, K.-H., Tai, K., Ng, E., and Muskulus, M. (2016). “Analytical gradient-based optimization of offshore wind turbine substructures under fatigue and extreme loads”. In: *Marine Structures* 47, pp. 23–41. DOI: 10.1016/j.marstruc.2016.03.002.
- Craig Jr., R. R. and Bampton, M. C. C. (1968). “Coupling of Substructures for Dynamic Analyses”. In: *AIAA Journal* 6(7), pp. 1313–1319. DOI: 10.2514/3.4741.
- Damiani, R., Dykes, K., and Scott, G. (2016). “A comparison study of offshore wind support structures with monopiles and jackets for U.S. waters”. In: *Journal of Physics: Conference Series* 753, p. 092003. DOI: 10.1088/1742-6596/753/9/092003.
- Damiani, R., Ning, A., Maples, B., Smith, A., and Dykes, K. (2017). “Scenario analysis for techno-economic model development of U.S. offshore wind support structures: Scenario analysis for techno-economic model development of U.S. offshore wind support structures”. In: *Wind Energy* 20(4), pp. 731–747. DOI: 10.1002/we.2021.
- Damiani, R. (2016). *JacketSE: An Offshore Wind Turbine Jacket Sizing Tool*. Technical Report NREL/TP-5000-65417. Golden, CO, USA: National Renewable Energy Laboratory.
- Damiani, R. and Song, H. (2013). “A Jacket Sizing Tool for Offshore Wind Turbines within the Systems Engineering Initiative”. In: *Offshore Technology Conference*. Houston, TX, USA. DOI: 10.4043/24140-MS.
- Damiani, R., Jonkman, J., Robertson, A., and Song, H. (2013). “Assessing the Importance of Nonlinearities in the Development of a Substructure Model for the Wind Turbine CAE Tool FAST”. In: *32nd International Conference on Ocean, Offshore and Arctic Engineering*. Nantes, France, pp. 1–16.
- Det Norske Veritas AS (2013). *Buckling Strength of Shells*. Recommended Practice DNV-RP-C202.
- Det Norske Veritas AS (2014). *Design of Offshore Wind Turbine Structures*. Offshore Standard DNV-OS-J101.
- Deutsches Institut für Normung (2010). *Eurocode 3: Bemessung und Konstruktion von Stahlbauten*. Norm DIN EN 1993.
- Dirlik, T. (1985). “Application of computers in fatigue analysis”. PhD thesis. University of Warwick.
- DNV GL AS (2016a). *Fatigue design of offshore steel structures*. Recommended Practice DNVGL-RP-C203.

- DNV GL AS (2016b). *Support structures for wind turbines*. Standard DNVGL-ST-126.
- Dubois, J., Muskulus, M., and Schaumann, P. (2013). “Advanced representation of tubular joints in jacket models for offshore wind turbine simulation”. In: *Energy Procedia* 35, pp. 234–243. DOI: 10.1016/j.egypro.2013.07.176.
- Efthymiou, M. (1988). “Development of SCF formulae and generalised influence functions for use in fatigue analysis”. In: *Proceedings of the Conference on Recent Developments in Tubular Joints Technology*. Surrey, UK, pp. 1–13.
- Farkas, J. and Jármai, K. (1997). *Analysis and design of metal structures*. Rotterdam: Balkema.
- Fischer, T., de Vries, W., and Schmidt, B. (2010). *Upwind Design Basis*. Tech. rep.
- Fletcher, R. (1987). *Practical methods of optimization*. 2nd ed. Chichester, New York: Wiley.
- Gebhardt, C. G., Hofmeister, B., Hente, C., and Rolfes, R. (2018). “Nonlinear dynamics of slender structures: a new object-oriented framework”. In: *Computational Mechanics*. DOI: 10.1007/s00466-018-1592-7.
- Gencturk, B., Attar, A., and Tort, C. (2012). “Optimal Design of Lattice Wind Turbine Towers”. In: *15th World Conference on Earthquake Engineering*. Lisbon, Portugal.
- Germanischer Lloyd (2012). *Guideline for the Certification of Offshore Wind Turbines*. Offshore Standard.
- Gill, P. E., Murray, W., and Wright, M. H. (1981). *Practical optimization*. London, New York: Academic Press.
- Glover, F. (1986). “Future paths for integer programming and links to artificial intelligence”. In: *Computers & Operations Research* 13(5), pp. 533–549. DOI: 10.1016/0305-0548(86)90048-1.
- Goldberg, D. E. (1989). *Genetic algorithms in search, optimization, and machine learning*. Reading, Mass: Addison-Wesley Pub. Co.
- Gutierrez, J. E., Zamora, B., García, J., and Peyrau, M. R. (2013). “Tool development based on FAST for performing design optimization of offshore wind turbines: FASTLognoter”. In: *Renewable Energy* 55, pp. 69–78. DOI: 10.1016/j.renene.2012.12.026.
- Guyan, R. J. (1965). “Reduction of stiffness and mass matrices”. In: *AIAA Journal* 3(2), p. 380. DOI: 10.2514/3.2874.
- Haake, G., Rolfes, R., Schaumann, P., Schlurmann, T., Lohaus, L., Achmus, M., and Huhn, H. (2009). “Research on Support Structures in the German Offshore Wind Farm alpha ventus”. In: *Proceedings EWECEC 2009*. Marseille, France.
- Häfele, J., Hübler, C., Gebhardt, C. G., and Rolfes, R. (2016). “An improved two-step soil-structure interaction modeling method for dynamical analyses of offshore wind turbines”. In: *Applied Ocean Research* 55, pp. 141–150. DOI: 10.1016/j.apor.2015.12.001.
- Häfele, J., Gebhardt, C. G., and Rolfes, R. (2018a). “A comparison study on jacket substructures for offshore wind turbines based on optimization”. In: *Wind Energy Science Discussions*. DOI: 10.5194/wes-2018-58.
- Häfele, J., Hübler, C., Gebhardt, C. G., and Rolfes, R. (2018b). “A comprehensive fatigue load set reduction study for offshore wind turbines with jacket substructures”. In: *Renewable Energy* 118, pp. 99–112. DOI: 10.1016/j.renene.2017.10.097.
- Häfele, J., Damiani, R., King, R. N., Gebhardt, C. G., and Rolfes, R. (2018c). “A systematic approach to offshore wind turbine jacket predesign and optimization: geometry, cost, and surrogate structural code check models”. In: *Wind Energy Science* 3(2), pp. 553–572. DOI: 10.5194/wes-3-553-2018.
- Haftka, R. T. and Gürdal, Z. (1992). *Elements of Structural Optimization*. Third revised and expanded edition. Dordrecht: Springer Science+Business Media.
- Haghi, R., Ashuri, T., van der Valk, P. L., and Molenaar, D. P. (2012). “Integrated Multidisciplinary Constrained Optimization of Offshore Support Structures”. In: *The Science of Making Torque from Wind*. Oldenburg, Germany.

- Hall, M., Buckham, B., and Crawford, C. (2013). “Evolving offshore wind: A genetic algorithm-based support structure optimization framework for floating wind turbines”. In: *OCEANS*. Bergen, Norway, pp. 1–10. DOI: 10.1109/OCEANS-Bergen.2013.6608173.
- Ho, A. and Mbistrova, A. (2017). *The European offshore wind industry - Key trends and statistics 2016*. Tech. rep. WindEurope.
- Ho, A., Mbistrova, A., and Corbetta, G. (2016). *The European offshore wind industry - key trends and statistics 2015*. Tech. rep. European Wind Energy Association.
- Hübler, C., Gebhardt, C. G., and Rolfes, R. (2017). “Development of a comprehensive database of scattering environmental conditions and simulation constraints for offshore wind turbines”. In: *Wind Energy Science* 2(2), pp. 491–505. DOI: 10.5194/wes-2-491-2017.
- Hübler, C., Gebhardt, C. G., and Rolfes, R. (2018a). “Assessment of a standard ULS design procedure for offshore wind turbine sub-structures”. In: *Journal of Physics: Conference Series* 1104, p. 012013. DOI: 10.1088/1742-6596/1104/1/012013.
- Hübler, C., Häfele, J., Gebhardt, C. G., and Rolfes, R. (2018b). “Experimentally supported consideration of operating point dependent soil properties in coupled dynamics of offshore wind turbines”. In: *Marine Structures* 57, pp. 18–37. DOI: 10.1016/j.marstruc.2017.09.002.
- Hübler, C., Gebhardt, C. G., and Rolfes, R. (2018c). “Methodologies for fatigue assessment of offshore wind turbines considering scattering environmental conditions and the uncertainty due to finite sampling”. In: *Wind Energy* 21(11), pp. 1092–1105. DOI: 10.1002/we.2216.
- International Electrotechnical Commission (2009). *Wind turbines – Part 3: Design requirements for offshore wind turbines*. Tech. rep. IEC-61400-3:2009.
- International Electrotechnical Commission (2010). *Wind turbines – Part 1: Design requirements*. Tech. rep. IEC 61400-1:2005 + AMD1:2010 CSV.
- Jonkman, J. (2007). *Dynamics Modeling and Loads Analysis of an Offshore Floating Wind Turbine*. Technical Report NREL/TP-500-41958. Golden, CO, USA: National Renewable Energy Laboratory.
- Jonkman, J. (2013). “The New Modularization Framework for the FAST Wind Turbine CAE Tool”. In: *51st AIAA Aerospace Sciences Meeting including the New Horizons Forum and Aerospace Exposition*. Grapevine, TX, USA. DOI: 10.2514/6.2013-202.
- Jonkman, J. and Musial, W. (2010). *Offshore Code Comparison Collaboration (OC3) for IEA Task 23 Offshore Wind Technology and Deployment*. Technical Report NREL/TP-5000-48191. Golden, CO, USA: National Renewable Energy Laboratory.
- Jonkman, J., Butterfield, S., Musial, W., and Scott, G. (2009). *Definition of a 5-MW Reference Wind Turbine for Offshore System Development*. Technical Report NREL/TP-500-38060. Golden, CO, USA: National Renewable Energy Laboratory.
- Kallehave, D., LeBlanc Thilsted, C., and Liingaard, M. (2012). “Modification of the API p-y formulation of initial stiffness in sand”. In: *Proceedings of the 7th International Conference Offshore Site Investigation and Geotechnics*. London, UK.
- Kang, B.-S., Choi, W., and Park, G. (2001). “Structural optimization under equivalent static loads transformed from dynamic loads based on displacement”. In: *Computers and Structures* 79, pp. 145–154. DOI: 10.1016/S0045-7949(00)00127-9.
- Kaufer, D., Fischer, T., Vorpahl, F., Popko, W., and Kühn, M. (2010). “Different approaches to modelling jacket support structures and their impact on overall wind turbine dynamics”. In: *10th German Wind Energy Conference*. Bremen, Germany.
- Kaveh, A. and Sabeti, S. (2017). “Optimal Design of Jacket Supporting Structures for Offshore Wind Turbines Using CBO and ECBO Algorithms”. In: *Periodica Polytechnica Civil Engineering*. DOI: 10.3311/PPci.11651.

- Kaveh, A. and Sabeti, S. (2018). “Structural optimization of jacket supporting structures for offshore wind turbines using colliding bodies optimization algorithm”. In: *The Structural Design of Tall and Special Buildings* 27(13), e1494. DOI: 10.1002/tal.1494.
- Kennedy, J. and Eberhart, R. (1995). “Particle Swarm Optimization”. In: *Proceedings of IEEE International Conference on Neural Networks IV*. Perth, Australia, pp. 1942–1948. DOI: 10.1109/ICNN.1995.488968.
- Kim, T., Hansen, A. M., and Branner, K. (2013). “Development of an anisotropic beam finite element for composite wind turbine blades in multibody system”. In: *Renewable Energy* 59, pp. 172–183. DOI: 10.1016/j.renene.2013.03.033.
- Kleineidam, P. (2005). “Zur Bemessung der Tragstrukturen von Offshore-Windenergieanlagen gegen Ermüdung”. PhD thesis. Leibniz Universität Hannover.
- Kooijman, H. J. T., Lindenburg, C., Winkelaar, D., and van der Hooft, E. L. (2003). *Aero-elastic modelling of the DOWEC 6 MW pre-design in PHATAS*. Tech. rep. DOWEC-F1W2-HJK-01-046/9.
- Kreiss, J., Ehrhart, K.-M., and Hanke, A.-K. (2017). “Auction-theoretic analyses of the first offshore wind energy auction in Germany”. In: *Journal of Physics: Conference Series* 926, p. 012015. DOI: 10.1088/1742-6596/926/1/012015.
- Kühn, M. (1999). “Design optimisation of an offshore wind energy converter by means of tailored dynamics”. In: *European Wind Energy Conference and Exhibition*. Nice, France.
- Kühn, M. (2001). “Dynamics and Design Optimisation of Offshore Wind Energy Conversion Systems”. PhD thesis. Delft University of Technology.
- Lavassas, I., Nikolaidis, G., Zervas, P., Efthimiou, E., Doudoumis, I., and Baniotopoulos, C. (2003). “Analysis and design of the prototype of a steel 1-MW wind turbine tower”. In: *Engineering Structures* 25, pp. 1097–1106. DOI: 10.1016/S0141-0296(03)00059-2.
- Long, H. and Moe, G. (2012). “Preliminary Design of Bottom-Fixed Lattice Offshore Wind Turbine Towers in the Fatigue Limit State by the Frequency Domain Method”. In: *Journal of Offshore Mechanics and Arctic Engineering* 134(3). DOI: 10.1115/1.4005200.
- Long, H., Moe, G., and Fischer Tim, T. (2011). “Lattice Towers for Bottom-Fixed Offshore Wind Turbines in the Ultimate Limit State: Variation of Some Geometric Parameters”. In: *Journal of Offshore Mechanics and Arctic Engineering* 134(2). DOI: 10.1115/1.4004634.
- Maki, K., Sbragio, R., and Vlahopoulos, N. (2012). “System design of a wind turbine using a multi-level optimization approach”. In: *Renewable Energy* 43, pp. 101–110. DOI: 10.1016/j.renene.2011.11.027.
- Meyer, M. (2002). “Reduktionsmethoden zur Simulation des aeroelastischen Verhaltens von Windkraftanlagen”. PhD thesis. Technische Universität Braunschweig.
- Michailides, C. and Angelides, D. C. (2012). “Multi Objective Optimization Performance of a Floating Flexible System”. In: *Proceedings of the Twenty-second International Offshore and Polar Engineering Conference*. Rhodes, Greece, pp. 636–643.
- Mohammadi, E., Fadaeinedjad, R., and Naji, H. R. (2018). “Using a new wind turbine emulator to analyze tower shadow and yaw error effects”. In: *Energy Conversion and Management* 174, pp. 378–387. DOI: 10.1016/j.enconman.2018.08.049.
- Molde, H., Zwick, D., and Muskulus, M. (2014). “Simulation-based optimization of lattice support structures for offshore wind energy converters with the simultaneous perturbation algorithm”. In: *Journal of Physics: Conference Series* 555, p. 012075. DOI: 10.1088/1742-6596/555/1/012075.
- Morison, J., Johnson, J., and Schaaf, S. (1950). “The Force Exerted by Surface Waves on Piles”. In: *Journal of Petroleum Technology* 2(05), pp. 149–154. DOI: 10.2118/950149-G.
- Muñoz-Esparza, D., Cañadillas, B., Neumann, T., and van Beeck, J. (2012). “Turbulent fluxes, stability and shear in the offshore environment: Mesoscale modelling and field observations at FINO1”. In: *Journal of Renewable and Sustainable Energy* 4(6), p. 063136. DOI: 10.1063/1.4769201.

- Muskulus, M. (2012). “The Full-height lattice tower concept”. In: *Energy Procedia* 24, pp. 371–377. DOI: 10.1016/j.egypro.2012.06.120.
- Muskulus, M. and Schafhirt, S. (2014). “Design Optimization of Wind Turbine Structures – A Review”. In: *Journal of Ocean and Wind Energy* 1(1), pp. 12–22.
- National Wind Technology Center Information Portal (2016). *FAST v8*. URL: <https://nwtc.nrel.gov/FAST8> (visited on 11/01/2018).
- National Wind Technology Center Information Portal (2018). *OpenFAST*. URL: <https://nwtc.nrel.gov/OpenFAST> (visited on 11/01/2018).
- Negm, H. M. and Maalawi, K. Y. (2000). “Structural design optimization of wind turbine towers”. In: *Computers and Structures* 74, pp. 649–666. DOI: 10.1016/S0045-7949(99)00079-6.
- Nocedal, J. and Wright, S. J. (2006). *Numerical optimization*. 2nd ed. Springer series in operations research. New York: Springer.
- NORSOK (2004a). *Design of steel structures*. Standard N-004 Rev. 2.
- NORSOK (2004b). *Structural design*. Standard N-001 Rev. 4.
- Oest, J., Sørensen, R., T. Overgaard, L. C., and Lund, E. (2016). “Structural optimization with fatigue and ultimate limit constraints of jacket structures for large offshore wind turbines”. In: *Structural and Multidisciplinary Optimization* 55, pp. 779–793. DOI: 10.1007/s00158-016-1527-x.
- Oest, J., Sandal, K., Schafhirt, S., Stieng, L. E. S., and Muskulus, M. (2018). “On gradient-based optimization of jacket structures for offshore wind turbines”. In: *Wind Energy* 21(11), pp. 953–967. DOI: 10.1002/we.2206.
- Oh, K.-Y., Nam, W., Ryu, M. S., Kim, J.-Y., and Epureanu, B. I. (2018). “A review of foundations of offshore wind energy convertors: Current status and future perspectives”. In: *Renewable and Sustainable Energy Reviews* 88, pp. 16–36. DOI: 10.1016/j.rser.2018.02.005.
- Pahn, T., Rolfes, R., and Jonkman, J. (2017). “Inverse load calculation procedure for offshore wind turbines and application to a 5-MW wind turbine support structure: Inverse load calculation procedure for offshore wind turbines”. In: *Wind Energy* 20(7), pp. 1171–1186. DOI: 10.1002/we.2088.
- Passon, P. and Kühn, M. (2005). “State-of-the-art and Development Needs of Simulation Codes for Offshore Wind Turbines”. In: *Copenhagen Offshore Wind 2005 Conference and Expedition Proceedings*. Copenhagen, Denmark.
- Passon, P., Kühn, M., Butterfield, S., Jonkman, J., Camp, T., and Larsen, T. J. (2007). “OC3–Benchmark Exercise of Aero-elastic Offshore Wind Turbine Codes”. In: *Journal of Physics Conference Series* 75, pp. 1–12. DOI: 10.1088/1742-6596/75/1/012071.
- Pavese, C., Wang, Q., Kim, T., Jonkman, J., and Sprague, M. (2015). “HAWC2 and BeamDyn: Comparison Between Beam Structural Models for Aero-Servo-Elastic Frameworks”. In: *European Wind Energy Association Annual Conference and Exhibition 2015*. Paris, France, pp. 1193–1201.
- Perelmuter, A. and Yurchenko, V. (2012). “Parametric Optimization of Steel Shell Towers of High-Power Wind Turbines”. In: *Procedia Engineering* 57, pp. 895–905. DOI: 10.1016/j.proeng.2013.04.114.
- Pontow, S., Kaufer, D., Shirzadeh, R., and Kühn, M. (2017). *Design Solution for a Support Structure Concept for future 20MW*. Tech. rep. INNWIND.EU deliverable report D4.3.6.
- Popko, W., Vorpahl, F., Zuga, A., Kohlmeier, M., Jonkman, J., Robertson, A., Larsen, T., Yde, A., Sætertrø, K., Okstad, K., Nichols, J., Nygaard, T., Gao, Z., Manolas, D., Kim, K., Yu, Q., Shi, W., Park, H., Vásquez-Rojas, A., Dubois, J., Kaufer, D., Thomassen, P., de Ruyter, M., van der Zee, T., Peeringa, J., Zhiwen, H., and von Waaden, H. (2014a). “Offshore code comparison collaboration continuation (OC4), Phase I-results of coupled simulations of an offshore wind turbine with jacket support structure”. In: *Journal of Ocean and Wind Energy* 1(1), pp. 1–11.



- Popko, W., Vorpahl, F., and Panagiotis, A. (2014b). "Investigation of Local Vibration Phenomena of a Jacket Sub-Structure Caused by Coupling with Other Components of an Offshore Wind Turbine". In: *Journal of Ocean and Wind Energy* 1(2), pp. 111–118.
- Popko, W., Georgiadou, S., Loukogeorgaki, E., and Vorpahl, F. (2016). "Influence of Joint Flexibility on Local Dynamics of a Jacket Support Structure". In: *Journal of Ocean and Wind Energy* 3(1), pp. 1–9. DOI: 10.17736/jowe.2016.jcr45.
- Quarton, D. C. (1998). "The Evolution of Wind Turbine Design Analysis - A Twenty Year Progress Review". In: *Wind Energy* 1, pp. 5–24. DOI: 10.1002/(SICI)1099-1824(199804)1:1+<5::AID-WE1>3.0.CO;2-I.
- Rademacher, W. (2012). *Die drei nördlichen Windkraftanlagen vom Typ REpower 5M*. License: CC BY-SA 3.0. URL: <https://commons.wikimedia.org/w/index.php?curid=19811340> (visited on 11/01/2018).
- Renewable Energy Policy Network for the 21st Century (2018). *Renewables 2018 – Global Status Report*. Tech. rep.
- REpower Systems AG (2004). *5M*. Tech. rep. Hamburg, Germany. URL: [http://www.besco.de/5m\\_de.pdf](http://www.besco.de/5m_de.pdf) (visited on 11/01/2018).
- Robertson, A., Wendt, F., Jonkman, J., Popko, W., Vorpahl, F., Stansberg, C. T., Bachynski, E. E., Bayati, I., Beyer, F., de Vaal, J. B., Harries, R., Yamaguchi, A., Shin, H., Kim, B., van der Zee, T., Bozonnet, P., Aguilo, B., Bergua, R., Qvist, J., Qijun, W., Chen, X., Guerinel, M., Tu, Y., Yutong, H., Li, R., and Bouy, L. (2015). "OC5 Project Phase I: Validation of Hydrodynamic Loading on a Fixed Cylinder". In: *Proceedings of the Twenty-fifth (2015) International Offshore and Polar Engineering Conference*. Kona, HI, USA, pp. 471–480.
- Robertson, A., Wendt, F., Jonkman, J., Popko, W., Borg, M., Bredmose, H., Schlutter, F., Qvist, J., Bergua, R., Harries, R., Yde, A., Nygaard, T. A., Vaal, J. B. d., Oggiano, L., Bozonnet, P., Bouy, L., Sanchez, C. B., García, R. G., Bachynski, E. E., Tu, Y., Bayati, I., Borisade, F., Shin, H., van der Zee, T., and Guerinel, M. (2016). "OC5 Project Phase Ib: Validation of Hydrodynamic Loading on a Fixed, Flexible Cylinder for Offshore Wind Applications". In: *Energy Procedia* 94, pp. 82–101. DOI: 10.1016/j.egypro.2016.09.201.
- Robertson, A. N., Wendt, F., Jonkman, J. M., Popko, W., Dagher, H., Gueydon, S., Qvist, J., Vittori, F., Azcona, J., Uzunoglu, E., Soares, C. G., Harries, R., Yde, A., Galinos, C., Hermans, K., de Vaal, J. B., Bozonnet, P., Bouy, L., Bayati, I., Bergua, R., Galvan, J., Mendikoa, I., Sanchez, C. B., Shin, H., Oh, S., Molins, C., and Debruyne, Y. (2017). "OC5 Project Phase II: Validation of Global Loads of the DeepCwind Floating Semisubmersible Wind Turbine". In: *Energy Procedia* 137, pp. 38–57. DOI: 10.1016/j.egypro.2017.10.333.
- Rolfes, R., Schaumann, P., Achmus, M., Huhn, H., Lohaus, L., and Schlurmann, T. (2013). *Ganzheitliches Dimensionierungskonzept für OWEA-Tragstrukturen anhand von Messungen im Offshore-Testfeld alpha ventus - Abschlussbericht GIGAWIND alpha ventus*. Ed. by R. Rolfes and P. Schaumann. Berichte aus dem Bauwesen. Aachen, Germany: Shaker Verlag.
- Rychlik, I. (1987). "A new definition of the rainflow cycle counting method". In: *International Journal of Fatigue* 9(2), pp. 119–121. DOI: 10.1016/0142-1123(87)90054-5.
- Sandal, K., Latini, C., Zania, V., and Stolpe, M. (2018). "Integrated optimal design of jackets and foundations". In: *Marine Structures* 61, pp. 398–418. DOI: 10.1016/j.marstruc.2018.06.012.
- Sarpkaya, T. (2010). *Wave forces on offshore structures*. Cambridge; New York: Cambridge University Press.
- Sartori, L., Bellini, F., Croce, A., and Bottasso, C. (2018). "Preliminary design and optimization of a 20MW reference wind turbine". In: *Journal of Physics: Conference Series* 1037, p. 042003. DOI: 10.1088/1742-6596/1037/4/042003.

- Schafhirt, S., Zwick, D., and Muskulus, M. (2016). “Two-stage local optimization of lattice type support structures for offshore wind turbines”. In: *Ocean Engineering* 117, pp. 163–173. DOI: 10.1016/j.oceaneng.2016.03.035.
- Schafhirt, S., Zwick, D., and Muskulus, M. (2014). “Reanalysis of Jacket Support Structure for Computer-Aided Optimization of Offshore Wind Turbines with a Genetic Algorithm”. In: *Journal of Ocean and Wind Energy* 1(4), pp. 209–216.
- Schaumann, P. and Böker, C. (2007). “Influence of Wave Spreading in Short-term Sea States on the Fatigue of Offshore Support Structures at the Example of the FINO1-Research Platform”. In: *DEWI Magazin* 30, pp. 51–57.
- Schaumann, P., Dubois, J., Achmus, M., Abdel-Rahman, K., and Seidel, M. (2011). “Local Dynamics of Jacket Support Structures for Offshore Wind Turbines”. In: *European Offshore Wind 2011*. Amsterdam, Netherlands, pp. 846–853.
- Seidel, M. (2007). “Jacket substructures for the REpower 5M wind turbine”. In: *Conference Proceedings European Offshore Wind 2007*. Berlin, Germany.
- Seidel, M. (2010). “Design of support structures for offshore wind turbines – Interfaces between project owner, turbine manufacturer, authorities and designer”. In: *Stahlbau* 79(9), pp. 631–636.
- Seidel, M., von Mutius, M., Rix, P., and Steudel, D. (2005). “Integrated analysis of wind and wave loading for complex support structures of Offshore Wind Turbines”. In: *Conference Proceedings Offshore Wind 2005*. Copenhagen, Denmark.
- Shi, Y. and Eberhart, R. (1998). “A modified particle swarm optimizer”. In: *The 1998 IEEE International Conference on Evolutionary Computation Proceedings*. Anchorage, AK, USA, pp. 69–73. DOI: 10.1109/ICEC.1998.699146.
- Smith, A., Stehly, T., and Musial, W. (2015). *2014-2015 Offshore Wind Technologies Market Report*. Technical Report NREL/TP-5000-64283. Golden, CO, USA: National Renewable Energy Laboratory.
- Song, H., Robertson, A., Jonkman, J., and Sewell, D. (2012). “Incorporation of Multi-Member Substructure Capabilities in FAST for Analysis of Offshore Wind Turbines”. In: *Offshore Technology Conference*. Houston, TX, USA.
- Sørensen, J. N. (2016). “Blade-Element/Momentum Theory”. In: *General Momentum Theory for Horizontal Axis Wind Turbines*. Vol. 4. Cham: Springer International Publishing, pp. 99–121. DOI: 10.1007/978-3-319-22114-4\_7.
- Sørensen, J. D. and Tarp-Joansen, N. J. (2005). “Reliability-based Optimization and Optimal Reliability Level of Offshore Wind Turbines”. In: *International Journal of Offshore and Polar Engineering* 15(2), pp. 141–146.
- Stieng, L. E. S. and Muskulus, M. (2018). “Reducing the number of load cases for fatigue damage assessment of offshore wind turbine support structures using a simple severity-based sampling method”. In: *Wind Energy Science* 3(2), pp. 805–818. DOI: 10.5194/wes-3-805-2018.
- Stolpe, M. and Sandal, K. (2018). “Structural optimization with several discrete design variables per part by outer approximation”. In: *Structural and Multidisciplinary Optimization* 57, pp. 2061–2073. DOI: 10.1007/s00158-018-1941-3.
- Stolpe, M., Wandji, W. N., Natarajan, A., Shirzadeh, R., Kühn, M., and Kaufer, D. (2016). *Innovative design of a 10MW steel-type jacket*. Tech. rep. INNWIND.EU Deliverable D4.3.4.
- Sutherland, H. J. (1999). *On the Fatigue Analysis of Wind Turbines*. Tech. rep. SAND99-0089. Albuquerque, NM, USA: Sandia National Laboratories.
- The Crown Estate (2012). *Offshore Wind Cost Reduction – Pathways Study*. Tech. rep.
- Thiry, A., Bair, F., Buldgen, L., Raboniand, G., and Rigo, P. (2011). “Optimization of monopile offshore wind structures”. In: *MARSTRUCT - 3rd International Conference on Marine Structures*. Hamburg, Germany, pp. 633–642. DOI: 10.1201/b10771-77.

- Tong, X., Zhao, X., and Karcianas, A. (2018). “Passive vibration control of an offshore floating hydrostatic wind turbine model: Passive vibration control of an offshore floating hydrostatic wind turbine model”. In: *Wind Energy* 21(9), pp. 697–714. DOI: 10.1002/we.2188.
- Uys, P. E., Farkas, J., Jármai, K., and van Tonder, F. (2007). “Optimisation of a steel tower for a wind turbine structure”. In: *Engineering Structures* 29. DOI: 10.1016/j.engstruct.2006.08.011.
- Van Kuik, G. A. M., Peinke, J., Nijssen, R., Lekou, D., Mann, J., Sørensen, J. N., Ferreira, C., van Wingerden, J. W., Schlipf, D., Gebraad, P., Polinder, H., Abrahamsen, A., van Bussel, G. J. W., Sørensen, J. D., Tavner, P., Bottasso, C. L., Muskulus, M., Matha, D., Lindeboom, H. J., Degraer, S., Kramer, O., Lehnhoff, S., Sonnenschein, M., Sørensen, P. E., Künneke, R. W., Morthorst, P. E., and Skytte, K. (2016). “Long-term research challenges in wind energy – a research agenda by the European Academy of Wind Energy”. In: *Wind Energy Science* 1(1), pp. 1–39. DOI: 10.5194/wes-1-1-2016.
- Van der Tempel, J. (2006). “Design of Support Structures for Offshore Wind Turbines”. PhD thesis. Delft University of Technology.
- Vemula, N., DeVries, W., Fischer, T., Cordle, A., and Schmidt, B. (2010). *Design solution for the upwind reference offshore support structure*. Tech. rep. UpWind deliverable report D4.2.6.
- Von Borstel, T. (2013). *Design Report Reference Jacket*. Tech. rep. INNWIND.EU deliverable report D4.3.1.
- Vorpahl, F. and Popko, W. (2013). *Description of the load cases and output sensors to be simulated in the OC4 project under IEA wind annex 30*. Tech. rep. Bremerhaven, Germany: Fraunhofer-Institut für Windenergie und Energiesystemtechnik.
- Vorpahl, F., Popko, W., and Kaufer, D. (2011). *Description of a basic model of the "UpWind reference jacket" for code comparison in the OC4 project under IEA Wind Annex XXX*. Tech. rep. Bremerhaven, Germany: Fraunhofer-Institut für Windenergie und Energiesystemtechnik.
- Walters, A.-M. (2016). “Keystone Engineering Designs First Commercial Offshore Wind Farm in the U.S.” In: *Process & Plant Engineering* 34(4), pp. 33–35.
- Wang, Q., Sprague, M., Jonkman, J., Johnson, N., and Jonkman, B. (2017). “BeamDyn: a high-fidelity wind turbine blade solver in the FAST modular framework”. In: *Wind Energy* 20(8), pp. 1439–1462. DOI: 10.1002/we.2101.
- Yoshida, S. (2006). “Wind Turbine Tower Optimization Method Using a Genetic Algorithm”. In: *Wind Engineering* 30(6), pp. 453–470. DOI: 10.1260/030952406779994150.
- Zaaijer, M. B. (2001). “Properties of offshore support structures for large scale wind turbines”. In: *Offshore Wind Energy Special Topic Conference*. Brussels, Belgium.
- Zaaijer, M. B. (2006). “Foundation modelling to assess dynamic behaviour of offshore wind turbines”. In: *Applied Ocean Research* 28, pp. 45–57. DOI: 10.1016/j.apor.2006.03.004.
- Zahle, F., Bak, C., Bitsche, R., Kim, T., Hansen, M. H., and Yde, A. (2013). “Towards an Integrated Design Complex for Wind Turbines”. In: *The 2nd NREL Wind Energy Systems Engineering Workshop*. Broomfield, CO, USA.
- Zwick, D. and Muskulus, M. (2015). “The simulation error caused by input loading variability in offshore wind turbine structural analysis”. In: *Wind Energy* 18(8), pp. 1421–1432. DOI: 10.1002/we.1767.
- Zwick, D. and Muskulus, M. (2016). “Simplified fatigue load assessment in offshore wind turbine structural analysis”. In: *Wind Energy* 19(2), pp. 265–278. DOI: 10.1002/we.1831.
- Zwick, D., Muskulus, M., and Moe, G. (2012). “Iterative optimization approach for the design of full-height lattice towers for offshore wind turbines”. In: *Energy Procedia* 24, pp. 297–304. DOI: 10.1016/j.egypro.2012.06.112.

# Lebenslauf

## Persönliche Daten

Name: Jan Häfele  
Geburtsdatum: 24.05.1987  
Geburtsort: Minden  
Nationalität: deutsch  
Familienstand: ledig

## Werdegang

1993 – 1997: Grundschule  
Bierpohlschule, Minden  
1997 – 2006: Gymnasium (Abschluss: Abitur)  
Besselgymnasium, Minden  
2006 – 2007: Zivildienst  
AHB- und Rehaklinik Porta Westfalica, Bad Oeynhausen  
2007 – 2012: Maschinenbaustudium (Abschluss: Dipl.-Ing.)  
Leibniz Universität Hannover  
2012 – 2013: Wissenschaftlicher Mitarbeiter  
Institut für Fahrzeugtechnik, Technische Universität Braunschweig  
2013 – 2018: Wissenschaftlicher Mitarbeiter  
Institut für Statik und Dynamik, Leibniz Universität Hannover

## Erklärung

Ich erkläre hiermit, dass ich

1. die Regeln der geltenden Promotionsordnung kenne und eingehalten habe und mit einer Prüfung nach den Bestimmungen der Promotionsordnung einverstanden bin,
2. die Dissertation selbst verfasst habe, keine Textabschnitte von Dritten oder eigener Prüfungsarbeiten ohne Kennzeichnung übernommen habe und alle von mir benutzten Hilfsmittel und Quellen in meiner Arbeit angegeben habe,
3. Dritten weder unmittelbar noch mittelbar geldwerte Leistungen für Vermittlungstätigkeiten oder für die inhaltliche Ausarbeitung der Dissertation erbracht habe,
4. die Dissertation noch nicht als Prüfungsarbeit für eine staatliche oder andere wissenschaftliche Prüfung eingereicht habe,
5. nicht die gleiche oder eine in wesentlichen Teilen ähnliche Arbeit und auch nicht eine andere Arbeit bei einer anderen Hochschule als Dissertation eingereicht habe,
6. damit einverstanden bin, dass die Dissertation auch zum Zwecke der Überprüfung der Einhaltung allgemein geltender wissenschaftlicher Standards genutzt wird, insbesondere auch unter Verwendung elektronischer Datenverarbeitungsprogramme.

Hannover, den 22.11.2018

Jan Häfele